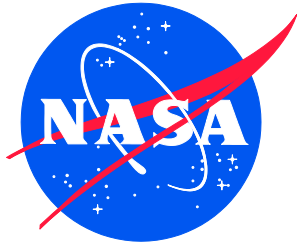


NASA/TM-2014-218505/Volume I
NESC-RP-13-00852



Evaluation of Agency Non-code Layered Pressure Vessels (LPVs)

*William H. Prosser/NESC
Langley Research Center, Hampton, Virginia*

NASA STI Program . . . in Profile

Since its founding, NASA has been dedicated to the advancement of aeronautics and space science. The NASA scientific and technical information (STI) program plays a key part in helping NASA maintain this important role.

The NASA STI program operates under the auspices of the Agency Chief Information Officer. It collects, organizes, provides for archiving, and disseminates NASA's STI. The NASA STI program provides access to the NASA Aeronautics and Space Database and its public interface, the NASA Technical Report Server, thus providing one of the largest collections of aeronautical and space science STI in the world. Results are published in both non-NASA channels and by NASA in the NASA STI Report Series, which includes the following report types:

- **TECHNICAL PUBLICATION.** Reports of completed research or a major significant phase of research that present the results of NASA Programs and include extensive data or theoretical analysis. Includes compilations of significant scientific and technical data and information deemed to be of continuing reference value. NASA counterpart of peer-reviewed formal professional papers, but having less stringent limitations on manuscript length and extent of graphic presentations.
- **TECHNICAL MEMORANDUM.** Scientific and technical findings that are preliminary or of specialized interest, e.g., quick release reports, working papers, and bibliographies that contain minimal annotation. Does not contain extensive analysis.
- **CONTRACTOR REPORT.** Scientific and technical findings by NASA-sponsored contractors and grantees.

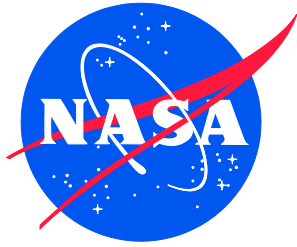
- **CONFERENCE PUBLICATION.** Collected papers from scientific and technical conferences, symposia, seminars, or other meetings sponsored or co-sponsored by NASA.
- **SPECIAL PUBLICATION.** Scientific, technical, or historical information from NASA programs, projects, and missions, often concerned with subjects having substantial public interest.
- **TECHNICAL TRANSLATION.** English-language translations of foreign scientific and technical material pertinent to NASA's mission.

Specialized services also include organizing and publishing research results, distributing specialized research announcements and feeds, providing information desk and personal search support, and enabling data exchange services.

For more information about the NASA STI program, see the following:

- Access the NASA STI program home page at <http://www.sti.nasa.gov>
- E-mail your question to help@sti.nasa.gov
- Fax your question to the NASA STI Information Desk at 443-757-5803
- Phone the NASA STI Information Desk at 443-757-5802
- Write to:
STI Information Desk
NASA Center for AeroSpace Information
7115 Standard Drive
Hanover, MD 21076-1320

NASA/TM-2014-218505/Volume I
NESC-RP-13-00852



Evaluation of Agency Non-code Layered Pressure Vessels (LPVs)

*William H. Prosser/NESC
Langley Research Center, Hampton, Virginia*

National Aeronautics and
Space Administration

Langley Research Center
Hampton, Virginia 23681-2199

July 2014

The use of trademarks or names of manufacturers in the report is for accurate reporting and does not constitute an official endorsement, either expressed or implied, of such products or manufacturers by the National Aeronautics and Space Administration.

Available from:

NASA Center for AeroSpace Information
7115 Standard Drive
Hanover, MD 21076-1320
443-757-5802

	NASA Engineering and Safety Center Technical Assessment Report	Document #: NESC-RP- 13-00852	Version: 1.0
Title: Evaluation of Agency Non-code LPVs			Page #: 1 of 193

Evaluation of Agency Non-code Layered Pressure Vessels (LPVs)

June 26, 2014

	NASA Engineering and Safety Center Technical Assessment Report	Document #:	Version:
		NESCP-RP-13-00852	1.0
Title:		Page #:	
Evaluation of Agency Non-code LPVs		2 of 193	

Report Approval and Revision History

NOTE: This document was approved at the June 26, 2014, NRB. This document was submitted to the NESC Director on July 21, 2014, for configuration control.

Approved:	<u>Original Signature on File</u>	<u>7/21/14</u>
	NESC Director	Date

Version	Description of Revision	Office of Primary Responsibility	Effective Date
1.0	Initial Release	William H. Prosser, NASA Technical Fellow for Nondestructive Evaluation	6/26/14

	NASA Engineering and Safety Center Technical Assessment Report	Document #:	Version:
		NESCP-RP-13-00852	1.0
Title:		Page #:	
Evaluation of Agency Non-code LPVs		3 of 193	

Table of Contents

Technical Assessment Report

1.0	Notification and Authorization	8
2.0	Signature Page	9
3.0	Team List	10
4.0	Executive Summary	12
5.0	Assessment Plan	14
6.0	Problem Description and Proposed Approach	17
6.1	History of LPVs	17
6.1.1	Original Patents, Manufacturers, and Benefits and Limitations of Construction Technique.....	17
6.1.2	ASME Boiler and Pressure Vessel Code	19
6.1.3	Additional Risk Factors for NASA Non-code LPVs	23
6.1.4	LPV Failure History.....	24
6.1.5	LPV Reliability Evaluation.....	28
6.2	Problem Statement	29
6.3	Planned Tasks	29
7.0	Data Analysis	30
7.1	Task 1 Summary	30
7.1.1	Center Request for Information (RFI) Responses.....	30
7.1.2	Summary of Previous or Ongoing LPV Related Work Identified at NASA Centers	39
7.1.3	External User Survey	59
7.1.4	Risk Assessment for Different LPV Regions	64
7.2	Task 2 – Limited Scope Testing and Analysis.....	74
7.2.1	LPV Material Evaluations Conducted at MSFC.....	75
7.2.2	WRS Modeling of LPVs.....	110
7.2.3	Evaluation of Two Digital Image Correlation Techniques to Detect LPV Deformations during Hydrotest	123
7.2.4	AE Testing of a Multilayer Pressure Vessel	141
7.2.5	Feasibility of using Phased Array Ultrasound to Inspect the Shell-to-Head Circumferential Welds in NASA Pressure Vessels	149
7.2.6	AE Laboratory Test Specimen Design	161
7.3	Assessment Team Comments on Proof Testing of LPVs	169
7.3.1	Methods of Proof Test Assessment.....	172
7.3.2	Proof Test Conclusions	175
7.4	Assessment Team Comments on LPV Replacement Strategy.....	175
8.0	Findings, Observations, and NESC Recommendations	177
8.1	Findings	177
8.2	Observations	181
8.3	NESC Recommendations	181

	NASA Engineering and Safety Center Technical Assessment Report	Document #:	Version:
		NESCP-RP-13-00852	1.0
Title:		Page #:	
Evaluation of Agency Non-code LPVs		4 of 193	

9.0	Alternate Viewpoint.....	184
10.0	Other Deliverables	184
11.0	Lessons Learned.....	184
12.0	Recommendations for NASA Standards and Specifications.....	184
13.0	Definition of Terms.....	184
14.0	Acronym List.....	185
15.0	References.....	187
16.0	Appendices (separate Volume 2)	193

List of Figures

Figure 5.0-1.	Typical Large Facility LPVs	15
Figure 5.0-2.	Cross-sectional Diagram of LPV	15
Figure 6.1.5-1.	Notional Bathtub Curve Illustrating Changes in Failure Rate versus Time/Cycles ...	29
Figure 7.1.2.3-1.	MSFC Vessel V0256 with Welds Stripped for Inspection.....	47
Figure 7.1.2.3-2.	Longitudinal Crack in Outer Layer of V0256	47
Figure 7.1.2.3-3.	PAUT Scan of Head-to-Shell Weld Region.....	49
Figure 7.1.2.3-4.	PAUT Scan of Head-to-Shell Weld Region.....	49
Figure 7.1.2.3-5.	PAUT Scan of Shell-to-Shell Weld Region	50
Figure 7.1.2.3-6.	PAUT Scan of Shell-to-Shell Weld Region	50
Figure 7.1.2.3-7.	PAUT Scans for Indication in C5 Weld O to N Location, Indicative of Slag.....	54
Figure 7.1.2.3-8.	PAUT Scans for Linear Indication in C5 Weld O to P Location, Indicative of Lack of Fusion.....	55
Figure 7.1.2.3-9.	PAUT Scans for Visible Crack in Outer Layer of V0256.....	56
Figure 7.2.1.1-1.	Vessel V0032 before Sectioning, Shown with Sister Vessels V0030 and V0035	78
Figure 7.2.1.1-2.	Vessel V0125 Shown after Sectioning	78
Figure 7.2.1.2-1.	V0032 Gross Sectioning Plan.....	90
Figure 7.2.1.2-2.	V0125 Sectioning Cut Plan	90
Figure 7.2.1.2-3.	V0032-1 Sectioned for Metallographic Microstructural Examination for Determining Material Orientation	91
Figure 7.2.1.2-4.	V0032-1 Cut Plan for Metallographic Microstructural Evaluation for Determining Material Orientation	92
Figure 7.2.1.2-5.	Microstructural Evaluation at 50× Magnification of A225 Material from Vessel V0032 showing Banding of Pearlite and Ferrite on Meridional Face.....	93
Figure 7.2.1.2-6.	Cut Plan for V0032 Charpy Impact Samples	95
Figure 7.2.1.2-7.	Charpy V-notch Impact Test Results for V0032 A225 Head Material	97
Figure 7.2.1.2-8.	Partial Cut Plan for Fracture Toughness and Tensile Test Specimens from A225 Head Material from V0032 Showing Salient Features of Full Cut Plan.....	98
Figure 7.2.1.2-9.	Comparison of Fracture Surfaces for Fracture Toughness Tests Performed in C-L Orientation and L-C Orientation	100

	NASA Engineering and Safety Center Technical Assessment Report	Document #: NESCP-RP- 13-00852	Version: 1.0
Title: Evaluation of Agency Non-code LPVs		Page #: 5 of 193	

Figure 7.2.1.2-10.	Master Curve Plot for 1143 Material.....	105
Figure 7.2.1.2-11.	Master Curve Plot for 1146 Material.....	106
Figure 7.2.1.3-1.	Microhardness Traverses Taken across the V0125 Head-to-Shell Weld.....	108
Figure 7.2.1.3-2.	Microhardness Traverses Illustrating Hardness Response Differences in Inner Layer and First Thinner Layer in V0125.....	108
Figure 7.2.1.3-3.	Cross-section for V0032-11, Evaluated by RT for Longitudinal Shell Welds Shown.....	109
Figure 7.2.2-1.	Four-layer Tank Considered for Weld Residual Stress Analysis	111
Figure 7.2.2-2.	VFT Weld Modeling System	113
Figure 7.2.2-3.	Axisymmetric Weld Models and Meshes.....	113
Figure 7.2.2-4.	Stress Strain Curves Used for Mechanical Portion of Analysis	115
Figure 7.2.2-5.	Hoop WRS Predictions for Layered Shell-to-Shell Weld.....	116
Figure 7.2.2-6.	Axial WRS Predictions for Layered Shell-to-Shell Weld.....	117
Figure 7.2.2-7.	Hoop WRS Predictions for Layered Shell-to-Head Weld.....	117
Figure 7.2.2-8.	Axial WRS Predictions for Layered Shell-to-Head Weld.....	118
Figure 7.2.2-9.	Line Path Definitions for Through Thickness Stress Plots	119
Figure 7.2.2-10.	Shell-to-Head Weld: Line Plot from ID to Outer Diameter (OD) along Centerline	119
Figure 7.2.2-11.	Shell-to-Head Weld: Line Plot from ID to OD along Layer Path 2-3.....	120
Figure 7.2.2-12.	Comparison of API-579 Solutions to Calculated Results for Both Shell-to-Shell and Shell-to-Head Tank Cases: Weld Centerline.....	121
Figure 7.2.2-13.	Comparison of API-579 Solutions to Calculated Results for Both Shell-to-Shell and Shell-to-Head Tank Cases: Layer 2-3 Path	122
Figure 7.2.3.1-1.	Pretest View of PV0236.....	125
Figure 7.2.3.1-2.	NDE Results Summarizing Known Vessel Flaws for Vessel PV0236	126
Figure 7.2.3.3-1.	Test Pressure Vessel Cleaned and Painted White	128
Figure 7.2.3.3-2.	Application of Vinyl Stencil and Spray-painting Process on Vessel	129
Figure 7.2.3.3-3.	Pressure Vessel with Completed Dot Pattern.....	129
Figure 7.2.3.3-4.	Two Views Depicting Placement of Digital Targets on Pressure Vessel.....	130
Figure 7.2.3.3-5.	Aramis Camera Pair in Test Configuration	131
Figure 7.2.3.4-1.	Aramis Three-Dimensional Fringe Plot of Computed Radial Values on Pressure Vessel.....	132
Figure 7.2.3.4-2.	Vessel Point Locations and Respective Displacement Plotted versus Stage Number.....	134
Figure 7.2.3.4-3.	Color Fringe Overlay of Axial Displacement (X-direction) at 4,200 psi.....	135
Figure 7.2.3.4-4.	Selected Axial Section Lines on Color Overlay of Axial Displacement (X-direction) at 4,200 psi	136
Figure 7.2.3.4-5.	Average Computed Radius of a Best Fit Cylinder from Aramis Data Results from Second Pressure Test.....	137

	NASA Engineering and Safety Center Technical Assessment Report	Document #: NESCP-RP-13-00852	Version: 1.0
Title: Evaluation of Agency Non-code LPVs		Page #: 6 of 193	

Figure 7.2.3.4-6.	Screenshot of Tritop Graphical User Interface Showing Pressure Vessel Point Cloud with Best-fit Cylinder	138
Figure 7.2.3.4-7.	Displacement Vectors Overlaid on Coded Target Locations at Pressurized End of Vessel.....	139
Figure 7.2.3.4-8.	Displacement Vectors Overlaid on Coded Target Locations at Sealed End of Vessel	139
Figure 7.2.4-1.	Drawing Detail of A. O. Smith Vessel PV0236.....	142
Figure 7.2.4-2.	Pressurization Plan	142
Figure 7.2.4-3.	Sensor Placement	143
Figure 7.2.4-4.	Crack Locations.....	144
Figure 7.2.4-5.	Crack Locations (continued)	144
Figure 7.2.4-6.	Corrosion between Layers on MSFC LPV V-32	145
Figure 7.2.4-7.	Location Event Amplitudes versus Time	146
Figure 7.2.4-8.	Location Calibration Plots.....	147
Figure 7.2.4-9.	Location Plot	147
Figure 7.2.4-10.	Trending Plots	148
Figure 7.2.5.1-1.	Examples of Common Operating Modes using a Phased Array Probe.....	150
Figure 7.2.5.2-1.	View from either Side of Calibration Block Showing SDHs.....	151
Figure 7.2.5.2-2.	View from Underside of Calibration Block Showing the Three RDHs in the Weld	152
Figure 7.2.5.2-3.	Ultrasonic Velocity Measurement Locations in First Test Block	152
Figure 7.2.5.3-1.	View of the Probe and Wedge used to Conduct Phased Array Half-V Sectorial Exams	154
Figure 7.2.5.3-2.	S-scans of Three SDHs on Head Side of Weld and A-scan of Each Hole at Angle of Peak Response.....	155
Figure 7.2.5.3-3.	S-scans Showing Lower Two SDHs on Multilayered Side of Weld and A-scan of Each Hole at Angle of Peak Response.....	156
Figure 7.2.5.3-4.	S-scans of RDH#2 Detected with Probe Flush with Weld and Skewed at 30°	157
Figure 7.2.5.3-5.	Sectorial Exam View of Three Radially Drilled Holes in Weld Root and A-scan of Each Hole at Angle of Peak Response.....	158
Figure 7.2.5.3-6.	Two S-scans Showing Unidentified Indications Not Associated with Known Flaws or Part Geometry.....	159
Figure 7.2.5.4-1.	Illustration of Full-V Beam Path to SDH#2.....	160
Figure 7.2.6-1.	AE Laboratory Specimen to be Tested from V0032 1146a Material.....	162
Figure 7.2.6-2.	Bar Graph Comparing Measured Signal Energies from Different-sized ¼-inch-thick Plates	164
Figure 7.2.6-3.	Early Waveform from Pencil-Lead Break on 36- by 72-inch Aluminum Plate.....	165
Figure 7.2.6-4.	Early Waveform from Pencil-Lead Break on 3- by 6-inch Steel Plate	165
Figure 7.2.6-5.	Early Waveform from Pencil-Lead Break on 4- by 8-inch Steel Plate	166

	NASA Engineering and Safety Center Technical Assessment Report	Document #:	Version:
		NESCP-RP-13-00852	1.0
Title:		Page #:	
Evaluation of Agency Non-code LPVs		7 of 193	

Figure 7.2.6-6.	Early Waveform from Pencil-Lead Break on 6- by 12-inch Steel Plate	166
Figure 7.2.6-7.	Full Waveform from Pencil-Lead Break on 36- by 72-inch Aluminum Plate	167
Figure 7.2.6-8.	Full Waveform from Pencil-Lead Break on 3- by 6-inch Steel Plate	168
Figure 7.3-1.	Proof Test Concept.....	171
Figure 7.3-2.	Proof Test Concept with Proof and Operational Critical Crack Size Curves.....	172

List of Tables

Table 7.1.2.3-1.	Head-to-Shell Weld.....	52
Table 7.1.2.3-2.	Shell-to-Shell Welds.....	52
Table 7.1.4-1.	LPV Regions or Operating Conditions that Present the Highest Risk for Potential Failure for NASA Non-Code LPVs	66
Table 7.1.4-2.	LPV Regions or Operating Conditions with Lower Risk for Potential Failure for NASA Non-Code LPVs	72
Table 7.2.1-1.	Definition of Terms Specific to LPV Materials Testing Discussed in this Section ...	75
Table 7.2.1.1-1.	Summary of Vessels Evaluated.....	79
Table 7.2.1.1-2.	Typical Material Properties for LPV Materials.....	79
Table 7.2.1.1-3.	Comparison of Tensile Data Obtained from V0032 against A. O. Smith Certification and Lot Acceptance Values.....	80
Table 7.2.1.1-4.	ICP Analytical Chemistry Composition Results for V0032 Inner Shell Material Compared with 1146a Specification Requirements	82
Table 7.2.1.2-1.	Charpy V-notch Impact Energy Results for V0032 A225 Head Material.....	96
Table 7.2.1.2-2.	T0 Transition Reference Temperature Data for 1143 Material from V0032 in Bounding Material Orientation	102
Table 7.2.1.2-3.	T0 Transition Reference Temperature Data for 1146 Material from V0032 in Bounding Material Orientation	104
Table 7.2.3.2-1.	Vessel Stress, Strain, and Deformation Computations at Two Pressure States based on Modulus of Elasticity of 2.95 E+07 psi	127
Table 7.2.3.4-1.	Data-indicated Pressure Values Associated with Stages Recorded in Aramis	133
Table 7.2.4-1.	AE System Parameters	143
Table 7.2.5.2-1.	Wave Velocity and Relative Signal Loss Measurements taken from Test Block	153

	NASA Engineering and Safety Center Technical Assessment Report	Document #: NESCP-RP- 13-00852	Version: 1.0
Title: Evaluation of Agency Non-code LPVs		Page #: 8 of 193	

Technical Assessment Report

1.0 Notification and Authorization

In coordination with the Office of Safety and Mission Assurance (OSMA) and the respective Center Pressure System Managers (PSMs), the NASA Engineering and Safety Center (NESC) was requested to formulate a consensus draft proposal for the development of additional testing and analysis methods to establish the technical validity, and any limitation thereof, for the continued safe operation of facility non-code (i.e., not in compliance with the American Society of Mechanical Engineers Boiler and Pressure Vessel Code, Section VIII, Division 1, in effect at the time of construction) layered pressure vessels.

The NESC Review Board approved the assessment plan on April 18, 2013. Dr. William H. Prosser was assigned to lead this assessment. The primary stakeholders for this assessment were the OSMA, as represented by Owen Greulich, Technical Discipline Manager for Pressure Systems, and the respective Centers responsible for the safe operation of these vessels, as represented by the PSMs. The PSMs from each NASA Center were asked to participate as part of the assessment team by providing, collecting, and reviewing data regarding current operations of these vessels.

	NASA Engineering and Safety Center Technical Assessment Report	Document #: NESCP-RP- 13-00852	Version: 1.0
Title: Evaluation of Agency Non-code LPVs		Page #: 9 of 193	

2.0 Signature Page

Submitted by:

Team Signature Page on File 7/25/14

Dr. William H. Prosser

Date

Signatories declare the findings, observations, and NESC recommendations compiled in the report are factually based from data extracted from program/project documents, contractor reports, and open literature, and/or generated from independently conducted tests, analyses, and inspections.

	NASA Engineering and Safety Center Technical Assessment Report	Document #:	Version:
		NESCP-RP-13-00852	1.0
Title:			Page #:
Evaluation of Agency Non-code LPVs			10 of 193

3.0 Team List

Name	Discipline	Organization
Core Team		
William Prosser	NESC Lead; NASA Technical Fellow for Nondestructive Evaluation	LaRC
Pravin Aggarwal	Structures	MSFC
Matt Adler	Materials	Jacobs ESSA (MSFC)
Gilda Battista	Materials	Jacobs ESSA (MSFC)
Douglas Fraser	ARC PSM	ARC
Pete Taddie	KSC PSM	KSC
Ernest Graham	MSFC/MAF PSM	MAF
Owen Greulich	OSMA Discipline Manager for Pressure Systems	HQ
Maan Jawad	LPV Consultant	Global Engineering and Technology, LLC
Edward Johnson	MSFC PSM	MSFC
Pat Johnston	PAUT NDE	LaRC
Kenny Le	JPL PSM	JPL
Son Le	SSC PSM	SSC
Max Leuenberger	JSC/WSTF PSM	WSTF
Nick Noparat	GSFC/WFF PSM	WFF
Cynthia Null	NASA Technical Fellow for Human Factors	ARC
Carlos Perez-Ramos	LaRC PSM	LaRC
Al Pulley	Pressure Vessels	MSFC
Ivatury Raju	NASA Technical Fellow for Structures	LaRC
Fayssal Safie	NASA Technical Fellow for Reliability and Maintainability	MSFC
Roy Savage	MTSO Program Analyst	LaRC
Keith Van Tassel	JSC PSM	JSC
Douglas Wells	Materials	MSFC
Stephen Wnuk	GRC PSM	GRC
Calogero Dirienzo	Pressure Vessels	GRC
Richard Wong	AFRC PSM	AFRC



NASA Engineering and Safety Center Technical Assessment Report

Document #:
**NESCP-RP-
13-00852**

Version:
1.0

Title:

Evaluation of Agency Non-code LPVs

Page #:
11 of 193

Name	Discipline	Organization
Consultants		
Alan Puchot	PAUT NDE	Southwestern Research Institute
Charles Duffer	PAUT NDE	Southwestern Research Institute
Bud Brust	Weld Residual Stress Analysis	Engineering Mechanics Corporation of Columbus
James Joyce	Fracture Mechanics	U.S. Naval Academy (retired), AMA
Dave Dawicke	Structures	AS&M
Matthew Melis	Photogrammetry	GRC
Justin Littell	Photogrammetry	LaRC
Andrew Ring	Photogrammetry	Ohio Aerospace Institute
Claud Hunter	Acoustic Emission	Jacobs Technology
James Walker	Acoustic Emission	MSFC
Eric Madaras	Acoustic Emission	LaRC
Administrative Support		
Linda Burgess	Planning and Control Analyst	LaRC/AMA
Jonay Campbell	Technical Writer	LaRC/NG
Tina Dunn-Pitman	Project Coordinator	LaRC/AMA

	NASA Engineering and Safety Center Technical Assessment Report	Document #: NESCP-RP-13-00852	Version: 1.0
Title: Evaluation of Agency Non-code LPVs		Page #: 12 of 193	

4.0 Executive Summary

The NASA Engineering and Safety Center (NESC) was asked to perform an assessment related to the approximately 300 older, layered pressure vessels (LPVs) that are in service at a number of NASA facilities. Although NASA has not experienced a catastrophic failure of an LPV, the high pressures and large volumes of these vessels could produce severe consequences in the event of a failure. These vessels were fabricated prior to the adoption of layered fabrication techniques as an acceptable construction methodology in the American Society of Mechanical Engineers (ASME) Boiler and Pressure Vessel Code (BPVC) [ref. 1]. Additionally, there are variances in the materials, fabrication, and inspection techniques used in these vessels with respect to the BPVC at the time of construction, as well as the later adopted BPVC that provided for LPV construction. Thus, these vessels are non-code and, consequently, are not compliant with Occupational Safety and Health Administration (OSHA) regulations [ref. 2] as required for federal agencies [ref. 3]. Further, these vessels are typically more than 50 years old and, as such, are at additional risk for age-related degradation, including fatigue, corrosion, and embrittlement, which can lead to fracture.

The scope of the assessment was to formulate a consensus draft proposal for the development of additional testing and analysis methods to establish the technical validity, and any limitation thereof, of these vessels for continued safe operation. It should be made clear that the establishment of the current safety of these vessels, or their safety for continued operations for any period into the future, was not within the scope of this assessment. In performance of this assessment, three tasks were executed. The first was to review the inventory, usage conditions, and ongoing and proposed risk mitigation methods for LPVs at all NASA Centers and for select locations at other Government facilities and in private industry. The second task was to conduct limited scope testing and analysis necessary to formulate final recommendations. Major activities for this task were defined based on the results of the first task. The third and final task was to coordinate a consensus draft proposal for the development of additional testing and analysis methods to establish the technical validity, and any limitation thereof, of LPVs for continued safe operation. The output of this task forms the basis for the recommendations contained in this report.

The assessment team found that the operation of these non-code LPVs does present an elevated level of risk compared with conventional code-compliant vessels. However, insufficient information is available to quantify that level of increased risk within the scope of this effort. The assessment team found that the Agency lacks a consensus approach to addressing the risks associated with the operation of these vessels. Also, although near-term actions are available and identified to reduce the risk of and consequences from catastrophic failure of LPVs, the level of risk reduction for many of these actions cannot be quantified. Longer-term efforts are required and are identified for characterizing and mitigating the risk for LPVs, and these should be focused on the highest risk operating conditions and regions of these vessels identified by the assessment team. Several additional discipline-specific findings are provided specific to materials testing, structural analysis, and nondestructive evaluation (NDE) technique

	NASA Engineering and Safety Center Technical Assessment Report	Document #: NESCP-RP- 13-00852	Version: 1.0
Title: Evaluation of Agency Non-code LPVs		Page #: 13 of 193	

developments that are applicable to better characterizing and reducing of LPV risks. The assessment team also observed that the Center Pressure Systems Managers (PSMs) who participated on the assessment team demonstrated understanding of the technical issues and concerns associated with non-code LPVs and a willingness to engage across Centers to develop improved approaches to mitigating risks associated with the continued use of these vessels. The assessment team also observed that significant efforts are underway outside this assessment that directly relate to the understanding of and continued safe use of LPVs at Centers.

The assessment team identified two sets of recommendations. The first set of recommendations consists of near-term actions that if enacted could reduce either the risk of or consequences from catastrophic LPV failure resulting from their continued use. Because of the lack of adequate materials property data, inspection methodologies, and analyses methods, the risks associated with the continued use of these vessels and the degree to which these recommendations would reduce that risk cannot be accurately estimated at this time. In addition, it is recommended that the Agency formulate and support an Agency-wide team to continue efforts to assess and reduce risks associated with LPVs and to develop a centralized database of information on the design, fabrication, materials, operation, inspection, maintenance, and repair of LPVs.

The second set of recommendations comprises the longer-term activities proposed to improve understanding of the risks associated with continued use of LPVs and to develop Agency processes to mitigate these risks. The assessment team recommends that the Agency expand efforts to gather LPV materials property data. In doing so, it is recommended first that a statistical analysis be performed to determine the number of LPVs and associated materials testing specimens needed to provide adequate bounding materials property data. To address a high-risk operating condition, notably the potential operation of these vessels at temperatures where brittle fracture is possible, it is recommended that measurements of the temperatures associated with ductile to brittle fracture behavior (initiated in Task 2) be completed. These measurements are necessary to establish appropriate minimum design metal temperatures (MDMTs) for future operation of LPVs. Additionally, it is recommended that additional materials property data be gathered to support analysis methods to evaluate and utilize proof test methodologies and to establish critical crack sizes for NDE detection criteria.

It is further recommended that the Agency expand efforts to develop and validate analysis methods to address the identified highest risk conditions and regions of LPVs. Using these analysis methods, it is necessary to assess the sensitivity of any results to uncertainties in the input variables, such as material properties, structural configurations, and weld residual stress conditions. It is recommended that analysis predictions of weld residual stresses for LPVs (initiated in Task 2) be completed and measurements made to validate these results. It is recommended that an analytical framework be established to evaluate proof test logic for these vessels and, where proof testing cannot be applied, to analyze the leak-before-break (LBB) capability of the LPV system. To aid in NDE development and validation and remaining safe life determination, it is recommended that an analytical framework be established to evaluate critical initial flaw sizes.

	NASA Engineering and Safety Center Technical Assessment Report	Document #: NESCP-RP- 13-00852	Version: 1.0
Title: Evaluation of Agency Non-code LPVs		Page #: 14 of 193	

It is also recommended that the Agency develop and, where possible, validate a number of NDE techniques to address the highest risk conditions and regions of LPVs. These include the phased array ultrasonic technique (PAUT), which has shown promise for inspecting the critical full penetration circumferential welds in LPVs. Other techniques recommended for development and validation include photogrammetry, both for validation of analysis methods and potential flaw detection in shell sections; acoustic emission (AE) techniques for detection of flaw growth in welds, heads, and shell sections; and radiographic and low-frequency electromagnetic methods for potential flaw detection in welds, heads, and shell sections.

Lastly, the assessment team entertained significant discussion regarding whether to make any recommendations regarding the need for consideration of plans for replacement of these vessels, which would cost an estimated \$1–2M per vessel and would result in ancillary cost and schedule impacts while a vessel undergoing replacement is off-line. In the end, the assessment team stopped short of such a recommendation for a variety of reasons. However, all team members were in agreement with the obvious fact that replacement of these vessels would eliminate the additional risks associated with their continued use, in comparison with the better understood and more easily mitigated risks associated with monolithic code-compliant replacement vessels.

5.0 Assessment Plan

NASA has an active inventory at nine of its Centers or facilities of approximately 300 old, non-code LPVs in high-pressure service. Many of these are in close proximity to personnel and expose personnel and facilities to catastrophic consequences in the event of failure. The fabrication and inspection techniques in use at the time of construction for these older vessels were not included in the ASME BPVC; thus, these vessels are not compliant with the then-current ASME BPVC, or the 1968 ASME BPVC [ref. 4], as is now required by the Federal OSHA regulations (29 CFR 1910 and 1960, Occupational Safety and Health Standards) [refs. 2 and 3]. OSHA regulations do not provide for “grandfathering” of these older, non-code pressure vessels, which would allow these older vessels to be exempt from the existing regulations. Additionally, the layered construction technique makes the application of traditional NDE techniques, such as ultrasonic shear and straight-beam, radiography, and magnetic-particle inspection of the inner layers of these vessels, difficult if not impossible. This difficulty in detecting defects is further enforced when considering the types of NDE methods available and their detection capabilities at the time when these LPVs were constructed.

Figure 5.0-1 shows examples of typical large facility LPVs. Figure 5.0-2(a) shows a cross-sectional diagram of an LPV with a monolithic head, and Figure 5.0-2(b) shows a cross section of an actual vessel where the layers, weld, and monolithic head are clearly visible. The head for these vessels can be monolithic, as shown, or composed of multiple layers. All of the NASA LPVs have monolithic heads.



NASA Engineering and Safety Center Technical Assessment Report

Document #:
**NESCP-RP-
13-00852**

Version:
1.0

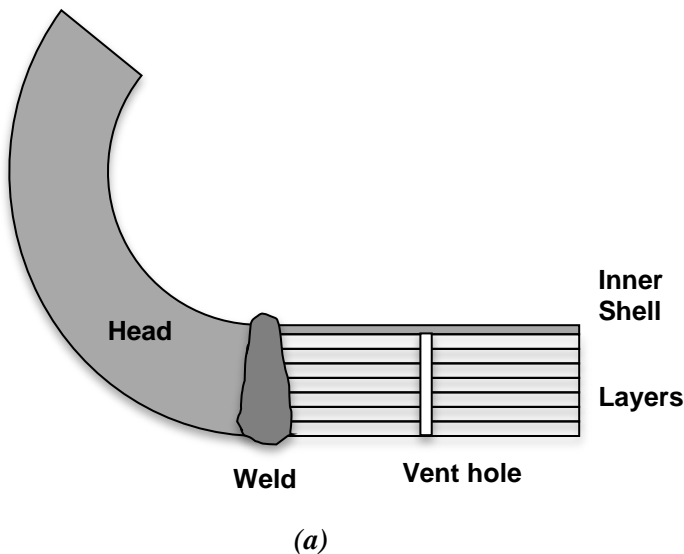
Title:

Evaluation of Agency Non-code LPVs

Page #:
15 of 193



Figure 5.0-1. Typical Large Facility LPVs



(a)
**Figure 5.0-2. Cross-sectional Diagram of LPV ((a) monolithic head
and (b) cross section of actual vessel)**

Although there has never been a catastrophic failure of this type of vessel at any NASA Center, there have been failures in industry (as described in Section 6.1.4) as recently as 2010, including at least one newer LPV that was ASME code-stamped. These NASA vessels have been in use for decades without an established Agency-wide-consensus technical basis for ensuring their safe operation.

	NASA Engineering and Safety Center Technical Assessment Report	Document #: NESCP-RP- 13-00852	Version: 1.0
Title: Evaluation of Agency Non-code LPVs		Page #: 16 of 193	

The assessment team was requested to formulate a consensus draft proposal for the development of additional testing and analysis methods that would be required to establish the technical validity, and any limitation thereof, of these vessels for continued safe operation. This assessment was to leverage common skills, capabilities, and data from within and outside NASA and to consider inspection, analysis, and monitoring techniques that could be applicable to these vessels. To accomplish this task, the assessment team was to evaluate failure risks associated with the inner shell, outer layers, heads, nozzles, and welds of these vessels. It was expected that the results of this assessment and the proposed follow-on testing and analysis could subsequently be used as a basis for the development of a future NASA standard that would be submitted to OSHA for use as an alternate and supplementary standard, as required by 29 CFR 1960 [ref. 3].

An informational presentation to familiarize OSHA with the suggested approaches was a possible product of this assessment, with the understanding that this assessment was only a first step and that the resulting proposed testing and analysis method development was outside the scope of this assessment. Likewise, this assessment did not include the generation, review, and Agency approval of any NASA alternate and supplementary standard for OSHA. The tasks for this assessment included the following:

Task 1: Review inventory, usage conditions, and ongoing and proposed risk mitigation methods for LPVs at all NASA Centers and at select locations within other Government facilities, as well as in private industry. Major activities included:

- Hold virtual technical interchange meetings (TIMs) with Center PSMs to acquire available data on NASA usage of LPVs, to include inventory, usage conditions, and ongoing and proposed risk mitigation methods.
- Research locations and points of contact for external, non-NASA sites where similar vessels are currently in operation.
- Conduct phone interviews with non-NASA users of LPVs.
- Engage multilayer pressure vessel fabricators and additional experts (e.g., ASME or American Society for Testing and Materials (ASTM) technical committee members) as needed.
- Conduct a virtual TIM with the assessment team to collate review results and identify technical areas requiring further studies, opportunities for limited testing and analysis efforts to be considered, and preliminary initial recommendations.

Task 2: Conduct limited scope testing and analysis necessary to formulate final recommendations and a path forward. Major activities for this task were to be defined based on the results of task 1, for example:

- Proof of concept of NDE and *in situ* sensing methods.
- Destructive materials properties testing and associated analysis.
- Structural analysis of LPV response.

	NASA Engineering and Safety Center Technical Assessment Report	Document #: NESCP-RP- 13-00852	Version: 1.0
Title: Evaluation of Agency Non-code LPVs		Page #: 17 of 193	

Task 3: Coordinate development of a consensus draft proposal for the development of additional testing and analysis methods required to establish the technical validity, and any limitation thereof, of LPVs for continued safe operation. Major activities for this task included:

- Conduct final virtual TIM to identify highest priority risk mitigation methodologies and necessary future testing and/or analyses required to develop, evaluate, and validate these approaches.
- Develop findings, observations, and NESC recommendations and draft a final report for peer review and approval.

6.0 Problem Description and Proposed Approach

6.1 History of LPVs

6.1.1 Original Patents, Manufacturers, and Benefits and Limitations of Construction Technique

The methods of construction for LPVs were originally described in the United States (U.S.) in patents assigned to the A. O. Smith Corporation in the 1930s and 1940s [refs. 5 and 6]. During WWII, Krupp in Germany also developed a layered method of constructing high-pressure vessels. Rather than using a single monolithic layer of material, multiple layers are used to construct these vessels, as shown in Figure 5.0-2. Although in principle both the shells and the heads of cylindrical vessels can be fabricated with layers, most vessels fabricated in this manner, including all within NASA, have monolithic heads and layered shells.

This fabrication approach originated to address the difficulty at the time in building thick monolithic steel shells to withstand very high pressures. Thick steel products produced by the steel mills at that time had considerable variability in chemical composition and material properties and suffered from slag inclusions and poor impact properties; thin-plate materials with better and more consistent properties were more readily available. Of course, as stated, NASA's layered vessels still have thick heads and present risks associated with materials variability, which is discussed later.

The advantages of the layered vessel construction method for vessels to be used at high pressures included:

1. The high-strength steel necessary for construction was readily available in thin (typically ¼- to ½-inch) plates, which could be rolled into cylinders for the shell sections.
2. Thin plates could more readily be rolled into cylinders with lighter forming rolls and without heating.
3. Large overall thicknesses could be fabricated using multiple thin layers.
4. The thin plates generally had superior material properties (e.g., ductility, strength, and toughness) over equivalent thicker plates.

	NASA Engineering and Safety Center Technical Assessment Report	Document #: NESCP-RP- 13-00852	Version: 1.0
Title: Evaluation of Agency Non-code LPVs		Page #: 18 of 193	

5. Vent holes could be drilled through all of the layers except the inner shell of the vessels, as shown in Figure 5.0-2(a), ensuring that pressure did not build up between layers and also providing a means of detecting leakage, indicating inner shell failure before catastrophic rupture of the vessel. (Note that a similar technology was developed in parallel in Germany in the coal gasification industry for the war effort, where an inner layer was used as the pressure seal and the outer shell layers were vented).
6. Welding of the thin longitudinal seam joints in the thin plates was more easily accomplished versus welding joints in thicker plates.
7. Redundancy of layers ensured that even a crack in a layer at a location near a circumferential weld could not propagate through the full vessel wall without first propagating to and through the circumferential weld.
8. The fact that such a crack must propagate through the circumferential weld to get to any layer other than that immediately adjacent to it (i.e., to which it could propagate through the longitudinal weld fusing the two layers) also ensured that a crack not extending to the vicinity of the circumferential weld was essentially harmless (barring other lost layers, which could result in a simple overstress failure).

Disadvantages included:

1. The intermediate layers of the shell sections are difficult, if not impossible, to reliably nondestructively inspect after fabrication.
 - a. Ultrasonic methods could only be used to inspect the outer layer and, if access to the interior of the vessel was available, the inner shell. Ultrasound is not readily transmitted to the intermediate layers because of the discontinuity between the layers.
 - b. Radiographic techniques typically used for inspecting vessel welds do not work well because of the presence of the multiple layers. The presence of layers creates indications in radiographic images that may obscure flaw indications in the circumferential welds (called layer wash in the ASME BPVC).
 - c. The flaw sizes detectable using radiography are a function of the total wall thickness (which is in the 2.5- to 6-inch range for NASA's vessels), while the critical flaw size in a layer based on fracture mechanics is a function of the layer thickness.
 - d. Ability of radiography to detect cracks is limited if the crack is not closely aligned with the direction of the radiation (i.e., generally accepted maximum of about 5 degrees). Reference 7 specifies 4.3 degrees, while NASA-STD-5009 [ref. 8] requires a maximum of 5 degrees).
 - e. NDE methods and their detection capabilities available at the time of construction were more limited than those in use today.

	NASA Engineering and Safety Center Technical Assessment Report	Document #: NESCP-RP- 13-00852	Version: 1.0
Title: Evaluation of Agency Non-code LPVs		Page #: 19 of 193	

2. Analytical methods used to predict the structural response of layered vessels are simplified and generally do not consider, for example, the complexity of the geometry, including the potential for asymmetric gaps between layers or at layer-to-circumferential-weld locations, among other issues.
3. It is difficult to achieve contact between layers across the full surface of the rolled plate layers, which results in a lower strain transfer efficiency to the outer layers. To ensure that adequate contact is made, ASME BPVC criteria requires that the measured shell expansion during an LPV vessel hydrotest for new vessels be at least 50% of that which would be expected for a monolithic shell of equivalent thickness.
4. The vast majority of NASA's vessels were manufactured before ASME BPVC rules existed for such vessels, using high-strength shell layer and nozzle materials that were never incorporated into the BPVC. In addition, the A225 Grade B head material, which was listed in the BPVC at the time of construction, was eliminated from the code in the Summer 1979 Addenda to the 1977 Section VIII Code [ref. 9] for reasons that are currently not known. Consequently, these vessels are generally noncompliant with OSHA regulations and/or interpretations (which mandate ASME design and fabrication), and NASA cannot currently prove they are safe for use for any specific period of time.

LPVs have been fabricated by a number of companies. A. O. Smith fabricated vessels though the 1950s under the registered trademark name of "Multilayer Vessels." They licensed the technology in the 1960s to Chicago Bridge & Iron Company, Inc. (CB&I) and Hahn and Clay. The Nooter Corporation began manufacturing vessels in the 1960s under a different patent using spirally wound cylindrical sections rather than concentrically wound cylinders and used the trademark "Plywall Vessels." Struthers Wells also began fabricating layered vessels in the 1960s under another patented technique, where thicker cylinder sections were shrink-fitted to form the shell, under the name "Multiwall Vessels." LPVs are also currently manufactured overseas, but specifics were not researched for this work. ASME uses the generic name of layered vessels to refer to vessels constructed by these various methods. NASA has layered vessels from a number of different manufacturers. The greatest portion of NASA vessels were fabricated by A. O. Smith, followed by CB&I, with a few by other manufacturers.

6.1.2 ASME Boiler and Pressure Vessel Code

Section VIII of the ASME BPVC [ref. 1] provides rules for the construction of new pressure vessels. Newly constructed pressure vessels that fully comply with and are stamped in accordance with ASME BPVC Section VIII are considered to be "code" vessels. A new code-stamped vessel having appropriate safety pressure relief protection is normally accepted as having sufficient integrity and minimal risk to serve its intended purpose without further mitigations against potential failures for its design service life (i.e., barriers, restricted access, etc., are generally not required simply because an ASME vessel is in use). It is also the standard required by OSHA for both industry and federal workplaces. (In formal letters of interpretation, OSHA refers to "nameplate, records, and stamping," and concludes that actual ASME BPVC stamping, not just "equivalent construction," is required.) The BPVC is a code for new

	NASA Engineering and Safety Center Technical Assessment Report	Document #: NESCP-RP-13-00852	Version: 1.0
Title: Evaluation of Agency Non-code LPVs		Page #: 20 of 193	

construction and does not address any degradation or changes in service that might occur after completion of construction of a vessel.

Most of the NASA-owned LPVs are from the 1950s and 1960s. The ASME BPVC did not provide for the layered method of construction. Only monolithic vessels were addressed by the BPVC. The layered method of construction was added to the ASME BPVC in the Winter Edition of 1978 [ref. 10]. Paragraph A-140 of reference 9 includes the following statement:

“The rules in Section VIII, Division 1 and Division 2 which cover the construction of layered vessels have been developed to parallel each other as far as can be done within the parameters of each Division. The design criteria may influence the selection of the Division.”

Even the first treatment of layered vessels in the ASME BPVC in 1978 included extensive requirements beyond what is included in the balance of the BPVC, addressing material requirements, design, welding (including heat treatment), NDE, fabrication, inspection and testing, and pressure relief devices.

LPVs constructed prior to 1978 were not ASME “code-stamped” and, thus, are “non-code.” Although designed and constructed by reputable companies using documented and formalized procedures and generally good practices, these were not consistent with the BPVC at the time of manufacture, or with later additions, and generally had lower factors of safety than required by ASME for code-stamped vessels. Appendix A shows an example of a procurement specification for a NASA LPV in 1961. In section 1-5(d) of Appendix A for design conditions, it specifies that the design and fabrication of the vessel shall conform to one of the following:

- 1) ASME Code for Unfired Pressure Vessels (1956) [ref. 11] with the following exceptions:
 - (a) the pressure limitations stated therein shall not apply and
 - (b) the provisions covered by Code Interpretations Case 1205-3 [ref. 12] shall apply.
- 2) A. O. Smith Corporation’s specification MLS-30A [ref. 13] and A. O. Smith Corporation’s specification dated August 27, 1957 [ref. 14], for multi-layer construction of vessels above 3,000 psi.

ASME Code Case 1205-3 [ref. 12] refers to forged pressure vessels without welds. Since the ASME BPVC of 1956 did not allow LPV construction techniques, the resultant pressure vessel, in order to meet the terms of the procurement specification, would have to be either a monolithic forged vessel complying with the 1956 BPVC and Code Case 1205-3 (which covered such forged vessels), or a layered vessel. If layered, it would have been required to conform to the A. O. Smith specifications.

Further, in section 1-5(e) of Appendix A of the specification, it was specified that a safety factor of 3 could be used for the LPV being procured. The ASME BPVC at the time required a safety factor of 4, except for Code Case 1205-3 for forged vessels without welds, which also allowed for a safety factor of 3. Additionally, in section 1-7(a) of Appendix A for materials, it was stated that the steel selected for fabrication of the LPV did not necessarily have to be in strict accordance with the requirements of the ASME BPVC. Thus, in addition to the fact that the

	NASA Engineering and Safety Center Technical Assessment Report	Document #: NESCP-RP- 13-00852	Version: 1.0
Title: Evaluation of Agency Non-code LPVs		Page #: 21 of 193	

general layered construction method was not covered by the BPVC at the time of construction of the NASA LPVs, additional variances with respect to the BPVC were permitted on materials and safety factors. There is no information available as to any assessments of the safety of the non-code vessel being procured with respect to these variances from the BPVC at that time. Note that government safety regulations were much less prevalent at this time, and OSHA did not exist until created by the OSH Act of 1970.

When layered methods of construction were added into the BPVC, A. O. Smith, as well as competitors Nooter Corporation and Hahn and Clay, were heavily involved in the development of the rules. The different companies had different fabrication procedures, and the resulting ASME rules were developed using a consensus process; thus, the rules that resulted allowed for a number of fabrication techniques and did not reflect what any one company had done for previously constructed vessels. Thus, it is important also to evaluate how the non-code NASA LPVs were constructed relative to the later-introduced versions of the BPVC that permitted their construction. There are two aspects to the discussion of equivalence to code: (1) do the vessels comply with all of the requirements of the BPVC, and (2) if not, can a level of safety and reliability essentially the same as compliant vessels be demonstrated? The following discussion relates to the first of these questions; this report as a whole deals with the second.

Although an exhaustive line-by-line comparison of the fabrication techniques used by the different LPV manufacturers was not performed, a review of 21 drawings for vessels constructed by A. O. Smith revealed the following discrepancies:

1. Fifteen drawings showed shell nozzles of 2-inch pipe size or less, six did not. None of the 15 nozzles complies with the configuration required in the 1978 BPVC for such nozzles.
2. Part ULW-20 in reference 10 states, "When the nondestructive examinations outlined in ULW-50 through ULW-57 have been complied with, the weld joint efficiency (factor to allow for possible weld defects) for design purposes shall be 100%." No alternative to the 100% joint efficiency is offered, and the requirements in ULW-50 through ULW-57 are all stated as requirements with no alternatives offered. Therefore, the NDE requirements on the 21 drawings were compared with the ULW-50 through ULW-57 requirements, revealing the following:
 - a. Part ULW-51 requires that Category A and B joints (see Figure UW-3 in the BPVC for category definitions) in the inner shells of layered shell sections and in the inner heads of layered heads...shall be 100% radiographic tested (RT). This was required in all drawings.
 - b. Part ULW-52(a) requires 100% magnetic particle testing (MT) inspection of the longitudinal weld joints in layers welded to the previous surface. Some MT was specified on every drawing (indicating that any MT specified could be expected to be found on the drawings rather than in some other associated specification), but

	NASA Engineering and Safety Center Technical Assessment Report	Document #: NESCP-RP- 13-00852	Version: 1.0
Title: Evaluation of Agency Non-code LPVs		Page #: 22 of 193	

none of the drawings reviewed met the 100% MT requirement for longitudinal joints.

- c. Part ULW-54(a), “Full Thickness Welding of Solid Section to Layered Sections,” requires 100% RT inspection of weld-category A, B, and D joints attaching a solid section to a layered section of any thickness given in ULW-52. Other radiography was specified on every drawing, while no drawings specified radiography meeting this requirement. While this is an inspection that can be performed after the fact, the vessels as constructed did not meet this requirement; therefore, it may be expected that the weld quality will not consistently meet the requirement.
3. Any impact testing performed typically consisted of U-notch or keyhole-notch Charpy specimens, which have a 5-mm-deep notch that has a 1-mm radius at the base. These were not permitted in the BPVC after 1967, after which Charpy V-notch specimens, which have a 2-mm-deep notch with a 45-degree angle and a 0.25-mm radius at the base, were required. The development of the Charpy V-notch specimen occurred as a result of WW II ship failures caused by high ductile-to-brittle transition temperature steels similar to A225B. Earlier Charpy notch geometries were not sensitive to this phenomenon. (The Department of Transportation (DOT) also made this change related to DOT requirements for gas storage bottles the same year.)
4. One of the later revisions of the ASME BPVC was in 1989 [ref. 15]. This revision added the UCS-66 curves for determining MDMT. At the time these vessels were constructed, the MDMT was typically based only on material strength and did not take into account brittle fracture that may occur at lower temperatures, including the nameplate MDMT. There is evidence that some A. O. Smith vessels were keyhole impact tested at -40°F , consistent with code procedures of the day, but the keyhole method used was removed from the BPVC in the early 1967 and is not acceptable in current practice because it was shown beginning in the 1950s that brittle failure of ship plates could be correlated with Charpy V notch, but not with Charpy keyhole notch characteristics [ref. 16]. Thus, operating at or above the nameplate MDMT for these vessels may not ensure safety with respect to the potential for brittle failure.
5. Proprietary shell and nozzle materials used were not BPVC listed (approved) materials. These proprietary materials also failed to comply with the BPVC requirements for unlisted materials. Thus, complete material fracture characteristics are not readily available.
6. The head material, ASTM A225B, while included in some prior editions of the BPVC, was deleted as an acceptable material in the Summer 1979 Addenda of the 1977 Section VIII, Division 1 Code [ref. 9], and is not currently included in ASME BPVC Section II (Materials) [ref. 17].

	NASA Engineering and Safety Center Technical Assessment Report	Document #: NESCP-RP-13-00852	Version: 1.0
Title: Evaluation of Agency Non-code LPVs		Page #: 23 of 193	

7. While the allowable stress basis varied by customer and was typically specified in a procurement document, the design factor of safety (FS) of these vessels is known in at least one case to be as low as 1.66 on yield strength (which for these steels results in an FS of about 2.1 on ultimate tensile strength). Using 60% of yield as the allowable stress (FS of 1.66) results in overstress at the design pressure based on the BPVC allowable stresses at the time of construction in 1978 when LPV design was incorporated into the BPVC, and the current ASME Section VIII, Division 1 [ref. 1] criteria.

It is clear that the NASA LPVs are not only “non-code” with respect to the BPVC in place at the time of construction but also “non-code” with the subsequent code that allowed the construction method. While some of these variances can be addressed to reduce risk associated with continued use of these vessels, they will always remain “non-code” and present some level of elevated risk as compared with code vessels. Additionally, the use of “non-code” vessels is not compliant with the Federal OSHA regulations (29 CFR 1910, Occupational Safety and Health Standards) [ref. 2].

To reduce risk, some but not all NASA LPVs have been derated to pressures lower than their original nameplate maximum allowable working pressure (MAWP), some to a pressure low enough to comply with ASME equivalent allowable stress criteria. However, it is noted that derating alone does not make them equivalent to ASME vessels due to the many other code compliance factors noted above.

6.1.3 Additional Risk Factors for NASA Non-code LPVs

In addition to the risks associated with being non-code vessels, there are other elements that contribute to increased risk for continued usage of these vessels. The first is the age of these vessels. Many in use at NASA were fabricated in the 1950s and 1960s. Primary risks associated with aging include fatigue, corrosion, and embrittlement. As will be discussed below, a number of cracks have been detected in NASA LPVs that may be the result of fatigue. However, it is recognized that the NDE techniques available at the time of construction were not as advanced as those currently available; therefore, the potential exists that some subsurface defects have existed since the time of construction. Corrosion on the interior of NASA LPVs has been a lesser concern since, unlike vessels operated in the petrochemical industry that often contain corrosive products at elevated temperatures, NASA vessels are largely operated with nonreactive gases (except, in some cases, hydrogen) and at ambient temperatures. Corrosion on the exterior is more of a concern, as many NASA LPVs are located near the coast. However, exterior corrosion is readily detected and can be easily abated. With respect to embrittlement, other than vessels that were in hydrogen service, there is little reason to believe that the vessels have changed in properties since their initial fabrication, given the operating environment of NASA LPVs.

Another factor is that in many cases there is limited information about the usage history of these vessels, such as the number of pressure cycles, the ranges of operating pressures, and temperatures, etc. A number of these vessels were not originally constructed for NASA but were put in service for other Agencies or organizations and later obtained by NASA. Service history for those vessels prior to arrival at NASA is often nonexistent. Additionally, even for vessels in

	NASA Engineering and Safety Center Technical Assessment Report	Document #: NESCP-RP- 13-00852	Version: 1.0
Title: Evaluation of Agency Non-code LPVs		Page #: 24 of 193	

service within NASA for their entire life, there may be limited information on the usage, maintenance, and inspection and repair history, or information may be buried in old written files that are difficult to access. This lack of accurate usage information impacts the ability to perform an accurate fitness-for-service (FFS) assessment of the vessels. Another identified area of concern regarding these vessels within the Agency is the lack of consistency in how they are maintained, inspected, and operated.

6.1.4 LPV Failure History

It is estimated that the total number of LPVs, both code and non-code, that have been fabricated is less than 24,000. When A. O. Smith licensed the technology to CB&I in the mid-1960s, they estimated 15,000 layered vessels in existence. Production of layered vessels in the U.S. has slowed since then and has been about 20 per year since the mid-1960s. The rate of production for Nooter Corporation was two to three vessels per year, and these appear to be used mostly in the chemical process industry, such as for urea manufacturing.

There have been a number of known catastrophic failures of LPVs, all at chemical process plants (none at a NASA facility). Vessels that failed in the U.S. prior to 1978 were obviously non-code vessels. For some of the more recent failures, as well as failures outside the U.S., it was not documented as to whether the vessels were non-code or code. In one case, however, it was a newer, code-compliant vessel that failed. Thus, it is possible for both code and non-code LPVs to fail catastrophically. Poor maintenance and inspection practices often contributed to missing early signs of inner shell failure through the vent holes.

The following paragraphs describe some of the vessel failures.

Catastrophic vessel failures:

1. Clinton, Iowa, fertilizer plant, March 30, 1969 [ref. 18]. Failure started in the heat-affected zone (HAZ) of a repair weld at a nozzle. Two-thirds of the vessel blew away. The report noted that “Notwithstanding (sic) the general low fracture toughness of the vessel, it is doubtful that this failure would have occurred if the nozzle had a well radiused inside corner and if the flow tube had not been welded to this corner.”
2. Cartagena, Colombia, fertilizer plant, December 8, 1977 [ref. 19]. This lead-lined vessel was constructed by A. O. Smith and operated at 3,600 psi and 400°F. The failure occurred in the vicinity of the shell-to-shell weld. Indications show that the failure occurred first longitudinally, then circumferentially, resulting in separation of the vessel sections. The vent holes were plugged with carbamate (a compound derived from carbamic acid) and salt (from seawater), and inner shells were corroded where the failure is believed to have initiated.
3. Lake Charles, Louisiana, fertilizer plant, July 28, 1992 [ref. 20]. Reported by Occupational Safety and Health Review Commission Docket 93-0628. Technical details not included.

	NASA Engineering and Safety Center Technical Assessment Report	Document #: NESCP-RP- 13-00852	Version: 1.0
Title: Evaluation of Agency Non-code LPVs		Page #: 25 of 193	

4. Hebei Qianan, China, fertilizer plant, October 7, 1995 [ref. 21]. Layered vessel. Ten urea reactors scrapped in inspection and assessment after an explosion of one reactor. Li et al. report that 15 or more reactors were investigated due to cracking, some from the outside in, some from the inside out, and some from intermediate layers. Reason for cracking is given as stress corrosion cracking (SCC).
5. Pingyin, China, fertilizer plant, March 21, 2005 [ref. 22]. Reported failure due to SCC caused by forcing steam through vent holes as a leak detection mechanism.
6. Coffeyville Kansas, fertilizer plant, September 30, 2010 [ref. 23]. A 10-year-old ASME code-stamped vessel constructed by Hahn and Clay. Radial and transverse weld cracking in the head-to-shell weld, attributed to “environmental stress cracking” caused by the boiler feed water that was used inside the vessel jacket, resulting in complete failure of the circumferential weld at the head-to-shell junction. Similar cracking but no failure was reported in the weld to the bottom head. Both welds were replaced.
7. At least two additional known catastrophic failures, one in Johannesburg, South Africa, and one in Europe, but no further details were available.

There also have been much larger numbers of vessels that have developed cracks, requiring either repair or removal from service. A number of NASA vessels have developed cracks; some of these have been removed from service, and others have remained in service when it has been judged they can be adequately monitored for additional crack growth. Some examples of non-catastrophic vessel cracking are provided below. Where available, the published reports are referenced. However, in many cases, formal reports or documentation is not available, and reports of the damage observed were obtained from assessment team members who either observed the damage or were involved in responding to the cracks. In these cases, the team member who provided the information is identified. While the specific details of these events were not captured in formal reports, the available anecdotal information is still of interest in providing insight into the types of damage that can occur in these vessels.

1. Leakage: Kennedy Space Center (KSC), October 14, 1980, from a helium vessel constructed by A. O. Smith in March 1958 and procured by the Department of Defense (DOD) [refs. 10 and 11]. The crack was in the cylindrical shell along the longitudinal weld, variously reported as propagating from inclusions in the plate adjacent to the weld or from weld undercut on the inner diameter (ID). Overall condition of the vessel was reported as good.
2. Cracking: Ames Research Center (ARC), 1987: ARC salvaged 16 1,750-cubic-foot A. O. Smith pressure vessels from the DOD Jackass Flats nuclear test site. Pre-service NDE (visual testing (VT), MT, and RT) showed most vessels (i.e., 15) having BPVC rejectable indications, including six with cracks in the circumferential or longitudinal welds. Most rejectable indications, including all cracks, were repaired by CB&I in 1986, and the remainder were accepted as found. All vessels remain in service to the present. There have been no subsequent service-related defects discovered in their 26-year

	NASA Engineering and Safety Center Technical Assessment Report	Document #: NESCP-RP- 13-00852	Version: 1.0
Title: Evaluation of Agency Non-code LPVs		Page #: 26 of 193	

operational history at ARC. (Documented in pressure system certification reports at ARC.)

3. Cracking: Langley Research Center (LaRC), 1987(?): 12 vessels removed from service after extensive cracking in outer shell layer adjacent to the head-to-shell weld of one or more vessels, as well as internal cracking. Blowdown temperatures and shocking were believed to be involved in the internal cracking. (Witnessed by Greulich.)
4. Cracking: KSC, 2013: Two vessels removed from service with cracks in the center of the outer shell plate, not adjacent to any welds or other known stress concentrations. (Observed by Greulich. Date of removal from service is not known.)
5. Cracking: LaRC, 2014: Two vessels removed from methane service at B-1265 due to external cracking. One vessel had transverse weld cracking in the head-to-shell weld. One of the three transverse cracks was removed with light grinding, two were reported to extend 0.87 inches into the weld based on shear wave ultrasonic testing (UT). The other vessel had a longitudinal crack in the shell adjacent to the shell-to-shell weld. Photographic verification of magnetic particle inspection indications. (Reported by Christie Swarts of Jacobs Technology.)
6. Cracking: Marshall Space Flight Center (MSFC) (1990s): A vertical vessel was removed from service due to cracks suspected in layers based on AE. (Reported by Pulley; detailed records lacking.)
7. Cracking: MSFC (2011/2012): A large horizontal vessel (V0256) was removed from service due to a longitudinal crack approximately 2 ¼ inches long in the outer layer near the head-to-shell weld. (Viewed by Greulich and Prosser, August 2013.)
8. Cracking: Glenn Research Center (GRC): GRC reported in the NESC LPV team teleconference on February 27, 2014, that they have one or more vessels in service with one or more cracks in an intermediate layer that are being monitored using periodic RT. (Reported by Wnuk.)
9. Stennis Space Center (SSC) (out of a total of 22 vessels for which history was provided), reported cracking and other indications in both A. O. Smith and Struthers Wells vessels, including the following:
 - a. Four Struthers Wells vessels exhibited a number of cracks that were removed by grinding at various times. At least two of these vessels later showed additional cracking, even though one had been derated (it was later “downmoded,” i.e., removed from service, but not scrapped). In 1988, “Assessment concluded that previous history of cracking due to high residual stress from welding and not service related.”
 - b. One CB&I vessel exhibited cracking that was “removed by light grinding.”

	NASA Engineering and Safety Center Technical Assessment Report	Document #: NESCP-RP- 13-00852	Version: 1.0
Title: Evaluation of Agency Non-code LPVs		Page #: 27 of 193	

- c. Four Struthers Wells and one CB&I vessel were reported to have “leakage at vent holes,” though it is not clear whether action was taken based on these indications. In one case it was “determined leaks are from air trapped between vessel layers.”
 - d. In five cases, indications were not described as cracks were removed by grinding.
 - e. Numerous vessels showed indications under AE testing. Further inspection using UT or RT (through as much as 11 inches of material) was used to accept these vessels as having no rejectable indications.
10. All A. O. Smith LPVs at Eastman Chemical Company were repaired and finally removed from service due to cracking of outer layers, according to a verbal report to Greulich from a representative of Eastman Chemical.
11. Cracked LPVs are found in industry on a regular basis (numerous times per year) and removed from service; these are usually repaired and returned to service. (Reported by Jawad, who is often involved in these repairs due to his association with a company previously in the business of fabricating layered vessels and now performing repairs and process industry maintenance.)

Discussion of past failures

The typical degradation mechanism associated with the six confirmed catastrophic failures of LPVs in industry has been SCC, and the service typically involves elevated temperature operation. One case involved a weld repair. Two cases involved cracking reported to be caused by boiler feedwater or steam used external to the vessel and either injected through the vent holes for leak detection or through cooling jackets.

Some vessels at NASA and many in industry have been removed from service due to cracking, most often in the vicinity of circumferential welds, usually the head-to-shell welds. The crack in the shell-to-shell weld noted in item 5 above at LaRC is stated by Jawad to be highly unusual: it was the first longitudinal crack associated with a shell-to-shell weld that he had seen. Similarly, the cracks reported in item 4, located in the outer layer away from all welds, are reported to be unique.

Service at NASA is typically at ambient temperatures or below, often with cold service due either to ambient conditions in wintertime or blowdown service. A number of vessels have been removed from service due to cracking. The cracking in NASA vessels is generally assumed to be caused by pressure cycling. The cracks that occur in the shell adjacent to circumferential welds appear to be emanating from a region that is expected, based on the current weld residual stress study, to be in circumferential compression. While it is possible to repair these cracks, which is often done in industry, it is clear that a full understanding of their initiation and growth mechanism is lacking. This lack of understanding, combined with the crack in an intermediate layer in the GRC vessel reported in item 8 above, lead to the conclusion that until a reliable inspection method for intermediate layers is identified, intermediate shell layer cracks cannot be ruled out. This raises the possibility that multiple shell layers could be compromised without anyone being aware of it.

	NASA Engineering and Safety Center Technical Assessment Report	Document #: NESCP-RP- 13-00852	Version: 1.0
Title: Evaluation of Agency Non-code LPVs		Page #: 28 of 193	

Thus far, the authors of this report are not aware of any catastrophic failures outside the fertilizer industry. However, based on the number of cracks identified in shell sections and in the circumferential welds, the possibilities of either undetected cracks in multiple layers leading to a failure due to overstress or of a crack propagating through a circumferential weld in such a way as to result in failure appear to be real, with nontrivial likelihood.

6.1.5 LPV Reliability Evaluation

In general, quantitative reliability evaluation is accomplished through reliability prediction and reliability demonstration.

Reliability prediction is the process of quantitatively or qualitatively estimating system reliability using both objective and subjective data at the level for which data are available. Reliability prediction is performed either to integrate the reliability into the design up front so as to satisfy a certain design reliability requirement or to better understand the failure modes and causes associated with an existing system.

Reliability demonstration provides the basis for quantitatively estimating the reliability from objective data provided by the demonstration. It is generally performed after the system/component is qualified and ready for operation. Reliability demonstration is intended to supply additional information for reliability prediction.

Although no well-documented reliability evaluation exists for pressure vessels, according to NASA-STD-8719.17, “NASA Requirements for Ground-Based Pressure Vessels and Pressurized Systems (PVS)” [ref. 24], and based on literature, the failure rate per year for ASME code-stamped pressure vessels constructed after 1988 is expected to be 10^{-6} or less. Pressure vessels constructed before that time are expected to have a higher failure rate, which NASA assumes to be in the 10^{-3} to 10^{-6} per year range (i.e., one block more frequent in NASA’s risk assessment charts), though at the less-frequent end of that block, based on experience. The lower failure rate for vessels constructed after 1988 is expected because MDMT determination methods have improved since that time.

For LPVs, even though data exist regarding the numbers of vessels constructed and a number of known failures, it is not possible to perform a high-confidence reliability evaluation. Operational data for NASA or industry vessels is not well documented in terms of operation time, operation cycles, operating environment, current condition, etc. Without this information, any reliability evaluation performed would be speculative. This is further complicated by the significant age of NASA’s vessels, with unknown accumulated degradation and defects. If the vessels follow a notional bathtub curve, as shown Figure 6.1.5-1, which is not certain, then these old vessels may also be in the region of escalating failure rate. In this regime, reliability assessments would require the use of conditional failure probabilities to account for the LPV wear. To maintain the lower constant failure rate suggested by the bathtub curve, LPVs with significant aging would need to be replaced if their actual condition could not be adequately assessed for high-confidence life extension.

	NASA Engineering and Safety Center Technical Assessment Report	Document #:	Version:
		NESCP-RP-13-00852	1.0
Title:			Page #:
Evaluation of Agency Non-code LPVs			29 of 193

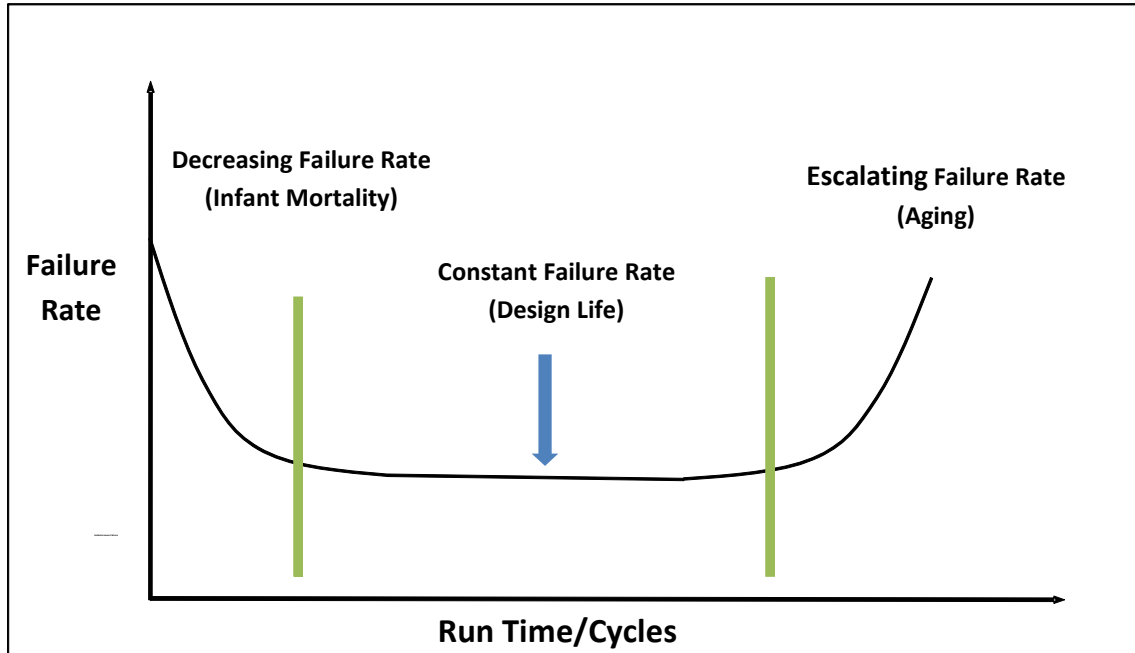


Figure 6.1.5-1. Notional Bathtub Curve Illustrating Changes in Failure Rate versus Time/Cycles

6.2 Problem Statement

Because of these identified risks and concerns, the NESC, in cooperation with the NASA Office of Safety and Mission Assurance (OSMA) and the respective Center PSMs, was requested to formulate a consensus draft proposal for the development of additional testing and analysis methods that would be required to establish the technical validity, and any limitation thereof, of these vessels for continued safe operation.

6.3 Planned Tasks

To accomplish the objective of developing a proposal for additional testing and analysis methods necessary for continued safe operation of LPVs, the assessment team was to evaluate failure risks associated with the inner shell, layers, heads, nozzles, and welds of these vessels. It is expected that the results of this assessment and the proposed follow-on testing and analysis subsequently can be used as a basis for the development of a future NASA standard that will be submitted to OSHA for use as an alternate and supplementary standard in accordance with 29 CFR 1960 [ref. 3]. This assessment was to leverage common skills, capabilities, and data from within and outside NASA and to consider inspection, analysis, and monitoring techniques that could be applicable to these vessels. The planned tasks for this assessment are listed in detail in Section 5.0 and included a review of how LPVs are maintained and operated both within and external to NASA as well as some limited scope testing and analysis.

	NASA Engineering and Safety Center Technical Assessment Report	Document #: NESCP-RP-13-00852	Version: 1.0
Title: Evaluation of Agency Non-code LPVs		Page #: 30 of 193	

7.0 Data Analysis

7.1 Task 1 Summary

7.1.1 Center Request for Information (RFI) Responses

To better understand the inventory, usage conditions, and ongoing and proposed risk mitigation methods for LPVs at all NASA Centers, the assessment team generated a request for information (RFI) that was sent to the PSMs at all Centers. A full copy of this RFI is included as Appendix B. The RFI requested information in eight general areas. These included detailed information about the inventory of LPVs, NDE used on the vessels, current additional risk mitigation approaches, previous risk mitigation approaches no longer used, risk mitigation approaches under development, recommendations for any additional risk mitigation methods that should be considered, special concerns about continued safe operation, and how the risks were being communicated to Center management. The detailed responses to the RFI and the accompanying spreadsheets with vessel information from each Center that has LPVs are also included in Appendix B.

From these responses, it was determined that non-code LPVs were in use at nine NASA Centers or facilities. These included ARC, GRC, Wallops Flight Facility (WFF), White Sands Test Facility, KSC, LaRC, Michoud Assembly Facility (MAF), MSFC, and SSC. A total of 376 vessels were reported, with 302 of these in active service and the remaining 74 inactive. There was a variety of reasons that vessels were not in active service, ranging from no identified current need to the existence of known defects within a given vessel. Depending on the owner of the vessel and the reason it was out of service, it was noted that some of these inactive vessels could be made available as specimens for future testing efforts. MSFC had the largest number of vessels of any Center with a total of 199, 173 of which were in current service. GRC had 86 with 57 in current service. ARC, KSC, and SSC all had on the order of 20 vessels, with the remaining Centers and facilities having smaller numbers. The vast majority of these vessels (i.e., 308) were manufactured by A. O. Smith; 40 were manufactured by CB&I; 23, by Struthers Wells; and the remaining few by other fabricators.

In reviewing and discussing the RFI responses from the Centers, two important points were identified. The first is that much of the important data that are needed to better characterize the risks associated with LPVs is in disparate formats, is difficult to access and retrieve, and in some cases, has been lost or was never tracked. This includes data such as design records and drawings, fabrication records, maintenance and inspection records and data, and operational usage data. Vessels not originally fabricated for NASA that were procured from other organizations may have minimal data regarding their use prior to acquisition from NASA. Even for vessels originally fabricated for NASA, the records may be more than 50 years old and have been subject to varying degrees of care and retention. The majority of these data exist only in paper format, with some documents scanned into local records. However, some design drawing documents have been scanned and made accessible Agency-wide.

	NASA Engineering and Safety Center Technical Assessment Report	Document #: NESCP-RP- 13-00852	Version: 1.0
Title: Evaluation of Agency Non-code LPVs		Page #: 31 of 193	

Another important point, not unexpected but readily apparent, was that there is not an Agency consensus on approaches to certification, recertification, inspection, maintenance, record keeping, or usage of these vessels. There is no consensus on what constitutes a certification or recertification of an LPV, or when it is required. Some Centers periodically “recertify” these vessels with their local procedures, while others do so only when a vessel is repurposed or not at all, although such an approach is not consistent with NASA’s PVS requirements documents. There is no consensus regarding intervals between required periodic maintenance and inspections, nor on which methods are required for those inspections. As will be discussed below, there is a variety of different inspection and analysis methods that are used across the Agency. Further, no consensus exists on the operating conditions under which these vessels are allowed to operate, such as the temperature at which they can be used or the safety factor that is required.

7.1.1.1 Summary of NDE or Other Inspections/Analyses Related to Continued Safe Usage

In discussions with the Centers, it was noted that NDE methods and detectability levels have changed over time and that the detection requirements for currently available NDE methods for LPVs are not well established. There are no formal defect size requirements established for the different regions of an LPV, due to the lack of validated analysis methods and limitations in available materials property data. Additionally, the capabilities of some of the methods that are used to inspect LPVs are not established or validated for these complex structures. Thus, the NDE data are used for “engineering evaluation,” and findings of flaw indications can lead to repair actions or removal of a vessel from service. However, the lack of findings of flaw indications does not necessarily ensure lack of defects or continued safe operation of LPVs. Further, as noted previously, the periodicity at which NDE is applied and which techniques are used vary from Center to Center.

Conventional surface inspection methods such as visual (VT) (including borescope), magnetic particle (MT), and dye penetrant (penetrant testing (PT)) methods are widely used at most Centers to inspect outer surfaces, exposed weld surfaces, and inner shells when access is available. The capabilities for these NDE methods are well established and documented, and there are no unique considerations for applying these methods to LPVs. However, their application is limited to exposed surfaces of these structures, and these methods are not completely effective unless surface coatings are removed.

UT methods are also utilized at some Centers to inspect the monolithic heads and the head-to-nozzle welds. UT is often used as a follow-up method to inspect regions of the outer and inner (when accessible) shell layers where surface techniques have indicated a flaw. UT in this case can provide information about the depth of the flaw in these layers, whereas the surface methods only indicate the presence of surface-breaking flaws. UT is also used to measure thickness and assess any loss of thickness due to corrosion. UT, however, cannot penetrate into the interior shell layers. It is not commonly used for complete scanning of the inner or outer shell layers. Conventional UT methods have not been successful for inspecting the full penetration

	NASA Engineering and Safety Center Technical Assessment Report	Document #: NESCP-RP-13-00852	Version: 1.0
Title: Evaluation of Agency Non-code LPVs		Page #: 32 of 193	

circumferential head-to-shell or shell-to-shell welds due to reflections from the layers boundaries.

RT has been used at some Centers to inspect the circumferential head-to-shell and shell-to-shell welds, as well as the longitudinal welds in shell layers. The presence of multiple shell layers adds irrelevant indications (i.e., layer wash) to radiographic images, which make detection of flaws more difficult. Although RT has been used to detect indications of cracks in layered sections and welds, some of which have been confirmed by destructive analysis and repair operations, the capabilities (i.e., flaw type and minimum detectable flaw size/probability of detection) of this method have not been established for application to these structures. Thus, the fact that flaw indications have not been found does not provide assurance that no flaws are present.

AE is one of the few methods that offers the potential for detecting crack growth within internal shell layers or longitudinal welds in these layers. A number of Centers have used AE to evaluate LPVs. Although AE methods have not been fully validated for application to LPVs, work in China [ref. 22] has shown at least one successful case of the detection of cracking in full penetration circumferential welds of an LPV. The crack was confirmed first with PAUT techniques and then by destructive material removal and visual examination.

Historically, there are two types of AE measurement systems. The first, known as parameter-based, or conventional, AE measurement does not actually record the full waveform for an AE signal. Instead, when a signal crosses a preset trigger threshold, analog circuits are used to rapidly measure certain parameters or features of the signals from each sensor, such as the peak amplitude, duration, arrival time, energy, etc. These parameters are then plotted for real-time visualization, as well as stored for later, more detailed analysis. Parameter-based AE systems were originally developed because high-speed digital waveform acquisition systems were not available at the time. The advantages of these systems include high data acquisition rates and the ability for near real-time data analysis and visualization. Resonant sensors are most often used with parameter-based AE systems as they provide the highest sensitivity response.

The second type of AE measurement system is known as waveform acquisition. As the name implies, this newer type of system digitally acquires from AE sensors each waveform whose signals cross the trigger threshold. The advantage of waveform systems is that the entire signal is acquired and available for more detailed analysis, which in turn can provide additional and more accurate information about the AE signal and its source. As an example, the signal arrival time, which is used to triangulate source location, can be more accurately determined. One limitation of these systems is that the larger amount of data acquired for each signal leads to a significant increase in data storage requirements. This increase in the amount of data for each signal can also lead to signals not being acquired at higher AE event rates due to dead time (i.e., time during which the system cannot accept new triggers) which occurs during data transfer/storage. Also, the capability of near real-time data processing and display during a test is more limited. Most often, broadband sensors, which have a lower sensitivity but a higher fidelity in reproducing the actual signal, are used with waveform acquisition systems. Some

	NASA Engineering and Safety Center Technical Assessment Report	Document #: NESCP-RP- 13-00852	Version: 1.0
Title: Evaluation of Agency Non-code LPVs		Page #: 33 of 193	

newer systems offer the ability to capture both parameter and waveform data in the same acquisition system.

There is also a variety of analysis methodologies for AE data from the two different types of AE systems. One particular methodology that has been developed for parameter-based AE data for metallic pressure vessels is known as MONPAC™ [ref. 25]. The MONPAC™ approach was developed from the analysis of parameter AE data from testing a large number of storage tanks and monolithic pressure vessels. Correlations with certain signal parameters and when they occurred in the vessel pressurization profile were developed to discriminate background extraneous noise and to identify signals of interest. Signals of interest are graded using intensity analysis to determine a course of action that ranges from no action, to performing additional NDE, to the immediate shutdown of the vessel with additional NDE. Since the proprietary database on which MONPAC™ is based is built on the testing of monolithic pressure vessels, its applicability to LPVs is not known.

Another approach to the analysis of waveform AE data is known as Modal AE (MAE). In MAE, the waveforms are analyzed based on knowledge of the specific wave modes that will propagate in the structure being tested. MAE has been demonstrated to be useful in discriminating extraneous noise and in identifying crack sources of interest based on the signal modal content.

Within NASA, both parameter and waveform AE data have been acquired during testing of LPVs. MONPAC™ and MAE analysis approaches have been employed, along with other analysis methods, such as location analysis. Efforts toward validation of the MAE method performed at NASA ARC in 2011 and 2012 [ref. 26] (funded by OSMA) are summarized later in this report. These efforts have included characterizing wave modes that propagate in these vessels, demonstrating signal transmission through the layered sections using simulated AE sources, and one test monitoring crack growth from a known crack in a full-scale vessel. While signals from the known crack were detected, they were of very small amplitude near the threshold for detection. Results from full-scale vessel testing with both the MONPAC™ and MAE methods have shown that substantial noise is detected in comparison with the testing of monolithic vessels, believed to be associated with the relative movement of the shell layers as the layers expand and rub against one another. This background noise makes detection of actual crack growth much more difficult than for monolithic vessels. Additional efforts are necessary to understand and validate the capabilities of AE techniques relative to the application to LPVs. In particular, the sensitivity of the AE technique to detect cracks of different sizes relative to critical crack sizes will need to be established.

Other testing or measurements reported by Centers included the use of hardness testing, as well as precision diameter tape (i.e., Pi Tape) measurements on LPVs for circumferential expansion as a function of pressure, consistent with current ASME BPVC Part-ULW requirements. A few Centers reported cleaning of vent holes and checking for leaks. However, it was not clear that all Centers cleaned or monitored vent holes or, for those Centers that did, how frequently this was done. Hydrostatic pressure testing to 1.42 times the MAWP was used by one Center as part of their initial certification of vessels. Other Centers have also applied the typical 1.5 times MAWP

	NASA Engineering and Safety Center Technical Assessment Report	Document #: NESCP-RP-13-00852	Version: 1.0
Title: Evaluation of Agency Non-code LPVs		Page #: 34 of 193	

hydrotest (required by the BPVC at the time of construction) when placing the vessels into service at NASA. AE testing has been performed during overpressure testing at a lower level, typically 1.10 times MAWP.

Some Centers reported the use of a number of different analysis approaches to estimate static strength (burst pressure) and fatigue life (pressurization cycles to failure), as well as additional permissible cycles following proof/overpressure testing of LPVs. In all cases, it was noted that many assumptions were necessary for these analyses, especially with regard to material properties, flaw size detection capabilities for NDE, and the structural response of the layered shells. Further, it was noted that none of the analysis methods have been validated on LPVs. Most Centers expressed significant doubt with regard to the validity of these assumptions and, thus, the results of the analyses. Nonetheless, overpressure testing may demonstrate that additional remaining cyclic life exists and, thus, increase confidence that a near-term failure will not occur during normal operations; however, as previously noted, this cannot currently be accurately quantified.

7.1.1.2 Summary of Additional Risk Mitigation Approaches Currently in Use

Other approaches to either mitigate the risk of, or consequence from, catastrophic LPV failures that were reported by the Centers included the use of berms or other physical barriers around some vessels, as shown in Figure 5.0-1. However, these approaches cannot practically be employed uniformly across the Agency. Also, the degree to which any such barriers truly mitigate consequences was not investigated in this assessment. Location of the vessels to remote sites and limiting personnel access was also reported. Multiple Centers have intentionally derated vessel MAWP to reduce risk and increase safety factor, while others are operating below nameplate MAWP due to reduced pressure needs of the facility being serviced. In some cases, operational pressure cycles are limited and closely tracked. An additional approach employed by a couple of Centers is to have more frequent recertification intervals for LPVs, although the effectiveness of recertification is an open issue at present.

7.1.1.3 Summary of Risk Mitigation Methods no Longer Used

The Centers were also asked to report on any risk mitigation methods that were used in the past but are no longer used. Most Centers reported none, although a couple of Centers reported that the MAWP had been reduced to mitigate risk but was later increased because of operational impacts caused by the reduced pressure. Two Centers also reported that the use of AE (both the MONPAC™ and MAE approaches) had either been eliminated or was under review because of questions that recent validation test results had raised with regard to the capability of this method.

7.1.1.4 Summary of Risk Mitigation Methods under Testing and Development

In response to inquiries regarding risk mitigation efforts under testing and development, a number of responses were provided by the Centers and are described in this and subsequent sections. Details of these activities, which prior to this assessment were sometimes only communicated locally within the Centers performing the work, were communicated across the

	NASA Engineering and Safety Center Technical Assessment Report	Document #: NESCP-RP- 13-00852	Version: 1.0
Title: Evaluation of Agency Non-code LPVs		Page #: 35 of 193	

Agency to all Centers. This communication afforded other Centers the opportunity to provide input and, in some cases, data or materials that enhanced these ongoing activities. Additionally, in some cases these efforts served as a basis for Task 2 activities that were funded within this assessment. Communication of these efforts across the Agency and the resulting follow-on improvements was perhaps one of the more significant accomplishments of this assessment.

NASA MSFC, operator of the largest number of these vessels across the Agency, initiated several activities to address risk associated with LPVs. Efforts were underway in characterization of materials properties from a sacrificed vessel, development of new analysis methodologies that would include some of the structural details of layered vessel construction, and, working with SSC, characterization of a new NDE method, PAUT, for inspection of the full penetration circumferential head-to-shell and shell-to-shell welds. Details of some of these efforts will be described in a following section. As a result of the communication fostered in this NESC assessment, additional materials from other sacrificed vessels at other Centers were provided to MSFC to expand the materials property database and evaluate vessel-to-vessel variability. Additional efforts in materials characterization, structural analysis, and NDE were identified and funded as part of Task 2 of this assessment to augment some of the efforts already underway at MSFC.

MSFC also continues to perform MONPAC™ AE testing on field LPV vessels to build a database. Primarily, tests to date have used the MONPAC™ AE approach, as there is limited MAE instrumentation available at MSFC. Plans include procurement of additional MAE instrumentation to allow future testing to apply both methodologies. As the AE method is still not validated for LPVs, the information acquired is for engineering evaluation only. However, it is providing useful information on issues related to applying AE in the field on these vessels and on the assessment of the background noise produced and how this noise varies across different vessels that have undergone different periods of inactivity. No AE indications of crack growth have been detected in the recent history of vessel testing, including a vessel with a known crack that was tested at GRC as part of the photogrammetry work that was supported by MSFC (see Section 7.2.4 of this report). However, a vessel with a known crack (V256) has been removed from service, and plans are under development to perform hydrostatic testing while monitoring with AE.

NASA ARC had significant efforts completed and underway to work toward validation of MAE methods for application to LPVs. ARC has used MAE since 2001 [ref. 27], when a concurrent test was performed with both MAE and parametric AE vendors on a single vessel. As a result of that work, ARC contracted for MAE testing of all 16 active A. O. Smith vessels in 2002 and 2008 [refs. 28 and 29]. No relevant crack indications were identified during this testing. During this work, ARC demonstrated the transmission of AE signals between layers and from the inner layer to the outer layers. For these tests, pencil-lead breaks were used to generate simulated AE signals (per ASTM E-1419) in a part-through hole drilled in one vessel and on the inner layer surface, which were detected with minimal attenuation by sensors on the outer layers. They also demonstrated the ability to detect and accurately locate such pencil-lead breaks over 20 feet from the nearest sensor on their large vessels at the specified ASTM threshold sensitivity. However,

	NASA Engineering and Safety Center Technical Assessment Report	Document #: NESCP-RP- 13-00852	Version: 1.0
Title: Evaluation of Agency Non-code LPVs		Page #: 36 of 193	

since no actual crack was ever found (and none are known to exist), the ARC PSM concluded that full-scale testing was required to fully validate the method on LPVs. In principle, this could be accomplished by MAE monitoring of an LPV under pressure cycling to force crack growth from a starter notch. This was proposed as a research project to OSMA in 2010 and accepted as 2011/2012 work. ARC managed the work through its site wind tunnel engineering and operations contractor and the selected MAE vendor. This particular crack growth turned out to be harder to detect than expected, and more testing is needed. Discussion of the cyclic test results and conclusions are contained in Section 7.1.2.2, Appendix G of this report, and reported in reference 26. As part of the cyclic test effort, when cycling was completed, the vessel was sent to an independent laboratory for materials property characterization to validate the ability to calculate crack growth using newly measured fracture properties and the NASGRO[®] fracture analysis program via comparison to the actual crack extension. This very limited material assessment in the vicinity of the crack was supplemented in 2012 with Phase 2 work by the same laboratory to more fully characterize shell, head, weld, and HAZ material, with some unexpected results but good correlation between the analysis and crack measurements. The materials characterization efforts are discussed in Section 7.1.2.2 and Appendix H of this report and reported in references 41 and 42.

Based on discussions with the same testing laboratory, ARC also identified PAUT as a potential method for inspecting circumferential welds in these vessels, and the laboratory developed a proposal for initial development of this method using a section of the sacrificed test vessel as a calibration block. This proposal was accepted and included as part of Task 2 of this assessment, with task management transferred to LaRC. Again, additional details on these efforts are provided in following sections and appendices.

Finally, the NASGRO[®] fracture analysis program (which was originally developed by NASA) has never been fully developed for application to ground-based vessels, and the above work required simplified geometry and nonstandard use of program features that limit its usefulness to the PSMs. Stress intensity factor modeling and failure assessment diagram application development are needed to make it fully and efficiently useful to the Centers. Since NASGRO[®] is free to all NASA users, the ARC PSM also requested a proposal for that software development work from the same independent laboratory mentioned above (which develops NASGRO[®] under a Space Act Agreement). This was provided to ARC, and the proposal was later passed on to OSMA and NESC for consideration in future tasks.

NASA GRC reported on efforts to continue refinement of their customized UT bore probes for nozzle and nozzle-to-head weld inspections. This capability was originally developed by GRC, and, while it had been discussed to a limited extent among the PSMs under their OSMA working group, it was not widely understood and had not been implemented at any other Centers. With further validation, it might be an approach that finds application across the Agency. NASA GRC also noted some preliminary efforts to apply full-field optical measurement approaches, such as photogrammetry, for measurement of LPV surface deformation as a result of pressurization. There are two potential applications for such a measurement tool. First, the measured deformations, if suitably accurate and sensitive, can in principal provide a basis for validating

	NASA Engineering and Safety Center Technical Assessment Report	Document #: NESCP-RP- 13-00852	Version: 1.0
Title: Evaluation of Agency Non-code LPVs		Page #: 37 of 193	

analysis methods under development. Additionally, if it can be shown that the presence of flaws, including manufacturing anomalies and in-service defects, results in significant changes to the surface deformation of LPVs under pressure that are greater than the threshold noise/sensitivity level of the method, then the technique could possibly be used as a flaw screening method. Additional testing with this method was performed again as part of Task 2 and is described in more detail in Section 7.2.3 of this report. The ability to measure general surface deformation was demonstrated (e.g., vessel elongation and bending due to internal pressure). Efforts in detecting deformation variations due to known flaws were not successful, and additional analysis tools are needed to understand whether this would be possible, and if so, what size flaws might be detectable. Analytical efforts are needed to determine expected surface deformations due to various defects, such as major layer weld cracks or layer gaps. Usefulness of the technology will depend on whether motion due to defects is sufficient enough to not be masked by other vessel physical characteristics.

MAF reported that the operating pressures for their vessels had been reduced unless otherwise specifically required for a short-duration test. In such cases, additional requirements for operation were introduced, including evacuation of personnel from potential blast zones and installation of temporary or permanent berms. It was noted that such higher pressure operations typically only occurred one to three times a year and lasted only 1 or 2 days at a time.

7.1.1.5 Summary of Proposed or Recommended Risk Mitigation Methods

The Centers were also asked for input on any proposed or recommended risk mitigation methods. A number of responses were received, many related to ongoing work previously discussed. One NDE method not previously noted was identified as having potential to inspect through layered shell sections. This is the Saturated Low Frequency Eddy Current (SLOFEC™) technique, an electromagnetic inspection technique that has been used in efforts to detect corrosion in thick-walled steel piping [refs. 30 and 31]. Given that no current methods exist for inspecting the shell sections, some initial efforts to evaluate its capabilities for LPVs, at least with modeling, and if warranted, laboratory testing, are recommended.

Multiple Centers recommended additional efforts to validate AE techniques, including full-scale vessel testing with known and independently verified measurements of crack growth. Likewise, multiple Centers recommended additional efforts to develop and validate the PAUT method for inspecting circumferential welds. One Center suggested further work on photogrammetric techniques.

In a different area, one Center recommended the installation of manways to allow internal inspections of LPV inner shells. Another Center suggested the redesign of systems to provide local storage of low-pressure/high-capacity gas capabilities to reduce the requirements for, and risk associated with, high-pressure LPVs and systems currently in use. However, physical modification and/or replacement of the vessels was outside the scope of the NESCS's charter, and these were not pursued further.

	NASA Engineering and Safety Center Technical Assessment Report	Document #: NESCP-RP- 13-00852	Version: 1.0
Title: Evaluation of Agency Non-code LPVs		Page #: 38 of 193	

7.1.1.6 Summary of Special Concerns Noted

The Centers were asked to identify any special concerns they had with respect to LPVs. One response highlighted the variability that has been observed in previous testing to characterize the material properties of the A225 material used in LPV heads. The variability makes it difficult to use generic materials properties for this material in analyses and may lead to requirements to use either very low bounding properties or to the development of some methods to assess properties specific to individual vessels. The problems associated with the unknown relevance of past Charpy U-notch or keyhole data to current fracture toughness methodologies were also highlighted.

Several Centers highlighted concerns over the application of ASME Division 1 versus Division 2 methods to rate pressures for these vessels. Some noted that Division 2 was not appropriate because these vessels were not fabricated to all Division 2 requirements, while others suggested that Division 2 could be used safely. This was identified as an area that needs resolution, and it is noted that the OSMA PVS lead and at least one PSM strongly disagrees with the appropriateness of applying Division 2, as is discussed elsewhere in this report. Also, it was questioned as to when updated MAWP calculations should be required.

Another concern highlighted by multiple Centers was the need to understand the overall safety record for these vessels in industry, as well as to better understand the catastrophic failures that have occurred. In particular, the importance of understanding how the LPVs that failed were used was identified, as well as identifying the similarities and differences as to how NASA uses these vessels.

One Center highlighted the lack of internal access for inspection of vessel inner shells as a particular concern.

Another concern identified by multiple Centers was the difficulty that might result from attempts at implementing uniform processes across the Agency because of the variety of vessel designs and applications. It was noted that as an example, invasive inspection approaches might be acceptable for one Center and application but could create excessive problems and possible damage from contamination in other Centers and applications. The need for having tailored approaches for inspection and hazard mitigations was highlighted.

7.1.1.7 Summary of Processes/Time Periods for Communicating Risk to Center Management

The Centers were asked to provide insight as to the processes, time periods for reporting risk associated with these vessels to Center Management, and, in general, perceptions as to the awareness of Center management of the risks. The responses clearly indicated that the frequency and methods of reporting LPV risks to Center management and their awareness of the risks presented by continued use of these vessels varies significantly from Center to Center. The types of reporting and frequency of reporting ranged from quarterly reports to Center management with specific inclusion of risks and efforts to reduce risk for LPVs, to no reporting at all. Some Centers cited waivers for their operation that were approved at various times in the past, ranging

	NASA Engineering and Safety Center Technical Assessment Report	Document #: NESCP-RP- 13-00852	Version: 1.0
Title: Evaluation of Agency Non-code LPVs		Page #: 39 of 193	

from within the last couple of years to more than a decade ago. Further, it was noted that these waivers were not periodically reviewed, updated, or required to be reapproved. Most Centers generally reported that there was not a high degree of awareness of potential, albeit undefined, risks associated with LPVs at Center management levels, but that the potential risk was better known to personnel within the facilities or operations organizations, as well as the safety organizations.

7.1.2 Summary of Previous or Ongoing LPV Related Work Identified at NASA Centers

During the internal review as part of Task 1, it was determined that several Centers had previous and ongoing activities to help mitigate risks associated with these vessels. Several examples of these efforts are summarized in the following. Although some of these efforts were collaborative involving multiple Centers, it was important to note that information about much of the work and associated results were not being effectively communicated across the Agency. The lack of an Agency team or forum to address this problem sometimes resulted in information about the individual efforts being kept local to the Center or Centers performing the work. One significant accomplishment of this assessment was that information about these efforts has been communicated across the Agency and further collaboration on these efforts has been established.

7.1.2.1 MSFC Materials and Processes Laboratory LPV Activities

The MSFC Materials and Processing Laboratory conducted several preliminary activities to gain an understanding of the materials used in the non-code LPVs. These activities were in the area of material properties, NDE, and analysis. Available material properties were reviewed, and preliminary mechanical tests and metallurgical evaluations were performed. Several NDE inspection methods were investigated to provide a sufficient understanding of their relative screening efficacies in order to down-select appropriate NDE methods for future evaluations. Stress levels and corresponding limiting flaw sizes for vessels of concern were investigated using the ASME FFS [ref. 32] methods. In order to gain a better understanding of the structural loading inherent to LPVs, with specific interest in determining the location and sizes of flaws for a damage-tolerance-based FFS analysis, an analytical tool was developed to parametrically model the weld regions in LPVs. The results from this preliminary effort were used to request funding to proceed with an ongoing LPV effort, which was ultimately funded and is described in detail in Section 7.2.

7.1.2.1.1 Materials

Material testing objectives were to develop an initial understanding of material performance of LPVs, more specifically, the structurally significant material properties, including tensile and fracture mechanics behavior. Representative surplus vessels were identified to collect data to develop a materials database. Material sources available at MSFC included a CB&I vessel (V0125) and an A. O. Smith vessel (V0032) (see Appendix C). This included 1146a shell and A225 head material from V0032, and 1146 and 1143 shell and A225 head material from V0125, where the materials were identified from the original manufacturer's data reports. Both 1143 and 1146 were A. O. Smith designations, while A225 is an ASTM designation. Based on later

	NASA Engineering and Safety Center Technical Assessment Report	Document #: NESCP-RP- 13-00852	Version: 1.0
Title: Evaluation of Agency Non-code LPVs		Page #: 40 of 193	

testing, which is described in Section 7.2.1, the pedigree of the 1146a inner shell material from V0032 was shown not to be in question, but this was unknown at the time of the preliminary effort. Both vessels were slated for mechanical testing and NDE to determine if there were any meaningful differences between materials based on the vendor or material lot. Existing material property data were surveyed and compared with preliminary materials tests. Limited tensile properties collected at MSFC for the CB&I vessel did not show the expected margin over reported design strengths (see Appendix D), and microstructural tests showed unexpected possible material anisotropy.

Fracture toughness as a function of temperature was identified as the most influential material property for vessel assessment. The fully ductile fracture toughness (upper shelf) and the temperature at which the steel transitions to cleavage fracture (lower shelf) were determined to be of critical interest in the assessment of LPVs. The use of the T_0 reference temperature methodology from ASTM E1921-13, “Standard Test Method for Determination of Reference Temperature, T_0 , for Ferritic Steels in the Transition Range” [ref. 33], was chosen as a method to evaluate fracture mechanics toughness data as a function of temperature due to brittle transition effects. Cleavage versus ductile in terms of ASTM E1921-13 refers to the fracture mechanism, (i.e., cleavage of crystal planes versus ductile crack-growth crack mechanism). A brittle structural failure can mean either cleavage or ductile but implies a low toughness controlled failure relative to failure due to net-section yielding behavior. The E1921-13 approach was expected to minimize the number of test samples required to define the ductile-to-brittle transition curve. The E1921-13 method was considered especially advantageous because it uses a fracture-mechanics-based weakest link theory in the evaluation to maximize the information gained from testing from a limited number of tests and because E1921-13, as a statistical method, allows failure probability levels (confidence levels) to be statistically determined. The fact that it is a fracture-mechanics-based method rather than a correlation means that it gives accurate rather than conservative measurement of the temperature above which cleavage fracture is not to be expected, compared with nil-ductility-temperature (NDT) based approaches. This method was applied to generate confidence curves for several LPV materials (see Appendix E).

A consultancy between MSFC and a cleavage fracture specialist was researched and proposed to assist in planning the scope and performing the analysis for E1921-13 testing. To date, the Master Curve method has predominantly been used to evaluate steels in the nuclear industry, and it was expected that an expert consultant could help address some of the unique challenges that were anticipated.

Preliminary examination of several welds was also conducted to identify potential fracture planes to investigate. These locations included head-to-shell and shell-to-shell welds. The scope of this evaluation was to investigate the varied microstructure around the various welds (see Appendix D).

This initial effort led to the recommendation to procure funding to pursue:

1. Mechanical testing on LPV A225 base head material, to characterize the ductile-to-brittle fracture toughness versus temperature response. The initial literature research showed

	NASA Engineering and Safety Center Technical Assessment Report	Document #:	Version:
		NESCP-RP- 13-00852	1.0
Title:		Page #:	
Evaluation of Agency Non-code LPVs		41 of 193	

that the A225 material would likely have the most elevated transition temperature and may cleave at operating temperatures.

2. Mechanical testing on LPV shell materials including 1143 and 1146, to characterize the ductile-to-brittle fracture toughness versus temperature response.
3. Preliminary mechanical and microstructural testing in LPV weld materials, including:
 - a. A225 head-to-shell
 - b. shell-to-shell
 - c. longitudinal welds (inner shell and wraps)
 - d. A225 to 5002 nozzle (circumferential weld at base of nozzle), where 5002 is a common nozzle steel used in the majority of vessels

These activities are discussed in Sections 7.2.1.

7.1.2.1.2 AE testing of LPVs

AE testing at MSFC is used as a method of screening LPVs, with the goal of identifying active crack growth. The original plan at MSFC was to use the MONPAC™ testing procedure to screen for crack growth. However, because MONPAC™ is primarily intended for structurally significant defects (those close to failure), an additional analysis method was added to the MONPAC™ intensity analysis to allow screening for potentially catastrophic crack growth and smaller crack extensions. This approach does not require a MONPAC™ procedure change and uses three-dimensional and two-dimensional algorithm-based source location software that can locate smaller sources. The software accuracy is verified using a pretest calibration consisting of lead breaks and/or center punch strikes in known locations. The AE software sound velocity setting is then adjusted until the software accurately locates the breaks/strikes.

MSFC uses a Physical Acoustics Corporation 56 Channel DiSP™ Workstation (with 40 channels installed) with the following parameters and capabilities:

- Test parameters currently in use: threshold, 42 dB (decibels), 100–400 kHz frequency filter
- R15I-AST sensors: mid-range sensors, operating range 80–200 kHz
- WDI-AST sensors: wideband sensors, operating range 200–900 kHz
- Waveform option module: processor, buffer, memory, adjustable sample length and rate

Plans are for procurement of additional MAE instrumentation to allow future testing to apply both methodologies.

The current AE test plan at MSFC is to gather data from approximately 10% of the layered vessels in the MSFC active inventory to establish an initial data set for evaluation (17 to 20 vessels total). Ten layered vessels have been AE tested at MSFC to date. No AE signals that had characteristics associated with the propagation of structurally significant defects have been

	NASA Engineering and Safety Center Technical Assessment Report	Document #: NESCP-RP-13-00852	Version: 1.0
Title: Evaluation of Agency Non-code LPVs		Page #: 42 of 193	

detected. MSFC is also planning to conduct lab-scale AE testing later in fiscal year (FY) 2014, as funding allows, using layered vessel coupons to investigate crack extension and overall AE test effectiveness and sensitivity. The goal of this testing is to understand the amplitude of AE signals that might be produced in a typical AE test on an LPV, which is usually accomplished by a 10% overpressure at nominal operating ambient temperature conditions, and to evaluate the apparent feasibility of using AE to detect growing cracks in the LPVs during proof testing. Accordingly, the data of most interest will be crack growth at room temperature. The samples will be as large as can be machined and tested due to the constraints of the thin, curved pressure vessel materials. With regard to specimen dimensions, the thickness of the samples is one limitation that will affect the signal characteristics significantly; it will change the signal mode of propagation from bulk modes to plate modes. However, with the layers present in the tank this may occur naturally to some extent for the real signals that occur in the tank. Test specimens will be used that maximize the lateral extent since the effect of reflections from these lateral boundaries will impede observation of the original arriving mode and make it difficult to assess the direct arriving signal amplitude of interest. For these tests, the focus is only whether the crack grew and by how much, not necessarily on calculating the fracture toughness, which is to be accomplished separately. Detecting cleavage fracture at low temperatures, which would likely produce the largest amplitude and most easily detectable AE signals, will not be pursued.

Since the AE method is still not validated, the information acquired is for engineering evaluation only. However, the method is providing useful information on issues related to applying AE in the field on these vessels and on the assessment of the background noise produced and how it varies between different vessels that have undergone different periods of inactivity. A vessel with a known crack (V0256) has been removed from service, and plans are under development to perform hydrostatic testing while monitoring with AE.

7.1.2.1.3 Analysis

The infrastructure LPVs are considered industrial ground support equipment (GSE) for which safety rationale based on FFS is being developed. National consensus code approaches are customarily used on GSE because these approaches maintain proper conservatism and consistency in the FFS assessment. The current ASME BPVC [ref. 1] and ASME-FFS-1 (API-579) [ref. 32] and related document are being considered as the FFS anchor for the LPV assessments. Even though ASME FFS-1 (API 579) does not specifically address assessment methods for layered vessels, Part 9 of this Standard allows flexibility for tailoring and establishing an approach for assessing LPVs.

To establish a viable FFS approach for the LPV fleet requires not only a clear understanding of the material behavior fundamentals being investigated concurrently (as discussed in Sections 7.1.2.1.1 and 7.2.3) but also an understanding of the physical behavior resulting from the layered construction. These include the effects of unintended layer gaps, flaws in intermediate layers or layer welds, residual stress effects, and the effects of proof tests on the overall state of stress, for example. Since a real-time snapshot of the interior or in-between layers of LPVs is not always

	NASA Engineering and Safety Center Technical Assessment Report	Document #: NESCP-RP- 13-00852	Version: 1.0
Title: Evaluation of Agency Non-code LPVs		Page #: 43 of 193	

practical, analytical tools, such as finite element analyses, are being employed to gain an understanding of these physical fundamentals.

As part of this assessment, finite element analyses were conducted to investigate various parameters that affect the state of stress of an LPV as compared with the classical thick-walled pressure vessel solution. A modeling tool, LPV Analysis Tool (LAPVAT), was developed to automatically generate and post-process LPV finite element models using the Abaqus® Python™ interface. LAPVAT enables efficient parametric studies by allowing the user to input the dimensions of the vessel, the number of layers, the layer gaps, the material properties, meshing parameters, internal pressures, temperatures, angular section size, and other parameters. These inputs are used to automatically generate a three-dimensional model of a sector of an LPV including a head, the specified number of shell layers, and the head-to-shell weld region with contacts between layers. Details of the development of this tool and results may be found in Appendix G.

7.1.2.2 NASA ARC – MAE Validation and Materials Testing Efforts

AE testing is a method used to detect cracks or other damage sources in structures by detecting and analyzing acoustic waves that are produced by growth of the damage or the contact and rubbing of crack surfaces as a result of load or pressure being applied to the structure. An array of acoustic sensors is placed on the structure to detect AE signals. The detected AE signals are analyzed to locate the damage site by triangulation and to assess the damage and discriminate extraneous noise by analysis of the signals or features of the signals. A simple analogy of the AE technique is that of structural seismology, where the growing damage sources are the equivalent of earthquake sources within the structure.

MAE is an AE approach based on the capture and analysis of complete AE waveforms acquired with high-fidelity, broadband acoustic sensors. MAE analysis incorporates a physics-based understanding of the modes of acoustic propagation for the structure being tested and the relationship between the crack sources of interest and the resulting acoustic modes that are generated and propagated [refs. 34–36]. This is in contrast to the resonant sensors and analysis of signal features or parameters based on a preexisting database for similar structures, which are employed in a competing approach that has also been applied to LPVs, known as MONPAC™ AE [ref. 25]. MAE has the potential for providing more accurate location of AE sources and for improved characterization of AE sources and discrimination of extraneous noise as compared with conventional AE parameter analysis approaches.

Although MAE has not been previously fully validated for application to LPVs, it has been validated for a number of other related applications. One example is the application of MAE to retest DOT cylinders and submarine flasks that resulted in the award of a DOT Special Permit [ref. 37] and the Navy’s ongoing use of MAE for flask requalification. Previous conventional parameter-based AE approaches were demonstrated for detection and location of subcritical and critical size cracks in these solid-wall high-strength steel vessels [refs. 38 and 39]. MAE improved on these approaches by providing improved source location accuracy and the ability to discriminate noise. In these and other applications of MAE, Digital Wave Corporation (DWC)

	NASA Engineering and Safety Center Technical Assessment Report	Document #: NESCP-RP- 13-00852	Version: 1.0
Title: Evaluation of Agency Non-code LPVs		Page #: 44 of 193	

utilizes published ASTM standards [refs. 40–43] as they apply to MAE with respect to instrument calibration and system performance testing.

Because of its demonstrated success in detecting crack growth in other related applications involving steel pressure vessels, MAE was evaluated for and eventually applied to full-scale testing of LPVs at NASA ARC as well as at other NASA Centers. As part of this effort, NASA ARC has worked with DWC since 2001 to fully validate MAE for LPVs [refs. 26–29] with cyclic testing in 2011 and 2012 funded by the NASA OSMA. These efforts, which are described in more detail in Appendix G, have successfully demonstrated many aspects of MAE for LPVs including evaluation of modal wave propagation characteristics (i.e., modal content, velocity, and attenuation) of signals generated by simulated AE sources (i.e., pencil-lead breaks) in LPVs, demonstration of AE signal propagation through the layered shell thickness, and evaluation of LPV background extraneous noise. The only aspect of MAE that was not demonstrated in initial testing on the large vessels at ARC was detection of actual crack growth in an LPV because it was not feasible to achieve verifiable growth of an induced crack on these large vessels.

Even without the full validation of the MAE technique to detect growing known cracks in an LPV, it was the engineering judgment of both DWC and NASA PSMs at several Centers that the method could be used as a periodic inspection tool to determine whether any relevant, growing cracks existed in the vessels (i.e., large cracks growing with each pressure cycle, probably close to critical size). This was based on the known success of MAE for monitoring other steel pressure vessels and the success in demonstrating MAE propagation in LPVs. Thus, MAE was applied for full-scale testing on the ARC vessels with the intent that if MAE indicated the presence of any growing cracks, the vessels would be removed from service and efforts made to verify the presence of cracks through other forms of NDE. The vessels would then, if possible, be repaired. If any indicated cracks were confirmed, this would provide additional validation data for the method. However, none of the vessels at ARC exhibited MAE indications of crack growth. Thus, ARC concluded that an additional validation test was required in which MAE would be applied to monitor an LPV with a known, fully characterized growing crack.

Attempts at demonstrating MAE detection of crack growth in a LPV were performed using cyclic crack-growth tests on a much smaller LPV (44 cubic feet) that was obtained from KSC. This work was managed by ARC and their prime contractor, Jacobs Technology, under OSMA research funding, and carried out by DWC. The test vessel was pressure cycled 4,688 times, about half of which were between its nameplate rating of 6,600 psi and 1,000 psi, and the remainder at progressively higher pressures up to yield strength of the outer layer. MAE was recorded throughout. This effort was, however, only partly successful in that, while MAE was shown to be able to detect the actual growing crack under field test conditions, the crack exhibited low acoustic energy release and was essentially at the threshold of detectability for the AE system being used. As such, it would likely have been missed in a standard production field test. It was later determined that the crack was much smaller than the expected critical size (approximately 25%) [refs. 26 and 44], which results in lower AE signal amplitude. Incomplete knowledge (at the time of the test) of the higher toughness of the material in the vessels contributed to using too small an initial crack size in the previous demonstration test. Further,

	NASA Engineering and Safety Center Technical Assessment Report	Document #: NESCP-RP-13-00852	Version: 1.0
Title: Evaluation of Agency Non-code LPVs		Page #: 45 of 193	

limited funding precluded continuation of the vessel cycling to grow a larger crack closer to critical size with (presumed) greater intensity AEs. Tests on vessels with larger cracks (closer to the critical crack size) will be necessary to better demonstrate and fully validate the capability of MAE for detecting crack growth and to document the relationship between signal amplitude and detectable crack size. Details on both the cyclic pressure testing and MAE assessment work performed by DWC are contained in reference 26.

While additional full-scale cyclic testing is required to validate either modal or parametric AE, this cyclic test work suggested that research on AE monitoring of laboratory scale specimens under cyclic loading could provide important information regarding the absolute intensity of AEs from growing cracks as detected by the various approaches to AE. Although this is discussed in the literature with mixed results, current techniques could improve upon issues encountered in the past. This recommendation was accepted by the NESC and ongoing work at MSFC and LaRC in that regard is described in Section 7.2.6 of this report.

Upon completion of the MAE tests of crack growth on the smaller LPV, the vessel was sent to Southwest Research Institute[®] (SwRI)[®] for fractographic analysis of the crack growth and materials characterization efforts to assess some of the relevant properties for the vessel materials [refs. 44 and 45]. In particular, measurements of fracture toughness and fatigue crack-growth properties of the principal material components for this vessel were performed. This work focused on the inner and outer shell layers, material from one of the heads, and weld and HAZ material from one head-to-shell weld. For this limited sampling from this one vessel, tensile properties, impact energy, fracture toughness, and fatigue crack-growth properties were documented. When SwRI[®] incorporated these properties into a fracture crack-growth analysis (using NASA's NASGRO[®] software, for which they are a Space Act Agreement developer) of the starter notch that was machined into the outer shell, the calculated crack growth closely matched the actual growth experienced in the cyclic field test. Of note, critical fracture toughness for both shell and head material was shown to be greater than indicated by prior work done at LaRC in the 1970s [ref. 46], although impact energy absorption using the Charpy V-notch test (which is required by ASME) was measured to be much less at low ambient temperatures. In fact, both head and shell material exhibited brittle fracture characteristics at 0°F, which can be a significant problem at several Centers. While there are known issues with utilizing Charpy impact energy results to statistically predict brittle fracture behavior, further work is required to determine the NDT and safe operating temperatures for all of the material that comprises these vessels. This effort has begun at MSFC with a program to determine transition reference temperature in accordance with ASTM E 1921-13 [ref. 33] and ASME FFS-1/API-579 standards [ref. 32]. In addition, since destructive material testing cannot practically be performed on NASA's fleet of in-service vessels, a much wider sampling of materials from other similar vessels is needed to develop an adequate confidence level in applying the SwRI[®], MSFC, or any other test data obtained from specific surplus vessels to the in-service fleet. Details on both the phase 1 and phase 2 work performed by SwRI[®] are contained in a detailed summary in Appendix H, and the SwRI[®] reports are available in total as NASA Contractor Report documents [refs. 44 and 45].

	NASA Engineering and Safety Center Technical Assessment Report	Document #: NESCP-RP-13-00852	Version: 1.0
Title: Evaluation of Agency Non-code LPVs		Page #: 46 of 193	

7.1.2.3 SSC/MSFC Evaluation of PAUT Methods for Inspection of Full Penetration Circumferential Welds on LPVs

There are currently no NDE techniques available that are validated for volumetric inspection of cracks in the full penetration circumferential welds of LPVs (RT limitations were discussed previously). PAUT techniques have been identified as a potential method for inspection of these welds, and at least one report in the literature [ref. 22] has shown promising results. Preliminary evaluation performed for MSFC and SSC also demonstrated the potential of this method.

Background

In April 2013, personnel from Davis NDE, located in Hoover, AL, were invited to visit MSFC to provide a demonstration of PAUT equipment for potential use as a weld inspection tool for LPVs. Davis NDE had previously reported to the SSC PSM some success in detecting flaws in layered vessels located overseas using PAUT techniques. In a collaborative effort between SSC, MSFC, and GRC, a plan was made to have Davis NDE provide an overview of the PAUT technique and operating principles, along with a hands-on demonstration of the PAUT equipment. MSFC was chosen as the site for the equipment demonstration due to the close proximity of MSFC to the Davis NDE office and the fact that MSFC had an out-of-service vessel readily available for the weld scanning demonstration.

Davis NDE was not under contract with MSFC for any services and the initial visit was intended to be an equipment demonstration only, at no cost to the government. However, subsequent to the visit, Davis NDE was asked to perform a review and interpretation of the PAUT data and provide informal (courtesy) reports to MSFC. It was understood that the PAUT weld scans performed were not code-quality scans since there was no calibration standard available for PAUT equipment calibration or for code-required weld scan plan development. Therefore, the PAUT weld scan data provided in this report are for reference purposes only and may not be used to assess vessel V0256 FFS.

Initial Demonstration of PAUT Equipment

The initial proof-of-concept demonstration by Davis NDE included general setup and operation of Olympus Omniscan phased array equipment. MSFC provided a vessel head-to-shell weld coupon obtained from layered Vessel V0125. Davis NDE personnel discussed general PAUT equipment setup and operation, performed a weld scan of the vessel coupon to demonstrate the scanning technique and on-screen data presentation options, and provided a real-time interpretation and discussion of the screen data. This first demonstration was focused primarily on equipment setup and adjustment, various scanning techniques, transducer options, data presentation formats, calibration requirements, and critical variables associated with development of weld scan plans.

PAUT Demonstration on Vessel V0256

Davis NDE personnel were asked to perform an *in situ* scan of weld areas on MSFC vessel V0256, shown in Figure 7.1.2.3-1, which was previously depressurized and taken out of service. V0256 is a 1,250-cubic-foot, 5,000-psig layered vessel built by CB&I in 1963. The vessel was

	NASA Engineering and Safety Center Technical Assessment Report	Document #: NESCP-RP-13-00852	Version: 1.0
Title: Evaluation of Agency Non-code LPVs			Page #: 47 of 193

constructed with a monolithic head and a layered shell section consisting of 14 total layers (15/32-inch inner layer and 13 overwraps of 9/32 inches each) for a total shell thickness of 4 1/8 inches. Vessel V0256 also has a readily visible defect in the outer layer base metal, a longitudinal crack running perpendicular to the head-to-shell weld, which was originally detected during an MT inspection (see Figure 7.1.2.3-2).



Figure 7.1.2.3-1. MSFC Vessel V0256 with Welds Stripped for Inspection (A225 head material; MLP 1143 shell material)

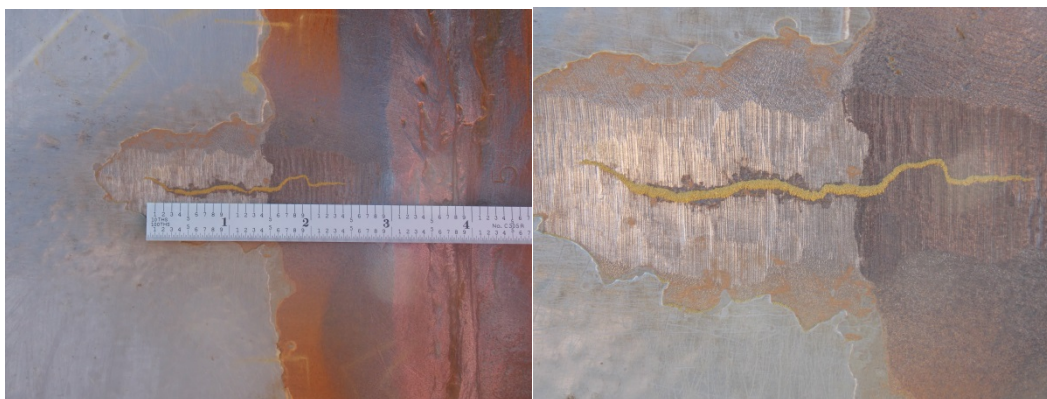


Figure 7.1.2.3-2. Longitudinal Crack in Outer Layer of V0256

Aside: Radiography had recently been performed on the full penetration welds of vessel V0256, not only to assess the quality of the vessel welds, but to gain more insight into the challenges of performing radiography on large, thick-wall layered vessels and to understand the extent and quality of volumetric weld data available from the radiography. Because MSFC has limited experience with performing radiography on large, thick-walled vessels, personnel from GRC traveled to MSFC to assist with the setup and provided setup tools commonly used at GRC. In

	NASA Engineering and Safety Center Technical Assessment Report	Document #: NESCP-RP- 13-00852	Version: 1.0
Title: Evaluation of Agency Non-code LPVs		Page #: 48 of 193	

short, radiography was being considered as another inspection tool for use by MSFC in evaluating the integrity of LPVs.

Vessel V0256 provided an opportunity for demonstration of the PAUT technique and equipment under field conditions and on a shell-to-shell weld, which was not available with the vessel V0125 coupons. Weld segments on V0256, including both head-to-shell and shell-to-shell weld regions, were prepared in advance of the PAUT demonstration by grinding the weld crowns flat to allow better coupling of the ultrasonic transducer with the vessel weld surface. Radiography was performed on V0256 prior to arrival of Davis NDE but resulted in only one positive indication, which could be used for comparison with the PAUT results.

Davis NDE personnel scanned the areas identified by MSFC, demonstrated various scan techniques, provided real-time data interpretation, and conducted hands-on training for the MSFC NDT technicians present. The line scan inspections on vessel V0256 were performed by setting the PAUT equipment gain to define both the weld root area and the shell section layers. Davis NDE indicated that this approach was used because no qualified procedure or calibration block was immediately available for this vessel inspection. Davis NDE personnel also scanned the longitudinal crack in the outer layer base metal and the adjacent head-to-shell weld in an attempt to better characterize the flaw.

Results

Figures 7.1.2.3-3 through 7.1.2.3-6 show PAUT scans of various indications observed in the vessel V0256 head-to-shell and shell-to-shell weld volumes. These figures demonstrate the PAUT capability to distinguish, to some extent, the shell layer edges from indications within the weld volume. In particular, Figure 7.1.2.3-5, which is a shell-to-shell weld scan, shows the symmetry of the individual layer tip reflections (indications) on both sides of the weld volume. In Figure 7.1.2.3-6, Davis NDE reports a discontinuity extending from the end of a layer into the weld volume.



NASA Engineering and Safety Center Technical Assessment Report

Document #:
**NESCP-RP-
13-00852**

Version:
1.0

Title:

Evaluation of Agency Non-code LPVs

Page #:
49 of 193

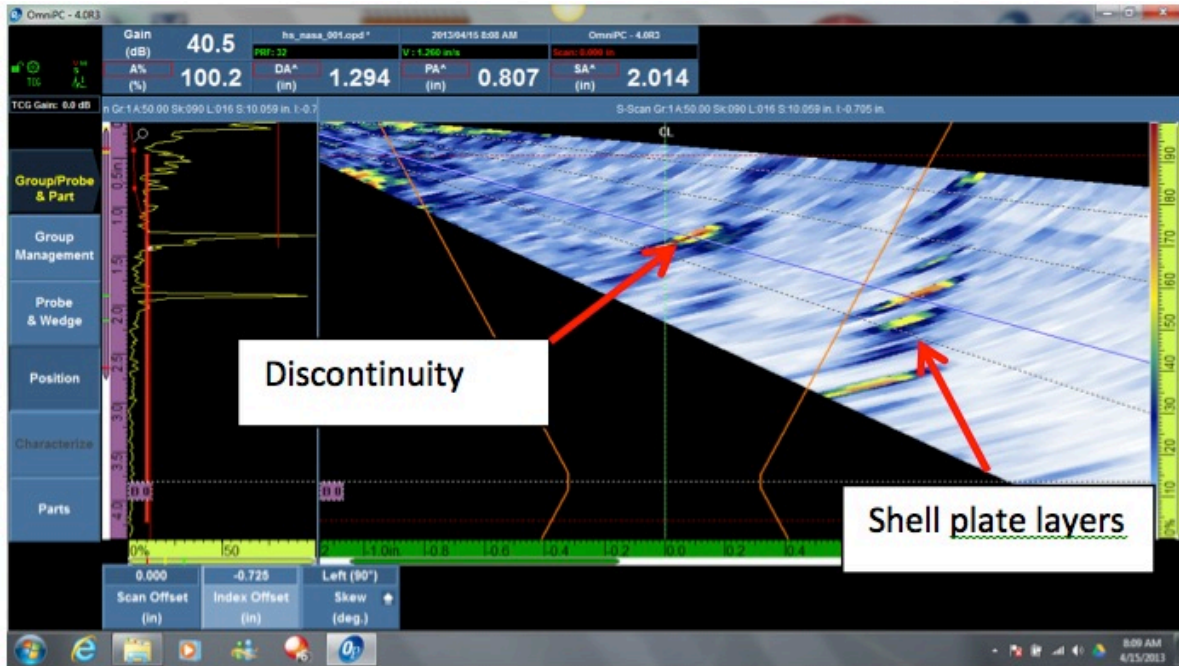


Figure 7.1.2.3-3. PAUT Scan of Head-to-Shell Weld Region (top portion)

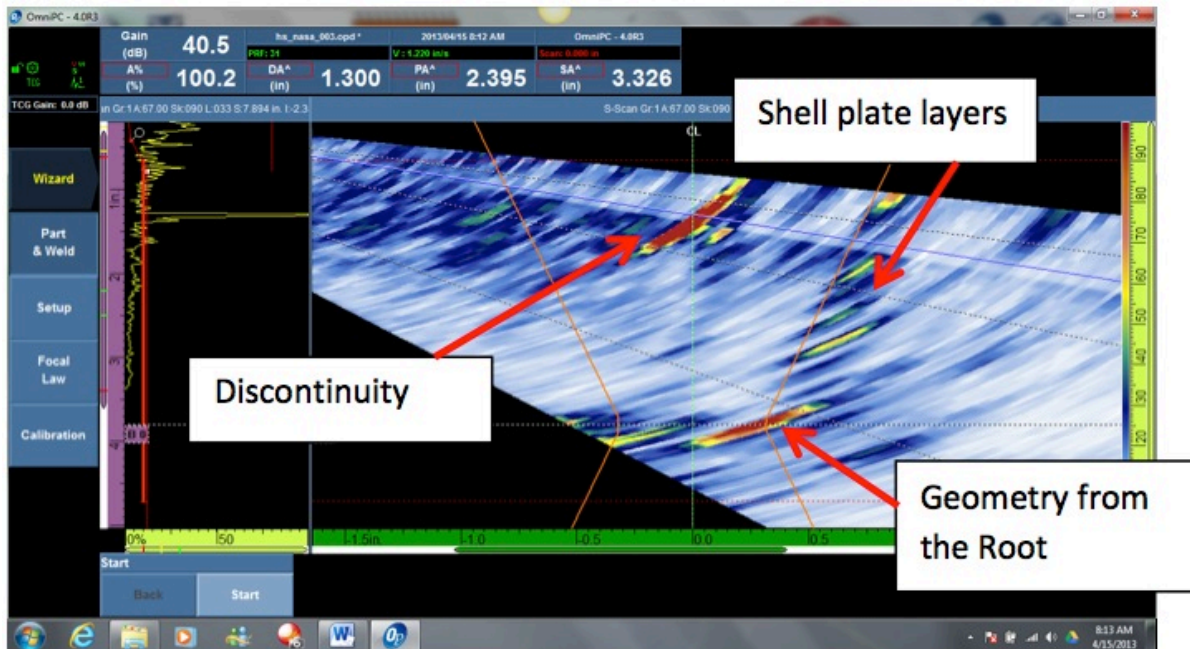


Figure 7.1.2.3-4. PAUT Scan of Head-to-Shell Weld Region (bottom portion)



Title:

Evaluation of Agency Non-code LPVs

Page #:
50 of 193

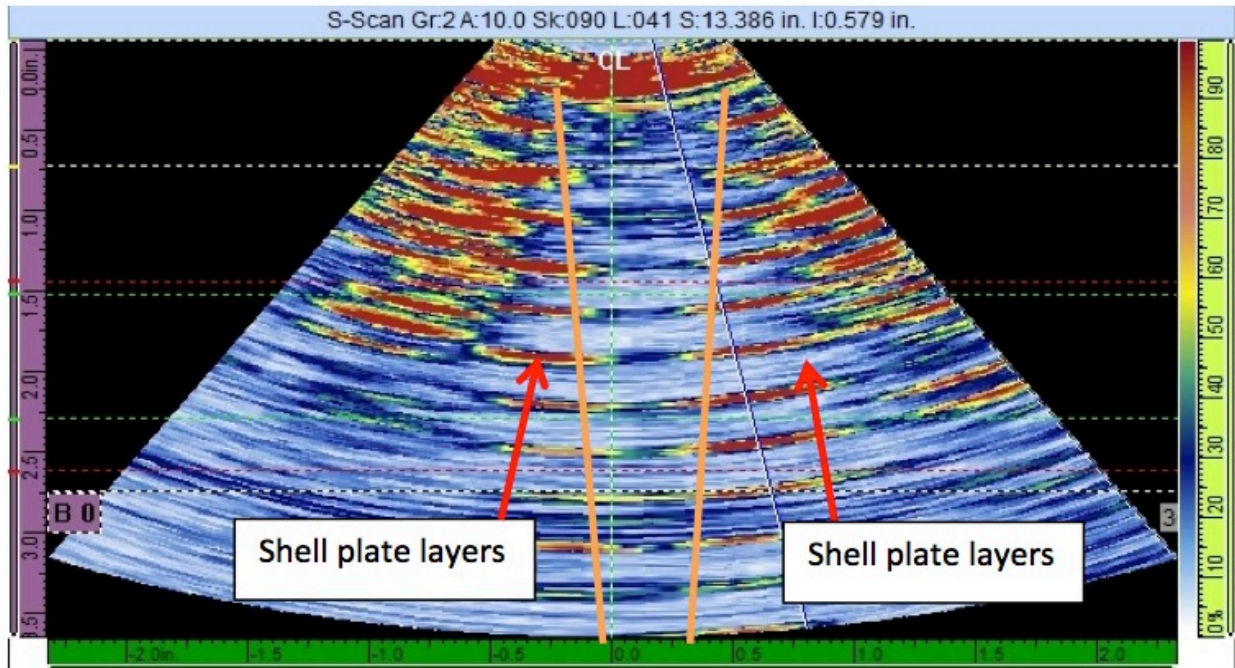


Figure 7.1.2.3-5. PAUT Scan of Shell-to-Shell Weld Region

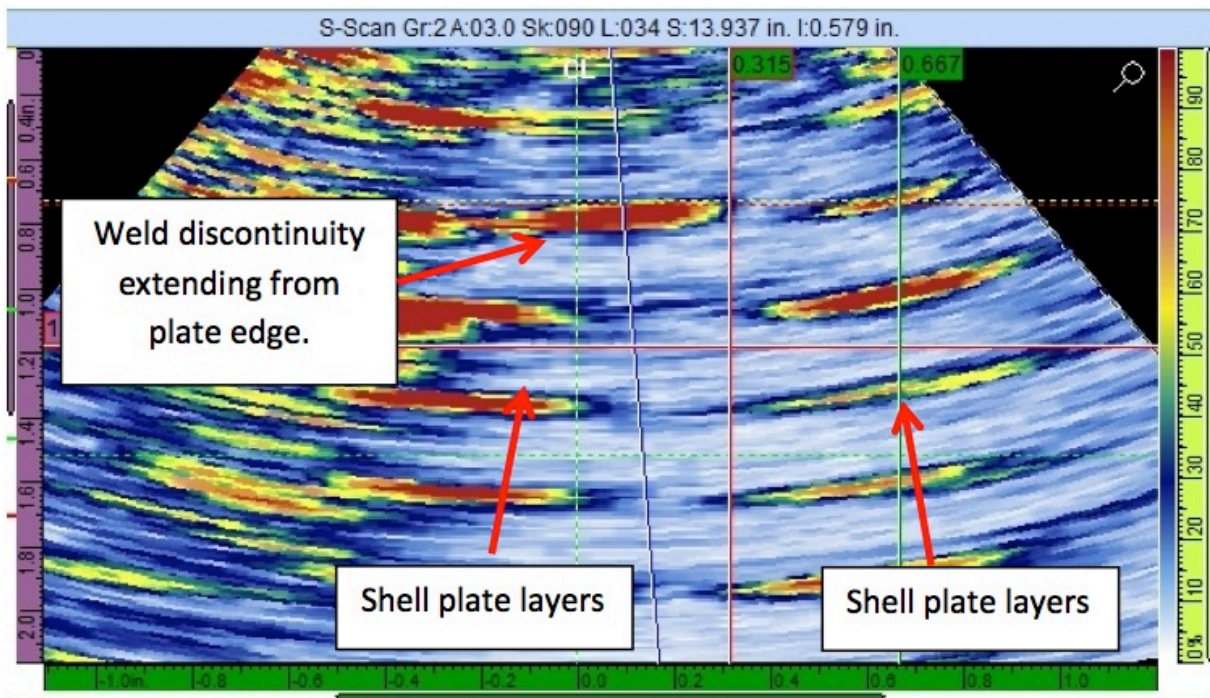


Figure 7.1.2.3-6. PAUT Scan of Shell-to-Shell Weld Region

	NASA Engineering and Safety Center Technical Assessment Report	Document #: NESCP-RP- 13-00852	Version: 1.0
Title: Evaluation of Agency Non-code LPVs		Page #: 51 of 193	

Davis NDE also provided tabular results of the weld scans for specific weld segments on vessel V0256 using both time based and linearly encoded scans. Davis NDE used both techniques to further demonstrate the scanning and data acquisition capabilities of the equipment. Table 7.1.2.3-1 shows the results for head-to-shell weld using linearly encoded weld scans. The linear encoding allowed Davis NDE to characterize the indications (i.e., height and length) and shows the relative location of the indications along the weld length. Table 7.1.2.3-2 shows results reported by Davis NDE for the vessel shell-to-shell weld using time-based scans rather than linearly encoded scans. Further characterization of the indications from these scans was not provided since the data were not encoded for this part of the demonstration.

The PAUT data interpretation by Davis NDE resulted in observations at each weld location scanned. Davis NDE personnel were asked to identify any and all observations, not just those that would be BPVC rejectable indications. Weld C3, location O-P is the only weld area of those scanned by Davis NDE personnel where radiography also indicated there was any indication within the weld volume. The MSFC American Welding Society film interpreter reported a BPVC rejectable indication of porosity at this weld location (C3/O-P).

As noted earlier, the data reviewed were not from code quality scans, which results in less than desirable confidence in the accuracy of the reviewed data. The records below are merely documentation of the indications presented in these scans and do not detail the overall component quality.



NASA Engineering and Safety Center Technical Assessment Report

Document #:
**NESCP-RP-
13-00852**

Version:
1.0

Title:

Evaluation of Agency Non-code LPVs

Page #:
52 of 193

Table 7.1.2.3-1. Head-to-Shell Weld

Identification	Meets Code	Fails Code	Linear	Planar	Rounded	Cluster	% DAC	Discontinuity				Scan Number	Comments (Surface/ Subsurface)		
								Height	Length	Sound Path	Depth From "A"			Distance	
														From X	From Y
Weld C1 (TOP)			X					.05"	.24"			0"	6.7"		Slag
			X					.18"	.35"			+ .7"	7.9"		LOF
			X					.10"	.27"			0"	9.3"		Slag
			X					.15"	.26"			0"	9.9"		Slag
			X					.09"	.28"			+ .2"	12.9"		Slag
			X					.28"	.37"			+ 1"	13.0"		LOF
			X					.07"	.14"			+ .2"	13.8"		Slag
Weld C1 (BOT)			X					.59"	2.9"			- .1"	7.5"		Crack
			X					.34"	.26"			+ .3"	11.3"		Slag
			X					.07"	.15"			0"	12.1"		Slag
			X					.44"	.21"			+ .1"	13.0"		Crack

Table 7.1.2.3-1 notes:

1. The head-to-shell data were encoded but scan axis positional information may differ slightly from the first to the second index position.
2. 100% weld coverage was not obtained in this scan.

Table 7.1.2.3-2. Shell-to-Shell Welds

Identification	Meets Code	Fails Code	Linear	Planar	Rounded	Cluster	% DAC	Discontinuity				Scan Number	Comments (Surface/ Subsurface)		
								Height	Length	Sound Path	Depth From "A"			Distance	
														From X	From Y
Weld C3 (L to K)			X										Slag		
			X										Slag		
			X										Crack-like		
Weld C3 (O to P)			X										Crack-like		
			X										Slag		

The only weld location scanned by Davis NDE which had indication (porosity) previously identified by radiography



NASA Engineering and Safety Center Technical Assessment Report

Document #:
**NESCP-RP-
13-00852**

Version:
1.0

Title:

Evaluation of Agency Non-code LPVs

Page #:
54 of 193

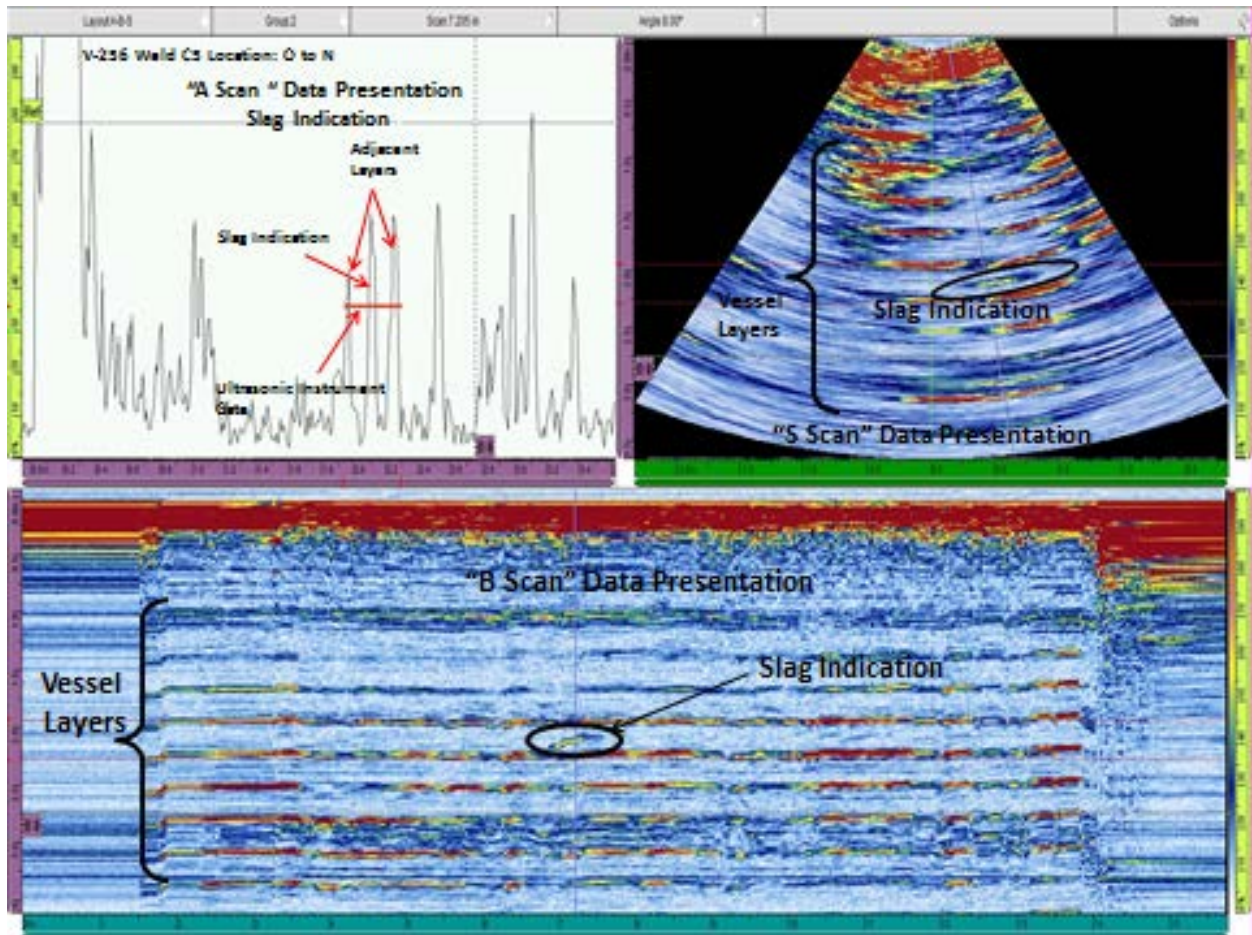


Figure 7.1.2.3-7. PAUT Scans for Indication in C5 Weld O to N Location, Indicative of Slag



Title:

Evaluation of Agency Non-code LPVs

Page #:
55 of 193

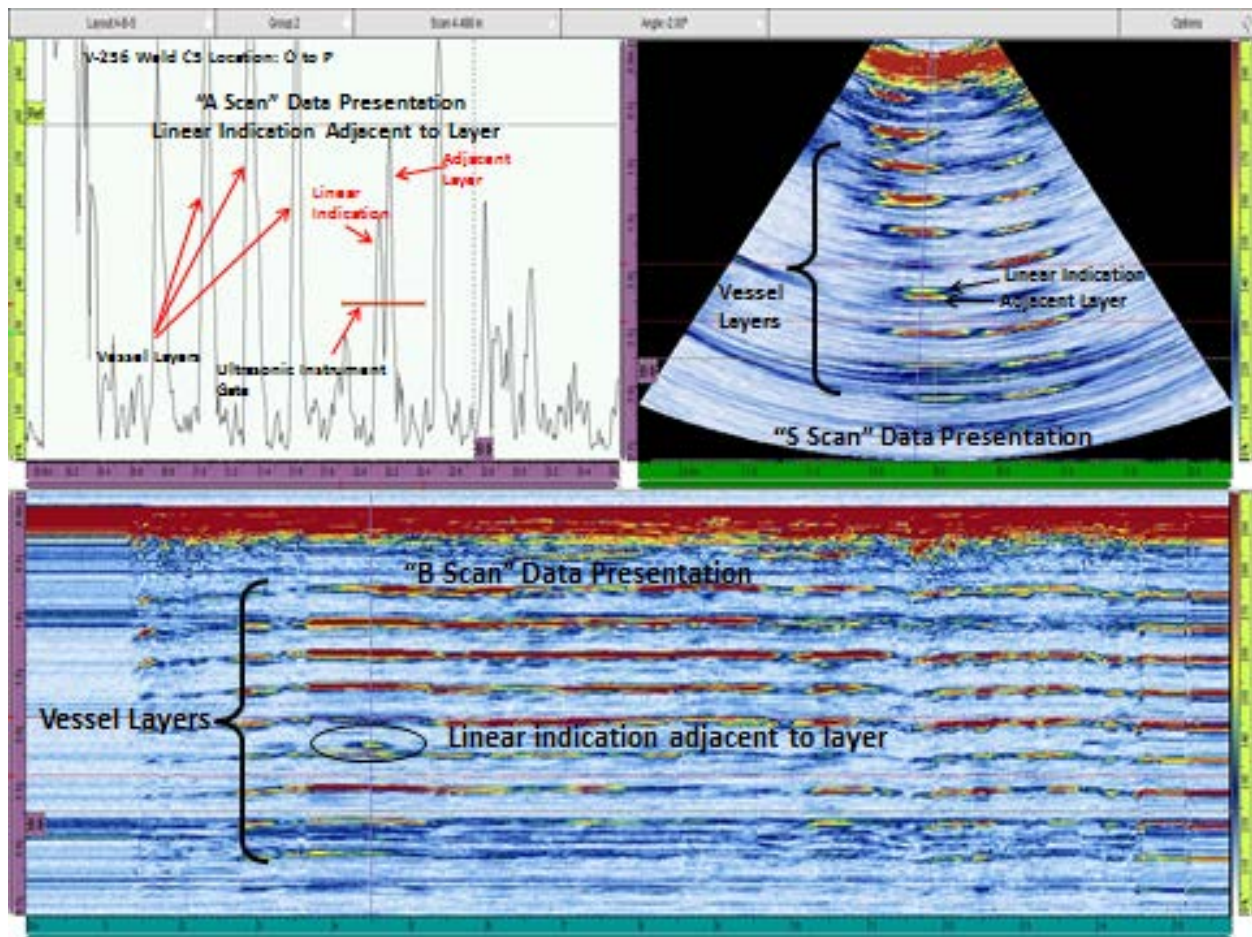


Figure 7.1.2.3-8. PAUT Scans for Linear Indication in C5 Weld O to P Location, Indicative of Lack of Fusion

	NASA Engineering and Safety Center Technical Assessment Report	Document #: NESCP-RP-13-00852	Version: 1.0
Title: Evaluation of Agency Non-code LPVs			Page #: 56 of 193

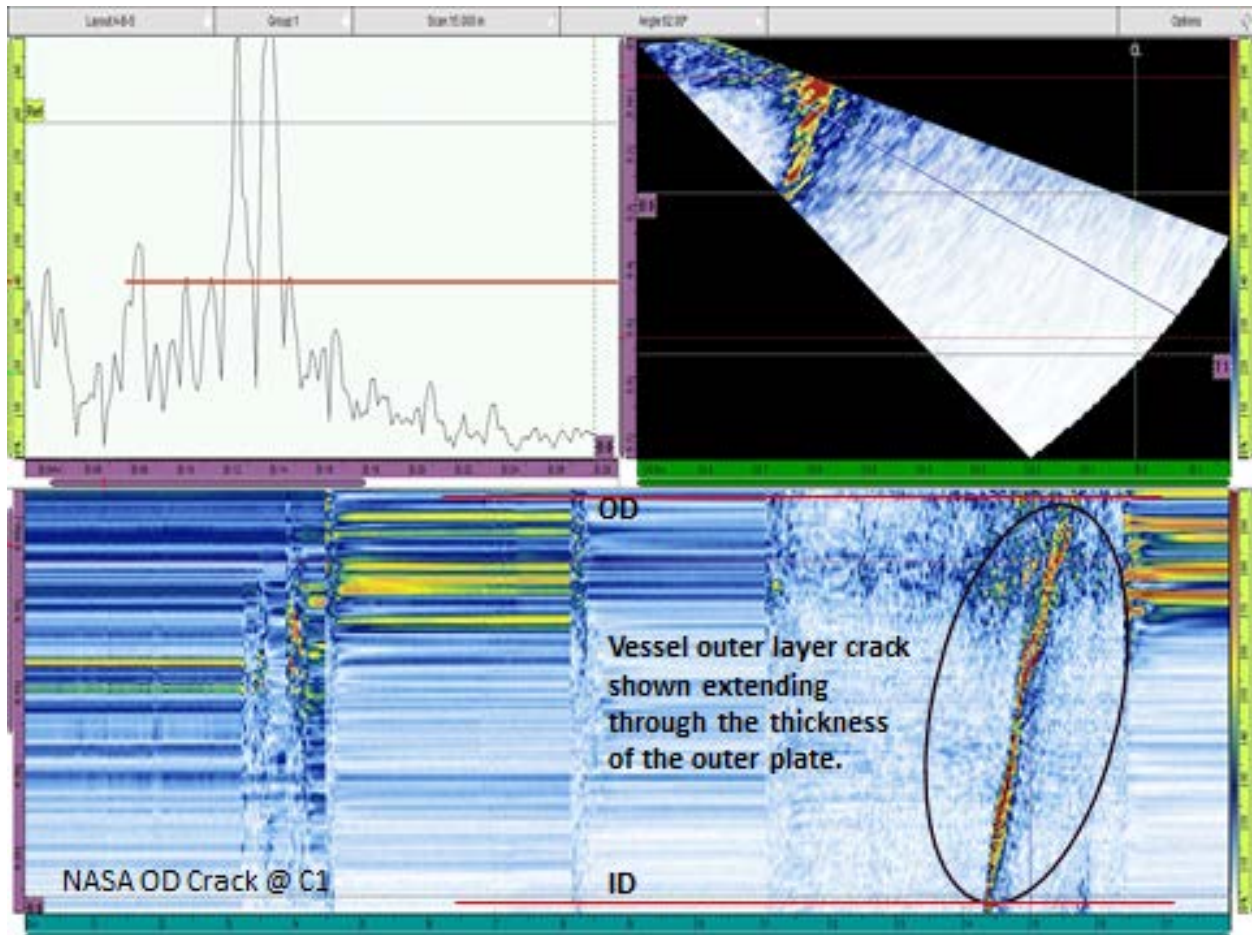


Figure 7.1.2.3-9. PAUT Scans for Visible Crack in Outer Layer of V0256

Observations and Conclusions

The demonstration by Davis NDE of the Olympus Omniscan PAUT equipment provided insight into the overall equipment operation and capabilities, as well as the weld scanning techniques. The amount of data and detail observed using the PAUT equipment far exceeded the amount of information available from the radiography or conventional UT in the specific weld areas inspected. The PAUT data shown in this report are only a small sample (screen view snapshots) of the data recorded during the V0256 weld inspection demonstration.

- No direct conclusions can be made from the comparison of PAUT data with radiography or conventional UT data on Vessel V0256 since there were few indications for comparison and there were no fully characterized flaws within the weld volumes that could be used for a quantifiable comparison. The PAUT weld scans of vessel V0256 were the most expedient means of obtaining PAUT data at the time to better understand the inspection technique and to assess general equipment capabilities. Many of the indications reported by Davis NDE in Tables 7.1.2.3-1 and 7.1.2.3-2 simply cannot be

	NASA Engineering and Safety Center Technical Assessment Report	Document #: NESCP-RP-13-00852	Version: 1.0
Title: Evaluation of Agency Non-code LPVs		Page #: 57 of 193	

confirmed at this time since radiography revealed no indications at these locations and no weld excavations have been performed.

- The PAUT technique appears to offer an immediate improvement over conventional UT inspection in the level of detail that can be observed for solid head to layered shell weld inspection. Although radiography and conventional UT could be used for inspection of the head-to-shell weld, PAUT offers the benefit of being a nonintrusive technique while providing beam steering capability to more fully investigate the area of interest, which is not available with conventional UT. (Beam steering refers to the PAUT capability to shift the phase of the signals from the pulser array, taking advantage of constructive and destructive wave interference and, in essence, directing (steering) the sound beam to specific areas of interest within the weld volume. Conventional UT does not provide this capability since only a single pulser-receiver is used.)
- The PAUT data appear to distinguish between indications of individual layers and indications in the weld volume. Further assessment will be needed to determine how defect orientation, size, and location (especially with respect to the shell layers) will affect capability and probability of flaw detection.
- The additional data presentations available with PAUT but not with conventional UT—the “S” and “B” scan data formats—allow a far more intuitive presentation of the weld volume and facilitate improved characterization and evaluation of flaw data. The improved data visualization in combination with the beam steering capability offers a powerful tool for weld inspection and assessment.
- The advantage that PAUT offers over conventional UT is somewhat offset by the additional training, interpretation skill required by the NDE specialist, and initial cost of the PAUT equipment. Individual assessment is required to determine whether PAUT benefits outweigh the associated cost especially in cases where other existing NDE techniques are already being employed with some success.
- PAUT does not provide a means of inspecting the longitudinal welds within a layered vessel other than those layers that are physically accessible (i.e., the outer shell and sometimes the inner shell) as the layer gaps are reflective surfaces and preclude passage of sound waves. However, PAUT may provide a means of inspecting a short distance into the layers immediately adjacent to the full penetration welds. Additional evaluation will be necessary to determine how far inspection capability extends into the layers, if at all, and how the weld geometry affects the probability of flaw detection.
- The Olympus Omniscan equipment provides capability to digitally store all equipment parameters and data from the inspection. Once the welds are scanned, the resulting data files can be reviewed at any time, and these data files provide a permanent record of the inspection. These data files also facilitate collaboration with others when evaluating and interpreting the inspection data.

	NASA Engineering and Safety Center Technical Assessment Report	Document #: NESCP-RP- 13-00852	Version: 1.0
Title: Evaluation of Agency Non-code LPVs		Page #: 58 of 193	

- PAUT requires a relatively flat weld crown to provide better coupling between the weld surface and the ultrasonic transducer. This requires time and effort to prepare welds, especially on larger vessels, but once the weld surfaces are properly prepared subsequent PAUT inspections can be performed without further weld preparation.
- Other, more general benefits of PAUT include:
 - PAUT can be performed with the vessel in service (on-stream), minimizing impact to ongoing operations.
 - Reduced vessel downtime in cases where PAUT is used in lieu of intrusive vessel inspection techniques. The reduced downtime can be substantial for vessels containing cryogenics, propellants, and high purity media due to both the pre-inspection and post-inspection activities required to open the vessel, inspect it, and return it to service (e.g., pre-inspection warming and the rendering of cryogenic and propellant vessels inert; post-inspection leak check, cleaning, sampling, inerting, and reestablishing media purity levels).
 - No personnel exclusion zones (as are required for radiography) are necessary for PAUT, allowing inspections to be performed during regular working hours and concurrent with other unrelated but ongoing operations. RT exclusion zones can be particularly intrusive to other operations when using a cobalt source, which would be necessary for radiography of the many heavy walled vessels at MSFC that are in close proximity to inhabited buildings and test facilities. All costs and benefits of each inspection method must be included in analyses, including such items as cost of NASA or NASA contractor personnel who may need to work overtime to monitor after hours operations.

Future Work

Additional work is planned to further explore the capabilities of PAUT for inspection of LPVs. The PAUT work that initially began as a collaborative effort between SSC, MSFC, and GRC now includes participation by the NESC.

A statement of work (SOW) was developed in late FY13 to further investigate and better quantify the capabilities and limitations of PAUT for detecting flaws in LPVs. The SOW and associated drawing were provided to Davis NDE to obtain a cost estimate to build a performance demonstration block that will simulate a layered vessel full penetration weld and will include a number of induced flaws with prescribed size, orientation, and location. ASME Code Case 2235 is being used as a basis for flaw size for the demonstration block and has been validated by the MSFC Material Laboratory personnel as an acceptable approach for this effort. In addition, ASME Section VIII Div I Part ULW [ref. 1] will be used as the basis for construction of the layered demonstration block. The primary objectives of this work will be to:

	NASA Engineering and Safety Center Technical Assessment Report	Document #: NESCP-RP- 13-00852	Version: 1.0
Title: Evaluation of Agency Non-code LPVs		Page #: 59 of 193	

- Further quantify the capability of PAUT to characterize known flaws in the weld volume (accuracy of flaw sizing and locating within the weld volume) and identify variables associated with flaw characterization.
- Investigate the effect of layer gap reflections in the area adjacent to the full penetration weld region and the ability of PAUT to distinguish layer gaps (layer tip reflections) from actual flaw indications in the weld volume.
- Determine whether PAUT can detect flaws that occur in the layers and do not continue into the circumferential weld, and if so, assess how far into the layers flaws can be detected.
- Further the development of weld scanning techniques, procedures, and scan plans for PAUT inspection of head-to-shell and shell-to-shell full penetration welds.

The start date for this follow-on work with Davis NDE is planned for mid-FY14. Additional work may be required beyond this planned effort to further assess PAUT capabilities, to address specific problem areas that are identified or to quantify the probability of flaw detection.

Additional efforts to develop a calibration block for PAUT evaluation was included as part of Task 2 of this assessment. The results from this activity are described in Section 7.2.5.

7.1.3 External User Survey

In addition to the internal survey of NASA Centers, select external users of non-code LPVs were contacted and questioned about their approaches to operating, inspecting, and maintaining these vessels. To assist in this external user survey, a nationally recognized consultant on these vessels, Dr. Maan Jawad, was added to the assessment. Dr. Jawad previously worked with a company that designed, fabricated, and repaired LPVs. He also has served extensively in numerous roles on the ASME Codes Committees responsible for the development and approval of codes for pressure vessels, including LPVs. As such, he had numerous contacts in industry where these vessels are in use. Additionally, he was able to provide general background information on the procedures for non-code commercial LPV certification and inspection.

In addition to the contacts provided by Dr. Jawad, several other contacts for additional industrial and government facility users of these vessels were gathered. In all, responses from seven different external LPV users were received. Most agreed to provide information only on the condition that their company names would not be included in the final report. Most of the external users surveyed were in the chemical processing industry, although some were in aerospace. In general, the LPVs used in the chemical processing industry were operated under significantly different conditions from those within NASA. They typically contained corrosive products and were operated at elevated temperatures. The vessels in use at aerospace facilities were operated under similar conditions to NASA LPVs, storing high-pressure noncorrosive gases and used under ambient temperature conditions but at times subject to low temperatures associated with blowdown operations or unusual weather conditions.

	NASA Engineering and Safety Center Technical Assessment Report	Document #: NESCP-RP- 13-00852	Version: 1.0
Title: Evaluation of Agency Non-code LPVs		Page #: 60 of 193	

In the following section, some general information regarding the certification and inspection procedures for non-code LPVs is provided. Then, some additional insight from the specific external users contacted in this survey is also provided.

7.1.3.1 General Procedures for Commercial Non-ASME Stamped LPVs

7.1.3.1.1 Certification

The rules for layered vessels were incorporated in the Sections VIII-1 and VIII-2 in 1978. Prior to that time, layered vessels were built in accordance with the manufacturer's in-house standards. Each manufacturer had its own construction standard. The design of these layered vessels was, as much as possible, in general accordance with VIII-1 [ref. 1]. Because of these variations from BPVC requirements, these layered vessels could not be put into service in states requiring code construction without first registering them with the state jurisdiction where the vessel was to operate. Jurisdictional requirements can vary greatly from state to state. However, the general registration process proceeds along the following lines:

- The manufacturer contacts the Chief Boiler Inspector of the state where the layered vessel is to operate and requests a "state special."
- The "state special" certificate is issued by the Board on Boilers and Pressure Vessels for that state. The Board consists of members who are normally appointed by the Governor and approved by the senate of that state. The board members represent various "interest" segments within the state and usually include representatives from manufacturing, academia, users, labor unions, insurance companies, technical consultants, etc.
- The manufacturer submits a package to the Board prior to their meeting (they typically meet four times a year) consisting of the following:
 - Design report showing the required thicknesses of various components such as heads, shell, nozzles, skirt, etc.
 - Manufacturing drawings showing materials used and details of construction.
 - Welding details and procedures in accordance with Section IX of the ASME BPVC.
 - NDE testing in accordance with Section V of the ASME Code.
 - Hydrotest information and procedures.
 - Any other pertinent information.
- The manufacturer's request is discussed at one of the meetings of the Board. Representatives from the manufacturer (typically, the chief engineer and chief metallurgist) are normally present at the meeting to answer any questions the Board may have.

	NASA Engineering and Safety Center Technical Assessment Report	Document #: NESCP-RP- 13-00852	Version: 1.0
Title: Evaluation of Agency Non-code LPVs		Page #: 61 of 193	

- The Board usually approves the registration request with additional requirements. These additional requirements vary greatly from state to state and may include changing the factor of safety, imposing additional fabrication and or testing requirements, etc.
- The Board issues a “State Special” certificate with a registration number. This number will be stamped on the vessel nameplate prior to operating the vessel.

7.1.3.1.2 In-Service Inspection

Commercial layered vessels are inspected during routine shut downs (normally every 2 to 5 years). For inspection guidance, the chemical industry normally follows the rules of the National Board Inspection Code (NBIC) [ref. 47], and the petroleum industry follows the rules of API 579 [ref. 32], although neither of these standards contains guidance specific to LPVs. Some large companies have their own proprietary in-house standards to supplement the standards mentioned above. Some of the features of layered vessels that are taken into consideration in the in-service inspection program in commercial applications are listed here.

- Vent holes: Vent holes are considered one of the most important safety features of layered vessels. Any cracks that occur in the inner shell during operation will result in leakage through the vent holes, which is detectable in principle by a number of different means.
 - Many companies, and especially those producing fertilizer, routinely monitor the depth of vent holes during planned shutdown to make sure they are not plugged with product (such as carbamate, which changes from liquid to solid immediately upon exposure to atmospheric pressure).
 - Many companies, especially those using lethal gases, connect all vent holes to a piping system that use sniffers, vacuum sensors, and pressure sensors to detect leaks caused by cracking of the inner shell.
- Residual stresses in circumferential welds: The ASME BPVC requires carbon steel welds greater than 1 ½ inches in thickness to be post-weld heat treated (PWHT) in solid wall construction. Heat treatment accomplishes two purposes. The first is to temper the welds, and the second is to reduce fabrication residual stresses. Such a requirement for PWHT is not mandated for layered construction. Thus, the circumferential thick welds in layered construction tend to have high hardness and high residual stresses, both of which are detrimental to the welds due to the possibility of both SCC and fatigue. Accordingly, the inside and outside of these welds are routinely dye-penetrant examined or magnetic-particle inspected during scheduled shutdowns to detect any possible cracks.

7.1.3.2 Responses from Specific External LPV Users

Three companies were contacted regarding their procedure for inspecting layered vessels. The information received is general in nature, with no specifics. This was to be expected due to liability issues. Two of the companies used the NBIC, which is for general guidance only.

	NASA Engineering and Safety Center Technical Assessment Report	Document #:	Version:
		NESCP-RP-13-00852	1.0
Title:		Page #:	
Evaluation of Agency Non-code LPVs		62 of 193	

API 579 was also mentioned as a reference, although API 579 does not contain specific rules for layered vessels.

Company A (chemical plant in Tennessee)

The company does not have in-house rules for inspection, repair, and alteration. The company follows the NBIC and state rules for operations.

- The company uses NBIC as a basis for all of their pressure-vessel inspection, repair, and alterations.
- The company supplements NBIC rules with the more rigorous rules of API 579 (when needed), subject to the state jurisdictional approval.
 - API 579 allows operation with full pressure and 90% remaining wall thickness (10% general corrosion) with appropriate NDE testing.
 - API 579 allows temporary operation of a vessel with a crack. The company uses very conservative K_{Ic} and crack-growth values and thorough NDE examination in order to allow a vessel to operate with a flaw until a scheduled shutdown, during which the flaw is removed and repaired.

Company B (refinery in California)

- The company does not have in-house rules for inspection, repair, and alteration but rather follows the NBIC, API 579, and state rules for operations.
- All inspection is done by the inspection department of the company in accordance with the NBIC.
- If the NBIC does not have rules that address a specific problem, then the inspection department contacts the engineering department for an evaluation using the rules in API 579.
- API 579 has three levels of evaluation. Level 1 is the most comprehensive, and level 3 is the least. The state jurisdiction requires that all repairs and alterations made in accordance with level 1 must be approved by the Chief Boiler Inspector of the state prior to implementation.

Company C (polyethylene and polypropylene plant in Texas)

- The company uses layered vessels when a process is highly corrosive and the stainless steel inner shell is needed for protection, and the vent holes are needed for leak detection.
- Because of the corrosive environment, the company uses AE for monitoring the layered vessels, which is performed by Stress Engineering (of Houston, Texas) during a hydrotest using a factor of 1.1 on operational pressure.
- The company encounters more problems with cracking when the layers are made of high-strength steel and the heads of lower strength steel.

	NASA Engineering and Safety Center Technical Assessment Report	Document #: NESCP-RP-13-00852	Version: 1.0
Title: Evaluation of Agency Non-code LPVs		Page #: 63 of 193	

- When cracking is detected, it is at the head-to-shell junction.
- The company inspects the layered vessels inside and out during normal shutdowns.
- The company does not normally use the NBIC since Texas is a non-code state.

Based on the above information, it can be concluded that the commercial segment uses available NDE and inspection tools. No particular new methodology or procedure has been developed for inspecting and monitoring layered vessels. However, these vessels are regularly inspected during planned shutdowns at intervals of 2 to 5 years.

Two other chemical companies provided responses. One noted that their vessels have jackets, which is where they have the most problems with cracking due to differential thermal expansion at elevated temperatures. Another company noted that they had undergone a process to rerate their LPVs to operate at higher pressures a number of years ago. This was based on results from analysis and MAE testing under hydrostatic proof testing. Unfortunately, they were not able to provide any details of the analysis or test results. Otherwise, both companies reported the use of similar inspection methods, including visual inspection, inspection of vent holes, and limited UT.

Two aerospace LPV users (one commercial company and one government facility) provided responses. Both indicated that their vessels were used for high-pressure, noncorrosive gases at ambient operating temperatures similar to NASA LPVs. Both also indicated that hydrostatic proof testing was used as part of the initial certification of the vessels. They also used visual inspections, UT, and radiography during initial certification. One user noted that their vessels were last certified for an additional operating period of 20 years and were approaching the end of this certification. They stated that they were unsure of what they would do to recertify the vessels for continued operation and were interested in the results from this assessment and follow-on testing to help in their decisions for recertification. Neither user was doing any materials testing work or evaluating any new NDE methods for these vessels, although one noted that they had discussed evaluating the applicability of PAUT.

7.1.3.3 Summary of Key Points from External User Survey

Although the external review consisted of contact with a limited number of commercial LPV users, no significant new approaches to inspection, analysis, and testing of these vessels were identified, nor were any efforts to develop materials property databases for the materials used in these older vessels. The commercial companies were largely applying hydrostatic proof testing and conventional NDE inspection methods such as visual inspection, MT, conventional UT, and radiography. The chemical industry performs detailed inspections of these vessels at regularly scheduled plant shutdowns every 2 to 5 years. Most admitted that they felt these methods were inadequate for key areas of the vessels such as the layered shells and the associated welds and the circumferential full penetration welds. As a result, most companies contacted were very interested in the results of this NESC assessment and any follow-on testing and highlighted the need to have an established standard or procedure for inspection and certification of these vessels.

	NASA Engineering and Safety Center Technical Assessment Report	Document #: NESCP-RP- 13-00852	Version: 1.0
Title: Evaluation of Agency Non-code LPVs		Page #: 64 of 193	

7.1.4 Risk Assessment for Different LPV Regions

Based on the information obtained in Task 1, the assessment team attempted to identify the highest risk operating conditions or regions of NASA LPVs. The purpose of this activity was to provide a basis for selection of additional efforts to be funded in Task 2, as well as to provide a basis for prioritizing the final team recommendations to be incorporated in this report. Information considered included the review of previous LPV catastrophic failures, as well as reports of commonly reported noncatastrophic damage; review of how NASA LPVs are operated, inspected and maintained in comparison with those in industry and, in particular, in comparison with those that have catastrophically failed; and the limitations of available materials property data, structural analysis methods, and NDE techniques as applied to LPVs.

Table 7.1.4-1 provides a summary of the high-risk LPV regions or operating conditions that were identified by this assessment team, along with the reasons for the high risk and potential actions to understand and/or mitigate the risk. The highest risk for NASA LPVs that was identified was the operation of the LPVs below the ductile-brittle transition temperature (i.e., NDT). The reason for this concern is that operation below the NDT can result in the propagation of any existing cracks by a lower energy brittle fracture mode resulting in an increased potential for catastrophic failure. Although the LPVs are typically operated above the MDMT that is either cited on the nameplate of the vessel or on the design drawings, as noted previously the MDMT values determined for these older, non-code LPVs were generally based on strength only and did not account for brittle fracture at lower temperatures of -20°F or greater. Some LPVs with lower nameplate MDMTs were keyhole impact tested consistent with BPVC requirements at the time, although this is not a code-accepted impact test method today. Further, data on the NDT for materials used in these vessels are not available. Thus, it is possible that some NASA LPVs are being used at temperatures near or below the NDT. To address this risk, characterization of the toughness and NDT is needed for all materials in NASA LPVs, including head, shell, weld, and weld HAZ materials. Measurements of these parameters from multiple vessels are needed to establish bounding NDT values that can be utilized to define more appropriate MDMT values for these NASA LPVs. Once the MDMT values are established, then operations can be restricted to ambient temperatures above these limits, or environmental controls such as enclosures or heaters can be utilized to maintain temperatures above these limits when ambient temperatures are too low. Alternatively, a reduction in operating pressure can be used to allow lower temperature operation in accordance with ASME BPVC. It should be noted that data showing previous safe operations of these vessels at lower temperatures may be beneficial. However, this does not fully mitigate this risk since, if new cracks have formed or cracks have propagated to critical sizes in the interval since the last exposure, then the risk of brittle fracture can exist for the next exposure to similar low temperatures.

The next high-risk region of NASA LPVs that was identified was that of the circumferential full penetration welds at either the head-to-shell, or shell-to-shell junctions of these vessels. This was cited to be of high risk because of the history of failures that have initiated in these areas, along with the current lack of capability to inspect this region. An additional concern is the lack of knowledge as to the stress state of this region, since these welds are not stress relieved in the

	NASA Engineering and Safety Center Technical Assessment Report	Document #: NESCP-RP- 13-00852	Version: 1.0
Title: Evaluation of Agency Non-code LPVs		Page #: 65 of 193	

fabrication process. With respect to the previous non-Agency failures relative to the NASA LPVs, it is noted that they occurred in vessels operating at higher temperatures with corrosive products, and there may have been environmental influences that contributed to the failures that are not applicable to NASA vessels. While possibly enhancing corrosion, however, the elevated temperatures reduce the risk seen due to low-temperature operation at NASA. To help mitigate risks associated with this region, analytical methods to predict the weld residual stress, as well as further predict stress states and critical initial flaw sizes, are needed. Evaluation and, if possible, validation of NDE methods to inspect this region are also needed. PAUT has shown some initial promise, and for this reason was included as one of the funded activities in Task 2. The capabilities of radiographic and AE methods for this regions need to be determined also. Alternatively, proof test logic may be applicable to reduce risk in this region.

The shell regions present elevated levels of risk in large part because of the lack of ability to inspect them except for the outer and inner (when internal access is available) layers. Additionally, one of the most common locations where cracks have been detected is in the inner or outer shell layers adjacent to the circumferential welds. This is anecdotally attributed to complex stress states, including bending where the head transitions into the shell though this longitudinal bending fails to explain longitudinal cracks that would normally be caused by circumferential stresses. However, currently available analysis models and materials property data are inadequate to provide detailed information on the stress states. The longitudinal welds in these layers are also a concern due to the lack of ability to inspect them and the varying degree to which they were inspected when initially fabricated. As with other high-risk areas, improved materials property data and analysis methods are needed to better understand the risk and estimate critical flaw sizes. AE is a potential technique for detecting propagating flaws in these regions, but this method needs to be further evaluated and, if possible, validated. Low-frequency electromagnetic NDE methods should also be evaluated for flaw detection capabilities in the shell regions.

Nozzles and nozzle welds are areas of increased risk, especially those through the shell sections. While some UT methods have been developed for nozzles and nozzle welds through the monolithic heads, these have not been fully validated and have not been evaluated for nozzles through the shell sections. Again, improved analysis capabilities are needed to better understand the risk, and development and validation of NDE methods such as UT, AE, or PAUT are needed to mitigate risks.

	NASA Engineering and Safety Center Technical Assessment Report	Document #:	Version:
		NESCP-RP-13-00852	1.0
Title:			Page #:
Evaluation of Agency Non-code LPVs			66 of 193

Table 7.1.4-1. LPV Regions or Operating Conditions that Present the Highest Risk for Potential Failure for NASA Non-Code LPVs

LPV Region or Operating Condition	Reasons for Elevated Risk	Potential Actions to Understand and/or Mitigate Risk
1. Operation of vessels below ductile-brittle transition temperature (i.e., NDT).	<ul style="list-style-type: none"> * Use of pressure vessels below NDT can lead to brittle fracture, resulting in catastrophic vessel failure. * NDT has not been established for head, shell, and weld materials in NASA LPVs. * NASA LPVs are used at ambient temperature conditions year round, which even in southern locations can be quite cold. * Some NASA LPVs are used in blowdown operational modes, which result in reduced vessel temperatures. 	<ul style="list-style-type: none"> * Characterize NDTs for head, shell, nozzle, and weld materials in NASA LPVs (including variability across multiple vessels). * Ensure MDMT is appropriately established relative to the measured NDT and restrict operation to temperatures above established MDMT. * Build enclosures with temperature control around vessels or utilize heating pads around vessels that must be operated when ambient temperatures are below established MDMT, or when operational conditions such as blowdown could result in such temperatures. * Reduce operating pressures to correspond to reduced operating temperatures in accordance with established procedures, such as the use of Figure UCS-66.1 of the ASME Section VIII, Division 1 BPVC [ref. 1].



NASA Engineering and Safety Center Technical Assessment Report

Document #:
**NESCP-RP-
13-00852**

Version:
1.0

Title:

Evaluation of Agency Non-code LPVs

Page #:
67 of 193

LPV Region or Operating Condition	Reasons for Elevated Risk	Potential Actions to Understand and/or Mitigate Risk
<p>2. Circumferential full penetration head-to-shell or shell-to-shell welds.</p>	<ul style="list-style-type: none"> * Known catastrophic vessel failures originated at head-to-shell or shell-to-shell welds. Examples are the LPV failures at Cartagena, Colombia (shell-to-shell weld failure) and Kansas (head-to-shell failure). Environmental effects also played a part in these failures. * No current validated NDE methods exist to provide adequate inspection for these welds. * Welds are not stress relieved, resulting in unknown residual stress states. * Current lack of materials properties and analysis techniques inadequate to characterize stress states and determine critical initial flaw sizes. 	<ul style="list-style-type: none"> * Evaluate and, if possible, validate PAUT, AE, and/or radiographic methods for inspection of these welds. * Perform external surface inspections (MT/PT). * Reduce inspection intervals for aging vessels. * Investigate analysis methods for determination of residual stresses. * Develop materials property database. * Develop and validate analytical techniques to assess stress states, fatigue crack growth, and critical initial flaw sizes at these welds.



NASA Engineering and Safety Center Technical Assessment Report

Document #:
**NESCP-RP-
13-00852**

Version:
1.0

Title:

Evaluation of Agency Non-code LPVs

Page #:
68 of 193

LPV Region or Operating Condition	Reasons for Elevated Risk	Potential Actions to Understand and/or Mitigate Risk
<p>3. Shell sections near head-to-shell welds</p>	<ul style="list-style-type: none"> * Most common flaws found and repaired in these vessels are cracks in outer and inner shell layers near or intersecting head-to-shell welds, although some flaws have been detected at this region in intermediate layers especially where the longitudinal welds intersect the circumferential weld. * Anecdotally attributed to complex stress states in this region that includes bending at this transition from head to shell, although current limited materials properties and analysis techniques are inadequate to provide detailed stress information. * Cracks at this location only observed directly at outer and inner (when accessible) layers. When repairs are made, additional cracks in interior layers adjacent to repaired layer have been found. Due to lack of NDE methods capable of inspecting interior layers, it is unknown whether similar cracks may exist in interior layers away from the repaired area, although some cracks have been detected in intermediate layers using RT. 	<ul style="list-style-type: none"> * Develop materials property database. * Develop and validate analytical techniques to assess stress states, fatigue crack growth, and critical initial flaw sizes at these locations. * Develop improved non-traditional NDE methods for inspecting interior shell layer when manways are not present to allow interior access to the inner layer. * Investigate capability of AE methods for detecting crack propagation in interior layers. * Investigate very low frequency electromagnetic NDE methods for detecting cracks within interior layers. * Evaluate and, if possible, validate radiographic methods for inspection of these regions. * Reduce operating pressure (also account for low operating temperatures if below MDMT).



NASA Engineering and Safety Center Technical Assessment Report

Document #:
**NESCP-RP-
13-00852**

Version:
1.0

Title:

Evaluation of Agency Non-code LPVs

Page #:
69 of 193

LPV Region or Operating Condition	Reasons for Elevated Risk	Potential Actions to Understand and/or Mitigate Risk
<p>4. Longitudinal welds in shell sections (especially at intersection with circumferential welds).</p>	<ul style="list-style-type: none"> * No current validated NDE methods for inspecting these welds other than on outer layer (and inner layer if internal access is available), although RT methods have been successful at detecting some flaws. * Degree of NDE inspection of these welds at time of fabrication is unknown or varied by manufacturer, and typically was not consistent with current code requirements. In some cases, RT inspection of inner shell longitudinal weld was performed, but no inspection of intermediate layer longitudinal welds. * Limited knowledge of materials properties, as constructed structural configuration (i.e., size of layer gaps, etc.), and analysis techniques inadequate to provide detailed stress analysis and establish initial flaw sizes (other than those assumed by the code) as well as critical flaw sizes. 	<ul style="list-style-type: none"> * Develop materials property database. * Develop and validate analytical techniques to assess stress states, fatigue crack growth, and critical initial flaw sizes at these locations. * Investigate capability of AE methods for detecting crack propagation in longitudinal welds of interior layers. * Investigate analysis of flaw tolerance within the layered shell and means for detecting overstress of outer shell via Pi Tape, photogrammetry, or other means. * Investigate very low frequency electromagnetic NDE methods for detecting cracks within longitudinal welds of interior layers. * Reduce operating pressure (also account for low operating temperatures if below MDMT).



NASA Engineering and Safety Center Technical Assessment Report

Document #:
**NESCP-RP-
13-00852**

Version:
1.0

Title:

Evaluation of Agency Non-code LPVs

Page #:
70 of 193

LPV Region or Operating Condition	Reasons for Elevated Risk	Potential Actions to Understand and/or Mitigate Risk
<p>5. Drain nozzles or other penetrations through shells and associated welds.</p>	<ul style="list-style-type: none"> * No current validated NDE methods to provide adequate inspection for these welds. * Welds not stress relieved resulting in unknown residual stress states. * Current lack of materials properties and analysis techniques inadequate to characterize stress states and determine critical initial flaw sizes. * Cross-bore openings are areas of stress concentrations and, thus, would have elevated stress intensity factors for cracks occurring in these regions. * Most likely sites for failure during burst tests * Greatest potential for adiabatic cooling and operation below MDMT. 	<ul style="list-style-type: none"> * Develop NDE methods as cited above for identification of defects. * Reduce inspection intervals for aging vessels. * Develop materials property database. * Develop and validate analytical techniques to assess stress states (including residual stresses), fatigue crack growth, and critical initial flaw sizes at these welds.



NASA Engineering and Safety Center Technical Assessment Report

Document #:
**NESCP-RP-
13-00852**

Version:
1.0

Title:

Evaluation of Agency Non-code LPVs

Page #:
71 of 193

LPV Region or Operating Condition	Reasons for Elevated Risk	Potential Actions to Understand and/or Mitigate Risk
<p>6. Shell sections in parent materials away from welds</p>	<ul style="list-style-type: none"> * Recent discovery of cracks in exterior layer of KSC vessels at locations remote from welds – unknown what factors contributed to occurrence of these cracks. * No current validated NDE methods for inspecting regions other than on outer layer and inner layer if internal access is available. * Lack of materials properties, as constructed structural configuration (i.e., size of layer gaps, etc.), and analysis techniques inadequate to provide detailed stress analysis and establish initial critical flaw sizes. 	<ul style="list-style-type: none"> * Further develop materials property database. * Develop and validate analytical techniques to assess stress states, fatigue crack growth, and critical initial flaw sizes at these locations. * Investigate capability of AE methods for detecting crack propagation in interior shell layers. * Investigate very low frequency electromagnetic NDE methods for detecting cracks within interior shell layers. * Investigate analysis of flaw tolerance within the layered shell and means for detecting overstress of outer shell via Pi Tape or photogrammetry or other means. * Reduce operating pressure (also account for low operating temperatures if below MDMT).

Regions within LPVs that were considered to be of less risk were also identified. These are summarized in Table 7.1.4-2 with the basis for this designation along with residual risk considerations and possible risk mitigations.

	NASA Engineering and Safety Center Technical Assessment Report	Document #:	Version:
		NESCP-RP-13-00852	1.0
Title:		Page #:	
Evaluation of Agency Non-code LPVs		72 of 193	

Table 7.1.4-2. LPV Regions or Operating Conditions with Lower Risk for Potential Failure for NASA Non-Code LPVs

LPV Region or Operating Condition	Reasons for Lower Risk	Residual Risks and Potential Methods to Mitigate
1. Monolithic vessel heads (other than when operating at temperatures below MDMT or at or near head-to-shell welds).	<ul style="list-style-type: none"> * While what is known of material fracture properties in this region is not encouraging, there is better capability of NDE methods for inspection of monolithic vessel heads, although NDE methods are not currently and consistently used to regularly inspect acreage of heads. * Analysis methods more adequate for predicting stress states and establishing initial critical flaw sizes in monolithic heads. 	<ul style="list-style-type: none"> * Material properties not well characterized for head materials – further develop materials property database. * Quality of thick head materials likely less than thin shell materials – develop materials property database, ensure critical initial flaw sizes established and validated inspection techniques used to ensure flaws that exceed critical initial flaw size are not present.
2. Welds at through-head nozzles or other penetrations.	<ul style="list-style-type: none"> * Available NDE methods for inspecting these welds. * Analysis methods more adequate for predicting stress states and establishing initial critical flaw sizes. 	<ul style="list-style-type: none"> * Material properties not well characterized for weld materials – develop materials property database * Different NDE methods/procedures in use at different Centers – determine best approach and standardize these inspections across the Agency.



NASA Engineering and Safety Center Technical Assessment Report

Document #:
**NESCP-RP-
13-00852**

Version:
1.0

Title:

Evaluation of Agency Non-code LPVs

Page #:
73 of 193

LPV Region or Operating Condition	Reasons for Lower Risk	Residual Risks and Potential Methods to Mitigate
3. Corrosion on vessel interior.	<ul style="list-style-type: none">* Unlike LPVs used in industry that contain corrosive products and operate at elevated temperatures, NASA LPVs contain high-pressure gases at ambient temperatures and are at low risk for internal corrosion.* For vessels with internal access, internal corrosion is readily detected and can be abated.	<ul style="list-style-type: none">* Difficult to inspect interior of vessels with no internal access. Use borescopes and collapsible UT probes on best effort basis.
4. Corrosion on vessel exterior.	<ul style="list-style-type: none">* Proper use of protective paints and coatings can minimize occurrence.* Readily detectable and can be abated.	<ul style="list-style-type: none">* Maintenance and inspection protocols vary from Center to Center – develop standardized process and ensure adequate funds available to inspect for exterior corrosion and apply protective coatings to minimize corrosion.

	NASA Engineering and Safety Center Technical Assessment Report	Document #:	Version:
		NESCP-RP-13-00852	1.0
Title:			Page #:
Evaluation of Agency Non-code LPVs			74 of 193

LPV Region or Operating Condition	Reasons for Lower Risk	Residual Risks and Potential Methods to Mitigate
5. Vent holes.	* Safety feature to detect cracks in internal layers resulting in product loss through vent holes.	* Occurrence of corrosion in the vent hole resulting in a plugged vent hole, preventing detection of internal layer cracks – inspect vent holes to ensure no blockage. * Provides potential path for moisture intrusion to layers, resulting in corrosion – evaluate and document any corrosion in layers around vent holes during vessel sectioning. * Periodic clean-out of vent holes, and protection from moisture without creating a pressure seal.

7.2 Task 2 – Limited Scope Testing and Analysis

As a result of the information and data gathered in Task 1, a number of limited scope testing and analysis activities were identified for support as part of Task 2. The purpose of these activities was to provide additional data to better formulate the final recommendations for this report. Additionally, these efforts provided a mechanism to augment some of the Center-led activities that were already ongoing. In addition to the OSMA funds that were provided for this NESC assessment, some additional NESC funds available at the end of the fiscal year were added to increase the number and scope of the Task 2 activities supported. The following Task 2 efforts were conducted and are summarized in the following sections:

- Characterization of material toughness transition temperature for specimens from head, inner shell, and shell layer materials.
- Evaluation of the toughness of different microstructural regions of LPV welds (e.g., weld, fusion zone, heat-affected zone, etc.).
- Weld residual stress (WRS) modeling of LPVs.
- Evaluation of photogrammetric methods for measurement of LPV deformation and potential flaw detection.
- Evaluation of PAUT methods for inspecting head-to-shell welds.
- AE laboratory specimen design.

	NASA Engineering and Safety Center Technical Assessment Report	Document #:	Version:
		NESCP-RP-13-00852	1.0
Title:			Page #:
Evaluation of Agency Non-code LPVs			75 of 193

7.2.1 LPV Material Evaluations Conducted at MSFC

This section describes current materials testing and analysis performed at MSFC related to this NESC LPV non-code vessel assessment. Although other LPV related characterization efforts independent of this NESC assessment are ongoing at MSFC, the following tasks were defined expressly as a part of this assessment effort:

- **Task 1:** Determine the toughness transition reference temperature T_0 per ASTM E1921-13 for A225 head material.
- **Task 2:** Determine the toughness transition reference temperature T_0 per ASTM E 1921-13 for cylindrical shell base metals.
- **Task 3:** Investigate the LPV weld regions microstructurally to develop recommended test methodologies for future evaluation.

A complete list of terminology and variables used in these sections is provided in Table 7.2.1-1 to assist the reader.

Table 7.2.1-1. Definition of Terms Specific to LPV Materials Testing Discussed in this Section

Term	Definition
1T	Syntax used to represent fracture toughness specimen dimensions; general form is nT , where the specimen thickness is n inches
a	Crack size (length), a lineal measure of the principal planar dimension of a crack
ASTM E 399-12	“Standard Test Method for Linear-Elastic Plane-Strain Fracture Toughness K_{IC} of Metallic Materials”
ASTM E 1820-11	“Standard Test Method for Measurement of Fracture Toughness”
ASTM E 1921-13	“Standard Test Method for Determination of Reference Temperature, T_0 , for Ferritic Steels in the Transition Range;” referred to as the Master Curve method
b_0	The initial remaining ligament, the distance from the crack tip to the back face of the specimen; a critical parameter for determining crack tip constraint
B_0	Full thickness of a fracture toughness specimen, ignoring side grooves if present
C	Used to designate the orientation of the crack or applied load for a toughness test specimen, indicating the circumferential direction around a pressure vessel
Compliance	Used for measuring crack length during fracture toughness testing; the ratio of specimen displacement increment to applied force increment (the inverse of specimen stiffness)
$C(T)$	Compact-tension specimen, a single-edge notched and fatigue cracked plate loaded in tension and used for fracture toughness tests
Δa	Change in specimen crack length during test, in this context, due to stable tearing



NASA Engineering and Safety Center Technical Assessment Report

Document #:
**NESCP-RP-
13-00852**

Version:
1.0

Title:

Evaluation of Agency Non-code LPVs

Page #:
76 of 193

Term	Definition
δ_j	Kronecker delta from ASTM E 1921-13 analysis, equal to 1 if the datum is valid or 0 if the datum is a substitute value related statistical censoring of invalid test results
E	Elastic modulus
FCC	Face-centered cubic crystal system, the only steel crystalline structure to which ASTM E 1921-13 is directly applicable
ICP	Inductively coupled plasma, a quantitative chemistry technique for determining chemical composition
J_C	Fracture toughness test result measuring the energy of fracture, taken as the point of cleavage instability prior to the onset of significant stable tearing crack extension, and meeting validity requirements of ASTM E1820-11
J_{IC}	Fracture toughness test result measuring the energy of fracture, defined at an average of 0.008 inches of stable, ductile crack extension, and meeting validity requirements of ASTM E1820-11
K_{IC}	Fracture toughness test result for linear-elastic measure of fracture toughness and meeting validity requirements of ASTM E399
K_{JC}	Fracture toughness test result obtained by converting a J_C value to a linear-elastic equivalent stress intensity factor
$K_{Jc(1T)}$	Fracture toughness test result obtained by adjusting a K_{JC} value to an equivalent value from a specimen of size 1T, accounts for statistical size effects on cleavage and used as an input to the T_0 analysis
$K_{JC(Limit)}$	Maximum allowed K_{JC} capacity of a specimen that will maintain a condition of high crack-front constraint at fracture based on specimen size; test results exceeding this limit must be statistically censored in order to be included in the ASTM E 1921-13 T_0 analysis
$K_{J\Delta a}$	Value of K_J at the crack extension limit; tests that terminate in cleavage in which slow stable crack growth exceeds the smaller crack extension limit of either $0.05b_0$ or 0.040 in. must be statistically censored to be used in the ASTM E 1921-13 T_0 analysis by substituting this value for K_{JC}
L	Used for designating the orientation of the crack or applied load for a toughness test specimen, indicating the material longitudinal direction or pressure vessel longitudinal axis
M	Used for designating the orientation of the crack or applied load for a toughness test specimen, indicating the pressure vessel meridional axis for hemispherical heads
R	Used for designating the orientation of the crack or applied load for a toughness test specimen, indicating the pressure vessel radial axis
RT_{NDT}	An index temperature determined from Charpy V-notch and nil-ductility temperature data that provides conservative bounding values of fracture toughness versus temperature

	NASA Engineering and Safety Center Technical Assessment Report	Document #:	Version:
		NESCP-RP-13-00852	1.0
Title:			Page #:
Evaluation of Agency Non-code LPVs			77 of 193

Term	Definition
RT_{T_0}	A Master Curve-based index temperature determined from fracture toughness data used as an alternative to RT_{NDT} as permitted by ASME Code Cases N-629 and N-631 that establishes an RT_{NDT} – like quantity from a T_0 value via the relationship $RT_{T_0} = T_0 + 35^\circ\text{F}$.
S	Used for designating the orientation of the crack or applied load for a toughness test specimen, indicating the material short-transverse direction
SE(B)	Single-edge notch bend specimens, see ASTM E1820
σ_{ys}	Yield strength
T	Used for designating the orientation of the crack or applied load for a toughness test specimen, indicating the material long-transverse direction
T	temperature
T_0	Reference transition temperature determined from ASTM E 1921-13 that represents the temperature at which the statistical median of the K_{Jc} distribution from 1T size specimens equals $100 \text{ MPa}\sqrt{\text{m}}$ ($91.1 \text{ ksi}\sqrt{\text{in.}}$) and statistically locates the fracture toughness versus temperature curve
$T_{35,50}$	Transition temperature from Charpy V-notch specimens that exhibit at least 35 mils of lateral expansion and not less than 50 ft-lbs of absorbed energy per ASTM E 23-12c.
T_{NDT}	nil-ductility-temperature from drop weight testing from ASTM E 208-06
u_{TS}	Ultimate strength
ν	Poisson's ratio
W	Width dimension for fracture toughness specimens; other specimen dimensions are commonly expressed relative to this width

7.2.1.1 Background on Vessels and Associated Materials

These three tasks are considered introductory in scope. They are intended to provide early guidance for evaluating the overall risk posed by the current LPV fleet, as well as to provide sufficient guidance to develop meaningful recommendations for future evaluations. These tasks do not provide a final answer with regard to the LPV material behavior. For example, the important issue of material property variability from lot-to-lot has not been addressed.

Tasks 1 and 2 involve evaluating the tensile strength and fracture toughness of the LPV base materials. These properties, particularly fracture toughness, are the most critical for a proper FFS assessment for the LPVs. Because these tests are destructive, the materials testing could only be performed on available sacrificial vessels. *In situ* evaluations on vessels in service are generally not practical. As testing for these tasks began, the surplus vessels available for sacrificial testing were limited to two MSFC vessels: V0032 (MV-50288-34) and V0125 (M-117). The parenthetical designations are the manufacturer's vessel numbers. Additional vessel materials were gathered as made available in preparation for future testing but were not evaluated as part of these tasks.



NASA Engineering and Safety Center Technical Assessment Report

Document #:
**NESCP-RP-
13-00852**

Version:
1.0

Title:

Evaluation of Agency Non-code LPVs

Page #:
78 of 193

Both V0032 and V0125 were of multilayered, right-cylinder construction manufactured by the A. O. Smith Corporation in 1962 and by CB&I in 1963, respectively, as shown in Figures 7.2.1.1-1 and 7.2.1.1-2. The body of vessel V0032 was constructed from six total layers (shells) with the inner layer nominally ½-inch-thick and the remaining five layers each nominally ¼-inch-thick, for a total nominal wall thickness of 1 ¾ inches. The body of V0125 was of similar construction, but with only four total layers, with the inner layer nominally ½-inch-thick and its remaining three layers each nominally ¼-inch-thick, for a minimum total thickness of 1.217 inches. The shells were fabricated from A. O. Smith 1143, 1146, and 1146a steel, which were proprietary, non-ASME material specifications. The hemispherical vessel heads were fabricated from monolithic, A225 Gr. B, a standard ASTM plate material. V0032 was 16 feet, 7.5 inches in total length, with an ID of 20 inches. V0125 was approximately 12 feet, 6.5 inches in total length, with a 24-inch ID. Table 7.2.1.1-1 summarizes the characteristics of these two vessels.



Figure 7.2.1.1-1. Vessel V0032 before Sectioning, Shown with Sister Vessels V0030 and V0035



Figure 7.2.1.1-2. Vessel V0125 Shown after Sectioning

	NASA Engineering and Safety Center Technical Assessment Report	Document #:	Version:
		NESCP-RP-13-00852	1.0
Title:			Page #:
Evaluation of Agency Non-code LPVs			79 of 193

Table 7.2.1.1-1. Summary of Vessels Evaluated

MSFC Vessel ID	Manufacturer Vessel ID	Manufacturer	Manufacture Date	Total Layers	Inner Shell Thickness (in)	Outer Shell Thickness (in)	Head Thickness (in)	Overall Length	Inner Shell Material	Outer Shell Material	Head Material	Nozzle Material	Shell ID (in)	MAWP (psi)	Purpose	Design Temperature
V0032	MV-50288-34	A. O. Smith	Sept. 1962	6	½	¼	2-3/16	16 ft. 7 ½ in.	1146a	1146a	A225 Gr. B FBX	ASTM A105 Gr II	20	5,500	Gaseous Hydrogen	Ambient
V0125	M-117	CB&I	Sept. 1963	4	½	¼	1.056	12 ft. 6 ½ in.	MLP 1143 Mod	MLP 1146	A225 Gr. B FBX	MLF 5002 Mod	24	3,500	High-Pressure Air	120 °F

7.2.1.1.1 Evaluated Base Materials, Tasks 1 and 2

Table 7.2.1.1-2 summarizes the primary base metals that are considered representative of the vast majority of the LPVs in service throughout the Agency. Each is a low alloy steel. The most common material for vessel heads is ASTM A225, Grade B, which is the subject of the Task 1 evaluations. The shell materials (i.e., 1143, 1146, 1146a) are the subject of Task 2. Though clearly important to the thorough and proper assessment of the LPVs, the nozzle materials (mainly MLF 5002) were not included in this assessment activity due to limitations in funding. For the base metals evaluated in Tasks 1 and 2, a decision was made to focus on only one lot of material during this assessment, primarily for the technical reasons that are described in detail in the discussion of the fracture toughness testing (Section 7.2.1.2). The focus on strength and toughness evaluations of base materials during this assessment does not imply that these are considered priorities over such testing in the LPV welds. To the contrary, the welds are considered the most critical aspect of the LPV material system, based, for instance, on the failure history of non-NASA vessels. However, the weld evaluations are considerably more complicated than the base metal evaluations. The prudent order of evaluation for this assessment was to begin in the relatively simpler base metals, leaving the detailed assessment of the welds as required forward work.

Table 7.2.1.1-2. Typical Material Properties for LPV Materials (plate materials are reported for thicknesses ranging from 0.180 to 0.375 inches, inclusive; data are taken from original manufacturer’s certifications)

Use	Common Designation	σ_{ys} (ksi)	u_{TS} (ksi)	Elongation (%)
Inner Layer	1143 [ref. 48]	75	90	22.0
Outer layers	1146 [ref. 49]	70	105–135	20.0
Inner/Outer Layers	1146a [ref. 50]	77	105–135	22.0
Heads	ASTM A225 Gr. B [ref. 51]	43	75	18.0
Nozzles	MLF 5002 Mod [ref. 52]	51	80	18.0

	NASA Engineering and Safety Center Technical Assessment Report	Document #:	Version:
		NESCP-RP-13-00852	1.0
Title:			Page #:
Evaluation of Agency Non-code LPVs			80 of 193

7.2.1.1.2 Selected Base Materials for Evaluation

With the focus on base materials limited to a single lot, the head material from vessel V0032 was selected for the Task 1 evaluation of the ASTM A225 Grade B material.

As shown in Table 7.2.1.1-2, the two MSFC sacrificial vessels provide access to three shell materials: 1143 and 1146 from V0125, and 1146a from V0032. The 1146 and 1146a materials were initially considered to have the same chemistries, but discovery of a CB&I material specification [ref. 53] for 1146 suggests that the 1146a material, with increased maximum allowable phosphorus and sulfur contents and an increased tensile strength, is a modified version of alloy 1146. While increased phosphorous can result in higher strength, it has been known since at least 1940 that sulfur and phosphorus can promote hot cracking and lower toughness in alloy steel welds [ref. 54], so it is unclear why an increase in the allowed maximum allowable phosphorus and sulfur would have been allowed. Considerable inconsistencies were also present in the historical 1146 and 1146a specifications available through the period manufacturers, which would ultimately require additional effort to settle, although a final, conclusive answer may prove elusive [ref. 55]. An evaluation of the constituent chemistry in currently tested and future lots of alloy 1146 and 1146a should be performed.

Though the original A. O. Smith paperwork indicates that 1146a was used to fabricate all V0032 shells (inner and outer), substantial differences in strength for the inner shell material were observed in the MSFC tests compared with the specification minimum properties and lot acceptance data provided for the V0032 inner shell material. These data are summarized in Table 7.2.1.1-3. The data brought the pedigree of the inner layer material into question. Replicate testing on the inner shell on multiple sample configurations ruled out that the data were the result of testing anomalies. Testing of the inner and outer ¼-inch layer materials resulted in tensile properties that were consistent with the A. O. Smith certification, indicating that the pedigree issue was limited to the ½-inch inner layer.

Table 7.2.1.1-3. Comparison of Tensile Data Obtained from V0032 against A. O. Smith Certification and Lot Acceptance Values

Specimen ID	Location	Sample Type	Orientation	σ_{ys} (ksi)	u_{TS} (ksi)	Elongation* (%)
380-11-1A-13	Inner Shell	Round, \emptyset 0.250 in.	L	50.8	76.6	32.3
380-11-1A-14	Inner Shell	Round, \emptyset 0.250 in.	L	50.8	77.1	32.5
380-1	Inner Shell	Round, \emptyset 0.113 in.	C	52.4	80.2	37.4
380-2	Inner Shell	Round, \emptyset 0.113 in.	C	45.3	80.8	33.8
380-3	Inner Shell	Round, \emptyset 0.113 in.	L	51.1	82.0	32.4
380-4	Inner Shell	Round, \emptyset 0.113 in.	L	53.3	82.1	29.9
380-21-33	Inner Shell	Flat, 0.250 in. Gage	L	48.1	74.0	34.4



NASA Engineering and Safety Center Technical Assessment Report

Document #:
NESCP-RP-13-00852

Version:
1.0

Title:

Evaluation of Agency Non-code LPVs

Page #:
81 of 193

380-22-34	Inner Shell	Flat, 0.250 in. Gage	L	49.1	74.5	35.5
380-19-31	Shell Layer 2	Flat, 0.250 in. Gage	L	93.0	124.1	24.1
380-20-32	Shell Layer 2	Flat, 0.250 in. Gage	L	92.5	124.6	24.5
380-40	Outer Shell	Flat, 0.250 in. Gage	L	88.5	119.5	24.8
380-41	Outer Shell	Flat, 0.250 in. Gage	L	87.1	120.0	24.7
V0032 Lot Acceptance 1	Inner Shell	Not Given	Not Given	88.4	114.4	36.0
V0032 Lot Acceptance 2	Inner Shell	Not Given	Not Given	91.8	124.8	29.0
V0032 Lot Acceptance 3	Inner Shell	Not Given	Not Given	90.7	117.0	28.0
V0032 Lot Acceptance 4	Outer Shell	Not Given	Not Given	90.0	116.4	25.0
V0032 Lot Acceptance 5	Outer Shell	Not Given	Not Given	93.4	118.7	28.0
A. O. Smith Spec	Base Metal	Not Given	Not Given	77.0	105 - 135	22.0
V0032 Certification	Base Metal	Not Given	Not Given	77.0	Not Given	Not Given

* Elongation values referenced in Table 7.2.1.1-3 are provided for reference only, as the extensometer used for testing was verified to only 8%.

The strength test results suggested that a potential undocumented substitution of softer material or heat treatment modifications to the 1146a may have occurred for the V0032 inner shell during construction, possibly to avoid problems with hydrogen embrittlement, since V0032 was designed for gaseous hydrogen storage. An industry consultant suggested that based on his past experience, a lower strength steel like A-285 or A516 Grade 70 may have been substituted for the 1146a [ref. 56]. It may be worthwhile to investigate the inner shells of the available sister vessels to V0032 to determine whether their properties also show a discrepancy. In the larger context, the discrepancy observed for V0032 indicates that the manufacturer's data records, the originating source of material pedigree information, are not infallible. Uncertainty in the pedigree of the material should be recognized as a risk associated with these vintage LPVs. Generally, it is not feasible to independently test and verify the material pedigree of the inner layer materials in a vessel due to limited physical access.

Once this material discrepancy was discovered, no further testing was performed on the 1146a material from V0032, although the thinner, higher strength 1146a material in the V0032 outer layers should be part of future evaluations. The pedigree of the V0032 inner layer material was evaluated by chemical analysis. X-ray fluorescence (XRF) analysis was attempted, with the hope of differentiating the material from other candidates, such as 516 or A-285, based on the presence of vanadium as a discriminator (i.e., 1146 has vanadium, where most potential candidates do not). XRF is best used as a comparator against known standards. Without such reference standards in this case, the XRF results were simply inconclusive; therefore, inductively

	NASA Engineering and Safety Center Technical Assessment Report	Document #:	Version:
		NESCP-RP-13-00852	1.0
Title:			Page #:
Evaluation of Agency Non-code LPVs			82 of 193

coupled plasma (ICP) analytical chemistry tests were performed. ICP is more time consuming but produces very accurate chemistries, including many trace elements in metals. The ICP chemistry results are shown in Table 7.2.1.1-4.

Table 7.2.1.1-4. ICP Analytical Chemistry Composition Results for V0032 Inner Shell Material Compared with 1146a Specification Requirements (this material was designated as 1146a on the originating A. O. Smith manufacturer's report)

Material	ICP (Run 1)	ICP (Run 2)	1146a Specification	Agreement
Manganese (Mn)	1.26	1.29	1.10 to 1.50	Yes
Phosphorus (P)	<0.02	<0.02	0.040 max	Yes
Silicon (Si)	0.261	0.247	0.20 to 0.35	Yes
Vanadium (V)	0.154	0.156	0.13 to 0.18	Yes
Nickel (Ni)	0.555	0.556	0.40 to 0.70	Yes
Chromium (Cr)	0.065	0.066	Not Given	NA
Copper (Cu)	0.048	0.048	Not Given	NA
Carbon (C)	Not Given	Not Given	0.18 to 0.25	Unknown
Sulfur (S)	Not Given	Not Given	0.05 max	Unknown

Note: Specification agreement for chromium and copper is described as not applicable (NA) since these elements often existed in steels with a scrap component.

The levels of manganese, phosphorus, silicon, nickel, and vanadium were confirmed to meet the 1146a specification requirements. Carbon and sulfur were not reported, as the ICP test cannot measure those trace elements. A separate, targeted test for carbon was considered but not performed due to cost. Chromium and copper were also reported in small quantities. Because of these subtle ambiguities, the V0032 inner shell material remains unidentified. Based on the strength data and the chemistry results, this soft inner layer material is not expected to be representative of the general population of LPV materials in use across the Agency and, thus, will likely not be investigated further. The base metals evaluated in Task 2 were, therefore, limited to the 1143 and 1146 materials from the V0125 vessel. These materials are considered to be generally representative of the nominal LPV materials used for the shells by A. O. Smith LPVs in NASA's infrastructure, with the caveat that the 1146 material is not as strong as 1146a and is expected to have slightly greater fracture toughness than 1146a. An evaluation of properly representative 1146a material should be performed.

In reference to Table 7.2.1.1-3, lot acceptance data are provided for the LPV materials that were evaluated. Lot acceptance testing for 1143 inner shell material for V0125 demonstrated a minimum 70-ksi yield and 91-ksi ultimate strength minimum in one material lot. It appears that the 1143 material from V0125 did not meet the yield strength specification minimum of 75 ksi, which again underscores the confusion associated with the observed specification inconsistencies.

	NASA Engineering and Safety Center Technical Assessment Report	Document #: NESCP-RP- 13-00852	Version: 1.0
Title: Evaluation of Agency Non-code LPVs		Page #: 83 of 193	

7.2.1.1.3 LPV Materials Collected for Future Evaluations

An ongoing aspect of this assessment activity has been to identify material resources in the form of vessels available across the Agency and elsewhere that may be sacrificed to provide needed materials for evaluation. This collection of vessel materials will be critical to fulfill the recommended future testing required to evaluate each of the base materials and welds properly. Furthermore, a bulk of material from a variety of vessels will be critical to assessing the expected material variability present in the LPV fleet across the Agency. A considerable amount of the vessel materials have been collected at MSFC and are being carefully retained in long-term storage in anticipation of this future testing. As part of this collection effort, an A225 head from a multilayer vessel at GRC, designated as GRC Vessel PV0296, was obtained, as well as all of the remnant pieces from a multilayer vessel designated by serial number MV-50466-8 that was tested at SwRI[®] as funded by NASA OSMA and managed by ARC [refs. 44 and 45]. Vessel MV-50466-8 was fabricated from 1146a and A225. The original manufacturer's data report for the PV0296 vessel was unavailable, but the report for a representative vessel produced and delivered at the same time by the same vendor designated as serial number MV-50405 demonstrates that the PV0296 head material is likely A225 Gr. B. Vessel V0031, a sister vessel of similar size, construction, and service history to V0032, was also available. No material testing was performed on PV0296, MV-50466-8, or V0031 in this assessment.

7.2.1.1.4 Material Anisotropy

The correlation between the structural and material orientations must be identified first to orient and extract appropriate test specimens. As a general rule for FFS assessments, fracture mechanics material property data are generated on the plane within the material that provides the least capability. For most thin-plate materials, specimens are extracted such that the crack is oriented parallel to the direction of elongated material grains, usually the longitudinal rolling direction. This typically produces bounding material properties. This philosophy for generating material data on the least capable orientation is required if the material orientation in the vessel is not certain. The small selection of sacrificial vessels under consideration in this assessment has illustrated that material orientation cannot be assumed to be consistent. While this assessment has proceeded mindful of determining bounding fracture properties in-plane, the behavior of cracks growing radially through the thickness of the materials has not been evaluated. Tests for this behavior in the thin-shell materials would typically use a surface-crack geometry. These studies were beyond the scope of the current assessment but should be considered for future evaluation. Material orientations are specified relative to the original plate corresponding the material longitudinal (L), transverse (T), and short-transverse (S) directions. The structural orientations of a vessel are described by the circumferential (C), longitudinal (L), radial (R), and meridional (M, spherical head) directions.

Due to inexperience with these types of pressure vessel steels, significant anisotropy was not initially anticipated in the planning stages of this assessment and was not a part of the budgeting process when allocating the available assessment funding. This oversight required time and testing resources to resolve, hindering the ability to achieve the scope that was anticipated in the

	NASA Engineering and Safety Center Technical Assessment Report	Document #: NESCP-RP- 13-00852	Version: 1.0
Title: Evaluation of Agency Non-code LPVs		Page #: 84 of 193	

testing tasks; thus, the 1143 and 1146 materials were more completely characterized than A225 due to these complications. Although unfortunately coming to the attention of the planning team too late, the material anisotropy was clearly identified in the SwRI[®] findings resulting from the mechanical testing they performed on an A. O. Smith vessel MV-50466-8 for NASA ARC [refs. 44 and 45].

Due to this anisotropic behavior, the material orientation for each piece of material needed to be determined prior to orienting the final set of test specimens. The shell materials proved fairly easy to orient, given that they maintained distinct orthogonal rolling directions. The only question to be resolved was whether the shell material longitudinal direction was oriented circumferentially around the vessel or along the vessel axis. Fracture toughness tests were performed in these two orientations (C-L and L-C) to determine the material orientation, which was always made clear by a large reduction in toughness in the longitudinal direction of the shell material. (Note that in the two-letter fracture toughness orientation designations above and elsewhere in this report, the first letter indicates the direction of applied loading, and the second letter indicates the direction of crack extension.) Identifying the bounding toughness orientation in the A225 head material was considerably more complicated. Both selective microstructural investigation and instrumented Charpy impact testing were used to help identify the material orientation. The microstructural evaluations were inconclusive, but the Charpy impact testing proved informative. Further details on the efforts to identify material orientation are provided in the discussions of Task 1 and Task 2 results.

7.2.1.1.5 Lot Variability

Though the LPV fleet is comprised of nominally the same steels based on the A. O. Smith designations previously discussed, the LPV fleet contains vessels fabricated over a span of years and by different vendors and the steels may have been processed by different mills using different rolling procedures. The LPV steels are expected to contain significant lot-to-lot variability; thus, one cannot assume the data obtained in this study are directly applicable to all LPVs without a further characterization of this variability.

The initial plan for this assessment was to test from as many different lots of material as possible to diversify the testing and characterize the lot-to-lot variability. This goal shifted primarily due to technical reasons and, to a lesser extent, schedule reasons. The technical reason for the shift to single material lot evaluation was that the E 1921-13 Master Curve test method used in this investigation is best applied to a macroscopically homogeneous material having uniform and isotropic strength and toughness properties. Therefore, the proper way to approach the transition toughness evaluation is to test a sufficient quantity of specimens to independently evaluate each lot. The result from each lot can then be compared for variability. A subsequent analysis combining data across lots can then be assessed for comparison.

7.2.1.2 Fracture Toughness Testing

Fracture toughness testing was the focus of this effort because fracture toughness as a function of temperature is the most important material property for FFS assessment of the vessels. The fully

	NASA Engineering and Safety Center Technical Assessment Report	Document #: NESCP-RP- 13-00852	Version: 1.0
Title: Evaluation of Agency Non-code LPVs		Page #: 85 of 193	

ductile fracture toughness (upper shelf) and the temperature at the transition to cleavage fracture (transition range) were of interest. The Master Curve methodology from ASTM E 1921-13 [ref. 57] was used to facilitate the assessment of the fracture toughness data and determine the fracture toughness versus temperature behavior for the LPV materials. The Master Curve method is a robust approach to characterizing the temperature dependent fracture toughness of ferritic steels with as few as six test samples. The following background information on the Master Curve method will provide a brief introduction to the concept and convey the rationale for choosing this method to evaluate the LPV materials instead of using the more traditional impact energy (Charpy) methods.

Other than obvious schedule and cost constraints, the choice of a fracture toughness test method is usually dictated by the expected failure mechanism of the material. The two primary mechanisms by which fracture occurs in ferritic steels are ductile rupture and cleavage. These are micromechanisms for fracture that describe the mechanism by which a material fails at the microstructural level. Care is needed not to confuse these mechanisms with terms such as “ductile” or “brittle,” which are often used to describe the failure behavior of structures or specimens. Note that a ductile rupture fracture may very well occur in an unstable, “brittle” manner. This is common in many alloys used in the aerospace industry, such as high strength aluminum or titanium alloys. Ductile rupture occurs in metals that fail by the growth and coalescence of voids initiating from loosened or broken inclusions and second-phase particles. Cracks extend through this void coalescence process, driven by plastic deformation, ultimately leading to fracture in either a stable or unstable manner. This is the typical failure mechanism for structural steels when they are kept sufficiently warm and not loaded in a highly dynamic manner. In contrast, cleavage fracture is a much lower energy process that progresses by the splitting of atomic planes with little associated plasticity, resulting in a flat and faceted fracture surface. The cleavage fracture process is of primary concern in structural steels at reduced temperatures or high loading rates [ref. 58].

For ferritic body-centered-cubic steels, the fracture mechanism undergoes a demonstrative transition from ductile rupture to cleavage as temperature decreases, which leads to a concomitant decrease in fracture toughness. This temperature dependency of fracture toughness is common to all ferritic steels. The material property of most importance to ferritic structural steels in LPV applications, therefore, is the ductile-to-brittle transition temperature curve that quantifies the fracture toughness loss with decreasing temperature and identifies the probability that a cleavage fracture will occur. Despite the common use of the term “transition temperature” that implies a discrete temperature below which steels fail by cleavage fracture, the reality is more subtle and complicated. An “upper shelf” exists where temperatures are sufficiently warm to ensure fracture progresses by ductile rupture mechanisms. Fracture toughness is greatest on the upper shelf and is generally consistent and repeatable. As temperatures decrease (or loading rates increase), the steel enters into a “transition range” where ductile rupture and cleavage are competing fracture mechanisms. In this range, the fracture behavior becomes considerably more variable since both mechanisms are operative and fracture toughness values drop below those of the upper shelf.

	NASA Engineering and Safety Center Technical Assessment Report	Document #: NESCP-RP- 13-00852	Version: 1.0
Title: Evaluation of Agency Non-code LPVs		Page #: 86 of 193	

Determining this temperature range where cleavage fracture becomes probable is critical to understanding the reliability of the LPVs. Cleavage fracture events often result in unexpected, catastrophic structural failures. Historically, brittle fracture has been characterized by a linear-elastic fracture toughness test to determine K_{IC} , which treats the material in front of the crack tip as a homogeneous and elastic continuum. This simplistic approach is insufficient to characterize cleavage where the fracture process is governed by the random distribution of cleavage initiators, such as carbide particles or inclusions, in the highly stressed zone of material just in front of the crack tip. This makes cleavage initiation a strongly stochastic process that follows a weakest link model. Therefore, a statistical approach is needed to adequately characterize cleavage fracture. ASTM Standard E 1921-13 [ref. 57] couples modern fracture mechanics and statistical methods to define a statistically based curve of fracture toughness versus temperature that is derived using only fracture-mechanics-based test data. The statistical nature of the method allows confidence bounds to be determined. This elastic-plastic method utilizes the J -integral at the point of cleavage instability, J_C , which is converted into a stress-intensity equivalent, K_{JC} , and uses these data to define a curve of median fracture toughness, K_{JC} versus temperature. Performing elastic-plastic J tests and deriving K from J , as opposed to conducting linearly elastic K tests directly, was necessitated by specimen size limitations imposed by the thin, cylindrical pressure vessel layers. Specimens for J test methods can be as much as $1/40^{\text{th}}$ the size required for linear-elastic K tests and still maintain sufficient constraint to produce toughness data that are unaffected by sample size [ref. 59]. It would not have been possible to perform linear-elastic fracture toughness tests per ASTM E 399-12 due to the thin-layer material constraints in LPV shells. Test specimens could not be made large enough to obtain the linear-elastic fracture toughness, K_{IC} .

Though the use of the J -integral method greatly relaxes specimen size requirements for testing fracture toughness, it does not altogether remove the effect of specimen size from the process of evaluating cleavage. Because cleavage fracture is a stochastic process, the amount of material sampled during a test will affect the likelihood of a cleavage event occurring. Therefore, the thickness of the specimen brings a size effect into the process by dictating the volume of material sampled along the crack front. This size effect is simply the increase in the likelihood of having a cleavage initiation particle along the crack front for samples of increased thickness. This influence of specimen size is accounted for in the statistical treatment of the test data in ASTM E1921-13. E 1921-13 uses a standard thickness of 25.4 mm (1 inch) and provides statistical relationships to relate thinner or thicker specimen tests to obtain a standard output. An extension of this logic then must be used in the application of the standard result to the structural application [ref. 60]. The relatively thin specimens dictated by the shell materials require more size correction than those extracted from the comparatively thick head material. These size corrections also play a role in the proper application of cleavage fracture toughness data obtained from laboratory specimens to the prediction of fracture behavior in real structures like the LPVs.

The E1921-13 approach is referred to as the Master Curve method because it has been demonstrated that the fracture toughness versus temperature behavior for most ferritic steels conforms to one universal curve shape [ref. 60]. The Master Curve method is empirically

	NASA Engineering and Safety Center Technical Assessment Report	Document #:	Version:
		NESCP-RP-13-00852	1.0
Title:		Page #:	
Evaluation of Agency Non-code LPVs		87 of 193	

derived and supported by a wealth of data that includes thousands of tests generated over more than three decades [ref. 61].

The universal Master Curve is made specific for a given material by being positioned on a plot of K_{JC} versus temperature by means of T_0 , the reference transition temperature. ASTM E 1921-13 prescribes both experimental and computational procedures that are used to determine the reference temperature T_0 . This one value, the T_0 reference temperature, is the only unknown that needs to be determined from the test data to fully establish the Master Curve for the subject material. T_0 is defined as the temperature at which a set of data obtained with 1-inch-thick specimens will have a median K_{JC} of $100 \text{ MPa}\sqrt{\text{m}}$ based on testing six or more specimens at a single temperature. While this definition of T_0 may seem somewhat arbitrary, because the shape of the Master Curve has been empirically predetermined, the T_0 definition simply serves as a standardized anchor for positioning the Master Curve on the temperature axis. It is important to realize that T_0 is not the same as the historically common NDT, T_{NDT} , though the two values are easily reconciled.

T_0 and T_{NDT} can be reconciled by utilizing available ASME code cases, which are official responses from ASME to the user community when meaningful inquiries are raised about the ASME code so that the knowledge base can be expanded, the code adapts, and repetitive inquiries are avoided. Relevant to the Master Curve method are ASME code cases N-629 and N-631, which establish the basis for using a Master Curve-based index temperature derived from T_0 as an alternative to T_{NDT} . These code cases directly permit use of the Master Curve index temperature:

$$RT_{T_0} = T_0 + 35^\circ\text{F} \quad (\text{Eq 7.2.1})$$

This is an alternative to RT_{NDT} , where RT_{NDT} is related to the NDT from ASME Section III and ASME NB-2331. For pressure retaining materials other than bolting applications, ASME NB-2331 requires that the reference NDT RT_{NDT} is established:

$$RT_{NDT} = \text{MAX}\{T_{NDT}, T_{35/50} - 60\} \text{ (in } ^\circ\text{F)}$$

where T_{NDT} is the NDT from drop-weight testing from ASTM E 208-06 and $T_{35,50}$ is the transition temperature from Charpy V-notch specimens that exhibit at least 35 mils of lateral expansion and not less than 50 ft-lb of absorbed energy per ASTM E 23-12c. The use of RT_{NDT} was intended to account for heat-to-heat differences in fracture toughness transition temperature and collapse the data more completely into a single curve, but it does not do so as well as the Master Curve.

The assumption in using the Master Curve index temperature is that it should provide the same implicit margin between K_{IC} and measured fracture toughness data as the accepted RT_{NDT} approach. While the fundamental relationship between T_0 and RT_{NDT} has unfortunately not been derived, comprehensive statistical analyses against existing fracture toughness data has shown that the relationship between RT_{T_0} and T_0 used in the ASME code cases N-629 and N-631 (i.e., $RT_{T_0} = T_0 + 35^\circ\text{F}$) bounds 97.5% of existing fracture toughness data [ref. 61].

	NASA Engineering and Safety Center Technical Assessment Report	Document #:	Version:
		NESCP-RP- 13-00852	1.0
Title:		Page #:	
Evaluation of Agency Non-code LPVs		88 of 193	

RT_{NDT} is considered conservative compared to the fracture toughness versus temperature relationship determined by T_0 . The two methods differ in their approach. T_0 is a statistically based fracture mechanics method that allows for a direct determination of the transition temperature, whereas T_{NDT} is defined by a relatively simple bounding method where the impact energy for fracture of blunt-notched specimens drops below a given threshold.

Defining RT_{NDT} from T_0 is straightforward as given by the ASME code cases. On the other hand, defining the proper MDMT for the LPV fleet from this value will require additional study. The use of a Master Curve derived T_0 to define the RT_{NDT} (and subsequently an MDMT) rather than a T_{NDT} based on an impact energy threshold is expected to reduce conservatism in that value. (Note: the Master Curve was born out of necessity to reduce known conservatisms in the traditional RT_{NDT} method, so the nuclear power industry could demonstrate adequate safety in aging structures in use beyond their original design service objectives.) The key distinction to underscore is that the Master Curve is consistent with a risk-informed framework for decision making that provides best estimates of fracture toughness by means of an explicit description of uncertainty. The Master Curve provides two key features: a statistical description of fracture toughness at a single temperature and the relationship between fracture toughness and temperature.

The process used by E1921-13 to establish the Master Curve indexing temperature T_0 is essentially a four-step procedure:

1. Six to eight fracture toughness specimens are tested as near to the estimated T_0 as possible as long as fracture occurs due to cleavage¹. Estimates of T_0 can be made from statistical offsets based on Charpy impact tests, if available. The elastic-plastic fracture toughness at cleavage instability, J_C , is determined and converted to its corresponding elastic fracture toughness K_{JC} . Test data must then be statistically censored according to two primary censoring limits before the data can be used in the T_0 analysis. Any specimens exceeding a ductile crack extension limit in which the slow stable crack growth before cleavage fracture is greater than 5% of the initial remaining ligament or that experience a loss of constraint are regarded as invalid and must be statistically censored before being included in the analysis. Any specimens that experience a loss of constraint must also be statistically censored. This statistical censoring, performed in accordance with ASTM E1921-13, means that the measured value is replaced with a smaller value close to J_C , the ductile initiation toughness as near to the test temperature as possible. Censoring is also necessary if the elastic-plastic fracture toughness exceeds a small-scale deformation limit $K_{JC(limit)}$ defined in E 1921-13 that depends on the specimen dimensions and the material's yield strength. For the steels tested here, this limit was not

¹ The fracture toughness tests are performed in accordance with ASTM E 1820-11, according to the basic test method from sections 8.1.2 and A2.4.2.1 without compliance unloading. As the basic test method is used, only this cleavage instability J_C is determined from a given test as opposed to a full J-R curve, which would be typical of unloading compliance fracture tests. That only J_C is determined as compared to the complete J-R curve is sufficient for determining T_0 . The basic method facilitates fracture testing when cleavage instability is expected, since unloads may occur in the vicinity of a cleavage instability and obfuscate the ability to determine cleavage initiation.

	NASA Engineering and Safety Center Technical Assessment Report	Document #:	Version:
		NESCP-RP- 13-00852	1.0
Title:		Page #:	
Evaluation of Agency Non-code LPVs		89 of 193	

approached, and this censoring was not required. Compact tension C(T) specimens are preferred over single-edge notch bend SE(B) specimens because T_0 differs for measurements made with C(T) and SE(B) specimen geometries due to differing constraints. C(T) specimens have higher constraint and produce higher (more conservative) T_0 temperatures. All test data generated for purposes of determining T_0 in this investigation were measured from C(T) specimens² [ref. 49]. All specimens must be tested in the crack orientation corresponding to the lowest toughness in the material.

2. The K_{JC} data are statistically corrected based on specimen thickness to the equivalent of a 1-inch-thick specimen, referred to as 1T. This correction reflects the fact that cleavage is a stochastic process, dependent on the length of the crack front. Inherent to this conversion is the assumption that there is a lower shelf at which fracture energy reaches an asymptotic limit and is independent of temperature. The conversion of data to the 1T equivalence is necessary because the Master Curve method physically assumes that the cleavage fracture mode is modeled by a weakest link process by which the fracture process is determined by the failure of a single cleavage initiation site and assumes that a random distribution of cleavage initiation sites exists through a given sample width. There is no special incentive for the choice to normalize to the 1T thickness, other than that provided a single, convenient, and common specimen width around which to develop a set of closed-form equations for T_0 .
3. The temperature T_0 at which the 1T equivalent K_{JC} is $100 \text{ MPa}\sqrt{\text{m}}$ is determined. The evaluation of T_0 from the test data inherently assumes that the toughness data are well described by the Master Curve. (This assumption can be confirmed if a sufficient quantity of data is generated, as was generally the case in this assessment.) Toughness data that are obtained closer to the T_0 temperature are preferentially weighted, and all tests must be within 50°C of T_0 to be considered valid. The 50°C window around T_0 exists because the weakest link assumptions become invalid as the upper and lower shelf temperatures are approached [ref. 60]. Some iteration on temperature is to be expected to determine T_0 ; thus, a provisional estimate of T_0 is needed after the first three to four fracture tests are completed to ensure test temperature remains within the 50°C window. The combination of a low upper shelf toughness K_{JC} that is below $100 \text{ MPa}\sqrt{\text{m}}$ and the thin specimens available required testing close to the $T_0 - 50^\circ\text{C}$ limit, which in turn required the testing of 8 to 10 samples rather than the minimum of 6. The extra data did, however, permit a better assessment of the E 1921-13 standard for the case of interest and as discussed below.
4. Based on the statistical procedures in ASTM E 1921-13, the median K_{JC} of the 1T data population corresponding to a 50% cumulative probability for fracture is determined and plotted. This curve is referred to as the Master Curve for the subject material. The

² A SE(B) fixture was manufactured, and a procedure for using the fixture for performing fracture tests on precracked Charpy V-notch samples was developed during this effort but was not used for measuring fracture data to be used in determining T_0 . This fixture and procedure, however, are available for future testing, as necessary.

	NASA Engineering and Safety Center Technical Assessment Report	Document #: NESCP-RP-13-00852	Version: 1.0
Evaluation of Agency Non-code LPVs			Page #: 90 of 193

Master Curve statistical model provides the ability to define probability levels other than the median, such as 95% and 5% probabilities of cleavage; thus, upper and lower statistically bounding confidence intervals are also calculated and plotted. The distribution of data with respect to the Master Curve should be evaluated to ensure that the curve-fit is loyal to the original data and described well by the Master Curve.

This four-step procedure was used for each of the base metal evaluations discussed in the following sections.

7.2.1.2.1 Task 1: A225 Head Material Fracture Toughness Reference Transition Temperature

In order to perform mechanical tests on the pressure vessels, they were coarsely sectioned into smaller segments to better accommodate machining test specimens. These cut plans are shown below in Figures 7.2.1.2-1 and 7.2.1.2-2.

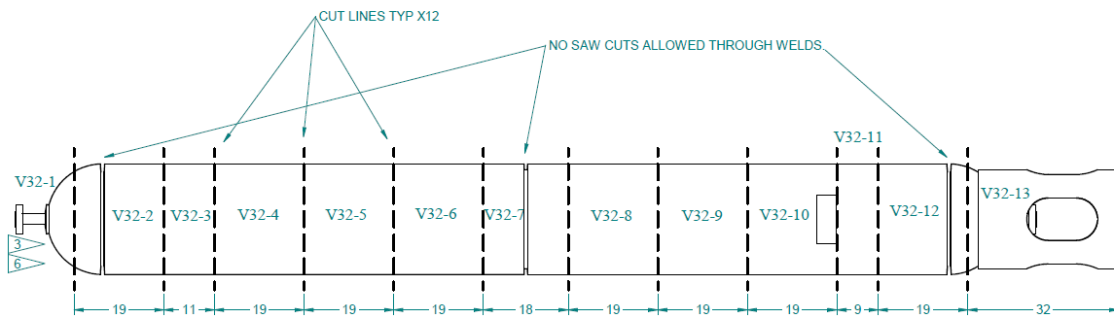


Figure 7.2.1.2-1. V0032 Gross Sectioning Plan (drawing number CP-380)

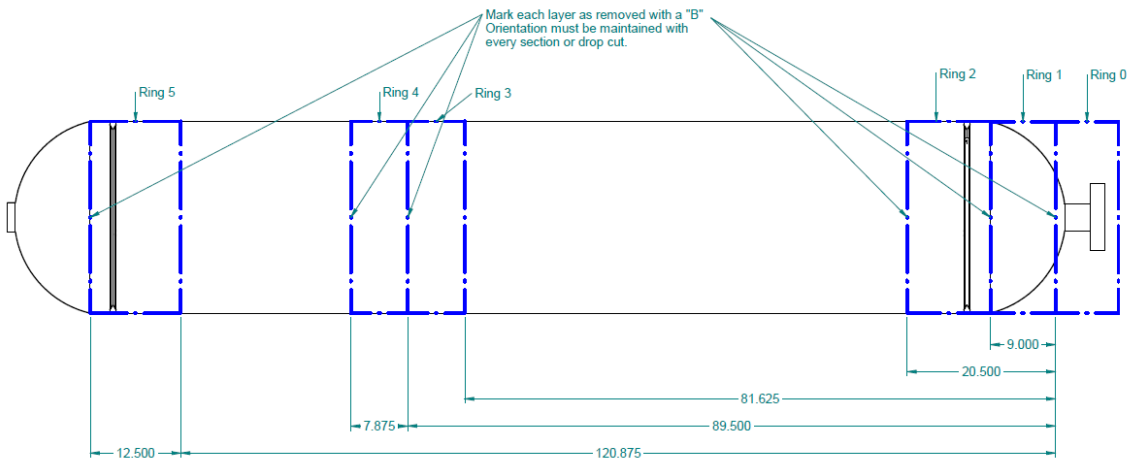


Figure 7.2.1.2-2. V0125 Sectioning Cut Plan (drawing number CP-344)

Task 1 of the materials characterization effort was to evaluate T_0 for the A225 head material. The A225 material testing was afforded highest priority based on historical accounts and anecdotal evidence that the A225 material may be the highest risk to cleavage at common vessel

	NASA Engineering and Safety Center Technical Assessment Report	Document #: NESCP-RP- 13-00852	Version: 1.0
Title: Evaluation of Agency Non-code LPVs		Page #: 91 of 193	

operational temperatures. The A225 testing initially focused on the heads from V0032 and the head material provided from the GRC PV0296 vessel. The decision to reduce focus to single lots for base metal testing led to using only V0032 head material in the current assessment. As mentioned in the prior discussion of anisotropy, the biggest challenge of the A225 material involved identifying the lowest toughness orientation in the head. At the time of this writing, the A225 T_0 test series is still ongoing. This section discusses the considerable efforts invested in determining microstructural orientation. The plan to determine microstructural orientation began with a traditional metallographic approach. When metallographic methods proved inconclusive, a series of Charpy impact tests were used to provide further quantitative insight.

Metallographic microstructural evaluations at 50 \times and 100 \times magnifications were performed on A225 material from V0032 and GRC V0296 for determining material orientation³. (Note: testing of the V0296 head was still ongoing when this report was prepared.) Nine total samples in three orthogonal planes (C-M, R-C, and M-R) were taken at three equidistant circumferential locations around each head with 45 $^\circ$ spacing between samples. Three samples were taken as close as possible to each nominal circumferential location as possible to expedite the metallurgical evaluation, instead of evaluating a single sample. Evaluation of a single sample would have required its polishing mold to be broken in order to evaluate a different sample face. As such, a small tradeoff in accuracy was accepted for expediency. Photographs and cut plans of the location in which blanks were evaluated from the V0032 head are provided in Figures 7.2.1.2-3 and 7.2.1.2-4.



Figure 7.2.1.2-3. V0032-1 Sectioned for Metallographic Microstructural Examination for Determining Material Orientation

³ Performed by Element in Houston, TX.



Title:

Evaluation of Agency Non-code LPVs

Page #:
92 of 193

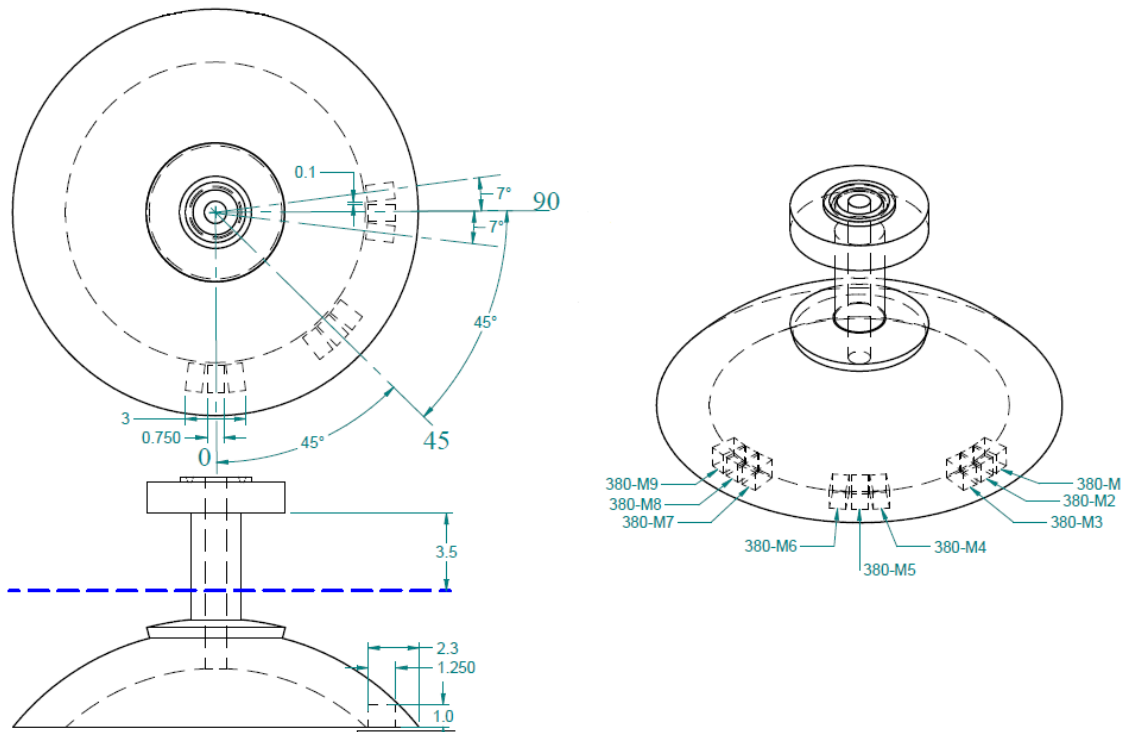


Figure 7.2.1.2-4. V0032-1 Cut Plan for Metallographic Microstructural Evaluation for Determining Material Orientation

The 0° location was chosen arbitrarily since there was no unique feature on the axisymmetric head that would indicate how the head was fabricated with respect to the parent plate. Each dimension of the metallurgical blanks was unique to maintain traceability of the macro orientations. The macros revealed no discernable microstructural evidence of the plate orientation prior to forming. For V0032, the microstructure appeared to be independent of the circumferential location with a uniform grain structure generally following the shape of the head. Although the same Nital etching process (3% nitric acid, balance methanol) was followed for the samples from both heads, the grain orientation for GRC V0296 was much less apparent in the microstructural samples and even less useful in determining material orientation.

The V0032 microstructure was dominated by what appeared to be considerable banding of pearlite and ferrite, which is undesirable (see Figure 7.2.1.2-5). The dark bands are pearlite, and the lighter bands are ferrite. This banding is possibly a result of microsegregation of alloying metals during the solidification of the original ingot, which was not ideally homogenized during the subsequent heat treatment. Alloying elements always segregate to some extent during the solidification of steel. Elements that are especially prone to segregation are carbon, phosphorus, sulfur, silicon, and manganese [ref. 62]. Manganese is especially problematic because it lowers the chemical activity of carbon in austenite, from which pearlite is formed. The manganese-rich areas are, thus, the last to transform and are mostly pearlite [ref. 63]. During the microstructural evaluations, the banding features were observed regardless of the sample orientation or angular

	NASA Engineering and Safety Center Technical Assessment Report	Document #:	Version:
		NESCP-RP-13-00852	1.0
Title:			Page #:
Evaluation of Agency Non-code LPVs			93 of 193

location. These microstructural features likely obscured any visible anisotropy introduced into the material from the original plate production.

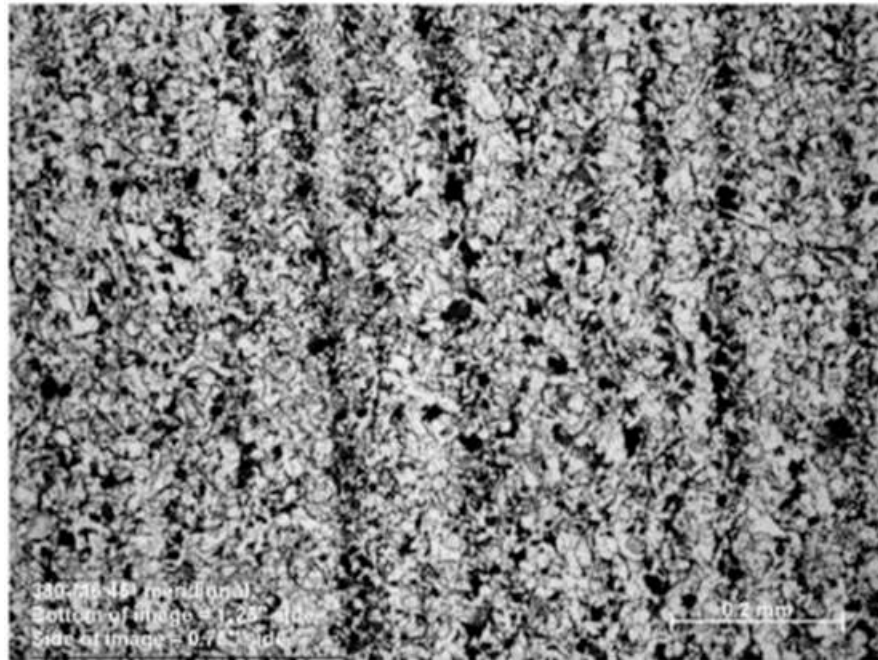


Figure 7.2.1.2-5. Microstructural Evaluation at 50× Magnification of A225 Material from Vessel V0032 showing Banding of Pearlite and Ferrite on Meridional Face (both radial and circumferential faces demonstrated similar features)

These inconclusive microstructures, showing either no orientation or spherical banding following the head, were not expected. There was an expectation that the prior plate microstructure would remain dominant. Although exact historical records are incomplete, information on the typical head fabrication process was obtained from an industry consultant⁴. For forming a head such as V0032, the steel mill would start with a thick slab of commercial A225 and roll the plate at a temperature close to 1,000°F between two rolls to reduce the thickness. In this process, one primary direction would be stretched the most and become dominant—the plate longitudinal (L) direction. The orthogonal direction in the flat plane of the plate is identified as the transverse (T) direction. Based on the desired surface area of the hemisphere, the head manufacturer would cut an appropriately sized disk out of the plate. The head manufacturer would usually heat the blank disk to around 800 to 900°F and press it between male and female dies in small increments in order to attain the desired head dimensions and form.

Based on this manufacturing process, the head forming operations would not be expected to eliminate the prior plate microstructure, but rather the plate material orientation was projected over the head while retaining much of the original orthogonality. If the prior plate

⁴ Information provided by Maan Jawad, Consultant.

	NASA Engineering and Safety Center Technical Assessment Report	Document #: NESCP-RP- 13-00852	Version: 1.0
Title: Evaluation of Agency Non-code LPVs		Page #: 94 of 193	

microstructure remains, then the microstructure would continuously change circumferentially around the head, lining up with a prior plate orientation every 90°. The lack of such structure implies that the head material may have experienced an intermediate thermal treatment to eliminate the plate microstructure. Determining grain orientation by macros is commonly difficult in steels, particularly when the macros are arbitrarily oriented, as in this case. Given the inconclusive nature of these microstructural studies, a more quantitative approach with Charpy specimens was undertaken.

Instrumented Charpy V-notch tests according to ASTM E 2298-13 [ref. 64] were performed as a quick, relatively inexpensive yet quantitative way to determine the material orientation in the A225 head material from V0032. Due to deciding to focus on one lot of material, impact tests on the GRC V0296 head were not performed under this assessment. Instrumented Charpy tests utilize strain gages to capture the load versus displacement record at specimen impact. It is a more robust method than traditional Charpy tests, even if the load versus displacement is used only qualitatively as an aid to evaluate the fracture mechanism between a brittle and ductile failure. The instrumented test is also preferred for its precision in measuring fracture energy; it is more precise than monitoring pendulum height after impact. This precision also serves to lower the minimum range of impact energies that can be reliably measured, which can be important with cleavage. Given cost considerations, samples were limited to two at each of the three circumferential locations in two orthogonal orientations, M-C and C-M. Note that the direction of loading and crack extension is the same for Charpy specimens; therefore, in the two-letter orientation designation for the Charpy specimen, the first letter indicates the direction of the long axis of the specimen, and the second letter indicates the direction of crack extension. The cut plans for these samples are shown in Figure 7.2.1.2-6. Sample size was ASTM E23-12c type A, with a 10-mm by 10-mm square cross section and 55 mm long—the standard specimen used for ferrous metals.

The results of these Charpy tests are shown in Table 7.2.1.2-1 and Figure 7.2.1.2-7. All tests were conducted at 0°F. Regarding the test temperature, these tests were not intended to determine the transition temperature but were simply used to reveal the least tough microstructural orientation in the material for subsequent fracture testing. The prior work by SwRI[®] indicated that 0°F would be a good choice for determining anisotropy for this material because orientation impact energy differences appeared to be largest at 0°F in their tests [ref. 44]. More informative fracture toughness tests were considered for determining the material orientation, but due to the required quantity the Charpy tests were more financially viable.



NASA Engineering and Safety Center Technical Assessment Report

Document #: **NESCP-RP-13-00852**

Version: **1.0**

Title:

Evaluation of Agency Non-code LPVs

Page #: **95 of 193**

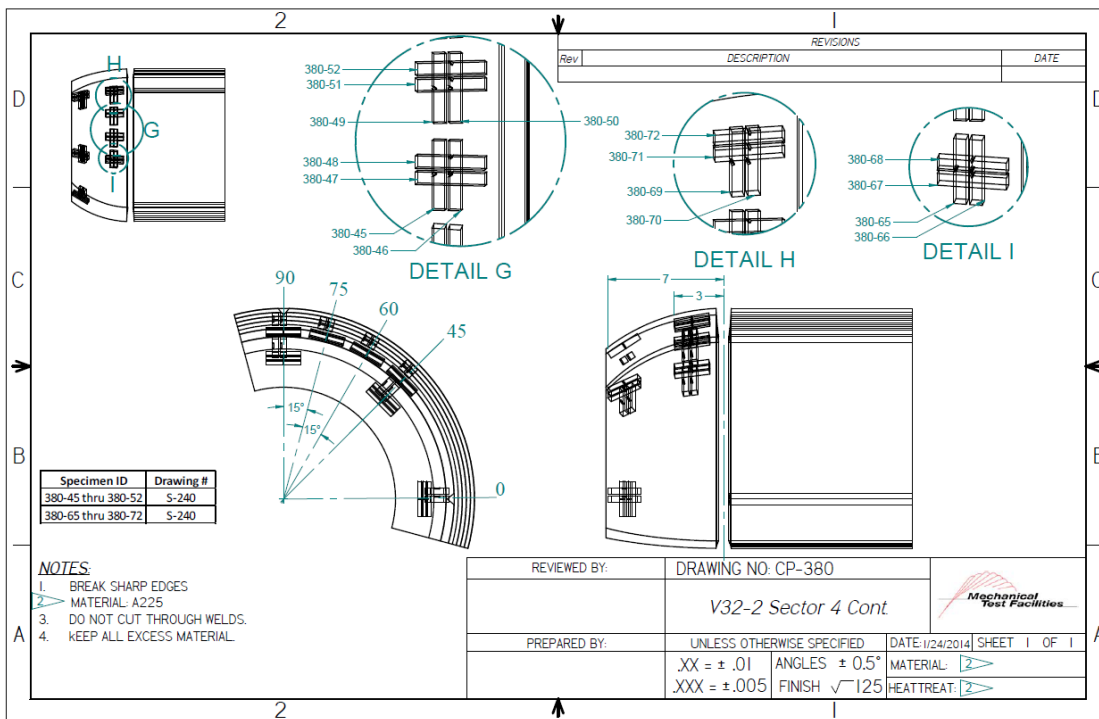
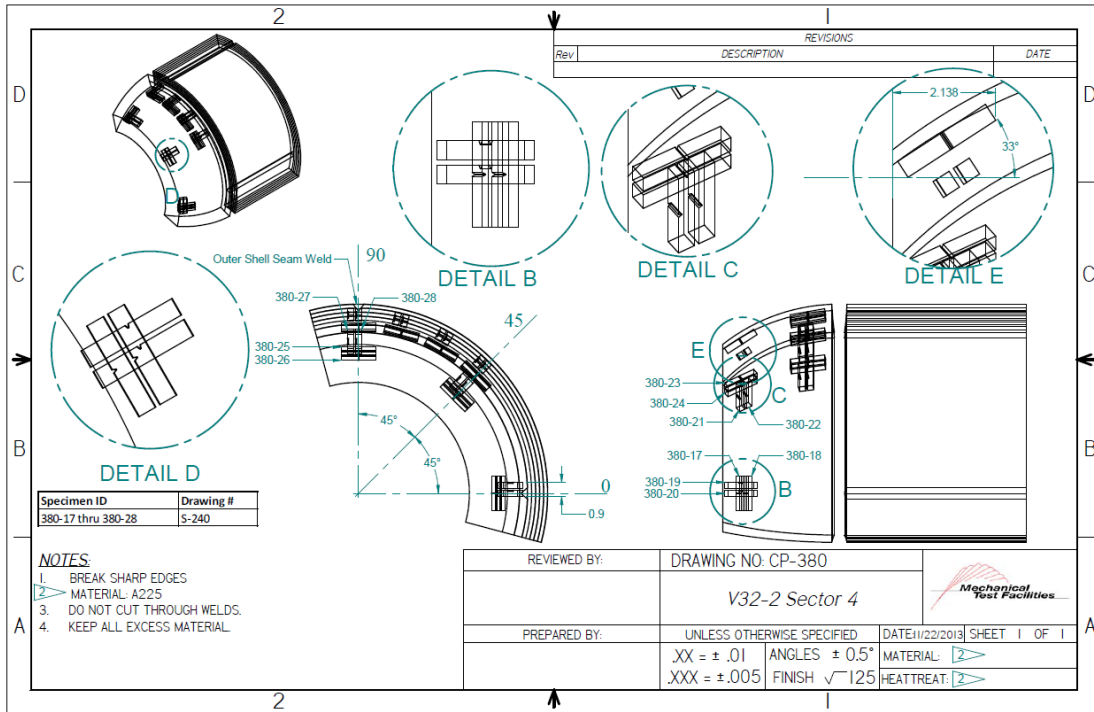


Figure 7.2.1.2-6. Cut Plan for V0032 Charpy Impact Samples

	NASA Engineering and Safety Center Technical Assessment Report	Document #:	Version:
		NESCP-RP-13-00852	1.0
Title:			Page #:
Evaluation of Agency Non-code LPVs			96 of 193

Table 7.2.1.2-1. Charpy V-notch Impact Energy Results for V0032 A225 Head Material

Sample ID	Vendor Test ID	Temp (F)	Theta (deg)	Meridional Location	Orientation	Impact Energy (ft-lbs)	Lat Exp (mils)	% Shear
CP-380-17	U09577	0	0	1	C-M	73.88	39	80
CP-380-18	U09578	0	0	1	C-M	66.83	34	40
CP-380-19	U09579	0	0	1	M-C	84.60	42	40
CP-380-20	U09580	0	0	1	M-C	90.85	44	40
CP-380-21	U09581	0	45	1	C-M	39.36	20	30
CP-380-22	U09582	0	45	1	C-M	34.28	20	30
CP-380-23	U09583	0	45	1	M-C	142.86	71	90
CP-380-24	U09584	0	45	1	M-C	135.21	71	80
CP-380-25	U09585	0	90	1	C-M	43.74	23	50
CP-380-26	U09586	0	90	1	C-M	42.60	22	30
CP-380-27	U09587	0	90	1	M-C	123.06	57	80
CP-380-28	U09588	0	90	1	M-C	111.80	55	70
CP-380-45	U33589	0	60	2	C-M	36.03	19	20
CP-380-46	U33590	0	60	2	C-M	36.91	18	20
CP-380-47	U33591	0	60	2	M-C	136.89	66	80
CP-380-48	U33592	0	60	2	M-C	186.76	81	100
CP-380-49	U33593	0	75	2	C-M	47.24	24	30
CP-380-50	U33594	0	75	2	C-M	44.66	26	35
CP-380-51	U33595	0	75	2	M-C	168.58	72	100
CP-380-52	U33596	0	75	2	M-C	163.52	75	100
CP-380-65	U47089	0	45	2	C-M	43.89	27	20
CP-380-66	U47090	0	45	2	C-M	39.18	19	20
CP-380-67	U47091	0	45	2	M-C	167.64	74	80
CP-380-68	U47092	0	45	2	M-C	200.16	72	100
CP-380-69	U47093	0	90	2	C-M	44.31	23	30
CP-380-70	U47094	0	90	2	C-M	44.50	27	40
CP-380-71	U47095	0	90	2	M-C	177.24	78	100
CP-380-72	U47096	0	90	2	M-C	162.75	67	90

Note: Testing at 0 degrees F was to establish materials properties and should not be interpreted as a basis to safely operate LPVs at this temperature.

The Charpy impact results showed that the C-M orientation produced significantly lower impact energies than the M-C orientation with invariance to the sample circumferential location. This matches the observed orientation of the microstructural banding in the V0032 head material. It is possible that the material anisotropy effects in the V0032 head are being dominated by this banding structure. Future tests on head material without the banded microstructure may yield different results. It is suggested that all future efforts to identify the material orientation for pressure vessel heads predominantly utilize Charpy impact testing. Having attempted microstructural orientation evaluation in the A225 head material in the SwRI® work, the GRC PV0296 head material, and the V0032 head, none of these investigations has provided the clarity of the Charpy impact data. Despite this finding, as future A225 material is evaluated it is suggested that the basic microstructure of the head material be documented for features such as banding.



Title:

Evaluation of Agency Non-code LPVs

Page #:
97 of 193

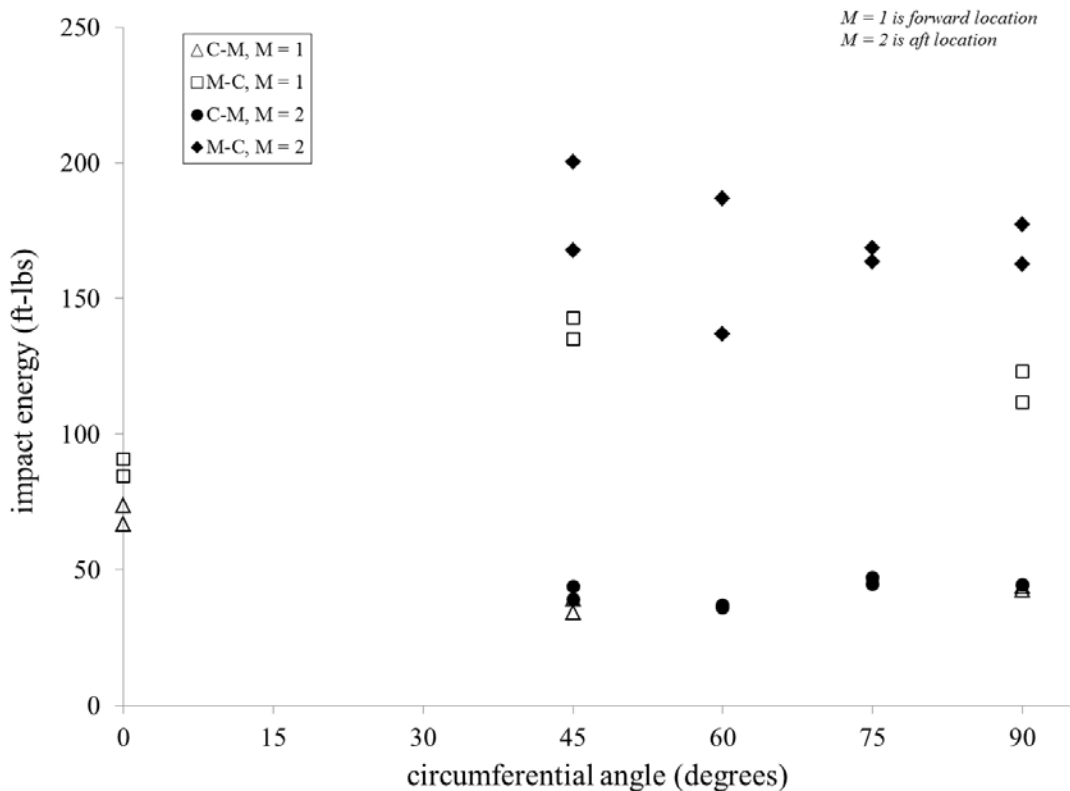


Figure 7.2.1.2-7. Charpy V-notch Impact Test Results for V0032 A225 Head Material
(note strong separation between C-M and M-C orientations without dependence on circumferential angle)

Based on the Charpy impact results, a cut plan was developed for A225 material from V0032, which is shown in Figure 7.2.1.2-8. All fracture toughness specimens are to be tested in the C-M orientation, which was determined as the lowest toughness orientation. Based on the unexpected delays caused by the time required for identification of material anisotropy, these fracture toughness specimens are still in process at the time of this writing. Due to time constraints, a survey through the thickness of the A225 head was also not performed to determine the bounding radial location for the samples. Accordingly, fracture samples are planned to be tested at two radial locations as shown in the cut plan. The feasibility of combining these two radial location data sets will be investigated in future work.



NASA Engineering and Safety Center Technical Assessment Report

Document #:
**NESCP-RP-
13-00852**

Version:
1.0

Title:

Evaluation of Agency Non-code LPVs

Page #:
98 of 193

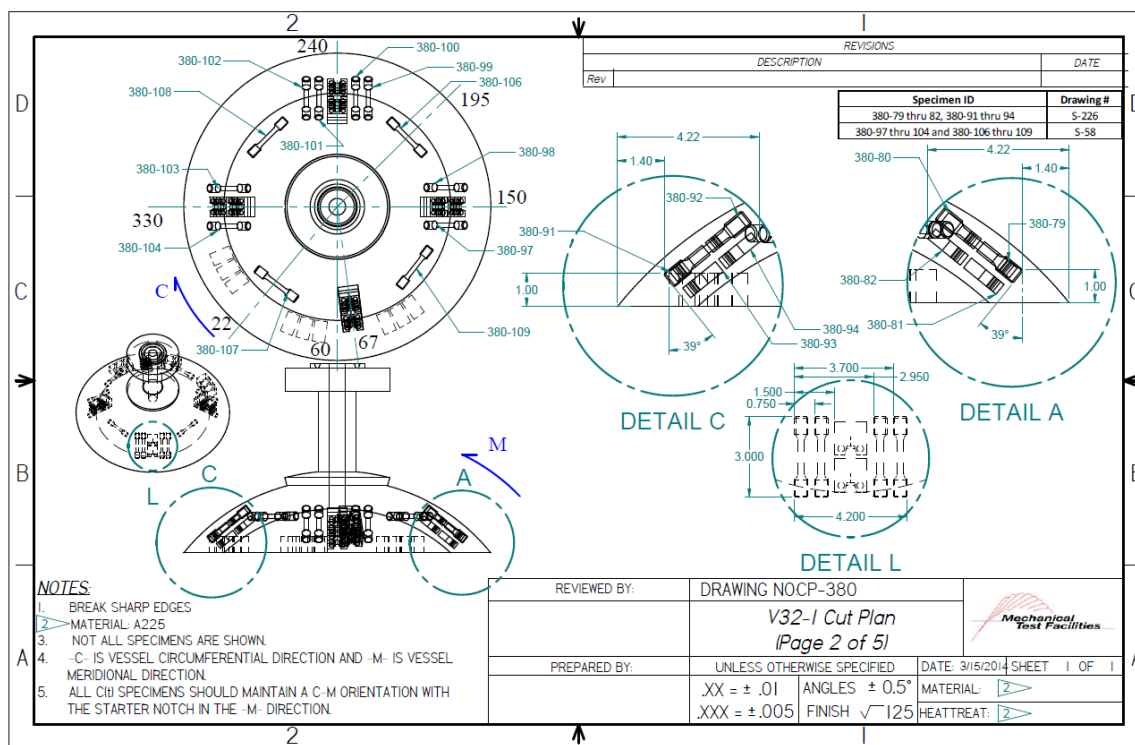


Figure 7.2.1.2-8. Partial Cut Plan for Fracture Toughness and Tensile Test Specimens from A225 Head Material from V0032 Showing Salient Features of Full Cut Plan (the full cut plan shows detailed views of all specimens, but those views are self-similar to the views currently shown and are omitted for simplicity)

7.2.1.2.2 Task 2: Shell Materials Fracture Toughness Reference Transition Temperature

The objective of Task 2 of the materials characterization effort was to determine the toughness transition reference temperature T_0 per ASTM E 1921-13 [ref. 33] for the LPV shell materials. This study was limited to 1143 and 1146 shell materials. Absent from this study was the 1146a material, which was initially based on the assumption that 1146 and 1146a were expected to produce nearly equivalent properties. The 1143 material was tested from the inner shell of vessel V0125. Where possible, inner shell material was preferred for testing because the greater thickness meant that thicker fracture toughness specimens could be machined and less of a statistical size correction would need to be made to account for the weakest link cleavage process. The 1146 material was not available from an inner shell and was tested from the outer layers of V0125. In reference to the master cut plan for V0125, the 1143 and 1146 samples were all taken from section 4. This selection was arbitrary but helped minimize the costs of performing additional machining operations on large vessel sections. Testing of these materials was confined to single vessels and layers so that the material would be representative of a single material lot.

	NASA Engineering and Safety Center Technical Assessment Report	Document #: NESCP-RP-13-00852	Version: 1.0
Title: Evaluation of Agency Non-code LPVs		Page #: 99 of 193	

Prior to testing the shell materials, as with A225 head material, material orientation needed to be determined with respect to the vessels such that samples could be machined from the material in the lowest toughness orientation. Based on the assumption of logical manufacturing processes where the shells are rolled from thin sheets and from prior SwRI[®] testing results [ref. 44], this task was inherently much more direct for the shells than the head because there were only two possible complementary layouts for the shell materials:

1. The longitudinal (L) direction of the plate material was coincident with the longitudinal (L) direction of the vessel. This would be evaluated with C-L fracture samples.
2. The longitudinal (L) direction of the plate material was coincident with the circumferential (C) direction of the vessel. This would be evaluated with L-C fracture samples.

To determine the material orientation, two standard ASTM E 1820-11 [ref. 65] fracture toughness tests were each performed at room temperature in the C-L and L-C orientations for each material and vessel section tested. These data were used to determine the material orientation, which would allow for test samples to be produced for determining T_0 from the Master Curve method.

For the 1143 material, fracture toughness tests performed at room temperature on the inner shell of section 4 from V0125 showed that the initiation fracture toughness was approximately 40% lower for the C-L orientation than for L-C. Fracture surfaces are shown in Figure 7.2.1.2-9. Neither of these tests produced a fully valid J_{IC} or K_J value, but the results were sufficiently advisory on material anisotropy. Given this outcome, all specimens for determining T_0 from the Master Curve method for 1143 V0125 section 4 materials were obtained in the C-L orientation. Inspection of the fracture surfaces for the two orientations confirmed the results, as the L-C surfaces were much more ductile than the C-L surfaces. Since the C-L orientation represents that the specimen loading direction was in the vessel circumferential direction with a crack plane in the vessel longitudinal direction, then, given the observed anisotropy, this inner shell was oriented in the lowest fracture toughness orientation with respect to the hoop loading direction in the vessel. This suggests that material anisotropy was not a consideration in the original vessel design, further confirming the need to use the lowest toughness orientation throughout any FFS evaluations of the LPV fleet. However, the results from the current study may not apply universally to all vessels; thus, in conducting further fracture toughness testing on materials from different lots and different manufacturers, it will be necessary first to determine the weakest orientation.

For the 1146, material taken from the outer shells of section 4 from V0125 showed that the initiation fracture toughness was approximately 45% lower for the C-L orientation than L-C; thus, all 1146 specimens were also made in the C-L sample orientation.

It is important to note that, to reduce material and labor costs, plates were sometimes rolled into cylinders with the plate transverse direction in the vessel longitudinal direction and sometimes in the vessel circumferential direction.

	NASA Engineering and Safety Center Technical Assessment Report	Document #:	Version:
		NESCP-RP-13-00852	1.0
Title:			Page #:
Evaluation of Agency Non-code LPVs			100 of 193

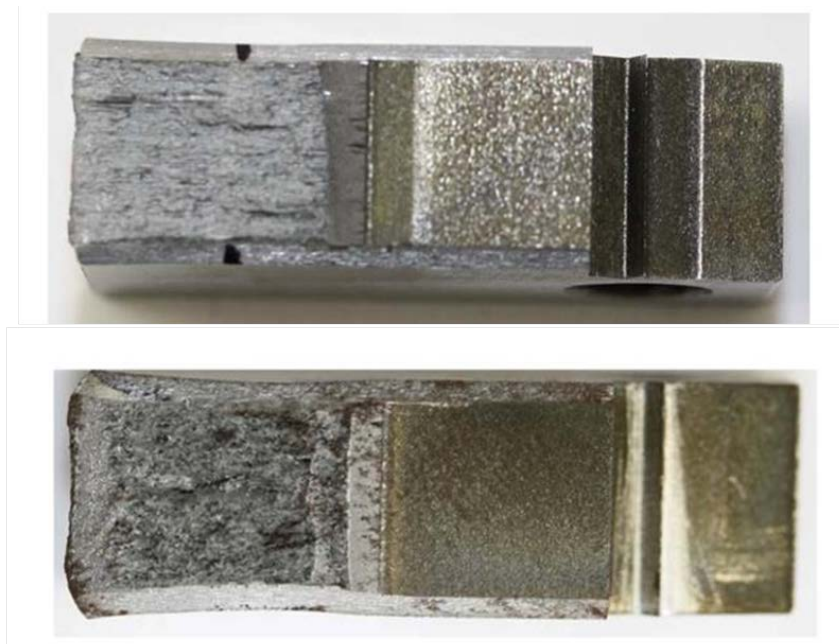


Figure 7.2.1.2-9. Comparison of Fracture Surfaces for Fracture Toughness Tests Performed in C-L Orientation (upper image) and L-C Orientation (lower image)

A total of 18 basic method fracture toughness tests were performed on C-L 1143 C(T) specimens over the range of -20 to -180°F . This range was required because the test temperatures were continually decreased until the samples failed due to cleavage, a requirement for the Master Curve method. The initial temperature selected for testing was -20°F based on the available Charpy impact energy data obtained by SwRI[®] for the LPV materials [refs. 44 and 45] and the procedure from ASTM E 1921-13, Section 8.4.1 [ref. 25], but significantly colder temperatures were required for cleavage.

The fact that colder temperatures than initially predicted were needed to produce cleavage in the 1143 material is advantageous for the FFS outcome of LPVs fabricated with 1143 material. However, this meant that more tests than initially planned were required to produce a large enough data set to evaluate T_0 per ASTM E 1921-13. In total, one fracture toughness test was performed at -20°F , one at -70°F , four at -120°F , five at -170°F , and four at -180°F , for a total of 15 tests. The data are shown in Table 7.2.1.2-2. Of the 15 tests, 9 were fully valid and 6 have not yet been included in the current analysis due to failing certain data qualification limits⁵. The Kronecker delta shown in the table indicates whether the K_{JC} data point is a fully valid data point

⁵ The six tests that are currently excluded are not unconditionally excluded. In fact, ASTM E 1921-13 explicitly contains a special censoring process for such data so that they may be included in the analysis. This censoring procedure was attempted but is currently incomplete because i) there is a difficulty with applying the censoring procedure for the LPV materials that exhibited a very flat crack resistance R-curve (indicating that the fracture resistance did not monotonically increase with growing crack size) and ii) even though the E1820-12 Basic Method is advantageous for measuring cleavage initiation fracture toughness, the Basic Method is not conducive to the censoring procedure.

	NASA Engineering and Safety Center Technical Assessment Report	Document #:	Version:
		NESCP-RP-13-00852	1.0
Title:		Page #:	
Evaluation of Agency Non-code LPVs		101 of 193	

or whether a data qualification limit was exceeded. When $\delta_j = 0$ at the j th K_{JC} value, then a data qualification check has failed and that data point must be censored in order to be included in the analysis. Data are used unconditionally when $\delta_j = 1$. Censoring, as defined by E1921-13, is a specific, conservative substitution process to ensure the data are well described by cleavage. The term itself may be somewhat misleading since censoring often means deleting or removing, but in the context of E1921-13 censoring does not mean that the data are eliminated from the analysis. Instead, if certain qualification limits are not satisfied, then in order to be included in the analysis, statistical censoring requires that a conservative estimate for K_{JC} must be substituted for the K_{JC} datum that was obtained. This statistical censoring is necessary since the method applies a standard statistical analysis to measured data. Statistical censoring is an accepted method with a long history, and E 1921-13 has simply adapted it for its purposes. The two qualification limits for censoring are:

- The loss of plastic constraint
- Excessive ductile crack growth before the onset of cleavage

First, the plastic constraint condition requires that the specimen remaining ligament $b_0 = W - a_0$ have sufficient size to maintain a condition of high crack-front constraint at fracture. This constraint is the three-dimensional stress state at the crack tip, and a high constraint condition is required to conservatively measure cleavage fracture toughness. The maximum K_{JC} capacity of a specimen is given by E 1921-13 as

$$K_{JC(Limit)} = \frac{Eb_0\sigma_{ys}}{30(1 - \nu^2)}$$

K_{JC} data that exceed this requirement must be first used in a data censoring procedure to be included in the analysis. The censored data must be replaced in the analysis by the $K_{JC(limit)}$ value. The argument is that while the value of K_J at the onset of cleavage is unknown for this specimen, it exceeds $K_{JC(limit)}$, and this information should be included in the statistical analysis of the data set. In the case for the steels investigated, none of the tests failed this censoring requirement.

Second, a K_{JC} datum is also invalid if too much slow, stable crack growth occurs before cleavage failure. The limit allowed for this stable portion of crack growth is the smaller of either 0.05 b_0 or 0.040 inches (b_0 is the length of the remaining uncracked ligament after precracking but prior to testing). This latter condition is necessitated because the E1921-13 method is premised on a physical model that assumes a cleavage failure mechanism, and the volume of material sampled grows dramatically as the crack moves through the material. For the size of the C(T) specimens tested in this effort, this meant that ductile crack growth was not allowed to exceed approximately 0.025 inches before the sample failed due to cleavage to be considered a valid test, which is determined by post-test measurements of the fracture surface. This post-test measurement is a standard procedure in fracture testing. As shown in Table 7.2.1.2-2, six tests failed this data qualification limit and could not be used in the T_0 analysis without censoring.

	NASA Engineering and Safety Center Technical Assessment Report	Document #:	Version:
		NESCP-RP-13-00852	1.0
Title:			Page #:
Evaluation of Agency Non-code LPVs			102 of 193

Table 7.2.1.2-2. T_0 Transition Reference Temperature Data for 1143 Material from V0032 in Bounding Material Orientation

Sample	B_0 , in	T , °F	J_C , in-lbf/in ²	K_{JC} , ksi√in	$K_{JC} (1T)$, ksi√in	δ_j
344-4-38	0.3738	-179.8	60.1	43.7	38.1	1
344-4-41	0.3753	-180.1	69.2	46.9	40.6	1
344-4-42	0.3743	-170.5	93.9	54.6	46.7	1
344-4-44	0.3735	-170.8	100.3	56.4	48.1	1
344-4-46	0.3735	-180.2	106.7	58.2	49.5	1
344-4-24	0.3748	-170.1	117.6	61.1	51.8	1
344-4-39	0.3742	-179.9	199.5	79.6	66.2	1
344-4-23	0.3748	-120.2	220.0	83.6	69.4	0
344-4-25	0.3762	-170.1	227.3	85.0	70.5	1
344-4-28	0.3742	-171.5	234.2	86.2	71.4	1
344-4-22	0.3752	-121.5	241.6	87.6	72.5	0
344-4-17	0.3770	-20.1	334.9	103.1	84.7	0
344-4-20	0.3757	-121.6	353.2	105.9	86.9	0
344-4-18	0.3767	-70.2	403.0	113.1	92.6	0
344-4-19	0.3743	-120.3	405.5	113.5	92.7	0

A separate validity criterion requires that the test temperature be within $\pm 50^\circ\text{C}$ of T_0 . If this condition is not met, then the data do not describe cleavage behavior well in the transition regime. In this case, no censoring procedure is appropriate, and the data must be excluded from the T_0 analysis per ASTM E 1921-13. This requirement can be procedurally difficult to meet since T_0 is not known *a priori* and is, in fact, what is being measured. Fortunately, while many tests were close to violating this condition, none actually did so.

Sufficient data were produced for calculating T_0 , even with the interim exclusion of the censored data. Based on the nine valid tests, T_0 was determined to be -71.0°C (-95.8°F). This should be considered a provisional but generally representative T_0 since the censoring process has not been performed and the inclusion of censored data is expected to change T_0 slightly. This provisional T_0 is expected to be conservative compared with the fully qualified T_0 determined with the censored data included.

The reference transition temperature T_0 is not equivalent to T_{NDT} , but a Master Curve-based index temperature RT_{T_0} can be determined, which can be used as a substitute for RT_{NDT} . This can be determined based on equation (7.2.1) to be $RT_{T_0} = T_0 + 35^\circ\text{C} = -71.0^\circ\text{C} + 35^\circ\text{C} = -36.0^\circ\text{C}$ (-32.8°F) for the 1143 material.

	NASA Engineering and Safety Center Technical Assessment Report	Document #: NESCP-RP- 13-00852	Version: 1.0
Title: Evaluation of Agency Non-code LPVs		Page #: 103 of 193	

It is noteworthy to consider that because T_0 was not known before completing the tests and analysis, it is not surprising that some tests did not fail due to cleavage before the ductile crack extension limit was reached as test temperatures were iteratively decreased. Historical testing of nuclear grade materials, which are much tougher than the materials tested for the LPV program, conventionally violate the plastic constraint data qualification limit. Due to considerably lower toughness, this was not of concern for the LPV materials; no tests came close to violating this limit. Conversely, there were many tests on the LPV materials that failed the ductile crack extension limit, which upon thorough analysis revealed some difficulties in censoring based on this limit. Censoring is required in the case of excessive ductile crack growth before fracture because if the sample experienced an appreciable amount of ductile crack growth before failure, then the fracture is not described as cleavage. In such cases, the measured fracture toughness following considerable crack extension needs to be bounded by a lower K value in order for the cleavage fracture assumption to be valid. This lower K value is determined as the lesser of either (1) K_{JIC} at the coldest possible temperature at which it can be measured or (2) the value of $K_{J_{\Delta a}}$, which is the value of K in the specimen at the point in the test where the 0.025-inch ductile crack extension limit, was violated.

In regard to the LPV material tests, the issue is that these limiting K values are difficult to determine given the LPV material behavior and the test method that was used. Determining the $K_{J_{\Delta a}}$ value requires knowledge of the ductile J -integral resistance curve as the crack grows, which requires crack length data as it grows throughout the test. The test method used in this assessment does not provide that feedback. This choice involves a trade between running tests inexpensively with some that may not be valid, versus a more time intensive and complicated test that provides crack length feedback. At the beginning, the choice was to utilize the simpler method, and this approach has been sufficient. However, this choice has also left a number of tests lingering with the ductile crack extension invalidity. It remains undetermined whether a change to the more complicated test is warranted to avoid these invalid tests.

The other means of getting a proper censoring reference test is to determine the coldest value of J_{IC} feasible to provide the K_{JIC} . A few tests were attempted for the 1143 material at -120°F but were unsuccessful. During the tests, increases in displacement occurred without a corresponding change in load, indicating a test issue such as ice buildup on the measurement gage or possible carbide or manganese locking [ref. 66]. These tests will be further pursued to obtain a proper censoring K_{JIC} . As an alternative in the absence of such data, ASTM E 1921-13, Section 10.2.2, requires the use of the highest uncensored $K_{Jc(1T)}$ in the data. In the 1143 data set, this corresponds to specimen 344-4-25, with a value of $70.5 \text{ ksi}\sqrt{\text{in}}$. This exceeds the $K_{Jc(1T)}$ value for only 344-4-23 and, thus, does not make a reasonable censoring value for that specimen. However, this value would be acceptable in the absence of a better alternative to use as a censoring value for the five other censored tests. At the time of this writing, this procedure has not yet been applied.

It was determined from this test program is that testing at colder temperatures and then testing warmer, as needed, is likely a more effective method than testing in a decreasing temperature pattern. The former method is likely to converge more quickly on the temperatures required for

	NASA Engineering and Safety Center Technical Assessment Report	Document #:	Version:
		NESCP-RP-13-00852	1.0
Title:			Page #:
Evaluation of Agency Non-code LPVs			104 of 193

cleavage. One caveat to this is the cautionary note that testing at exceptionally cold temperatures is not recommended because the test temperature must be within 50°C of T_0 for it to be useable in the T_0 analysis. It is noted that for both the 1143 and the 1146 material the testing temperatures ultimately required to produce cleavage pushed close to the extent of this allowable testing window. Too much weight should not be placed on Charpy impact methods, which can be overly conservative.

A total of 17 basic method fracture toughness tests were performed on C-L 1146 material over the range 32°F to –60°F. To date, 1 test was performed at 32°F, 1 at –20°F, 2 at –50°F, and 13 at –60°F. The data are shown in Table 7.2.1.2-3. Of the 17 total tests, 11 were fully valid and 6 will require censoring and have not been included in the current analysis. When considering only the fully valid data, sufficient data were measured for calculating T_0 . This provisional T_0 was determined to be –2.6°C (27.3°F). Based on Equation (7.2.1), RT_{T0} is determined to be –2.6°C + 35°C = 32.4°C (90.3°F). The 1146 material clearly has a much higher T_0 than the 1143 material, which was not predicted based on the strength properties shown in Table 7.2.1.1-3. This provisional T_0 is considered generally representative but is expected to change when the censored data are included in the analysis. Censoring the 1146 data according to ASTM E 1921-13, Section 10.2.2, is not possible because the highest uncensored $K_{Jc(1T)}$ in the data corresponds to specimen 344-4-30, with a value of 68.1 ksi√in. This exceeds the $K_{Jc(1T)}$ value for all of the uncensored specimens and, thus, is not a reasonable censoring value.

Table 7.2.1.2-3. T_0 Transition Reference Temperature Data for 1146 Material from V0032 in Bounding Material Orientation

Sample	B_0 , in	T , °F	J_C , in-lbf/in ²	K_{Jc} , ksi√in	$K_{Jc} (1T)$, ksi√in	δ_j
344-4-49	0.191	–59.8	94.6	54.9	42.4	1
344-4-51	0.1905	–60.8	116.7	61.0	46.4	1
344-4-14	0.1995	–60.8	142.8	67.5	51.0	1
344-4-29	0.2453	–60.1	140.6	66.9	52.4	1
344-4-35	0.2442	–60	141.3	67.1	52.5	1
344-4-52	0.1901	–59.8	164.3	72.4	53.9	1
344-4-50	0.1906	–59.7	165.0	72.5	54.0	1
344-4-15	0.1978	–60.1	179.9	75.7	56.5	1
344-4-34	0.244	–60.3	179.8	75.7	58.5	1
344-4-48	0.1901	–60.5	209.9	81.8	60.1	0
344-4-33	0.2435	–60	192.6	78.4	60.4	1
344-4-16	0.1985	32	221.4	84.0	62.0	0
344-4-12	0.1962	–50.3	238.7	87.2	64.0	0



NASA Engineering and Safety Center Technical Assessment Report

Document #:
**NESCP-RP-
13-00852**

Version:
1.0

Title:

Evaluation of Agency Non-code LPVs

Page #:
105 of 193

344-4-13	0.1993	-50.8	257.3	90.5	66.4	0
344-4-11	0.1968	-20	268.3	92.5	67.6	0
344-4-32	0.2435	-59.8	249.5	89.2	67.9	0
344-4-30	0.245	-60.9	250.4	89.3	68.1	1

All specimens tested to determine T_0 for both the 1143 and the 1146 material were of C(T) geometries, with the specimen thicknesses maximized given the constraints of the thin shell layers. The cut plans specified cutting the specimens to the full thickness with minimal cleanup. Multiple nominal thicknesses were tested for the 1146 material for no other reason than that the machinists became more adept with experience at maximizing the specimen thickness.

Master Curve plots for the 1143 and 1146 materials are shown as the red lines in Figures 7.2.1.2-10 and 7.2.1.2-11, respectively. Ninety-five-percent confidence bounds have been determined according to E 1921-13 and are also shown as the black dashed lines.

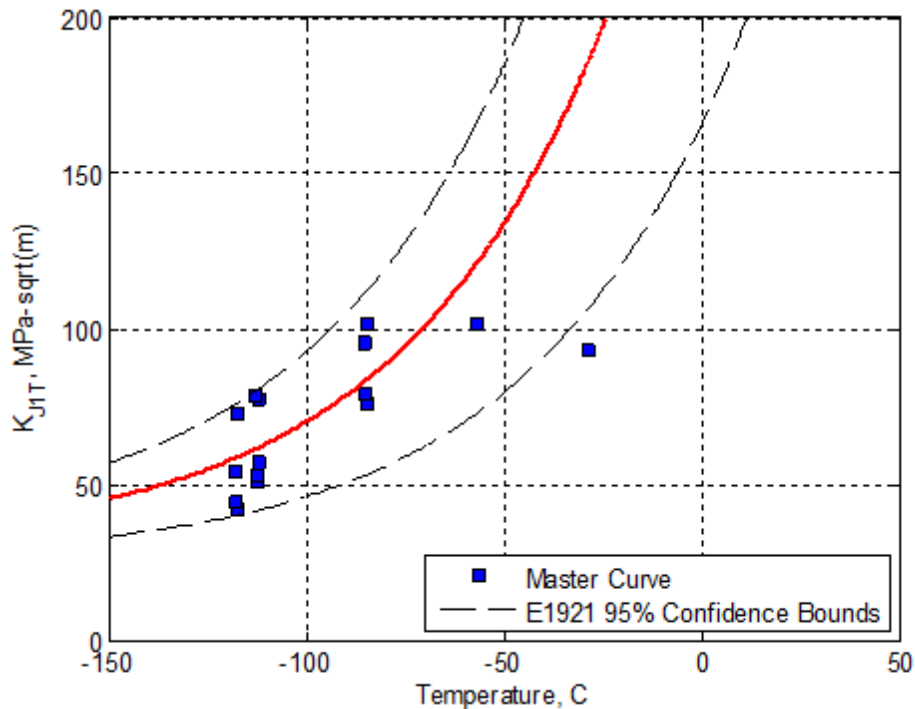


Figure 7.2.1.2-10. Master Curve Plot for 1143 Material

	NASA Engineering and Safety Center Technical Assessment Report	Document #:	Version:
		NESCP-RP-13-00852	1.0
Title:			Page #:
Evaluation of Agency Non-code LPVs			106 of 193

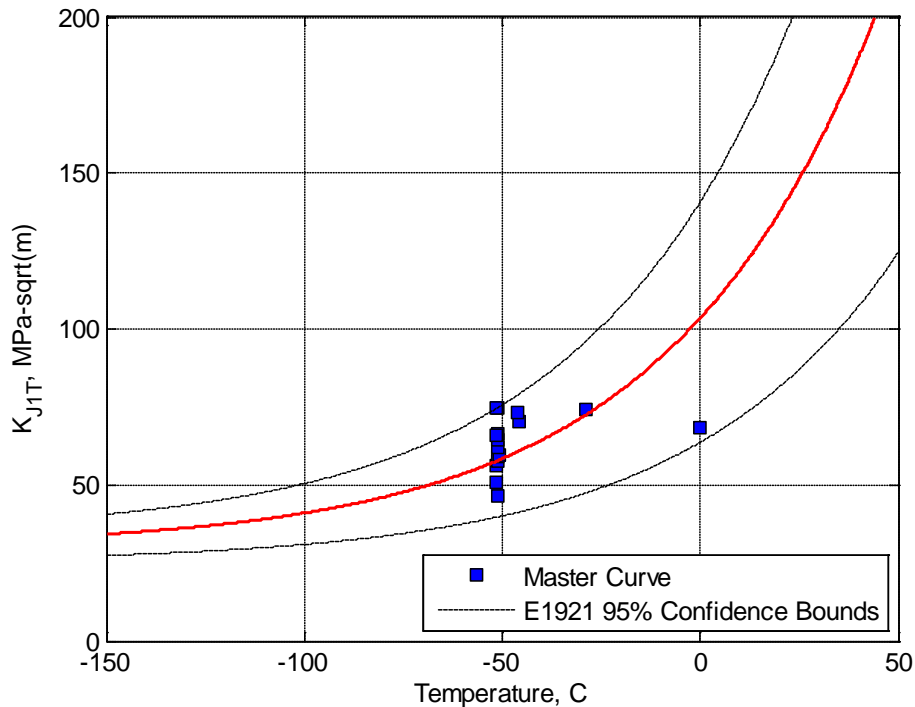


Figure 7.2.1.2-11. Master Curve Plot for 1146 Material

Note that certain details of determining T_0 have been purposely omitted from this report, as they were not considered germane to the principal LPV scope. Except for the use of only non-censored data, the analysis for T_0 was done according to ASTM E 1921-13. Since not using censored data removes the highest toughness data from the analysis, any revised T_0 will be higher and, hence, less conservative than the values reported here. These details and all supporting data are planned to be completely provided in a separate NASA Technical Memorandum.

7.2.1.2.3 Use of Fracture Toughness Values from T_0

The work described in the previous sections for generation of T_0 values for the head and shell materials marks the first step in the process of determining the performance of these materials in the presence of defects as a function of the use temperature and material thickness (as related to potential crack front length). It must be clear that the T_0 value is only a reference value anchored at a toughness of 100 MPa√m for an equivalent 1-inch-thick specimen. The 1-inch-thick reference specimen size establishes the 1-inch crack front length as the standard sampling volume of material relative to randomly occurring cleavage initiators, such as carbide particles. The T_0 value must not be confused with the MDMT used to limit vessel temperature in use. The T_0 value should be considered only a convenient way to express the fracture toughness of the material as a function of temperature with a statistically substantiated model of the data. There are a number of ways future work may utilize these T_0 values to arrive at a MDMT for a given vessel. First, as discussed in Section 7.2.1.1.5, it is important to recognize that the fracture

	NASA Engineering and Safety Center Technical Assessment Report	Document #: NESCP-RP- 13-00852	Version: 1.0
Title: Evaluation of Agency Non-code LPVs		Page #: 107 of 193	

toughness testing performed to date represents the performance of only a single lot of the 1143 and 1146 alloys. Additional evaluation of T_0 across many lots, including all alloys and welds, representing the larger LPV fleet is needed before obtaining T_0 values that may be considered representative of the entire LPV population. Once fully representative values for T_0 are produced, there are two likely ways that the T_0 value will be used to evaluate an MDMT. The first is to use the T_0 model for thickness correction to develop a set of curves for the LPV materials along the lines of the Charpy exemption curves shown in Section VIII, part UCS-66 [ref. 1]. This family of curves, covering a variety of specific pressure vessel steels, has classically been used to set the MDMT as a function of material thickness for vessels fabricated from the specified materials or by the bounding curve (A) for general carbon steels. This approach is consistent with the traditional Section VIII design criteria and provides a rationale for MDMT independent of the actual defect state within the vessels; however, its safe application to older, non-code vessels requires further evaluation. A second approach to using T_0 to develop an MDMT is to use a vessel-specific FFS logic, using rationale based on fracture mechanics assessment in accordance with ASME FFS-1 [ref. 32]. This approach has the advantage of adapting to a given vessel's use conditions (i.e., pressure and temperature), so it may provide additional flexibility. Although this approach is perhaps more appropriate to the older, non-code LPVs because it starts with the assumption that the vessel includes crack-like defects, the need for this assumption is also the distinct disadvantage of this method. As discussed in detail in this report, the LPV design currently precludes quantitative NDE. This leaves the FFS approach potentially unanchored in many sections of the LPV. Regardless of approach, there remains a considerable body of research to properly define the MDMT for the LPV fleet. The currently reported T_0 values are merely the beginning of the process.

7.2.1.3 Evaluation of Weld Microstructural Regions

The third task of this assessment involved investigating various representative welds of the LPV system to begin the process of specifying a method for fracture toughness testing in the weld regions. The welds are significantly more likely to contain defects that cause concern for the FFS of the LPV fleet; therefore, the toughness of the welds is of considerable interest. The evaluation of the weld material is complicated by the presence of nonuniform microstructure and residual stress. The toughness of the weld can vary significantly within the same joint, such as the weld nugget, the fusion lines, or the HAZs on either side. A common method to begin the process of understanding the propensity for toughness debits across a weld is to look at the local hardness in the microstructure across the various zones of the weld. Frequently, the zone with the lowest toughness will present itself with the highest local hardness. To evaluate this, each of the representative welds in the V0125 vessel was cross-sectioned and mounted for microstructural evaluation. A microhardness traverse was done across representative sections of the weld. One example is shown in Figure 7.2.1.3-1 for the head-to-shell weld of V125. The small white marks are reflections from the dents made by the microhardness indenter. Figure 7.2.1.3-2 shows the results of three of the hardness traverses.



Title:

Evaluation of Agency Non-code LPVs

Page #:
108 of 193

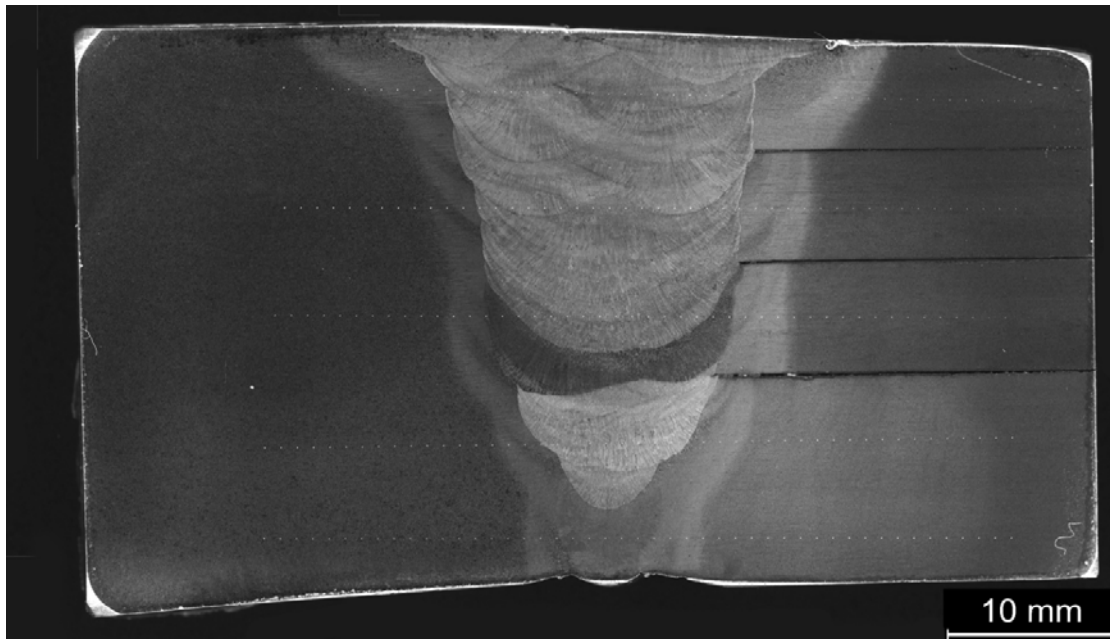


Figure 7.2.1.3-1. Microhardness Traverses Taken across the V0125 Head-to-Shell Weld

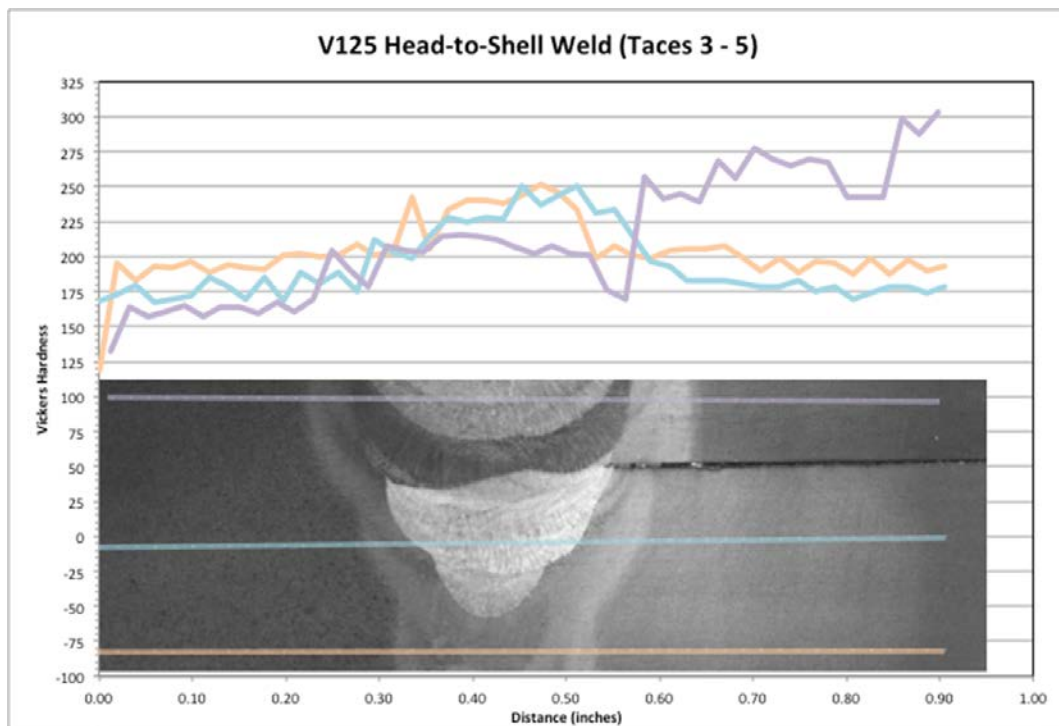


Figure 7.2.1.3-2. Microhardness Traverses Illustrating Hardness Response Differences in Inner Layer and First Thinner Layer in V0125

	NASA Engineering and Safety Center Technical Assessment Report	Document #:	Version:
		NESCP-RP-13-00852	1.0
Title:			Page #:
Evaluation of Agency Non-code LPVs			109 of 193

The microhardness profiles are well behaved, showing gradual changes across the weld zones and no isolated regions of particularly high hardness. Because the LPV welds do not receive a post-weld heat treatment, it was expected that the hardness would vary more than observed in these data. This is a preferred result from the perspective of the weld performance—there do not appear to be high-strength/low-toughness zones within the welds, but reducing the burden for testing the various zones across the welds does not help as was hoped. Though of largely uniform hardness, the microstructures (and residual stresses) do vary across the weld. The weld location of least toughness will have to be determined through toughness testing. Though not accomplished as part of this assessment, preliminary weld region toughness tests are currently in planning.

As another means of evaluating weld quality while helping to determine any systematic occurrence of weld process defects, a radiographic inspection of 1146a wrapping-layer longitudinal-seam welds was performed on approximately 50 inches of weld from section 11 of V0032 after the vessel section was dissected to reveal the welds [ref. 67]. For this vessel, each layer is joined to the adjacent layer by a single longitudinal seam weld, as shown in Figure 7.2.1.3-3. The five longitudinal welds in the 10-inch-long section comprised the 50 inches that were inspected. Sampling the quality of these seam welds is important because there is currently no NDE method available for the longitudinal shell welds for intact LPVs and because the original LPV mechanical drawings typically specified only limited NDE inspection, including RT of inner shell longitudinal welds and some MT of longitudinal shell welds. Data from these inspections are not available.

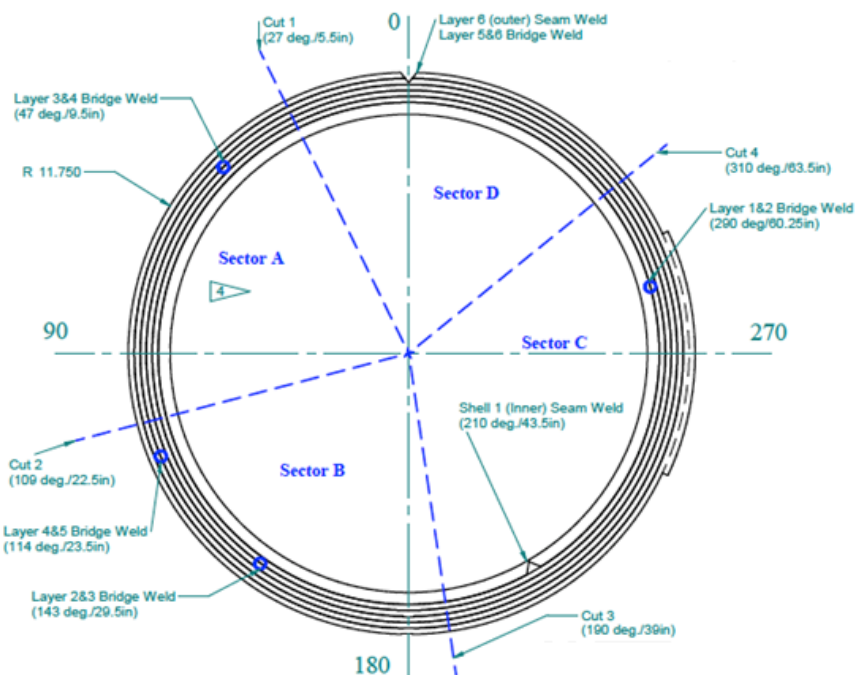


Figure 7.2.1.3-3. Cross Section for V0032-11, Evaluated by RT for Longitudinal Shell Welds Shown

	NASA Engineering and Safety Center Technical Assessment Report	Document #: NESCP-RP- 13-00852	Version: 1.0
Title: Evaluation of Agency Non-code LPVs		Page #: 110 of 193	

The inspections performed in the current evaluation were conducted on dissected sections comprised of two layers with an individual longitudinal weld. The goal was to determine the typical weld quality, including the location, type, size, and number of defects per linear foot of the welds, and whether a pattern emerges in the nature of these observed defects. Pattern refers to any outstanding characteristic or feature in the observed defects, with special interest in features that might impact the final FFS rationale. RT was a first attempt at characterizing the longitudinal shell welds, with the understanding that one of the limitations of RT is that it does not reliably detect cracks that are not open and are not optimally oriented with respect to the direction of the beam.

The V0032 section 11 results showed considerable porosity and lack of fusion, with all welds inspected failing the inspection criteria per ASME Section VIII [ref. 1], Appendices 4 and 12. Appendix 4 is specific to rounded RT indications. Appendix 12 is referenced so that lack of fusion can be included as a rejectable indication, as the BPVC does not include this callout under RT. Given this unfavorable inspection result, five additional longitudinal seam welds from V0032 section 8 were inspected utilizing the same inspection method [ref. 68]. Section 8 was a 19-inch-long segment, which at the time of this writing brings the total inspected length of V0032 longitudinal welds to approximately 145 inches. All of the longitudinal seam welds inspected in V0032 to date have failed to meet ASME Section VIII due to lack of fusion and porosity.

An additional set of RT inspections was performed on ring 4 from V0125 to determine possible vessel-to-vessel longitudinal weld quality differences [ref. 69]. As a four-layer vessel, this included the inspection of three welds, each approximately 8 inches in length. In contrast to V0032 (an A. O. Smith vessel), no rejectable conditions were found in the longitudinal seam welds of V0125 (constructed by CB&I). Overall, the quality issues that were observed (lack of fusion and porosity) are probably more indicative of weld processing issues than material quality issues. Additional RT inspection is needed to build a sufficient family of data to provide a broader assessment. This work is currently ongoing with additional evaluations planned for V0032 and V0125 and other available vessel materials.

7.2.2 WRS Modeling of LPVs

Introduction

Remaining life assessment of the aging NASA LPV vessels requires that a fatigue and fracture mechanics FFS assessment be performed. The WRS caused during LPV fabrication can strongly affect both fracture response and fatigue life⁶. The purpose of this effort is to perform weld analyses of several different typical layered vessels to determine the WRS fields in the layered shells. Two NASA vessels were chosen for WRS analysis: (1) a small, four-layer vessel and (2) a large, 14-layer vessel. This report summarizes the results for the small four-layer vessel; the results for the larger vessel will be reported later. These analyses will be compared with those of monolithic shells to determine the layering effect on WRS fields. If the layering effect

⁶ WRS can affect corrosion growth, but this is not considered a problem in the NASA LPV tanks.

	NASA Engineering and Safety Center Technical Assessment Report	Document #: NESCP-RP-13-00852	Version: 1.0
Title: Evaluation of Agency Non-code LPVs		Page #: 111 of 193	

is found to be small, it is possible that the WRS fields for use in fracture assessment may be obtained from monolithic vessels, which permit much easier analysis. In addition, if the layering effect is small, the use of solutions that appear in the API-579 code [ref. 32] may be permissible.

Geometry

Only the results for the four-layer tank circumferential weld are provided here. The smaller vessel was evaluated first because of its simpler construction (fewer layers) so that the layered vessel weld analysis procedure could be refined before addressing a larger vessel. The description of this tank is discussed in [ref. 70]. A schematic of the weld geometry as modeled can be seen in Figure 7.2.2-1.

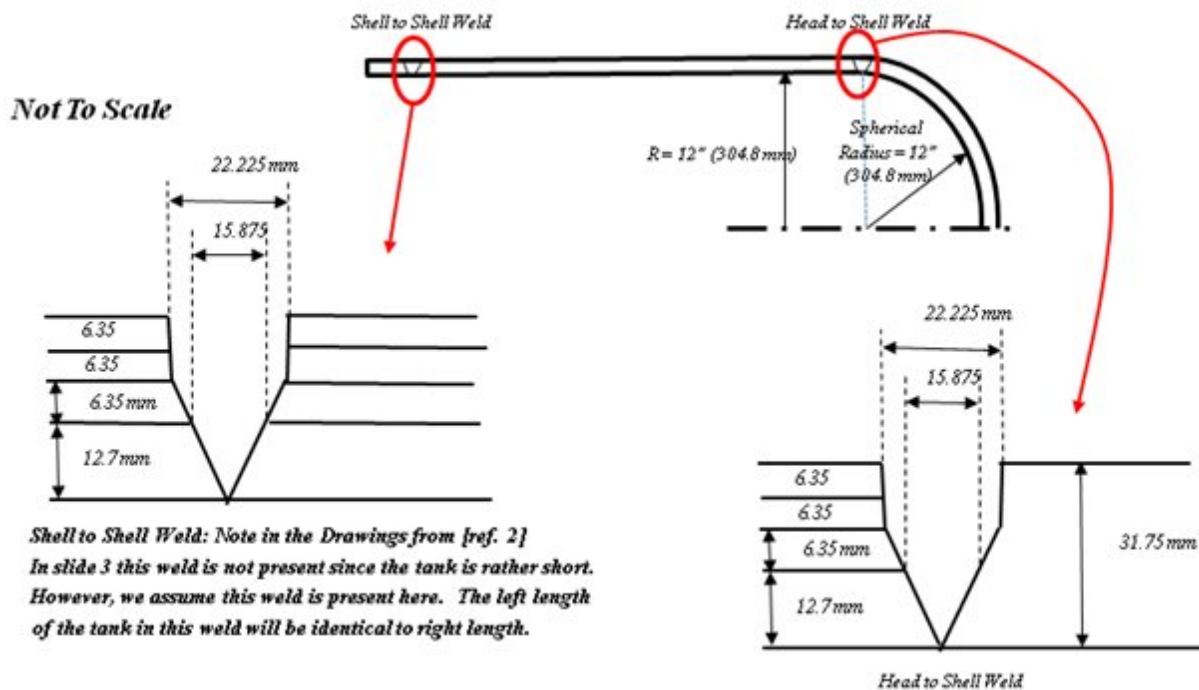


Figure 7.2.2-1. Four-layer Tank Considered for Weld Residual Stress Analysis

As seen in Figure 7.2.2-1, a shell-to-shell and a head-to-shell weld were considered. This represents a 3,500-psig, 609.6-mm (24-inch) diameter, and 3098.8-mm (122-inch) long vessel of vessel type M117. This vessel has an inner shell thickness of 12.7 mm (0.5 inches) and three layers of 6.35-mm (0.25-inch) thickness, for a total thickness of 31.75 mm (1.25 inches). In addition, the shell-to-shell and head-to-shell welds were also modeled as monolithic vessels (without the layers) in order to compare the layered analysis results with the monolithic results. Note that the four-layer model had a head the same size as the shell. However, many heads have smaller diameters than the shell, which is often the case with NASA's fleet of LPVs since primary stress in the hemispherical heads is only one-half that in the cylindrical shells. The 14-layer tank being analyzed now includes the taper transition. The taper transition between

	NASA Engineering and Safety Center Technical Assessment Report	Document #:	Version:
		NESCP-RP-13-00852	1.0
Title:		Page #:	
Evaluation of Agency Non-code LPVs		112 of 193	

such sections, including the severity of the taper, has a yet-to-be-determined effect on the stress results and should be considered in the future.

Weld Modeling Procedure

The Computational Weld Model: The analysis was performed using the Virtual Fabrication Technology (VFT™) computational weld modeling code [ref. 71]⁷. As seen in Figure 7.2.2-2, VFT has three modules:

1. GUI (graphical user interface), which is used to define weld passes, material data, weld sequence, etc. (i.e., GUI in Figure 7.2.2-2).
2. Thermal module, which calculates the temperature time histories at each nodal point as each pass is deposited. Here, the possibility of gap resistance between the plate layers is ignored since the plates are generally assumed to be tight against each other. Based on discussions with a former layered vessel manufacturer⁸, the thermal conductance in the radial direction at the layered regions was modeled as being 25% of the thermal conductance in the other directions.
3. The structural solution is performed using Abaqus® with a weld-specific material user routine (labeled “UMAT” in Figure 7.2.2-2), which is written to handle the unique aspects of welding such as material melting/resolidification, annealing caused by material heating above the phase transformation temperature, temperature-dependent hardening up to melting (800°C to 900°C suffices for ferritic steels), etc. The possibility of phase transformation plasticity effects is ignored since data are not available.

Finite Element Weld Model – The finite element weld models are shown in Figure 7.2.2-3, where the upper left model is layered shell to monolithic head, the upper right is layered shell to layered shell, the lower left is monolithic shell to monolithic head, and the lower right shows the monolithic shell-to-shell weld. The layers are identified via the different colors, as are the weld grouping elements. A total of 14 passes are modeled. Note that the simplified model using “rectangular” weld passes has been shown to have little effect on WRS results, as long as the relative pass sizes are realistic. For the structural solution, there were convergence difficulties caused by the use of contact⁹ between the layers. This was mainly caused during deposition of each pass when the material properties in the weld being deposited and near the interface contact zones were very low (low stiffness). However, the convergence difficulties were overcome by using restart analyses where solution parameters were continually modified.

⁷ Numerous publications of the theory and examples of weld residual stress and distortion calculations are available (for example, see references 67 through 70, and the many references cited therein, for more model details). Emc2 developed and uses VFT for many problems for weld modeling analysis, fatigue, and corrosion assessment of welded structures. In addition, VFT is leased by a number of organizations including Caterpillar, Knowl's Atomic Power Laboratory (KAPL), U.S. Nuclear Regulatory Commission (NRC), Babcock and Wilcox (B&W), and Rolls Royce (United Kingdom).

⁸ Maan Jawad, private discussions.

⁹ Frictionless contact was used.



Title:

Evaluation of Agency Non-code LPVs

Page #:
113 of 193

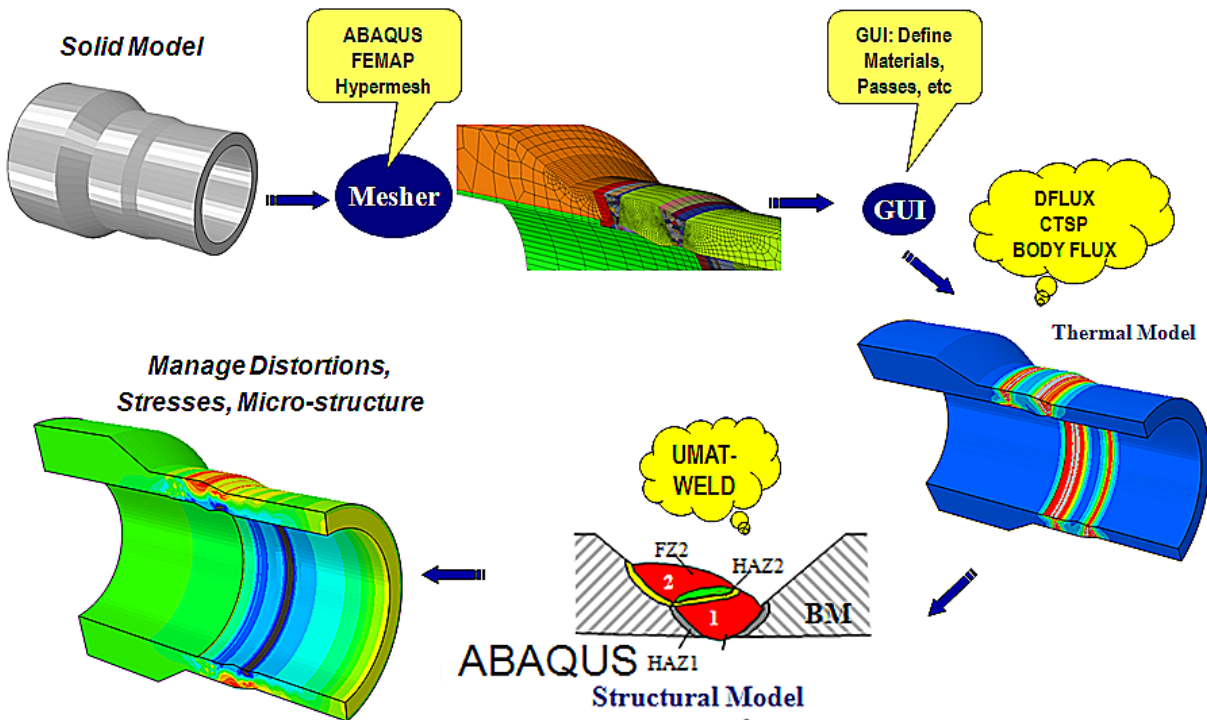


Figure 7.2.2-2. VFT Weld Modeling System

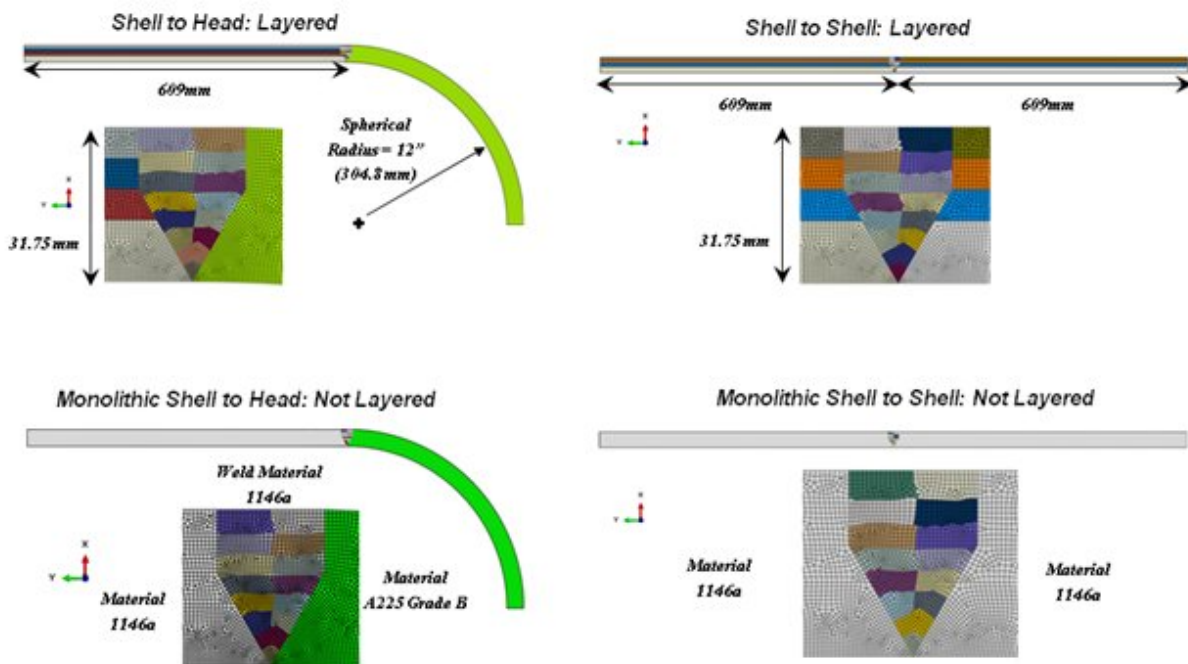


Figure 7.2.2-3. Axisymmetric Weld Models and Meshes

	NASA Engineering and Safety Center Technical Assessment Report	Document #: NESCP-RP- 13-00852	Version: 1.0
Title: Evaluation of Agency Non-code LPVs		Page #: 114 of 193	

Material isotropic hardening was initially used for the weld analyses. With classical plasticity theory used here, the stress state must be on the yield surface during plastic straining. With isotropic hardening, the yield surface expands during this plastic straining due to hardening. With kinematic hardening, the yield surface moves rigidly during plastic straining with the size of the yield surface remaining the same as the original size (i.e., the yield stress). Mixed hardening permits both translation and expansion of the yield surface and is considered most accurate. Isotropic hardening tends to produce upper bound results in WRS predictions. The material data used for the weld metal should be obtained in the annealed condition because the shrinkage during solidification is modeled. Here, the annealed data are not available. Therefore, the analyses were performed using linear kinematic hardening¹⁰. It is believed that use of kinematic hardening might be most appropriate here since the as-welded material data were used. However, this is only an experience-based guess at this point. Both results are presented here since isotropic hardening results should produce conservative predictions of FFS. It is noted that material data are not available to model mixed hardening.

An accurate analysis requires material data for each material from room temperature up to melting. As seen in Figure 7.2.2-3, the materials in the four-layer tank are 1146a for the shell and A225 Grade B for the head. The weld metal also was assumed to be 1146a. Since stress-strain data were not available for these materials, the properties used were obtained by scaling known stress strain curves for another similar pressure vessel steel (A516) based on the actual yield stress data tested by SwRI[®] [ref. 45]. Based on prior work in the nuclear industry, it is believed that this approach produces estimates of the stress strain response for the layered tank materials that are quite reasonable. The curves used to perform the weld analysis are shown in Figure 7.2.2-4. Since actual properties for the weld material were not known, any weld overmatch was not modeled. If it exists, it would result in increases in the WRS fields roughly by the ratio of the yield stresses between the base and weld materials.

¹⁰ Mixed (Chaboche) hardening would be best to use since cyclic loading does occur as each weld pass is deposited near prior passes. However, the material data necessary for this are not available.



Title:

Evaluation of Agency Non-code LPVs

Page #:
115 of 193

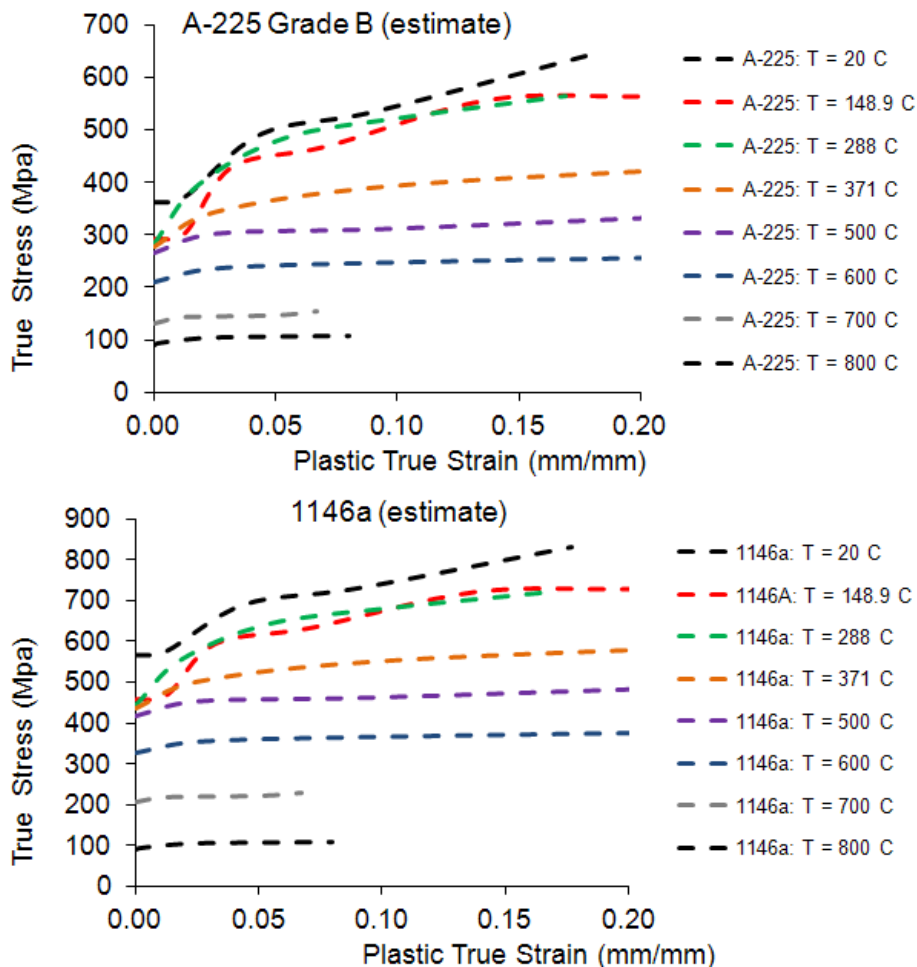


Figure 7.2.2-4. Stress Strain Curves Used for Mechanical Portion of Analysis

WRS Results

While no direct validation of the residual stress predictions was made here, the predictions of radial distortion and the corresponding gapping seen near the welds were qualitatively predicted. However, as mentioned in the previous section, extensive validation of the procedures and predictions of WRS and distortions have been made as indicated in references 72 through 76, the references cited therein, and user and validation manuals. It turns out that the hydrotest pressure of the vessel (38.06 MPa/5,250 psi), which was performed at a pressure of 1.5 times the nameplate design pressure of 3,500 psi (24.13 MPa), tends to relax the as-welded WRS fields, so this process was modeled as well. This hydropressure induces plasticity in and near the weld, which has the effect of relaxing the WRS magnitudes. This result was not initially anticipated based on experience with modern code vessels. However, since this layered vessel was fabricated from higher strength steel than is common today (105 ksi tensile strength, 75 ksi yield) and was designed with a significantly lower FS on shell tensile strength (2.86 FS) than code vessels at the time (i.e., 4) or modern BPVC vessels (i.e., 3.5), the stress due to pressure loading

	NASA Engineering and Safety Center Technical Assessment Report	Document #:	Version:
		NESCP-RP-13-00852	1.0
Title:			Page #:
Evaluation of Agency Non-code LPVs			116 of 193

is much higher than exists in code vessels. In hindsight, it is not surprising that a 1.5× overpressure test would cause more inelastic strain than anticipated with resulting residual stress relaxation.

Figure 7.2.2-5 shows contour plots of hoop WRS fields in the layered shell-to-shell circumferential weld. The upper illustration shows isotropic hardening, and the bottom shows linear kinematic hardening results. As discussed above, it is believed that the linear kinematic hardening results are most appropriate since the as-welded properties for the weld metal had to be used. However, results are shown using both hardening laws since isotropic hardening provides the most conservative predictions for FFS assessments. For the fracture assessment, it may be desirable to use the most conservative predictions if they are not overly conservative.

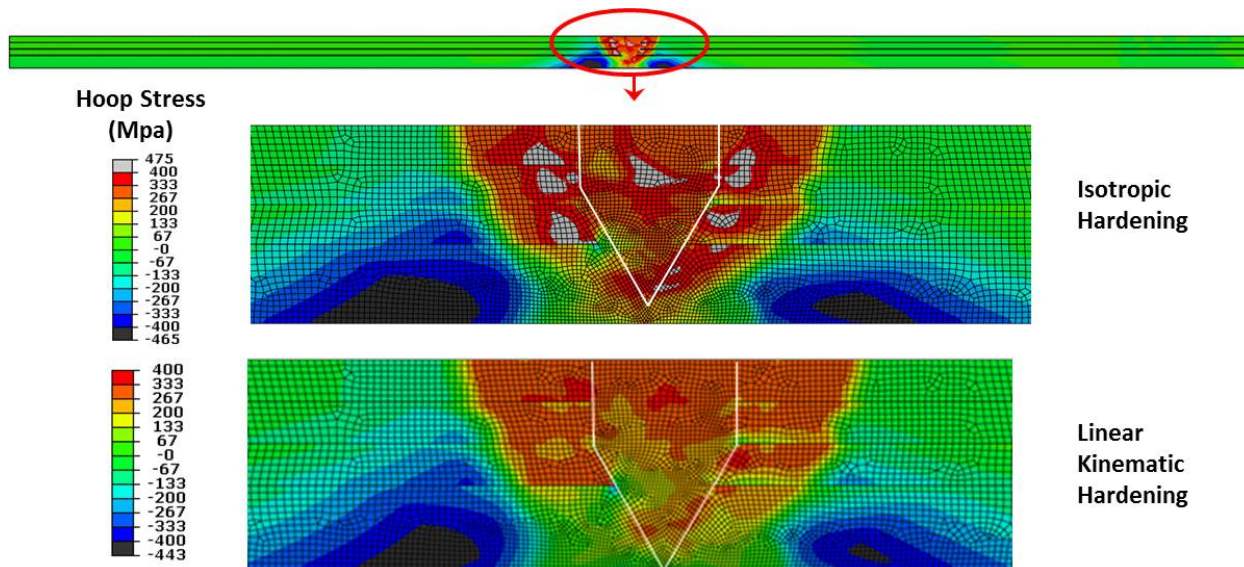


Figure 7.2.2-5. Hoop WRS Predictions for Layered Shell-to-Shell Weld

Figure 7.2.2-6 shows contour plots of axial WRS fields in the layered shell-to-shell circumferential weld. The upper illustration shows isotropic hardening, and the bottom shows linear kinematic hardening results. Somewhat higher axial stresses are seen near the ID and alternate between tension and compression at each layer. This is clearly different behavior compared with a monolithic analysis (which was performed but not reported in this high-level summary). Figures 7.2.2-7 and 7.2.2-8 show similar contour plots for hoop and axial stress, respectively, for the shell-to-head weld. For the most part, the WRS in the shell-to-head weld are slightly higher than for the shell-to-shell weld.



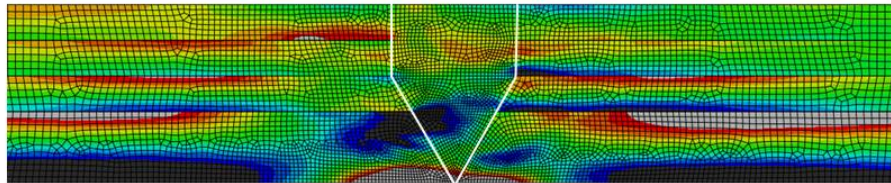
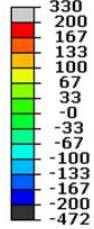
Title:

Evaluation of Agency Non-code LPVs

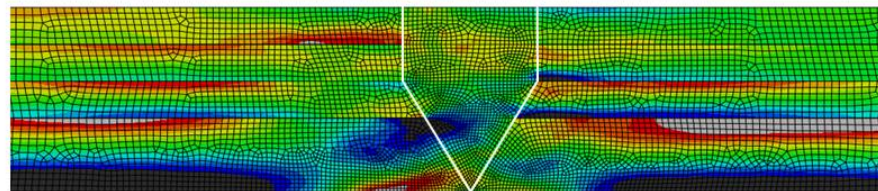
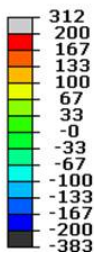
Page #:
117 of 193

Axial Stress

(Mpa)

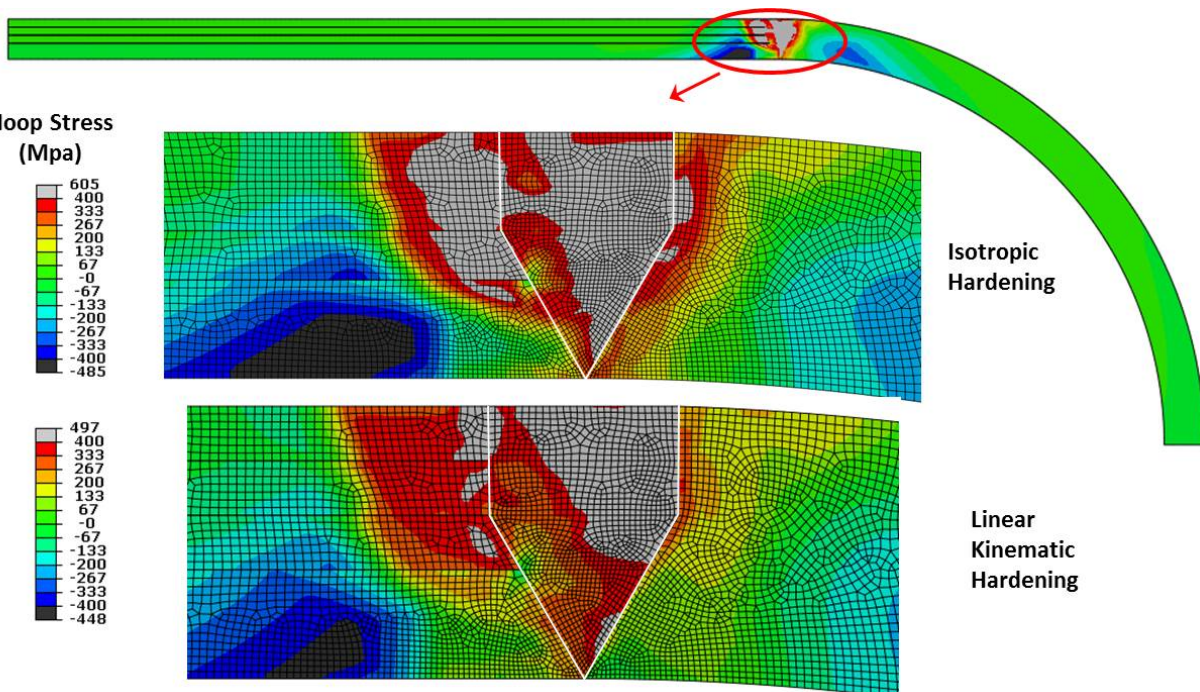


Isotropic
Hardening

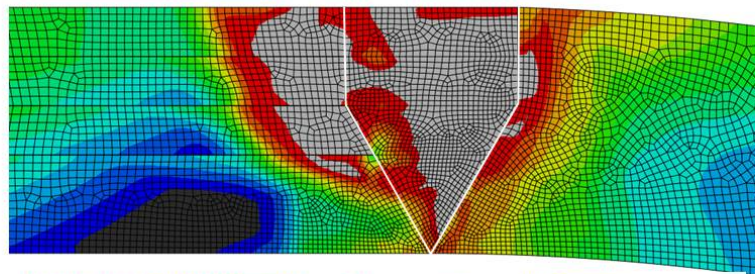
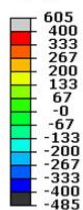


Linear
Kinematic
Hardening

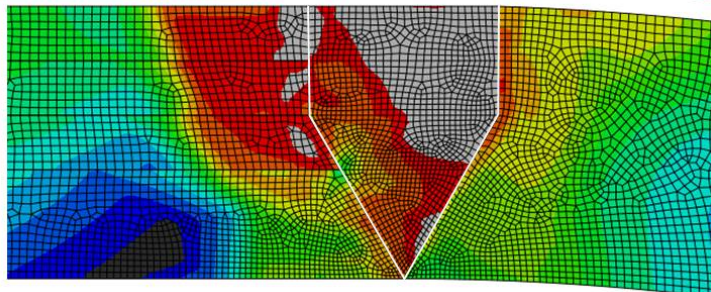
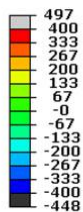
Figure 7.2.2-6. Axial WRS Predictions for Layered Shell-to-Shell Weld



Hoop Stress
(Mpa)



Isotropic
Hardening



Linear
Kinematic
Hardening

Figure 7.2.2-7. Hoop WRS Predictions for Layered Shell-to-Head Weld

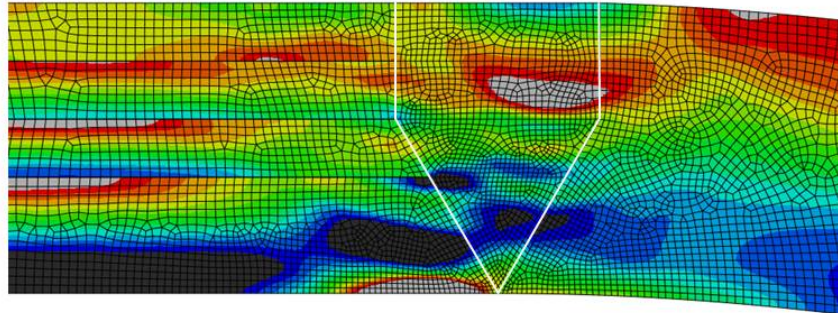
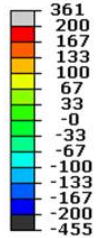


Title:

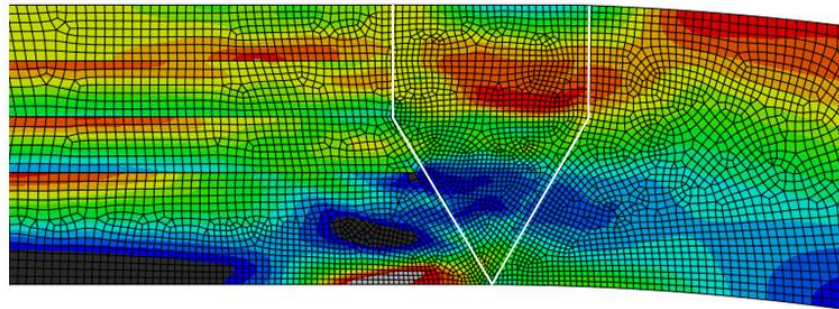
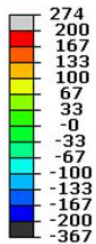
Evaluation of Agency Non-code LPVs

Page #:
118 of 193

Axial Stress
(Mpa)



Isotropic
Hardening



Linear
Kinematic
Hardening

Figure 7.2.2-8. Axial WRS Predictions for Layered Shell-to-Head Weld

WRS Line Plots and Comparison to Monolithic Results – It is useful to compare line plots of the WRS fields from the layered shell cases to monolithic vessel cases to determine the importance of including the layers in the analysis. As discussed above, solutions using the layers with contact are more challenging and can lead to convergence difficulties. Moreover, if the layer effect can be neglected, then solutions from API-579 (or other sources) can be used to estimate the stress intensity factors using the weight function approach in Appendix C of API-579. In addition, it is often easier to compare the stress fields directly with line plots.

As seen in Figures 7.2.2-5 through 7.2.2-8, the WRS distributions vary spatially in the weld region, as well as in the HAZs. For fracture mechanics assessment it is most proper to include this variation when calculating fracture parameters (e.g., the stress intensity factor, K) by using (for instance) the finite element alternating method (FEAM)¹¹ to insert cracks at various locations within the WRS field and then determining the K value. However, API-579 conservatively permits the use of a through-thickness line definition of WRS (for use with Appendix C stress intensity factor weight function tabulations), which is assumed to be invariant throughout the weld and the HAZ¹².

¹¹ FEAM is a convenient method for quickly obtaining stress intensity factors within WRS fields.

¹² Of course, this assumption is overly conservative since the WRS field clearly varies throughout the weld and HAZ, as can be seen in Figures 7.2.3-5 through 7.2.3-8.

	NASA Engineering and Safety Center Technical Assessment Report	Document #:	Version:
		NESCP-RP-13-00852	1.0
Title:			Page #:
Evaluation of Agency Non-code LPVs			119 of 193

In this section, line plots are provided and compared. Line plots of stress are provided along three paths, as illustrated in Figure 7.2.2-9. One represents a plot through the weld centerline, one intersects layer 1 with the weld (path 1), and one intersects layers 2 and 3 and the weld (path 2-3). Figure 7.2.2-10 illustrates line plots of axial and hoop WRS for the shell-to-shell case. The solid black and solid red lines compare results between isotropic and kinematic hardening. It is seen that the axial stress differences are relatively small except at the ID of the vessel. *It is noted that the differences between isotropic and kinematic hardening are much greater in the as-welded condition prior to application of the hydrotest.* The dashed lines in Figure 7.2.2-10 are for the monolithic case. The monolithic shell results do not compare well for the axial stresses and are conservative for hoop stresses.

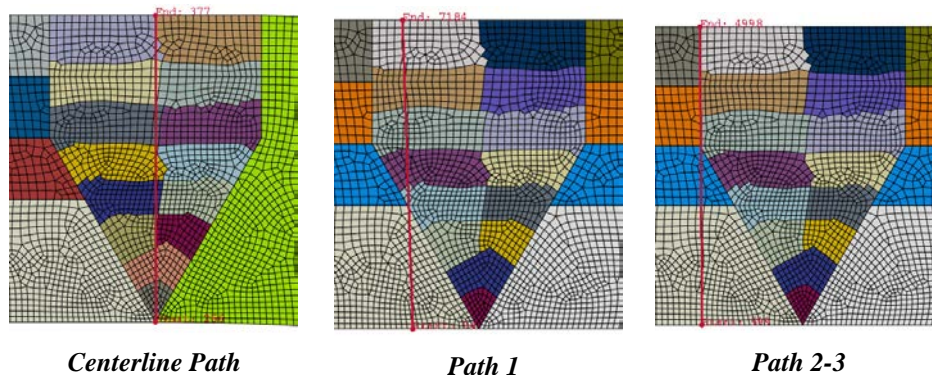


Figure 7.2.2-9. Line Path Definitions for Through Thickness Stress Plots

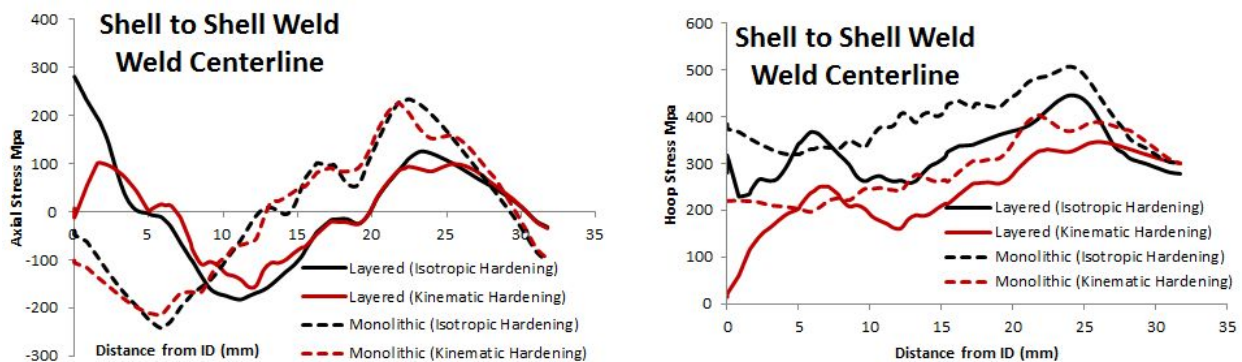


Figure 7.2.2-10. Shell-to-Head Weld: Line Plot from ID to Outer Diameter (OD) along Centerline

Figure 7.2.2-11 illustrates the line plots of the axial and hoop WRS fields along the layer path 2-3 (see Figure 7.2.2-9) for the shell-to-head case. The axial stresses are highest at the ID for both the isotropic and kinematic hardening cases. For low toughness materials, this may lead to a fully circumferential crack that, if undetected, could possibly grow through-wall with cyclic pressure loadings and eventually lead to a head blowout, although this was not specifically modeled and evaluated and would require crack-growth rate analyses and loading history assumptions that are well outside the scope of this study. The axial stresses for the monolithic case are somewhat similar to the layered case here. On the other hand, the monolithic shell-to-

	NASA Engineering and Safety Center Technical Assessment Report	Document #:	Version:
		NESCP-RP-13-00852	1.0
Title:			Page #:
Evaluation of Agency Non-code LPVs			120 of 193

head case produces higher hoop stresses than the shell case. One can also see that the stresses have “jumps” near the layer-to-weld intersections where a natural crack exists. Other plots like this show similar trends and suggest that modeling the actual shell behavior is more important than using the monolithic results. The effect of tapered head-to-shell transitions must also be determined.

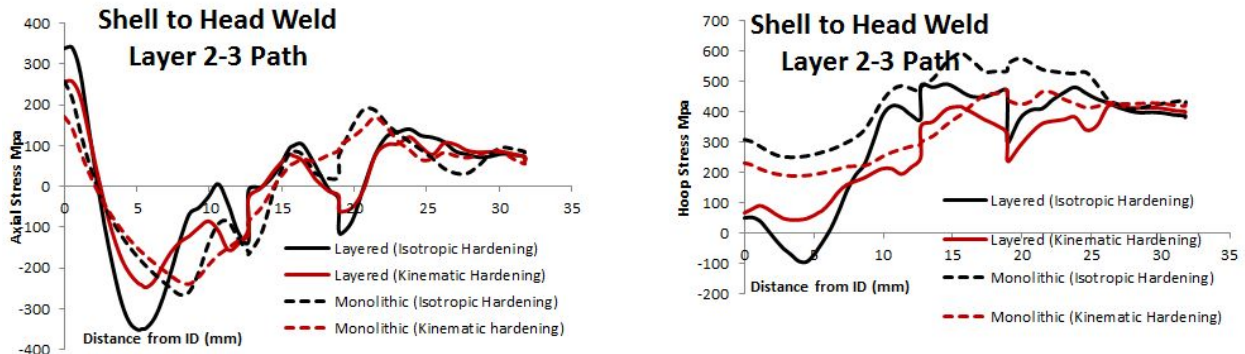


Figure 7.2.2-11. Shell-to-Head Weld: Line Plot from ID to OD along Layer Path 2-3

Comparison to API-579 Solutions

One of the goals of this effort was to determine whether the procedure in Appendix E of API-579 [ref. 32] for estimating WRS fields in pipes and vessels could apply to NASA LPVs. The API-579 estimates are meant to be upper bound generic solutions used in lieu of finite element WRS-based solutions¹³. Figure 7.2.2-12 compares the WRS analyses for both the layered cases for the shell-to-shell (top) and shell-to-head (bottom) cases, respectively. The use of the API-579 solution for both axial and hoop stresses (for evaluating circumferential and axial cracking, respectively) appears to be conservative for most points through the thickness¹⁴. For the shell-to-shell case, the isotropic hardening axial stresses near the ID are highest. However, if the API-579 solutions are used for cracks near the OD of the vessels, then fracture predictions will likely be too conservative as axial stresses approach 700 MPa and hoop stresses 800 MPa from the API solutions. Note that the API-579 estimated solutions for the shell-to-head case use the material yield stress for the shell material (layer side of weld).

As discussed above, the API-579-estimated WRS fields assume that the stresses are constant spatially throughout the weld. This is not true based on Figures 7.2.2-7 and 7.2.2-8 contour plots. Therefore, it is also useful to examine line plots at a location away from the weld centerline. Figure 7.2.2-13 illustrates the WRS fields along the layer path 2-3 (see Figure 7.2.2-9), which is along the line near the top of the vessel where “natural cracks” exist due the structure of the layered vessel. It is seen that the API-579 solutions for hoop stress are conservative throughout the thickness and probably too conservative from midway through the

¹³ Users of API-579 always have the option of developing their own WRS fields from welding.

¹⁴ It is noted that the API-579 solutions are not developed for the shell-to-head case, but it can be assumed to apply regardless.



NASA Engineering and Safety Center Technical Assessment Report

Document #:
**NESCP-RP-
13-00852**

Version:
1.0

Title:

Evaluation of Agency Non-code LPVs

Page #:
121 of 193

thickness to the OD. The API-579 axial stresses are conservative throughout except right at the ID and somewhat near mid thickness. Again, the API-579 solutions near the OD are probably overly conservative.

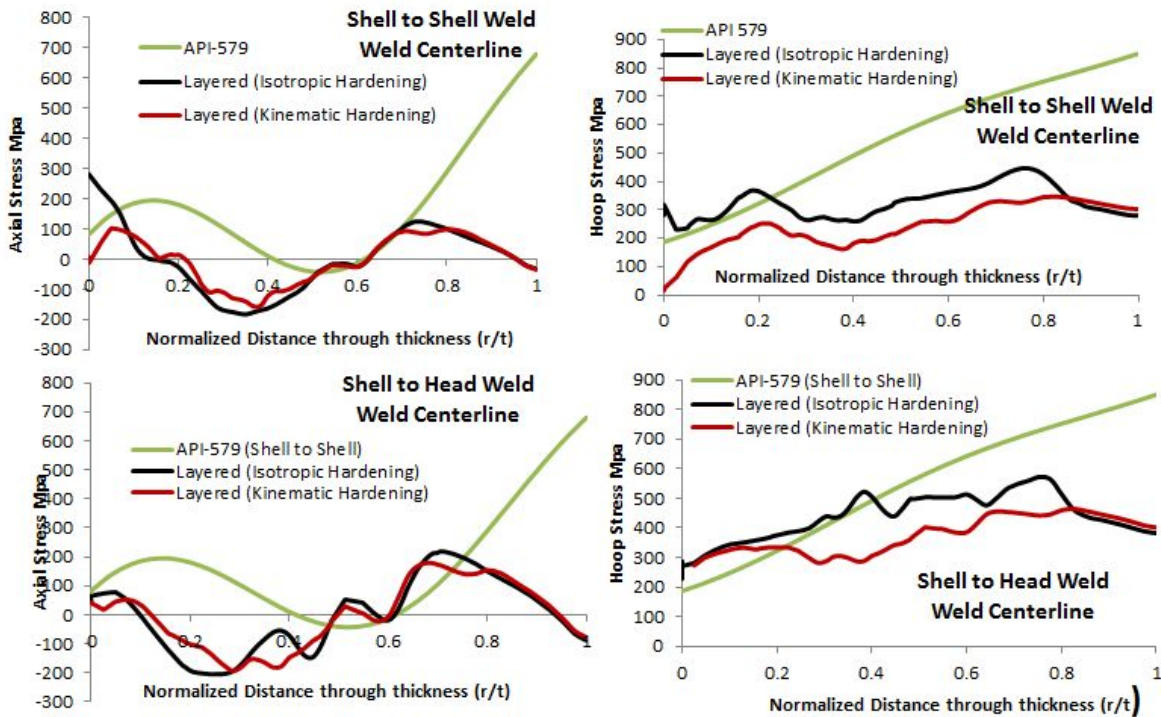


Figure 7.2.2-12. Comparison of API-579 Solutions to Calculated Results for Both Shell-to-Shell and Shell-to-Head Tank Cases (axial, left; hoop, right): Weld Centerline



Title:

Evaluation of Agency Non-code LPVs

Page #:
122 of 193

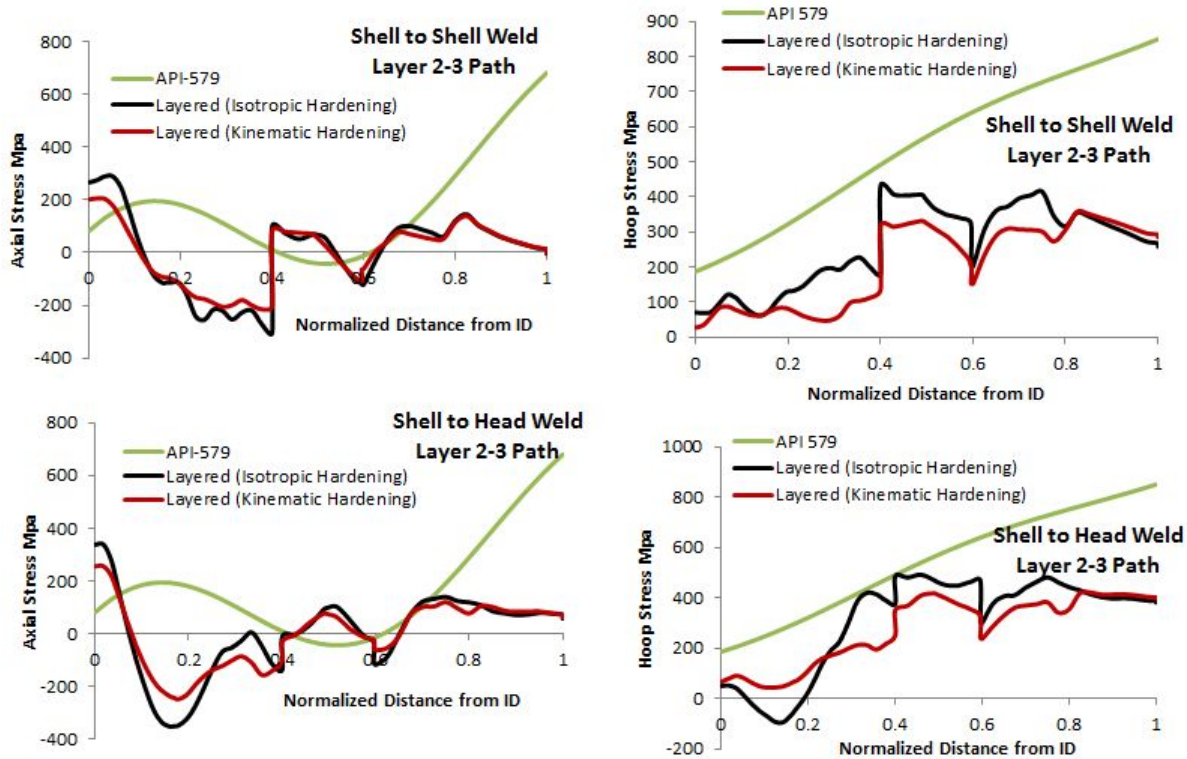


Figure 7.2.2-13. Comparison of API-579 Solutions to Calculated Results for Both Shell-to-Shell and Shell-to-Head Tank Cases (axial, left; hoop, right): Layer 2-3 Path

Measurement of Weld Residual Stress Fields

It may be useful to obtain a sample of WRS measurements in order to validate the predictions since full material test data are not available. There are several state-of-the-art methods that are often used in order to obtain through-thickness WRS fields, including neutron diffraction, deep hole drilling, and the contour method (see reference 73 for a summary of all three methods). Because of the nature of LPVs it appears that deep hole drilling might be most useful here. It is noted, however, that there are often scatter in measurements and differences in measurements between the different methods. Therefore, it is often useful to obtain measurements using two different methods.

Summary and Conclusions

From the analyses of the four-layer vessels, the following conclusions are drawn:

- WRS predictions using isotropic hardening are almost always highest in absolute value for hoop stresses (versus other hardening models), while axial stresses are quite similar except near the ID. Because there is a lack of material property data, both sets of results are presented at this time.

	NASA Engineering and Safety Center Technical Assessment Report	Document #: NESCP-RP-13-00852	Version: 1.0
Title: Evaluation of Agency Non-code LPVs		Page #: 123 of 193	

- Hoop WRSs are conservatively predicted using a monolithic geometry, neglecting the layers for both shell-to-head and shell-to-shell welds. However, predictions may be overly conservative from an FFS standpoint.
- The use of API-579 WRS solutions will likely be overly conservative, and calculated WRS fields where the correct hydrotest pressure is applied can be used if the API solutions for FFS predictions are overly constraining.
- Axial and hoop WRS tend to be maximum along path 2-3, which is near the edges of the weld near the region of layer-to-weld convergence. Axial and hoop WRS spikes occur near the region where the path intersects layer/weld interfaces due to the sharp crack-like interface. This could possibly be a crack initiation location for both circumferential and axial cracks.
- Results for a 14-layer vessel are nearly complete and will be presented soon.
- Calculations of stress intensity factors in these WRS fields need to be made for cracks positioned at different locations near the weld in order to perform FFS and remaining life calculations.
- A second hydrotest pressure of 1.5 times design load was applied, and this had little effect on reducing the WRSs. However, when a second hydrotest pressure 10% higher (41.86 MPa rather than 38.06 MPa) the WRSs were reduced with a maximum reduction of about 5% (hoop stresses) and 7% (axial stresses). This might be considered for life extension if the additional higher-pressure hydrotest did not cause damage.

7.2.3 Evaluation of Two Digital Image Correlation Techniques to Detect LPV Deformations during Hydrotest

NASA has a long history of safe pressure vessel operation that is largely attributable to a rigorous vessel certification program. Vessel certification entails inspections to detect and assess the effect of damage such as corrosion and cracking. Damage to solid wall vessels is readily detectable through standard NDE inspection techniques. However, damage to the shell sections of LPVs is hard to detect using standard NDE inspection techniques. For example, a crack within an intermediate layer is generally confined to the affected layer and cannot be detected using visual or surface NDE inspection techniques. Such cracks could propagate undetected into critical head-to-shell welds, leading to catastrophic vessel failure without warning. This type of intermediate layer damage could partially compromise shell integrity and might produce local shell deformations that could be detectable via photogrammetric techniques. The ability to detect defects using this approach could be compromised by the effect of layer gaps, which result in a reduced outer shell deformation. For example, ASME requires that an LPV have a minimum of only 50% of the outer shell deformation as measured by Pi Tape, compared with a monolithic shell.

Full-field optical deformation techniques, which include scanning vibrometers, various types of interferometry techniques, and digital image correlation have become more commonplace within

	NASA Engineering and Safety Center Technical Assessment Report	Document #: NESCP-RP- 13-00852	Version: 1.0
Title: Evaluation of Agency Non-code LPVs		Page #: 124 of 193	

the past decade. Digital image correlation applications have vastly expanded due to the advancements in sensor hardware capability and computer processing power needed for the pattern recognition and point tracking algorithms. In recent years, the testing paradigm has dramatically shifted from the use of physical instrumentation gages to optical techniques to capture deformation and motion.

NASA has previously used commercial digital image correlation systems in a number of areas, including the Space Shuttle Program. For the *Columbia* Accident Investigation and the Return to Flight Program, deflections of reinforced carbon-carbon test panels from impact tests were captured and used to validate analysis models for flight rationale. In the current timeframe, optical metrology is used at nearly every NASA field center on a daily basis. References are provided to illustrate the wide range of research and engineering applications of optical metrology in areas of material characterization [refs. 77–80], structural analysis [refs. 80–83], and biomechanics [refs. 84–87].

The test in this report used two photogrammetric techniques to measure deformations of a scrap LPV during hydrotest pressure excursion from 0 to 4,200 psig (150% of vessel design pressure). The objective of the test was to document gross vessel deformations, as well as specific surface locations where underlying flaws were known to exist via previous radiographic inspection. The hydrostatic test was conducted at GRC from August 20 to 23, 2013, and consisted of four total excursions from 0 to 4,200 psig. As part of this exercise, the team from MSFC conducted an AE survey on the first excursion with the intent to identify the applicability of AE to find internal flaws in pressure vessels. Results of the AE effort are presented in Section 7.2.4 of this NESC report.

7.2.3.1 Test Article

The test article, shown in Figure 7.2.3.1-1, was a scrap A. O. Smith LPV MV-50405A-31 (GRC vessel PV0236) with a 52-inch internal diameter, 24 feet long, with an internal volume of 306 cubic feet. The vessel was fabricated with two solid heads and a shell section consisting of an inner shell with seven overwrap layers. Manufacturer design pressure was 2,800 psig. The hydrotest pressure was 4,200 psig (150% vessel design pressure), which was the original hydrotest pressure of the vessel at manufacture in 1959. Prior to testing, the vessel was dormant for roughly 20 years due to internal crack-like defects located within vessel shell layers near the head-to-shell welds. These flaws were discovered by radiographic inspection in the early 1990s.

	NASA Engineering and Safety Center Technical Assessment Report	Document #: NESCP-RP-13-00852	Version: 1.0
Title: Evaluation of Agency Non-code LPVs		Page #: 125 of 193	



Figure 7.2.3.1-1. Pretest View of PV0236 (vessel measures 52-inches ID × 24 feet long, has an internal volume of 306 cubic feet and a design pressure of 2,800 psig, has a layered shell construction, and was fabricated in 1959)

Prior to testing, the vessel was re-inspected with radiography and ultrasound techniques to better quantify internal flaws for correlation with both the acoustic and optical measurement methods. Radiography was performed on both vessel head-shell welds, and an ultrasonic bore-probe inspection was performed on both nozzle welds. The radiographic inspection confirmed several crack-like indications in the vessel shell near both head-shell welds. Ultrasonic inspection revealed lack of fusion in the front fusion zone of both nozzle welds. These NDE findings are summarized pictorially in Figure 7.2.3.1-2. Referring to the figure, there are three crack-like indications in the vessel shell near head-shell weld C-1, measuring between roughly 0.25 inches and 0.56 inches, and one 0.27-inch crack-like indication in the vessel shell near head-shell weld C-2. The depth of these flaws within the vessel shell is unknown. There is a lack of fusion in the front fusion zones of both nozzle welds consistent around the entire weld circumference.



Title:

Evaluation of Agency Non-code LPVs

Page #:
126 of 193

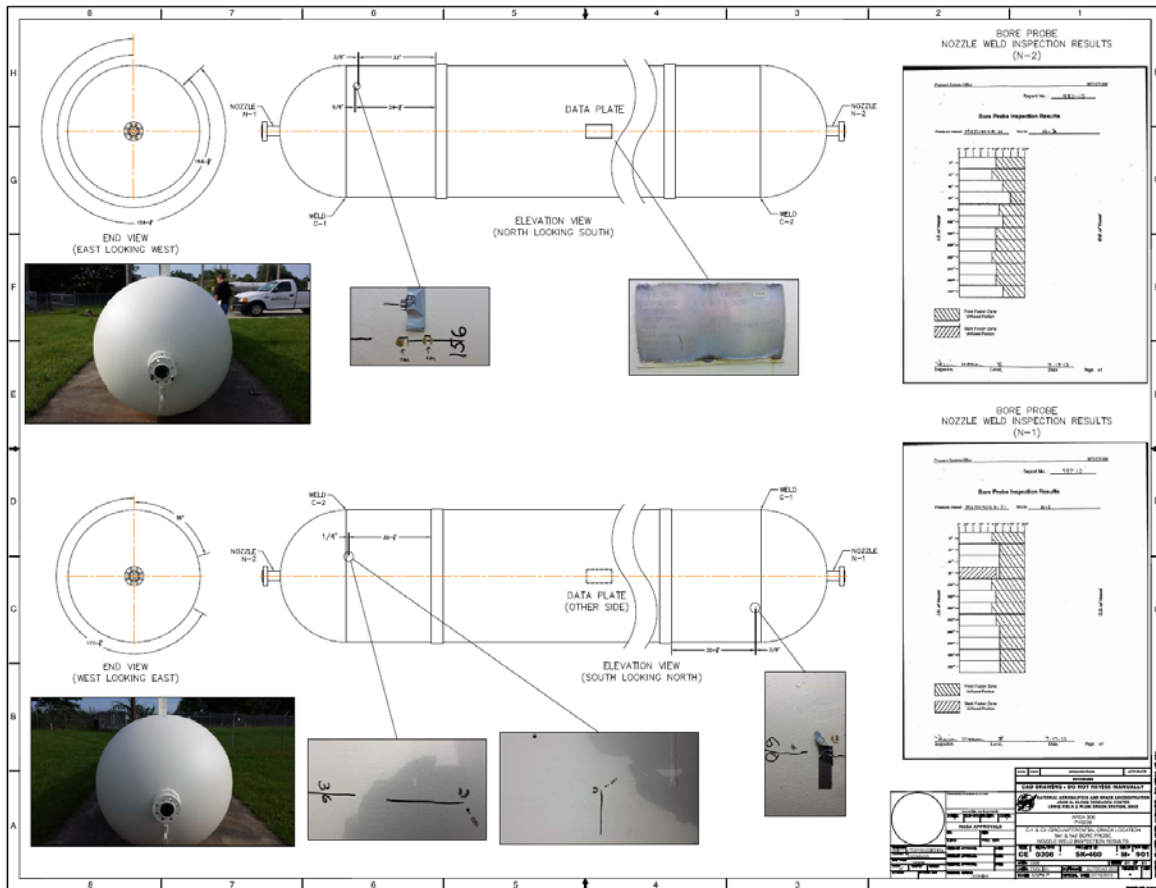


Figure 7.2.3.1-2. NDE Results Summarizing Known Vessel Flaws for Vessel PV0236

7.2.3.2 Digital Image Correlation Methods

Digital image correlation is the acquisition of engineering data from digital images of an object from different perspectives for determination of object shape and deformation at different states or loading conditions. Two different commercially available measurement systems were employed on this test: Aramis and Tritop, developed by the German company, GOM mbH.

Aramis computes full-field three-dimensional surface deformation and strains from stereo image sets taken at any selected time interval throughout a test sequence. These image sets are acquired by two image sensors fixed to a rigid beam apart from one another and focused on the object of interest being tested. Aramis utilizes pattern mapping/tracking algorithms to determine object deformations in the image pairs between discrete time intervals, and typically requires a high-contrast dot or speckle pattern to be applied to the test object of interest to ensure high-fidelity data capture. Post-test, the Aramis measurements can be viewed as full three-dimensional color contour images or plotted against load, time, or other desired values for engineering analysis.

	NASA Engineering and Safety Center Technical Assessment Report	Document #:	Version:
		NESCP-RP-13-00852	1.0
Title:			Page #:
Evaluation of Agency Non-code LPVs			127 of 193

Tritop is a quasi-static photogrammetry technique that generates shape and deformation results from sets of photographs, taken from arbitrary points of view, of an object with a handheld, high-quality, 12-megapixel digital single-lens reflex camera. Tritop computes the spatial centroidal locations of dots and specialized “coded targets” placed at selected locations on the surface of a test article to generate a three-dimensional point cloud. Using multiple sets of photographs, one or more point clouds of the test article can be generated at various test static states and then compared with the baseline data. From these comparisons, Tritop calculates highly accurate three-dimensional positional changes for each dot and target, enabling effective visualization of structural motion between states. Typical data reduction from Tritop shows vector plots resolved into a defined coordinate system representing the motion of each of the points in the point cloud.

To calibrate both of these optical systems, a calibration object is required to orient the camera spatial locations and establish a scale to ensure the software uses accurate dimensions. For this test sequence, a 2-meter carbon fiber cross, with digital targets placed at known dimensional locations, was used for calibration. For Aramis, calibration of the stereo camera set takes place prior to the actual test by recording a few dozen images of the cross located at several different locations in the cameras field of view. With Tritop, the calibration artifact remains in the field of view for a number of the handheld images, enabling the software to perform calibration at the same time it is calculating the spatial locations of the targets.

A preliminary study was performed to establish that both Aramis and Tritop were capable of resolving the expected deformations for the vessel. Hand calculations were performed to establish theoretical vessel stress, strains, and deformations under 2,800 and 4,200 psig loading pressures, for a fully intact vessel, a vessel with one layer lost, and a vessel with two layers lost. These parameters are summarized in Table 7.2.3.2-1. At the 4,200 psig state expected results were nominally 1,692 microstrain circumferentially (hoop strain) and an axial vessel elongation of about 0.185 inches.

Table 7.2.3.2-1. Vessel Stress, Strain, and Deformation Computations at Two Pressure States based on Modulus of Elasticity of 2.95 E+07 psi

	AT DESIGN MAWP (2,800 PSIG)			AT 150% MAWP (4,200 PSIG)		
	All layers intact	One layer lost	Two layers lost	All layers intact	One layer lost	Two layers lost
Nominal Vessel Thickness (in)	2.1875	1.9375	1.6875	2.1875	1.9375	1.6875
Ave Hoop Stress (PSIG) ⁽¹⁾	33280	37574	43141	49920	56361	64711
Ave Hoop Strain, $\mu\epsilon$	1128	1274	1462	1692	1911	2194
Circumferential Vessel Growth (in)	0.200	0.224	0.254	0.300	0.335	0.382
Axial Shell Growth (in)	0.124	0.139	0.160	0.185	0.209	0.240

The Aramis displacement resolution is linearly dependent on the physical length captured by each pixel on the sensor. This means that the smaller the length that Aramis is measuring, the more accurately it can record deformation. Thus, tradeoffs are commonly made when trying to optimize the combination of sensor distance to the test object and focal length of the lens (representing the size of the Aramis field of view) to establish the theoretical optimal accuracy of the test setup.

	NASA Engineering and Safety Center Technical Assessment Report	Document #: NESCP-RP-13-00852	Version: 1.0
Title: Evaluation of Agency Non-code LPVs		Page #: 128 of 193	

It was determined that one-half of the vessel would be imaged for each pressure cycle. This was a balance between capturing a large overall view of the vessel, while maintaining acceptable displacement resolution. The 5-megapixel sensors capture an image array of 2,448 pixels wide by 2,050 pixels high. With the field of view being about 14 feet, or 168 inches, this would yield an effective pixel width of 168 inches/2,448 pixels, which equals 0.0686 inches per pixel. GOM mbH publishes a theoretical accuracy to 1/30th of a pixel (0.0686/30), resulting in a ± 2.3 thousandths of an inch theoretical maximum accuracy displacement for the 14-foot field of view on the vessel. Referring back to Table 7.2.3.2-1, this value is well below the expected vessel expansion of 0.300 inches and axial growth of 0.185 inches at 4,200 psi. This basic analysis calculation provided the confidence that Aramis would theoretically be able to accurately capture the vessel deformations throughout the planned test.

7.2.3.3 Vessel Preparation

As mentioned in the earlier section, Aramis correlates stereo image pairs through sophisticated pattern recognition and tracking. In all cases of Aramis use, a high-contrast stochastic black and white pattern must be applied to the surface for measurements to be made. The stochastic pattern, in many cases, is created by preparing the surface to be white. A black pattern is then applied over the white base. The pattern can be accomplished using airbrushes, artificial patterned stamps, stencils, or, in many cases, a large number of circular dots applied at random. For the dot technique, each dot typically must be on the order of five to seven pixels in diameter. Using these criteria for the established field of view established a nominal dot diameter from 0.34 to 0.48 inches. The dot patterns were applied using a precut stencil. As can be seen in Figure 7.2.3.1-1, the vessel surface paint was in poor condition and required significant preparation to ensure an optimal pattern for Aramis. The vessel was striped, cleaned, and repainted entirely white in preparation for a black dot pattern application, as shown in Figure 7.2.3.3-1.



Figure 7.2.3.3-1. Test Pressure Vessel Cleaned and Painted White (black squares on the vessel are unpainted areas to accommodate AE sensors)



NASA Engineering and Safety Center Technical Assessment Report

Document #:
**NESCP-RP-
13-00852**

Version:
1.0

Title:

Evaluation of Agency Non-code LPVs

Page #:
129 of 193

For application of the black dots, 60-inch-wide vinyl stencils, cut on a Graphtec vinyl cutter, were adhered to the vessel. The large size of the stencils required multiple individuals to assist with the application process. The vinyl adhesive enabled easy removal and reuse on another section of the vessel. With the stencils in place, the vessel was spray painted. Figure 7.2.3.3-2 depicts the stencil application and spray painting of the vessel in progress; Figure 7.2.3.3-3 shows the tank with the completed dot pattern.



Figure 7.2.3.3-2. Application of Vinyl Stencil (left) and Spray-painting Process (right) on Vessel



Figure 7.2.3.3-3. Pressure Vessel with Completed Dot Pattern

	NASA Engineering and Safety Center Technical Assessment Report	Document #: NESCP-RP- 13-00852	Version: 1.0
Title: Evaluation of Agency Non-code LPVs		Page #: 130 of 193	

As mentioned in the earlier discussion on Tritop, digital or coded targets, printed on adhesive paper, are used to establish unique point locations on a test article between two states. Prior to running the final pressure cycle, the coded targets were adhered to the vessel at various locations. Particular locations of interest were the end caps of the pressure vessel and several circumferential lines along the axis of the vessel. Target size required for any given test was established in a similar manner as dot size was for Aramis. In order for Tritop to generate an accurate point cloud from the targets, an adequate number of targets must be common in overlapping images, which can be used to “stitch” the points together from image to image. This requirement can sometimes result in a greater number of targets being affixed to the test article than needed for successful or desired data capture on a test, which was the case with this investigation. The primary interest with Tritop was to identify circumferential and axial deformation of the vessel between the 0- and 4,200-psi endpoints, resulting in targets applied in concentrations on the end caps and on circumferential lines. The length of the vessel created the need for many “nonessential” targets to be added to the vessel to ensure proper stitching from end to end. Figure 7.2.3.3-4 shows two images depicting digital target placement on the pressure vessel. In both images, the carbon fiber calibration artifact is visible. Figure 7.2.3.3-5 shows the Aramis camera pair in testing configuration on beam for the first pressure cycle.



Figure 7.2.3.3-4. Two Views Depicting Placement of Digital Targets on Pressure Vessel

	NASA Engineering and Safety Center Technical Assessment Report	Document #: NESCP-RP-13-00852	Version: 1.0
Title: Evaluation of Agency Non-code LPVs		Page #: 131 of 193	



Figure 7.2.3.3-5. Aramis Camera Pair in Test Configuration (note acoustic sensors on vessel)

7.2.3.4 Experimental Results

Three pressure cycles were documented with Aramis, and one was documented using Tritop. The scope of this exercise was to verify whether Aramis and Tritop could capture deformations of the pressure vessel at levels of fidelity that would be useful in future engineering assessments of pressure vessels throughout the Agency.

Aramis Results

Aramis offers a wide variety of techniques for post-processing the image correlation data. Color contour overlays of deformations and strains in user-defined coordinate systems can be generated, as well as X-Y plots of the data as a function of any desired variables, such as time, load, etc.

Upon completing the image correlation process, Aramis provides a numerical indicator called an intersection deviation, which establishes a level of confidence that the cameras remained calibrated throughout the entire image capture sequence. In all three of the pressurization cycles, the Aramis intersection deviations indicated that the cameras remained calibrated. The correlated data sets yield a spatial, three-dimensional representation of the pressure vessel. An example is shown in Figure 7.2.3.4-1, which shows the computed surface radius value (from the computed centroidal axis of the vessel) at every location of the pattern. A close inspection of the figure reveals the weld lines on the saddle strap and where the axial shell meets the end cap.

	NASA Engineering and Safety Center Technical Assessment Report	Document #: NESCP-RP- 13-00852	Version: 1.0
Title: Evaluation of Agency Non-code LPVs		Page #: 132 of 193	

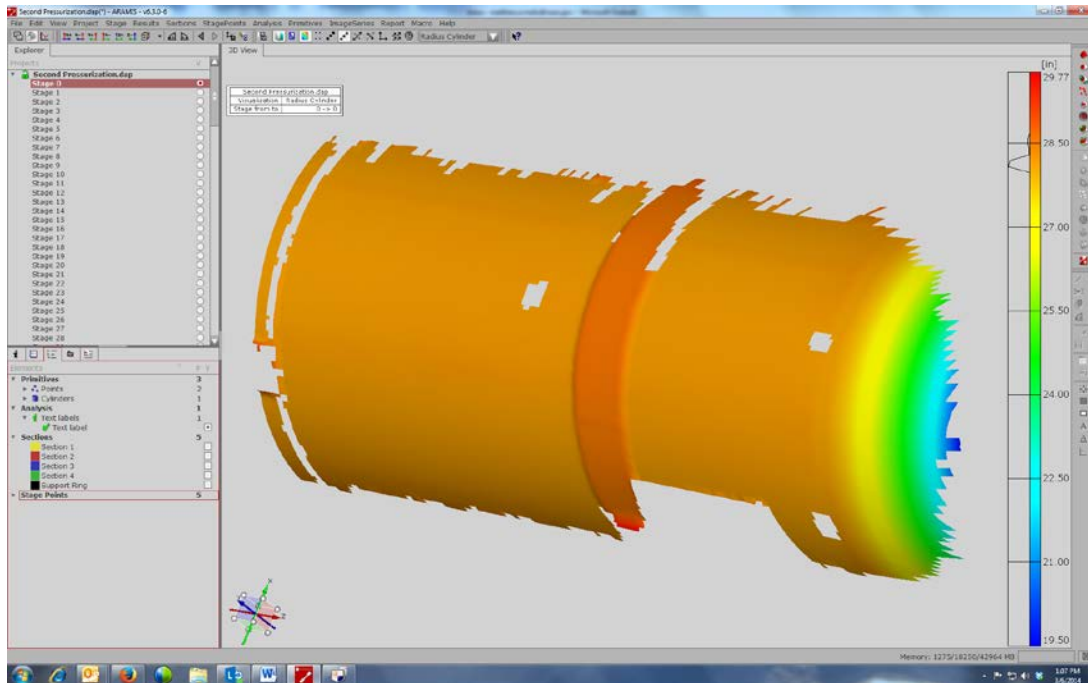


Figure 7.2.3.4-1. Aramis Three-Dimensional Fringe Plot of Computed Radial Values on Pressure Vessel

A useful feature provided by Aramis is the ability to generate a variety of geometric primitives from the computed three-dimensional shapes, including cylinders, which enables users to conduct further comparisons, define coordinate systems, and check Aramis data against known physical quantities. One item that was investigated using the Aramis data was analysis of the overall radius of the vessel. This was completed by creating a best-fit cylinder averaged from the Aramis data. From this cylinder, a Cartesian coordinate system was defined along the X-axis, representing the axial centroid of the vessel. In addition, the diameter of the cylinder created represented an average measured diameter of the vessel surface. These values yielded an average radius of 28.131 inches, or a diameter of 56.263 inches. From Table 7.2.3.2-1, adding the nominal thickness of the vessel wall of 2.188 inches to the nominal 52-inch ID results in a vessel OD of 56.375 inches, nominally within about one-tenth of an inch of the measured data. With the stated vessel measurements not accounting for layers of paint on the vessel and manufacturing irregularities (which can be seen on the vessel with the naked eye), it is fair to assume that Aramis is accurately capturing the spatial dimensions of the vessel.

During all of the tests, five sets of images were taken at each pressure level of interest. This was done for two reasons: it helped identify the true “noise floor,” or the amount of uncertainty in the data throughout the test, and at the same time enabled averaging of the data afterward to obtain more representative plots of the physical deformation. Aramis saves the images as time histories, called “stages,” such that the number of stages in the data file is the number of image pairs recorded during that particular test. Graphically, data sets are presented below using stages for the X-axis to enable a broader visualization of the data. Table 7.2.3.4-1 is for reference in

	NASA Engineering and Safety Center Technical Assessment Report	Document #:	Version:
		NESCP-RP-13-00852	1.0
Title:			Page #:
Evaluation of Agency Non-code LPVs			133 of 193

interpreting these figures. Single stages were recorded at 100-psi increments as the vessel was vented back to 0 psi. These stages were not included in the table to optimize space for this report.

Table 7.2.3.4-1. Data-indicated Pressure Values Associated with Stages Recorded in Aramis

Test 2

Pressure (psi)	Stage Numbers
0	0-4
0	5-9
250	10-14
500	15-19
750	20-24
1000	25-29
1250	30-34
1500	35-39
1750	40-44
2000	45-49
2250	50-54
2500	55-59
3000	60-64
3250	65-69
3500	70-74
3750	75-79
4000	80-84
4200	85-89
0	127-131

After detailed analysis of the data, it was discovered that the camera system was potentially compromised because its view had slightly shifted multiple times during the first and third pressure tests. Several factors may have contributed to this, but it is believed that the wind and saturated ground may have played a primary role in these induced motions. The large, 8-foot camera beam may have been susceptible to the moderate gusts that were experienced during the first excursion. Although the camera pair remained calibrated (as determined from the intersection deviation), shifted camera view angles created somewhat nonsensical deformation results. Aramis does employ algorithms that are able to remove some of the nonsensical motion; however, without tracking a fixed reference system (i.e., the background fence or the ground) the motion only due to the physical shifts of the cameras could not be decoupled from potential vessel motion due to the pressurization. Consequently, results from the first and third pressure tests were not presented in this report.

Note that the boundary conditions on this vessel were not completely understood. Both saddle bands were stitch-welded to the vessel, and the saddle supports sat, unconstrained, on the concrete support pad. As a consequence, drawing conclusions from displacement measurements on just one-half of the vessel was much more difficult without knowledge of how the saddle supports were displacing on the concrete pad throughout the test. During the development of the photogrammetry test plan, inadequate focus was placed on this subject, which will be examined in our conclusions. The surface strain analysis below, however, compensates for some of the ambiguity in the deformation data.

	NASA Engineering and Safety Center Technical Assessment Report	Document #: NESCP-RP-13-00852	Version: 1.0
Title: Evaluation of Agency Non-code LPVs		Page #: 134 of 193	

Predicted axial deformations and hoop strain will be the primary values used for comparative purposes with Aramis measurements. In post analysis, measured data can be taken from any desired point location within the data field. The left-hand image in Figure 7.2.3.4-2 depicts an Aramis image for the second excursion with the relative locations on the vessel where displacement data were taken, along with the positive direction of the vessel cylindrical axis. The graph on the right-hand side of the figure plots the axial deformation of those points as a function of stage number. Refer to Table 7.2.3.4-1 for correlation of pressure to stages. From the graph in Figure 7.2.3.4-2, the relative noise can be estimated to have an average on the order of 2.5- to 3.0-thousandths of an inch, which is in line with the expected 2.3×10^{-3} -inch system capability.

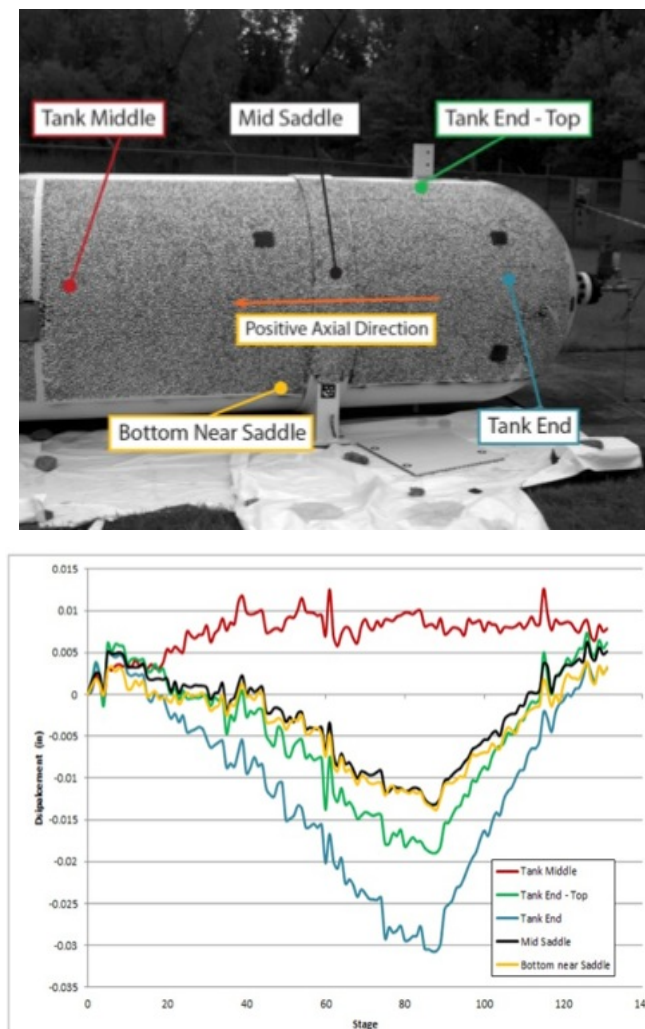


Figure 7.2.3.4-2. Vessel Point Locations and Respective Displacement Plotted versus Stage Number

The displacement curves in the graph show a somewhat intuitive deformation profile. The largest magnitude displacements are at the “vessel end” point, with the other points deforming

	NASA Engineering and Safety Center Technical Assessment Report	Document #:	Version:
		NESCP-RP-13-00852	1.0
Title:			Page #:
Evaluation of Agency Non-code LPVs			135 of 193

less as their locations move in the positive axial direction of the vessel. Note that the “vessel middle” point actually begins to deform in the positive axial direction, indicating it to be near the “midpoint,” at which point the vessel expands away in both axial directions. The maximum displacement at the vessel end was measured to be on the order of 0.05 inches. The prediction from Table 7.2.3.2-1 calls for a total axial shell displacement of 0.185 inches at 4,200 psi. At this point in the analysis, no conclusions can be drawn between Aramis and predicted displacements, as data do not exist to indicate how the other half of the vessel is deforming. This would be required for a meaningful comparison to the predicted value. The Tritop survey did, however, include the entire vessel; those results are presented below.

As stated earlier, Aramis provides the ability to overlay color fringe plots onto the actual test images. Figure 7.2.3.4-3 shows the axial deformation overlay at the maximum 4,200-psi pressure load, providing validation of a uniform continuous expansion of the vessel. Note that the bottom of the vessel expands slightly more than the top, which may possibly be due to interaction with the saddle bands or manufacturing irregularity. The large gap in the data in the lower right corner of the vessel results from data being disregarded because of coverage issues during the start of the test.

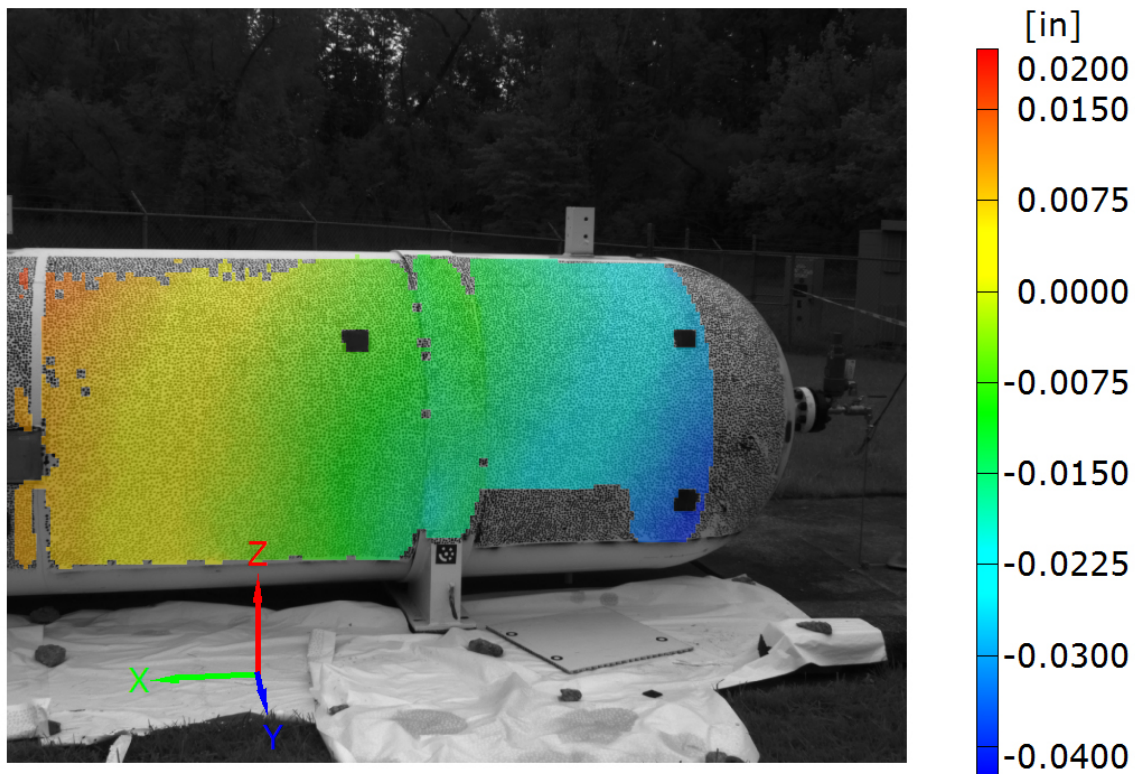


Figure 7.2.3.4-3. Color Fringe Overlay of Axial Displacement (X-direction) at 4,200 psi

In addition to axial displacements, axial strains were also of interest for comparison to expected values. Section lines are created in Aramis at several selected locations and directions on the



Title:

Evaluation of Agency Non-code LPVs

Page #:
136 of 193

Aramis data field to obtain the strains along that line. Aramis measures the difference in displacement between the two endpoints of the section line, effectively creating an optical extensometer over its length. Three section lines were selected along the axial direction of the vessel to generate strain data. Figure 7.2.3.4-4 shows the vessel location of two “medium” and one “large” length section lines, with their respective strain plots as a function of stage number. Note that the longer section line is slightly less noisy due to the greater averaging that results over a longer physical length on the vessel. This longer section line is more representative of the overall growth of the vessel during pressurization.

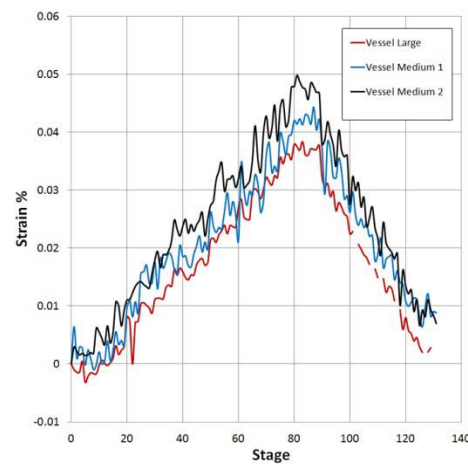
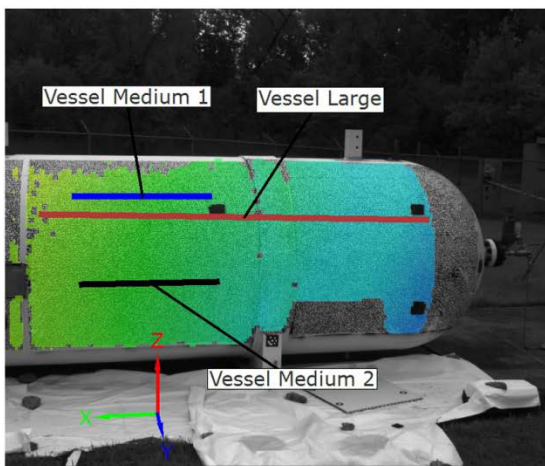


Figure 7.2.3.4-4. Selected Axial Section Lines on Color Overlay of Axial Displacement (X-direction) at 4,200 psi

The strain-stage plot in Figure 7.2.3.4-4 shows a nominal range of vessel strain from 380 to 500 microstrain. Assuming a uniform expansion of the vessel and applying these strains to the initial axial shell length of 223 inches yields a resultant expansion of 0.085 to 0.111 inches computed by Aramis. Referring to Table 7.2.3.2-1, the predicted expansion of the vessel can be seen to be 0.185 inches, about 67% greater than the Aramis measurement.

A final measurement to be computed was the hoop strain of the vessel. This was accomplished by computing the average outside diameter of a best-fit cylinder calculated from the Aramis data at both the 0 and 4,200 psig states. Figure 7.2.3.4-5 shows a graph depicting the growth of the best-fit cylinder radius as a function of stage number. From the Aramis data, the average outside vessel radius was 28.1313 and 28.1986 inches at 0 and 4,200 psig, respectively. Calculating the circumferential strain from this value $((28.1986 - 28.1313)/28.1313)$ yields 2,392 microstrain. This value is about 40% higher than the calculated value taken from Table 7.2.3.2-1, presuming all shell layers were intact and uncompromised.



Title:

Evaluation of Agency Non-code LPVs

Page #:
137 of 193

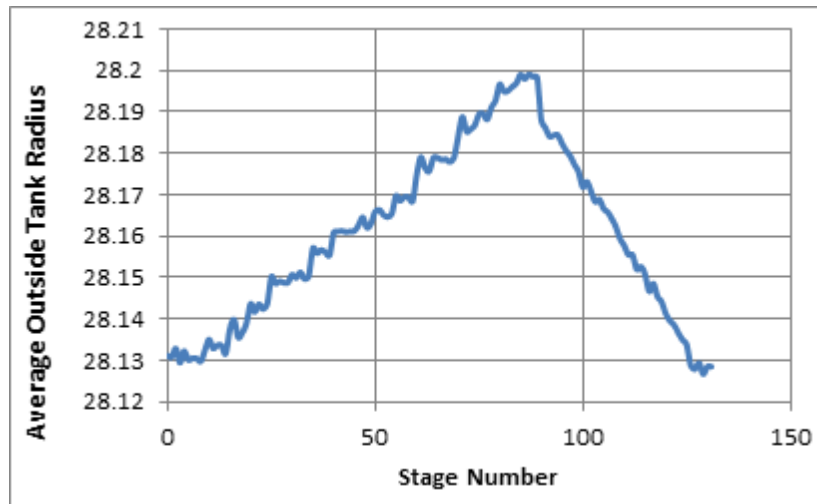


Figure 7.2.3.4-5. Average Computed Radius of a Best Fit Cylinder from Aramis Data Results from Second Pressure Test

Tritop Results

A Tritop survey of the vessel was conducted at 0 and 4,200 psig pressure conditions in an attempt to identify the differences in vessel deformations between those two states. The effort was successful in obtaining Tritop measurements at several locations on the vessel but was limited in terms of the number of data points from which measurements could be taken. This was largely due to operator inexperience with understanding the software requirements for adequate digital target coverage on a large structure such as the pressure vessel. Figure 7.2.3.4-6 depicts a snapshot from the Tritop GUI depicting the generated point cloud from targets on the pressure vessel with a best-fit cylinder created from the data points.



Title:

Evaluation of Agency Non-code LPVs

Page #:
138 of 193

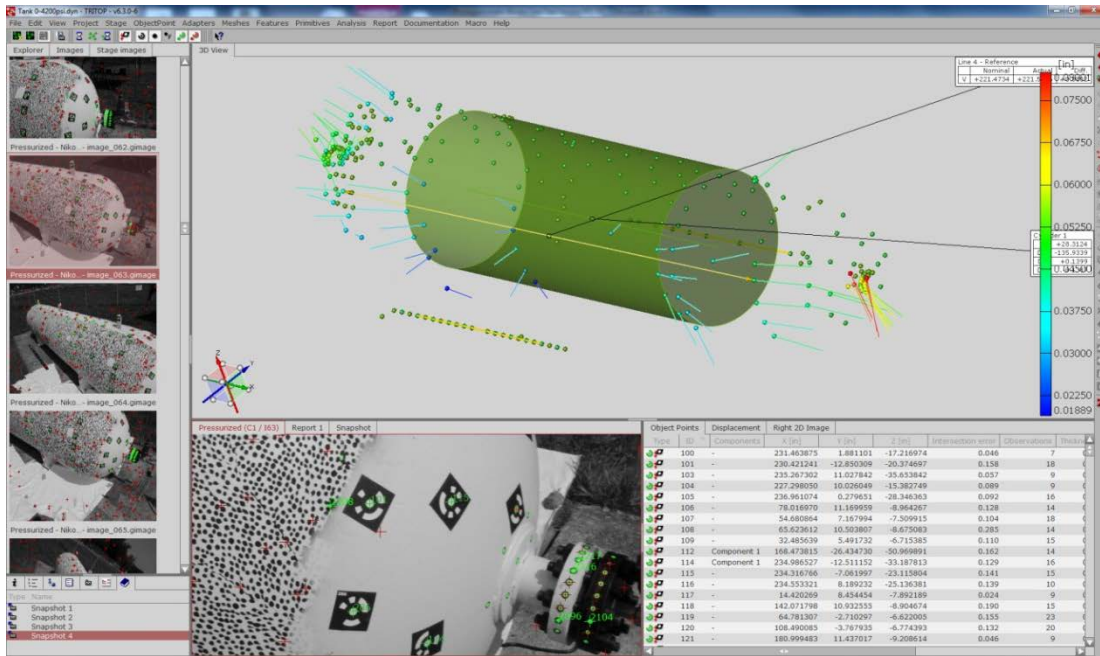


Figure 7.2.3.4-6. Screenshot of Tritop Graphical User Interface Showing Pressure Vessel Point Cloud with Best-fit Cylinder

Tritop computes vector displacements between the two pressure states and represents their magnitude and direction at each point in the cloud where the data were considered valid. In addition, color assignment representing displacement magnitude is included in this figure. Note that there are many points in this plot that do not have associated vectors placed upon them. The lack of data at these points is a due to a combination of an inadequate density of digital targets placed on the vessel and an inadequate number of photographs taken to get a complete data analysis of all points on the vessel.

Displacement results can be plotted virtually on any photograph included in the Tritop data set in any coordinate system the user chooses to define. Figures 7.2.3.4-7 and 7.2.3.4-8 are examples showing vector displacements of targets at both ends of the pressure vessel. Note that not all of the coded targets in these photographs have associated displacement vectors, again due to the lack of targets/photographs required in this survey. In both figures, the leftmost photograph shows the resultant displacement vector directions and magnitudes, which are coordinate-system independent. The rightmost photos depict the axial deformation vectors of the vessel plotted along the axis of the best-fit cylinder computed from the data targets.

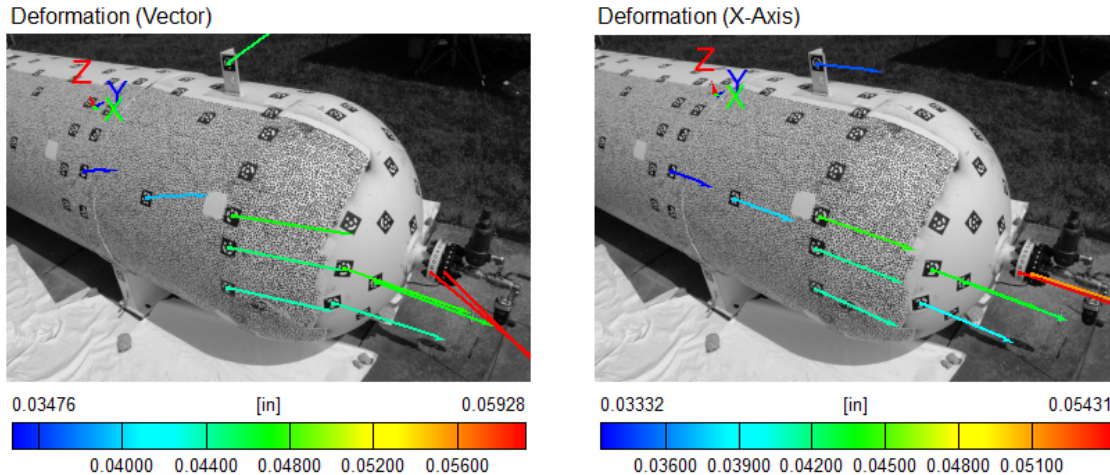


Figure 7.2.3.4-7. Displacement Vectors Overlaid on Coded Target Locations at Pressurized End of Vessel

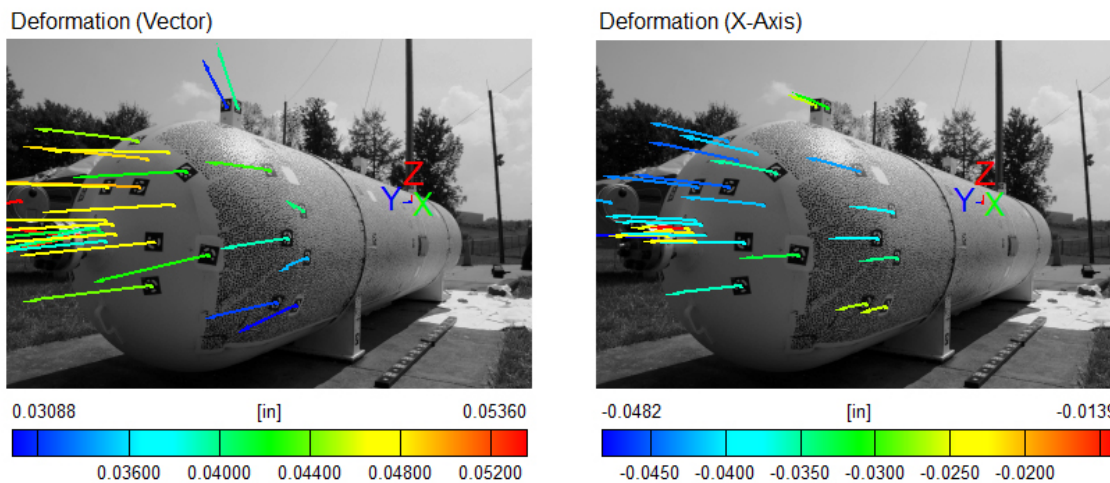


Figure 7.2.3.4-8. Displacement Vectors Overlaid on Coded Target Locations at Sealed End of Vessel

As intuitively expected, the vessel expands outward at both ends. Close inspection of the data in the Tritop database showed that targets placed on the flanges on each end of the vessel expanded outward about 0.05 inches on the feed line end and about 0.04 inches on the sealed end. Comparing the Aramis and Tritop deformations of points on the endcap weld lines showed general agreement. To get a direct comparison to the axial shell growth prediction, deformations were taken from two targets placed near the endcap welds at each end of the vessel along the same relative axial location. The straight-line distance calculated was 221.4734 and 221.5536 inches at respective vessel pressures of 0 psi and 4,200 psig, yielding a difference of 0.082 inches axial shell growth. This is less than half of the 0.185-inch growth prediction but closer to the predictions made from measurements with the Aramis system of 0.111 inches. An

	NASA Engineering and Safety Center Technical Assessment Report	Document #: NESCP-RP- 13-00852	Version: 1.0
Title: Evaluation of Agency Non-code LPVs		Page #: 140 of 193	

adequate number of data points were not available in the Tritop survey at the 4,200-psig pressure state to compute a reliable best-fit cylinder. Consequently, we were unable to extract a reliable value for hoop strain to compare with the Aramis results and the predicted values. The Tritop survey was of limited success due to a less-than-comprehensive data point set from which to analyze. This was confirmed by a Tritop error-predictor function, which indicated a less-accurate survey. Lessons learned outlined in the conclusion will ensure better results with potential future investigations using this tool.

7.2.3.5 Conclusions and Future Efforts

Results from the photogrammetry surveys produced measurement data that, in part, agreed with predictions and with one another. Due the lack of understanding of the true structural configuration of the vessel, along with manufacturing irregularities, it was impossible to conclude the true accuracy of either the predictions or the photogrammetry measurements. Regrettably, resources were not available to allow physical strain or displacement measurements to be made for this test to provide further validation of the predictions and photogrammetry. Lessons learned and conclusions are presented below.

Aramis Results

The quality Aramis data taken from the second pressure cycle excursion were considered acceptable and accurate to about 0.003 inches, based on both data analysis and the fact that internal Aramis error parameters were within acceptable limits for the data set.

- The strain and displacements in the region of known flaws were examined. No significant variations beyond the background noise of the systems were observed at these locations. However, it was anticipated that Aramis would not be effective in identifying such with the field of view used for this test series. Strain gages may provide the necessary sensitivity for detecting deformation response to small internal cracks or defects; however, a cost-benefit analysis and practicality assessment would have to be made.
- Environmental factors played a more significant role than anticipated in the stability of the Aramis camera system; wind, saturated soil, thermal shifts, and changes in lighting all presented challenges. These factors should be carefully considered and anticipated prior to future testing efforts.
- Including stationary points on the concrete pad to account for rigid body motion of the camera system may have salvaged the data from the first and third excursions. This should be a mandatory practice in future test efforts.
- Inadequate time was spent considering the potential deformation and translation behaviors of the vessel during a pressure cycle. Consequently, certain conclusions could not be drawn from the Aramis data, which were limited to a field of view of only half of the vessel during any particular excursion.

	NASA Engineering and Safety Center Technical Assessment Report	Document #: NESCP-RP-13-00852	Version: 1.0
Title: Evaluation of Agency Non-code LPVs		Page #: 141 of 193	

- A second Aramis system would have been of high value for this effort in order to capture the complete behavior of one side of the vessel. This would be of particular value for future testing efforts since Aramis facilitates the merging of data sets taken from multiple camera systems. Additional systems would enable capturing deformation of both sides of a pressure vessel.
- Aramis has the potential for detecting other types of potentially dangerous flaws: layer gaps, long cracks propagating within intermediate layers, etc. However, this was not demonstrated in this testing, and further analysis and testing is required to establish this capability.

Tritop Results

- The quality of the Tritop data was inadequate to conclusively assess its potential for evaluating deformations on large pressure vessels. This was due to the inexperience of the operators in using this technique, as well as time/schedule constraints associated with the survey.
- Careful advance consideration of the application of targets to the test article, along with the photo-capture strategy, is mandatory to acquiring a comprehensive, accurate deformation survey.
- Tritop is a substantially easier and more forgiving photogrammetry technique to use than Aramis to identify accurate quasi-static deformations at discrete points on a structure.

Based on known commercial successes and use of both the Tritop and Aramis products, it is fair to assume that both could have valuable applicability for quick and cost-effective deformation of LPVs during pressurization. Such data could have application for validating LPV deformation analysis techniques under development. Further, if it can be demonstrated that subsurface flaws generate measurable surface deformation disturbances, then these techniques might also have applicability for screening LPVs for flaws.

7.2.4 AE Testing of a Multilayer Pressure Vessel

In addition to the photogrammetry measurements performed during the pressurization of the LPV at GRC, AE testing was also performed during the first pressurization cycle. The MSFC Certification Team provided AE test support for this activity. As described previously, cracks in or near the head-to-shell welds on this vessel were previously identified using radiography; thus, the vessel afforded an excellent opportunity to acquire AE data from a vessel with known flaws. An excerpt of the A. O. Smith construction drawing for this vessel (PV0236) is shown in Figure 7.2.4-1.

The MAWP of PV0236 is 2,800 psig, and the hydrostatic test was conducted at 4,200 psig (2,800 psig \times 1.5). A pressurization plan was developed and implemented based on this test pressure. A chart of the pressurization plan is shown in Figure 7.2.4-2.



Title:

Evaluation of Agency Non-code LPVs

Page #:
 142 of 193

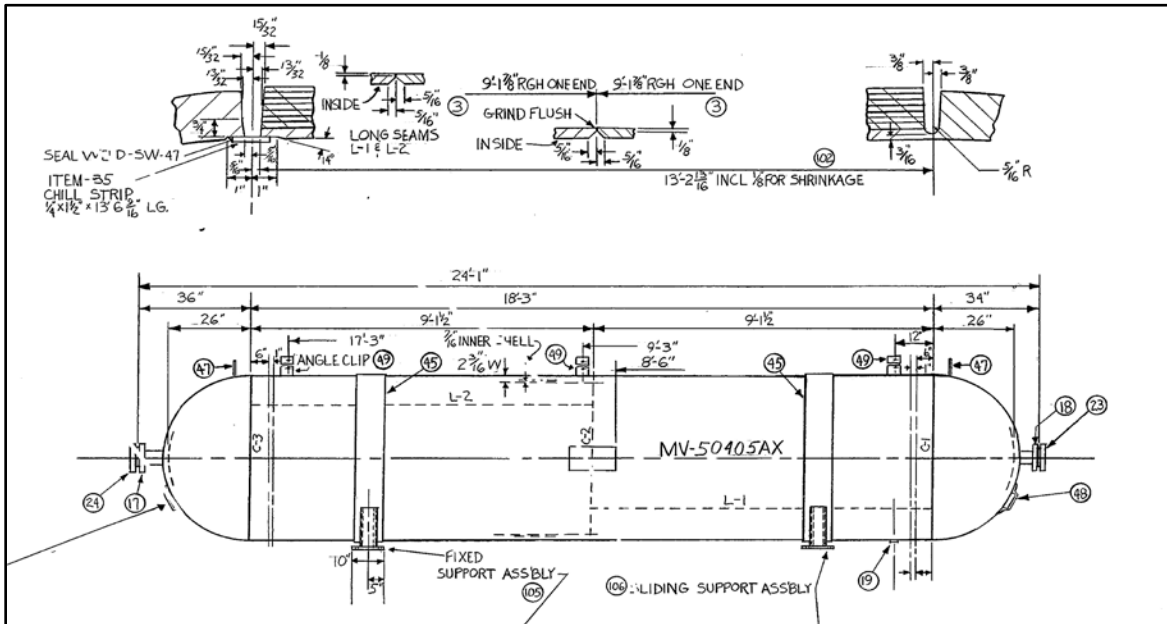


Figure 7.2.4-1. Drawing Detail of A. O. Smith Vessel PV0236

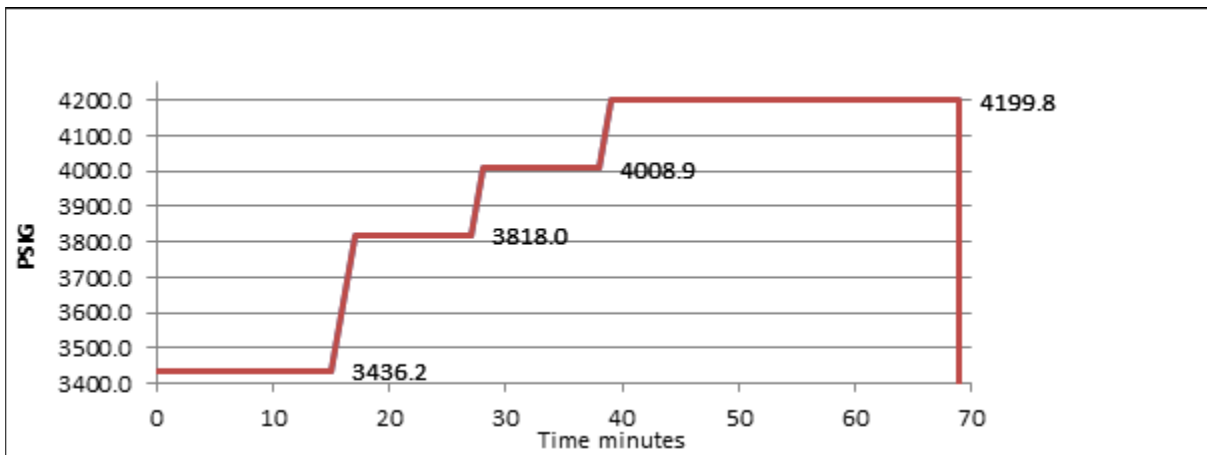


Figure 7.2.4-2. Pressurization Plan

The AE equipment used for this test was a 56-channel DISP56 AE workstation manufactured by Physical Acoustics Corporation. The vessel was instrumented with 19 AE R151 sensors having a resonant frequency of 150 kHz, per an AE sensor layout plan developed by the MSFC Certification Team. Three sensors were placed evenly on each circumferential weld, and the sensors on adjacent welds were installed 120° apart. Two additional sensors were installed on each head. The sensor layout plan is shown in Figure 7.2.4-3, and the AE system parameters are provided in Table 7.2.4-1.



NASA Engineering and Safety Center Technical Assessment Report

Document #:
**NESCP-RP-
13-00852**

Version:
1.0

Title:

Evaluation of Agency Non-code LPVs

Page #:
143 of 193

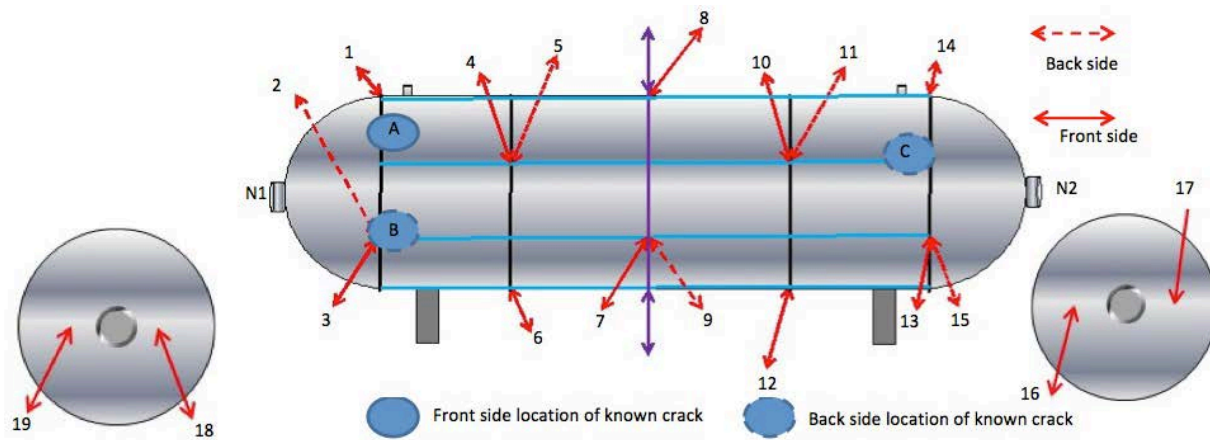


Figure 7.2.4-3. Sensor Placement

Table 7.2.4-1. AE System Parameters

AE Parameters	Peak definition time (PDT)	200 μ s
	Hit definition time (HDT)	800 μ s
	Hit lockout time (HLT)	1,000 μ s
	Pre-amp gain	40 dB
	Threshold	45 dB
External Parameters	Parametric multiplier	None
Location Parameters	Wave speed	200,000 inch/sec
	Event definition value	200 inches
	Event lockout value	400 inches
	Hits/events	Min = 6 Max = 8 Max Iteration = 256
	Evaluation threshold (dB)	70

Three cracks were known to exist in the vessel at the locations shown in Figures 7.2.4-4 and 7.2.4-5. Crack growth was not measured following the test. Worst-case expected crack growth

	NASA Engineering and Safety Center Technical Assessment Report	Document #:	Version:
		NESCP-RP-13-00852	1.0
Title:			Page #:
Evaluation of Agency Non-code LPVs			144 of 193

was estimated to be on the order 0.0001 inches by GRC Engineering (based on API 579, part 9, analysis over four overpressure excursions [ref. 32]). The locations of these cracks were not revealed to the MSFC AE test team until after the test was completed.

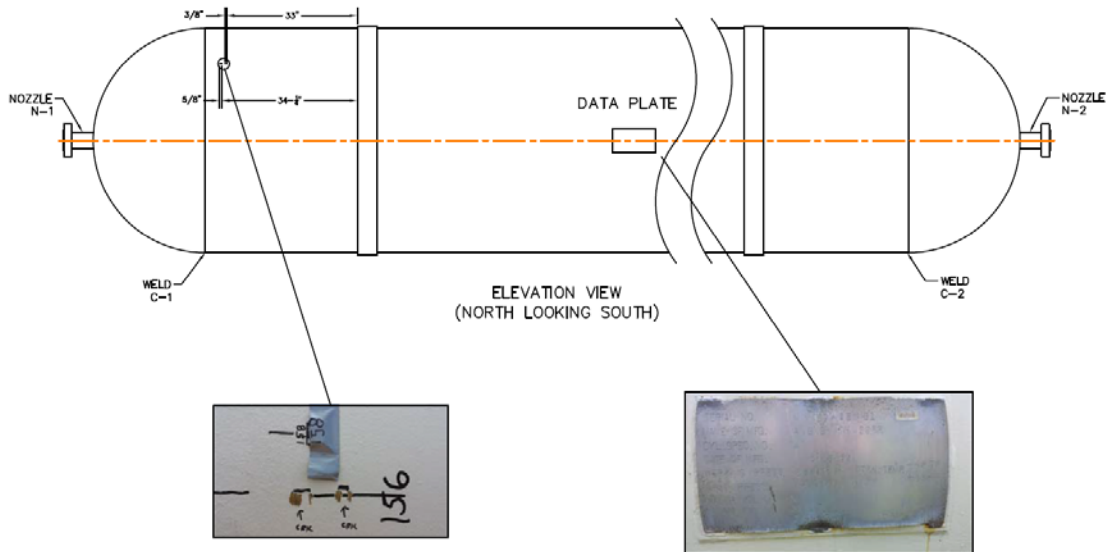


Figure 7.2.4-4. Crack Locations

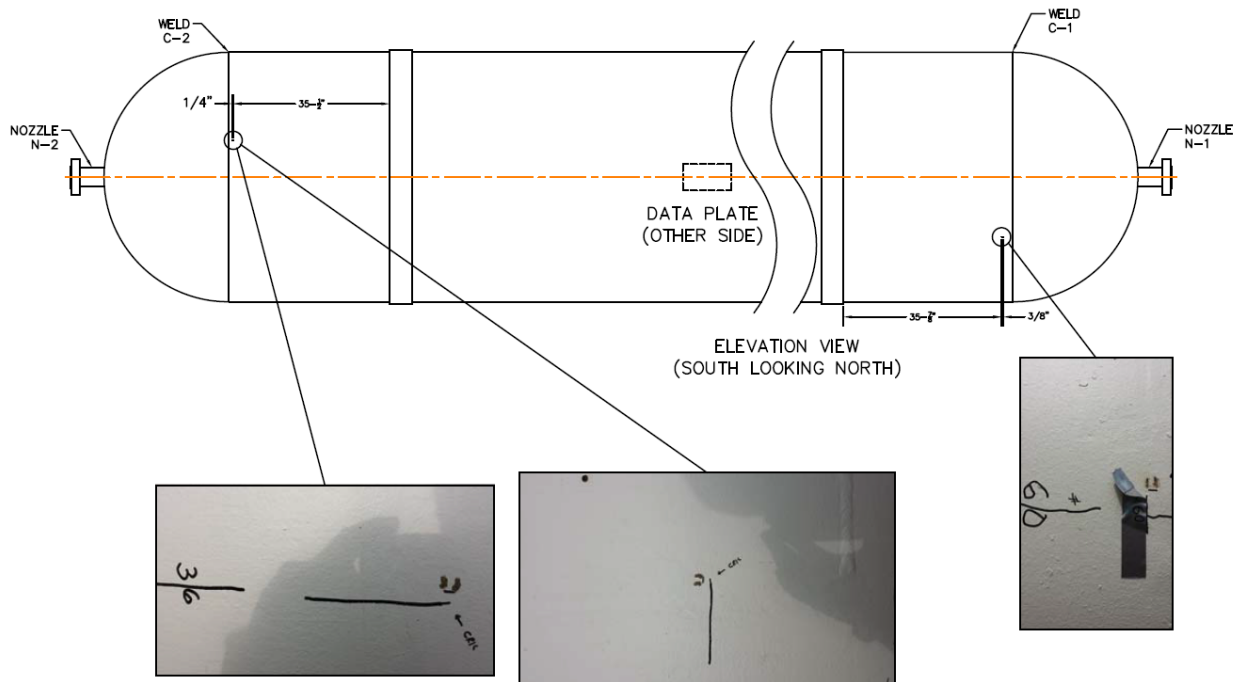


Figure 7.2.4-5. Crack Locations (continued)

	NASA Engineering and Safety Center Technical Assessment Report	Document #:	Version:
		NESCP-RP-13-00852	1.0
Title:		Page #:	
Evaluation of Agency Non-code LPVs		145 of 193	

General Analysis

During the AE test of PV0236, the extraneous noise levels were very high, and under normal circumstances, the test would have been terminated no later than 2 minutes into the first hold period. Using the criteria found in ASTM E569/E569M-13 [ref. 88], paragraph 5.5.6, background noise must be fully investigated and minimized before any AE monitoring can begin. However, since photogrammetry testing was being performed in parallel and this test was not intended to assess the structural integrity of the vessel, pressurization was continued. A major limitation for using AE testing for crack extension detection is extraneous noise. Extraneous noise levels must be controlled and minimized, when possible, to increase the probability for a crack extension to be detected.

It is believed but not confirmed that the extraneous noise was due to corrosion between the layers. PV0236 was stored unprotected from weather for more than 20 years. Similar AE background noise was also observed during a recent test of MSFC multilayered vessel V-32, which also was stored outside and unprotected for over 20 years prior to the test.

The pictures in Figure 7.2.4-6 are coupons cut from V-32 that reveal corrosion between the layers. During pressurization, it is presumed that the corrosion, in combination with the layer expansion and movement (layer rubbing), resulted in intense extraneous noise. V-32 was manufactured by A. O. Smith and has a ½-inch-thick inner shell and five ¼-inch-thick layers.



Figure 7.2.4-6. Corrosion between Layers on MSFC LPV V-32

The AE sensor locations on PV0236 were based on earlier investigations at MSFC related to overall detection sensitivity versus sensor spacing. This earlier work was performed using multilayered MSFC vessel V0343 with lead breaks performed on the inner wall of the vessel and the sensors located on the outer wall. A sensor spacing of 4.54 feet was used on PV0236. It is estimated that a 0.3-mm lead break at any point on the vessel inner wall would result in at least a 75-dB signal at one of the AE sensors.



Title:

Evaluation of Agency Non-code LPVs

Page #:
146 of 193

Location Analysis

The location algorithm was calibrated by means of a single set of five center-punch events located near sensor 7, performed pre- and post-test. Figure 7.2.4-7 shows a plot of amplitude versus time for each calibration run. The main strike can be clearly seen for each event, along with the subsequent ringing in the structure from that event. Also, note the high degree of noise between the center-punch events when there should be low levels of acoustic activity. Figure 7.2.4-8 locates the events on the vessel above sensor 7, where the punches took place. Utilizing the location calibration and applying the data from the pressure test, it can be seen that there is no significant clustering near known defect locations and the located events appear to be somewhat random across the acreage (reference Figure 7.2.4-9). There was no significant correlation with emissions from the saddle or nozzle areas.

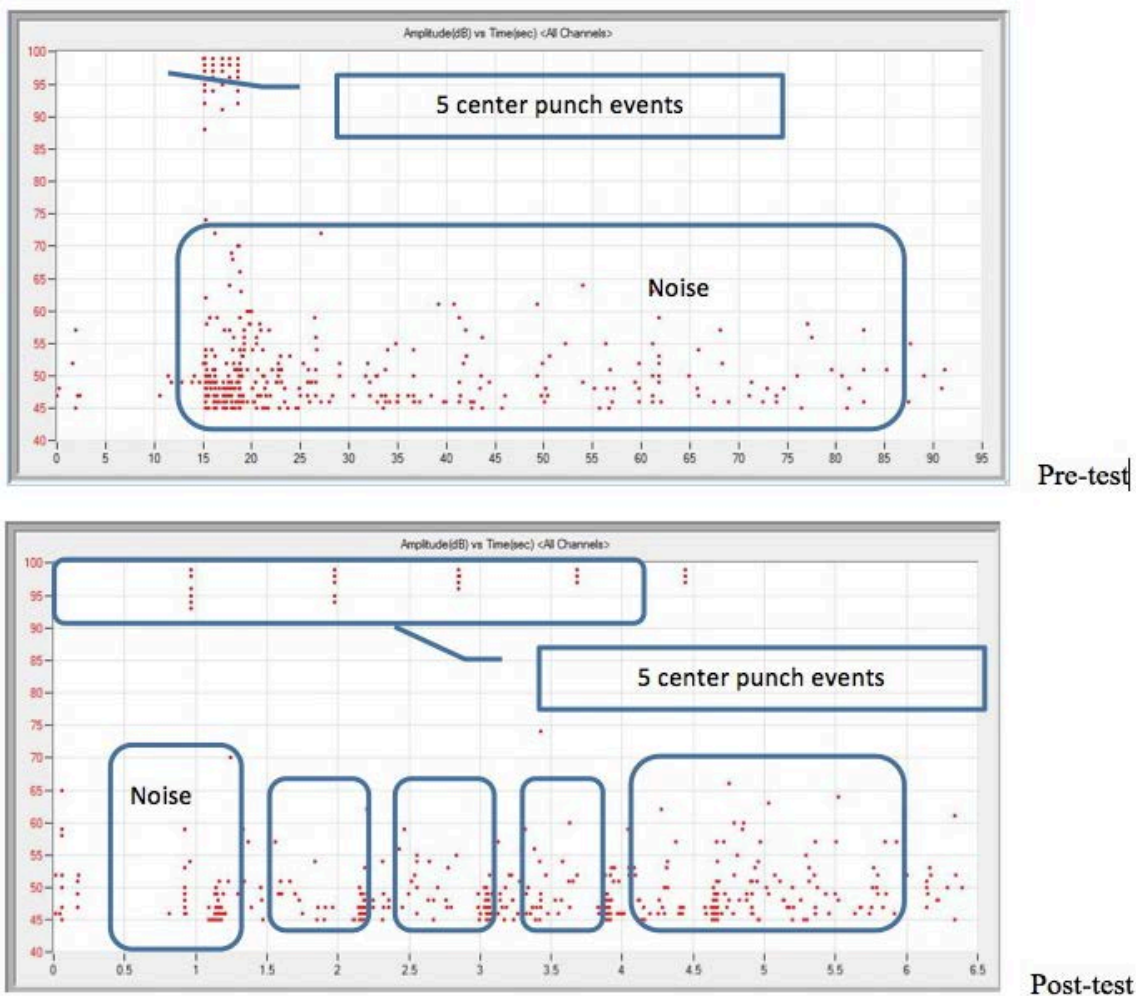


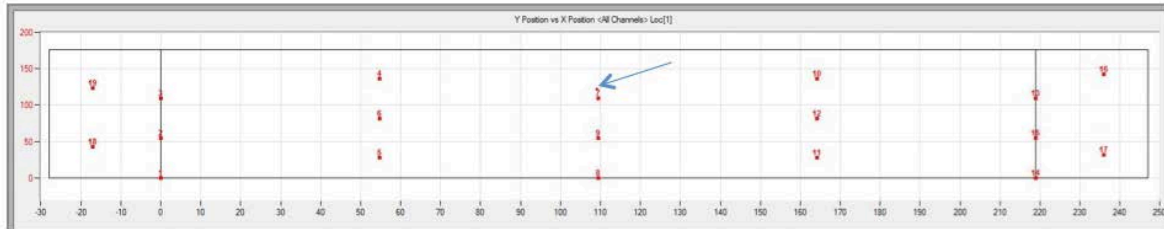
Figure 7.2.4-7. Location Event Amplitudes versus Time



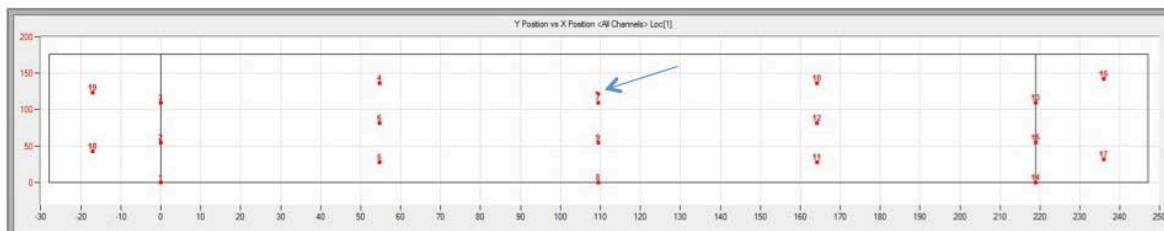
Title:

Evaluation of Agency Non-code LPVs

Page #:
147 of 193



Pre-test center punch



Post-test center punch

Figure 7.2.4-8. Location Calibration Plots

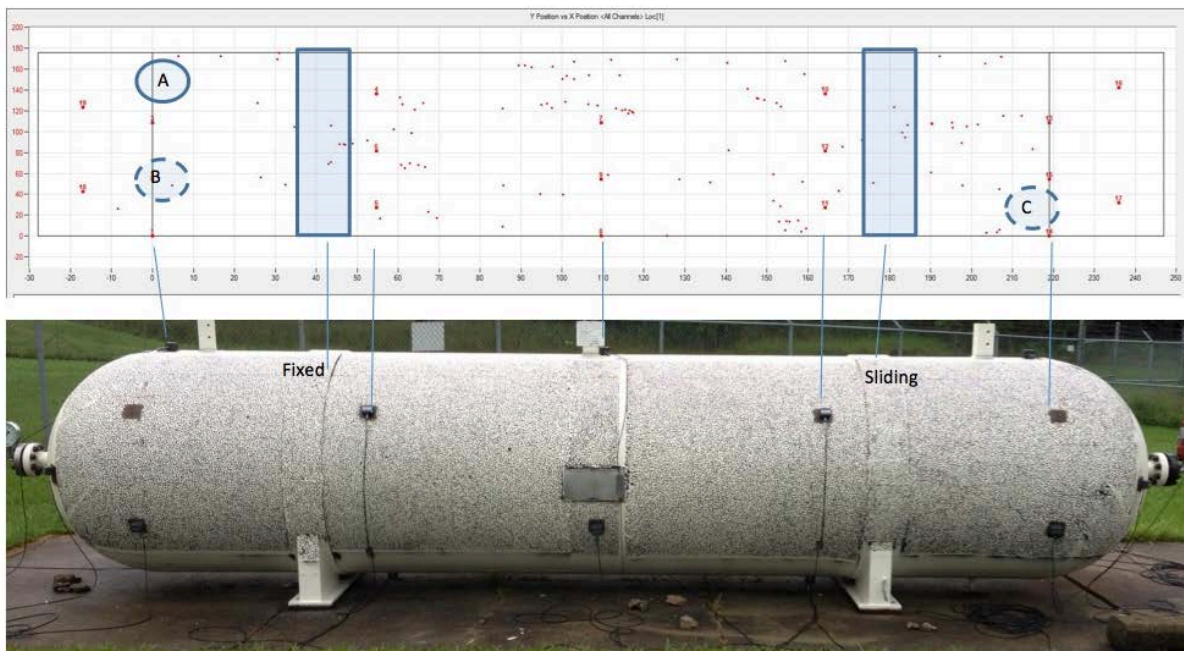


Figure 7.2.4-9. Location Plot

	NASA Engineering and Safety Center Technical Assessment Report	Document #:	Version:
		NESCP-RP-13-00852	1.0
Title:			Page #:
Evaluation of Agency Non-code LPVs			148 of 193

Trending Analysis

As can be seen in the amplitude-versus-time plot (Figure 7.2.4-10A), there were many significant (>80 dB) signals during ramp, as well as during hold periods. The amplitudes drop in magnitude during the hold, indicating some drop in AE severity, but were still very high. If these were inter-laminar rubbing noises, then they would mask any real crack-growth activity. Overall, there was significant low-level activity (<70 dB) during most of test.

The pressure data recorded for this test were logged manually from a calibrated pressure gage. It is difficult to obtain any quantitative data from the hits versus time plots in Figure 7.2.4-10 (B and D) without more accurate “real time” pressure data from a transducer. Here, only a qualitative assessment can be made from the data. The graphs show significant activity during each of the holds, approaching but not reaching a point where the activity stops. Ideally, the system should become completely quiet after 2 minutes of hold time. The activity, however, continued at about the same rate during each hold (parallel purple lines with approximately the same slope) and increased with each pressure ramp, as given by the increase in slope (green lines), which indicates that the vessel was becoming more acoustically active.

A measure of the “goodness” of the AE timing parameters can be obtained using the counts versus duration plot, shown in Figure 7.2.4-10C. For resonant sensors, it should be a single line, following the resonant frequency of the sensors.

In general, the activity is so numerous and covers such a large dynamic range that if these were inter-laminar rubbing noises, as assumed, they would mask any real crack-growth activity.

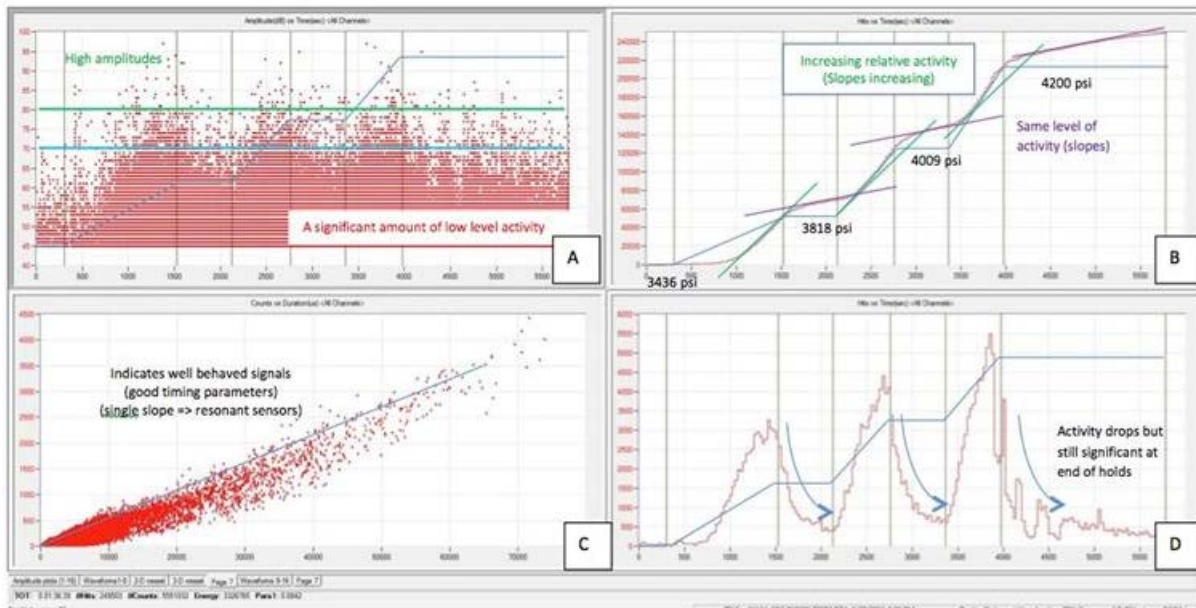


Figure 7.2.4-10. Trending Plots

	NASA Engineering and Safety Center Technical Assessment Report	Document #:	Version:
		NESCP-RP-13-00852	1.0
Title:			Page #:
Evaluation of Agency Non-code LPVs			149 of 193

Conclusions

The amplitude-versus-time and hits-versus-time plots reveal that there was significant low- and high-level activity throughout the test and that during hold periods the acoustic activity never returned to zero. This, coupled with the random nature of the location plots, tends to indicate that the activity resulted from inter-laminar rubbing. Also, considering that theoretical crack growth was estimated by GRC engineers to be only 0.0001 of an inch, the emissions from the inter-laminar rubbing and corrosion would likely mask any true crack-growth activity. Therefore, the results of the AE test results are inconclusive.

Further consideration will be given to the use of broadband sensors and a more rigorous pre-test location calibration procedure to determine if improvements can be made in differentiating flaw growth from elevated levels of background noise on multilayered vessels. MSFC is also preparing to perform lab-scale AE testing, which should help to answer questions related to sensor density and predicted energy levels from flaw extension in multilayered vessels.

7.2.5 Feasibility of using Phased Array Ultrasound to Inspect the Shell-to-Head Circumferential Welds in NASA Pressure Vessels

Due to the age and operating history of LPVs, it is possible that cracks have developed over time and could provide a potential failure mechanism during future operation. Of particular interest are the circumferential shell-to-head welds, as one such weld has already failed catastrophically in Kansas. The shell-to-head weld joins the domed head of the vessel to a cylindrical body that is composed of concentric plate layers that have been welded together. To ensure the safe future operation of these vessels, it is necessary to develop an inspection procedure to detect potential crack-like defects in the shell-to-head weld regions.

In a prior investigation conducted at SwRI[®], the feasibility of conducting ultrasonic inspection of the shell-to-head weld was investigated using standard single element transducers. In this preliminary investigation, SwRI[®] found that ultrasonic waves entering through the multi-layered body of the vessel tended to remain trapped within the outermost layer and could not effectively propagate to the shell-to-head weld. Alternatively, SwRI[®] attempted to direct sound into the shell-to-head weld via an ultrasonic beam entering the vessel through the head at an angle. The results of this work indicated that an angle beam inspection from the head side merited further investigation.

Given the relatively complex geometry of the part and the thickness of the weld, an effective inspection of the weld using conventional single element ultrasonic probes would require two-axis scanning of the part to sweep the beam through the area of interest. Furthermore, inspection may require several probe angles to provide full coverage of the weld. These factors would lead to an involved inspection and analysis procedure. Instead, a phased array probe may be used to provide more extensive coverage of the weld using a limited number of line scans around the vessel's circumference. In the interest of developing a relatively straightforward inspection method for the shell-to-head welds, SwRI[®] conducted several phased array exams on shell-to-

	NASA Engineering and Safety Center Technical Assessment Report	Document #:	Version:
		NESCP-RP-13-00852	1.0
Title:			Page #:
Evaluation of Agency Non-code LPVs			150 of 193

head weld samples with machined flaws to determine the feasibility of developing an ultrasonic phased array inspection procedure.

7.2.5.1 PAUT Background

UT phased array is based on electronically controlling the excitation and reception characteristics of a multi-element probe. Although there are several different phased array probe configurations, the most common phased array probe is a linear array composed of several narrow ultrasonic transducers that are spaced at some regular interval. During ultrasonic transmission, each element of the probe is excited with a phase delay relative to the other elements, where the phase delays of all elements are calculated to produce an ultrasonic beam with the desired directivity and focal characteristics. If a feature is present at the desired focal point, then the feature reflects a portion of the transmitted wave and the reflection returns to the probe. The received signal is captured and recorded by each element. Calculated phase shifts and gains are applied to each waveform, and then all waveforms are summed to produce an A-scan. The gains and phase delays for each element are calculated to enhance signals captured at the desired focal point and suppress signals originating from other locations within the part. By rapidly adjusting the firing sequence, gain, and phase delay of each element within the probe, the ultrasonic beam can be made to dynamically sweep or shift through the inspected part. Figure 7.2.5.1-1 shows the some common operating modes of a phased array probe in which varying the timing of the excitation of the individual elements according to different focal laws results in different effects on the resulting ultrasonic beam, such as focusing and scanning.

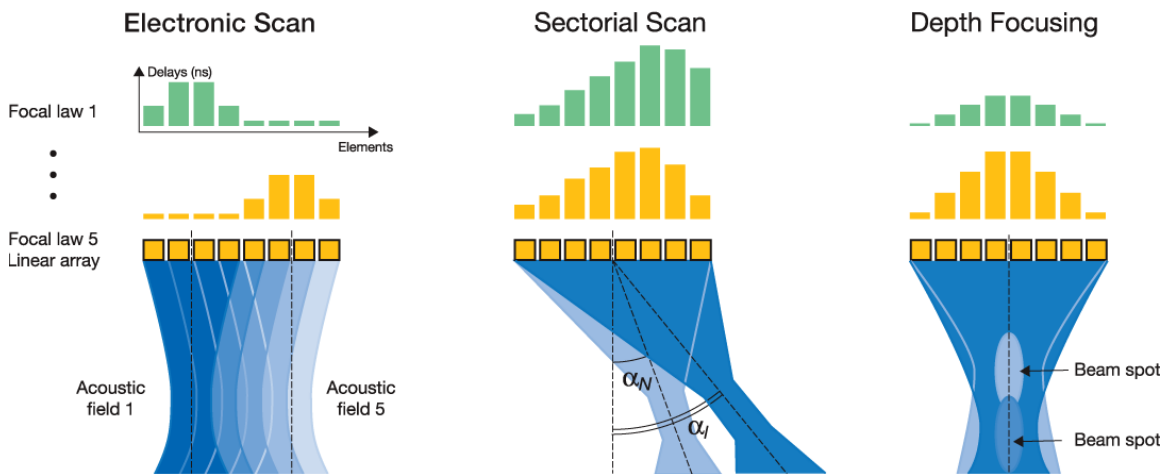


Figure 7.2.5.1-1. Examples of Common Operating Modes using a Phased Array Probe (used by permission from Olympus)

Phased array ultrasound inspection has several potential advantages over conventional ultrasound inspection. To test or interrogate a large volume of material, a conventional probe must be physically scanned over the area of interest. In contrast, the beam from a phased array probe can be moved electronically along one inspection axis without having to move the probe, effectively eliminating one scan axis in an inspection.

	NASA Engineering and Safety Center Technical Assessment Report	Document #:	Version:
		NESCP-RP-13-00852	1.0
Title:			Page #:
Evaluation of Agency Non-code LPVs			151 of 193

Another key advantage of phased array is the data visualization. In a conventional ultrasonic exam, the probe must be scanned over some area of the part (often in an X-Y grid), and an A-scan, or a time-amplitude plot of the reflected ultrasound, must be recorded at each probe location. These A-scans must then be post-processed to present the data in a visualization of the inspected part. This task can be time consuming and often requires off-site manipulation of the exam data. In a phased array system, the data from a scan can be immediately processed and displayed.

7.2.5.2 Inspection Feasibility Study

SwRI[®] conducted a series of ultrasonic tests to evaluate the feasibility of detecting several flaws distributed throughout the weld. The study was conducted using an Omniscan MX2, a commercially available instrument produced by Olympus NDT. Inspections were conducted with two 60-element 1-mm-pitch linear array phased array probes with frequencies of 3.5 and 7.5 MHz.

Test Blocks

Two test blocks were manufactured from samples cut out of a multi-layer, A. O. Smith pressure vessel MV-50466-8, the same vessel that was tested in references 40 through 42. Each test block measured 6 inches in width. They included roughly a 7-inch span of the vessel head and a 2.75-inch span of the multi-layer plate structure joined together by the shell-to-head weld. In the first block, a total of nine flat-bottom holes (FBHs) were drilled into the weld at varying depths and locations. An illustration of the six side-drilled holes (SDHs) in the test block is shown in Figure 7.2.5.2-1, and an illustration of the three radially drilled holes (RDHs) is shown in Figure 7.2.5.2-2.

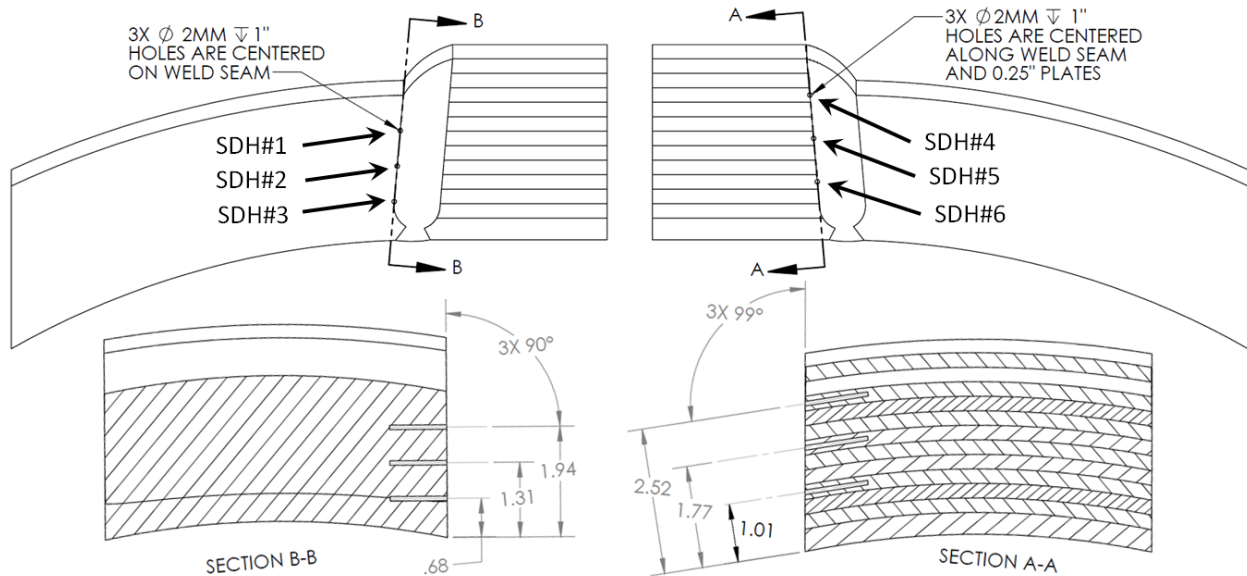


Figure 7.2.5.2-1. View from either Side of Calibration Block Showing SDHs



Title:

Evaluation of Agency Non-code LPVs

Page #:
152 of 193

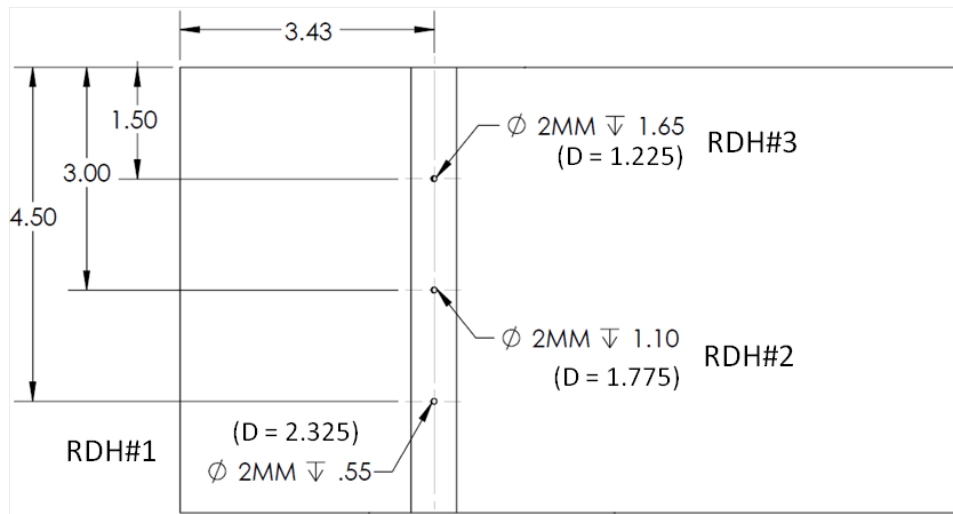


Figure 7.2.5.2-2. View from Underside of Calibration Block Showing the Three RDHs in the Weld

No flaws were added to the second block. At a later point, electronic discharge machine (EDM) notches that behave similar to crack-like flaws will be added to the second block. In the work to date, the second block was used to compare the phased array response to a specific location within the block with and without a known flaw.

Ultrasonic Velocity Measurements

Prior to conducting phased array inspections, the longitudinal wave and shear wave velocities were measured in the part at various frequencies. In addition to velocity, the relative signal level at each frequency and location was compared against a baseline signal level taken at 1 MHz through the width of the block. These measurements were taken in three locations in the first test block, as shown in Figure 7.2.5.2-3, and the measurement results are provided in Table 7.2.5.2-1.

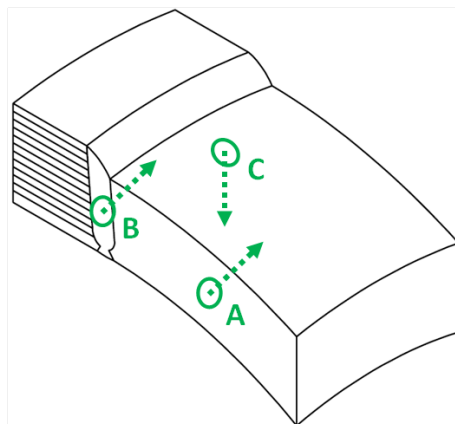


Figure 7.2.5.2-3. Ultrasonic Velocity Measurement Locations in First Test Block

	NASA Engineering and Safety Center Technical Assessment Report	Document #:	Version:
		NESCP-RP-13-00852	1.0
Title:			Page #:
Evaluation of Agency Non-code LPVs			153 of 193

Table 7.2.5.2-1. Wave Velocity and Relative Signal Loss Measurements taken from Test Block

Measurement location	Frequency (MHz)	Shear Wave		Longitudinal Wave	
		Velocity at 0° (mm/μs)	Velocity at 90° (mm/μs)	Velocity (mm/μs)	Signal loss relative to 1 MHz at location A (dB)
A	1			5.92	0.0
A	2.25			5.91	-1.7
A	5	3.24	3.25	5.92	-3.8
A	10			5.92	-5.3
B	1			5.89	-2.7
B	2.25			5.87	-1.3
B	5	3.21	3.21	5.88	-1.5
B	10			5.87	-3.1
C	1			5.99	-0.1
C	2.25			5.99	-0.8
C	5	3.28	3.29	5.99	-3.2
C	10			5.98	-7.4

Based on the relative signal strength measured at each frequency, there does not appear to be a significant difference in attenuation over the tested frequency range that would encourage the use of one inspection frequency over another. For the purpose of the phased array investigation, the average longitudinal velocity is assumed to be 5.90 mm/μs and the average shear velocity is assumed to be 3.23 mm/μs.

Initial Observations

The first phased array tests were conducted using the 3.5-MHz and 7.5-MHz probes with a 0° Lucite® wedge that was machined to have a concave contact surface that matched the vessel head's radius of curvature. In addition to serving as a coupling surface between the probe and the part, the wedge serves as a medium for the ultrasonic beam to develop before entering the part, which improves the focusing performance of the probe. Initial tests were conducted both as sectorial exams and as fixed angle linear electronic scans.

The initial exams showed that at both frequencies, significant signal loss was observed within the part, and high gains were needed to resolve the drilled holes. Although the attenuation at the two frequencies is not significant, the overall signal loss at both frequencies will be a limiting factor to detection sensitivity. At high gains, background noise caused by the part became significant enough to interfere with the flaw signal responses, and the lower frequencies tended to have much higher sensitivity to background noise. Based on this observation, the majority of later testing was conducted with the 7.5-MHz probe.

Many of the flaws were detectable in both the linear exams and the sectorial exams, but the linear exams tended to exhibit a greater number of extraneous signals and focal law artifacts. Furthermore, the sectorial exams were capable of covering a greater extent of the weld (from cap

	NASA Engineering and Safety Center Technical Assessment Report	Document #: NESCP-RP-13-00852	Version: 1.0
Title: Evaluation of Agency Non-code LPVs		Page #: 154 of 193	

to root) from one fixed location. Therefore, later tests tended to focus on the development of sectorial exams. Finally, the 0° curved surface wedge proved less effective than originally anticipated. In later exams, this wedge was replaced with a wedge with a flat coupling surface and an 18° incidence angle.

7.2.5.3 Exams Using Half-V Path

Testing demonstrated that eight of the nine drilled holes in the first test block could be detected with sectorial exams using a half-V path, which is illustrated in Figure 7.2.5.3-1. The only hole not seen was the uppermost SDH (SDH#4) on the multi-layered plate side the weld. This hole was located above the uppermost coverage of the sectorial beam sweep and, therefore, could not be detected with the half-V sectorial exam.

Figure 7.2.5.3-1 shows an image of the probe and wedge setup on the test block for the half-V sectorial exam. The exam coverage across the weld is highlighted in green on the side of the block. Due to the radius of curvature of the vessel head, the weld appears slightly canted toward the probe position. In the half-V exam, the leading edge of the wedge is allowed to ride flush along the shell-to-head weld. As the probe and wedge is pulled back from the weld, the effective orientation of the weld with respect to the probe changes. This is important because the estimated depths of the detected flaws are dependent on the assumed position of the weld. The acquisition software of the Omnican MX2 assumes that the weld is always normal to the beam entry surface, as indicated by the white lines in Figure 7.2.5.3-1.

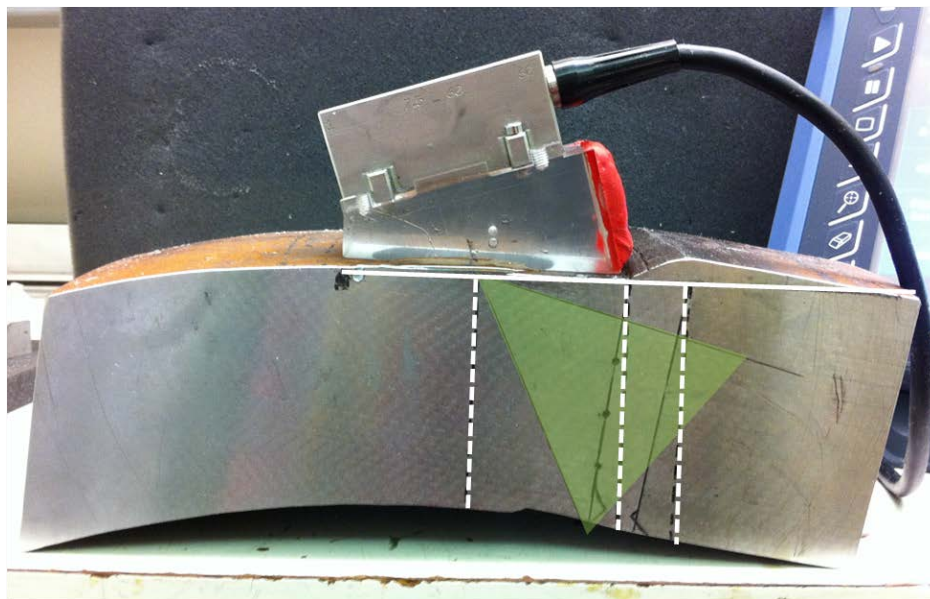


Figure 7.2.5.3-1. View of the Probe and Wedge used to Conduct Phased Array Half-V Sectorial Exams

Figure 7.2.5.3-2 shows the sectorial exam views (S-scan) of the three SDHs located on the head side of the weld. The uppermost flaw (SDH#1) was detected with a peak response of 78% full screen height (FSH) at a depth of 1.20 inches below the sound entry surface. SDH#2 was

	NASA Engineering and Safety Center Technical Assessment Report	Document #:	Version:
		NESCP-RP-13-00852	1.0
Title:			Page #:
Evaluation of Agency Non-code LPVs			155 of 193

detected with a peak response of 80% FSH at a depth of 1.90 inches, and SDH#3 was detected with a peak response of 74% at a depth of 2.55 inches. All flaws were detected within 0.2 inches of their true locations. Faint echoes from several of the plate layers (labeled C) can be seen in Figure 7.2.5.3-2. Signal artifacts caused by interactions between the wedge and the part (labeled A and B in the figure) are also observable in the S-scans. Each SDH echo is also accompanied by a second reverberation, which appears slightly below and behind the main echo.

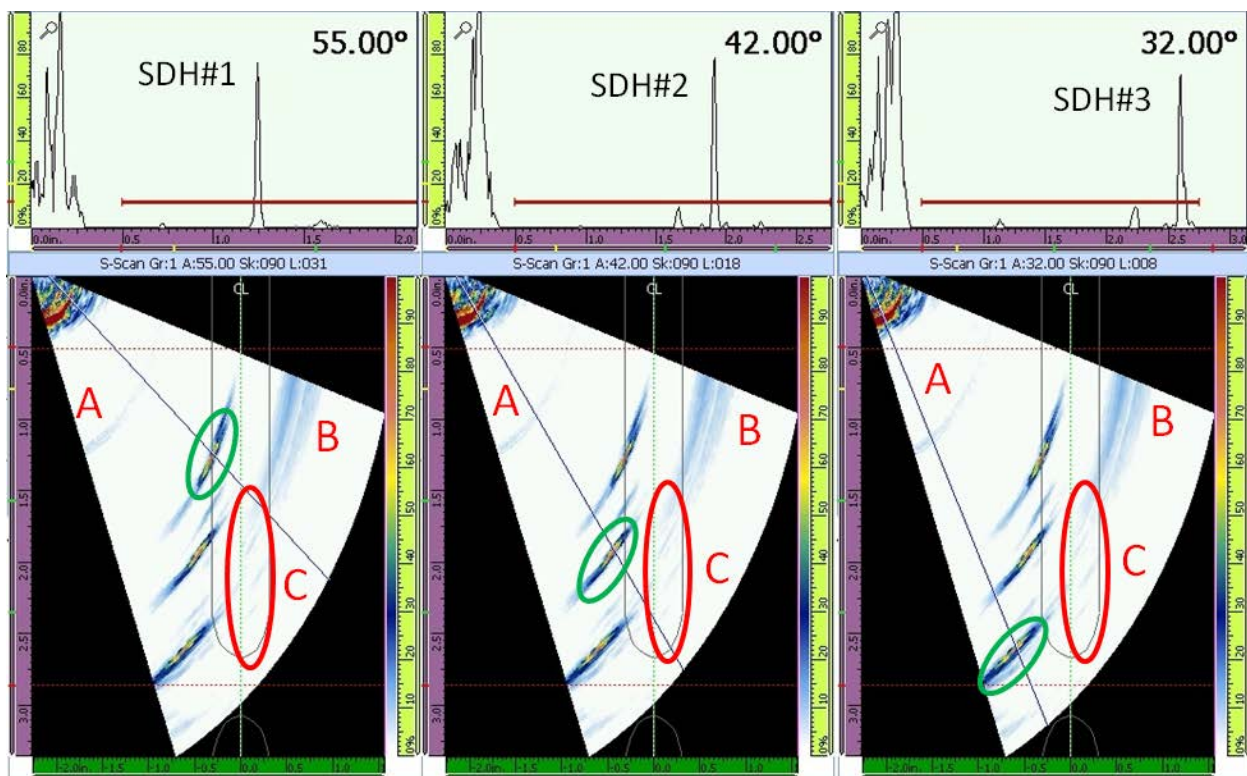


Figure 7.2.5.3-2. S-scans of Three SDHs on Head Side of Weld and A-scan of Each Hole at Angle of Peak Response

Figure 7.2.5.3-3 shows the S-scans of the lower two SDHs located on the multilayered plate side of the weld. SDH#5 was detected with a peak response of 26% FSH at a depth of 1.35 inches, and SDH#6 was detected with a peak response of 28% at a depth of 2.10 inches. Signal artifacts caused by interactions between the wedge and the part (labeled A and B) are also observable in the S-scans. At low angles, a reverberation (labeled D) is observable. This reverberation is produced by an abrupt change in thickness in the vessel head at the inner surface of the part. Both flaw signals are preceded by one or more signals that have not been identified (labeled E and F). These signals are noted to be unrelated to the flaw signals because their circumferential extents across the part do not coincide with the circumferential extents of the SDH signals.



Title:

Evaluation of Agency Non-code LPVs

Page #:
156 of 193

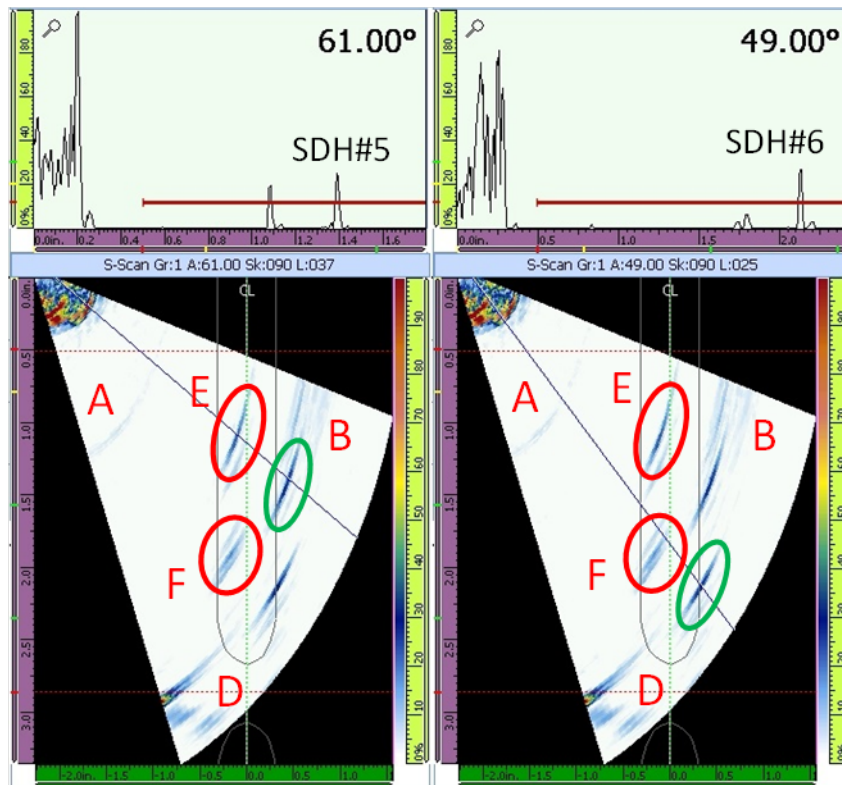


Figure 7.2.5.3-3. S-scans Showing Lower Two SDHs on Multilayered Side of Weld and A-scan of Each Hole at Angle of Peak Response

Due to their orientation, the RDHs exhibited a fainter response than the side drilled holes. Furthermore, due to their location within the part, signals from the RDHs tended to interfere with signals from the plate layers and with other extraneous signals detected throughout the test block, making detection of these holes difficult. As a result, exams for the RDHs were conducted both with the probe flush with the weld as in the previous exams, and with the probe skewed by some angle (usually 30° to 40°). Figure 7.2.5.3-4 shows S-scans of RDH#2 detected using both probe orientations. As the probe is skewed, the metal path to the hole increases, causing its apparent depth to increase. This can be corrected by updating the position of the probe on the part within the instrument. Unfortunately, there is no convenient way to notate the probe skew angle within the instrument.

By skewing the probe, fewer signals from the plate layers were detected, but the gain required to detect the holes increased, making the exam more sensitive to background noise. As a result, the S-scans tend to appear more cluttered with extraneous signals, but the extraneous signals appear over much shorter circumferential spans and are easier to discern from the flaws. Given the number of interfering signals detected when scanning flush with the weld and the amount of background noise detected when scanning at some angle, it may be necessary to conduct inspections around the weld using two probe orientations.



Title:

Evaluation of Agency Non-code LPVs

Page #:
157 of 193

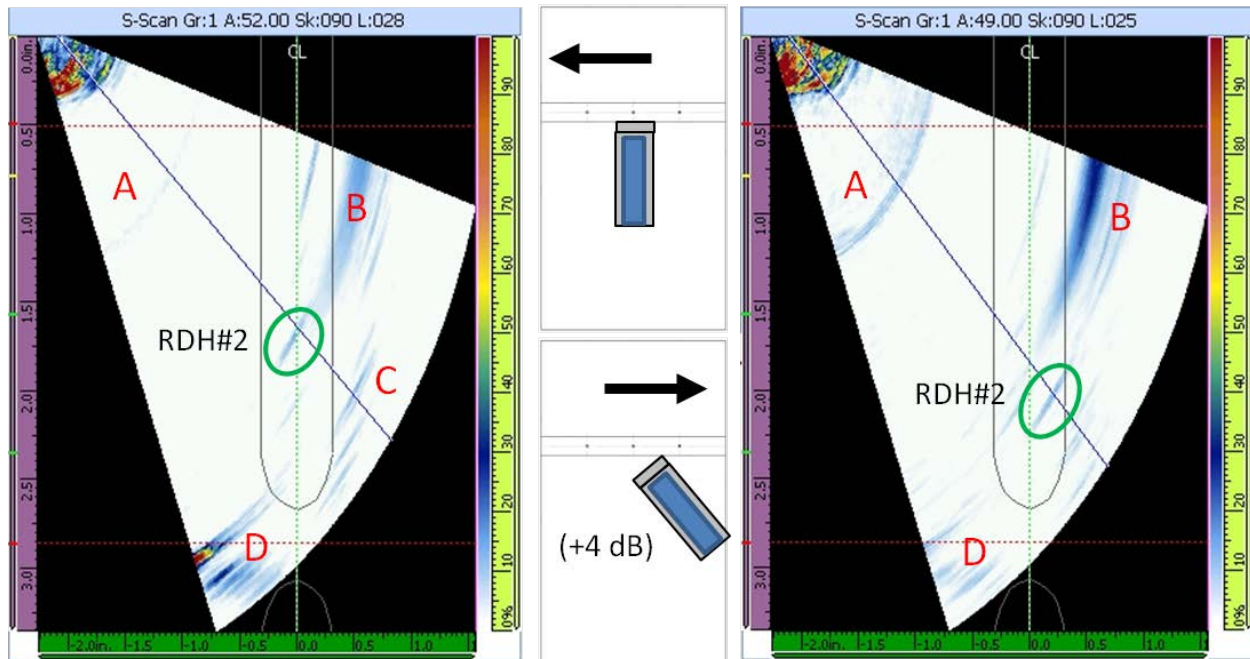


Figure 7.2.5.3-4. S-scans of RDH#2 Detected with Probe Flush with Weld (left) and Skewed at 30° (right)

Figure 7.2.5.3-5 shows the S-scans of the RDHs acquired with the probe skewed at a 30° angle. RDH#1 was detected with a peak response of 10% FSH and a depth of 2.34 inches (2.70 cos(30)), RDH#2 was detected with a peak response of 9% FSH and a depth of 1.73 inches (2.00 cos(30)), and RDH#3 was detected with a peak response of 10% FSH and a depth of 1.26 inches (1.45 cos(30)). A 4-dB increase in the instrument gain was required to capture these signals.



Title:

Evaluation of Agency Non-code LPVs

Page #:
158 of 193

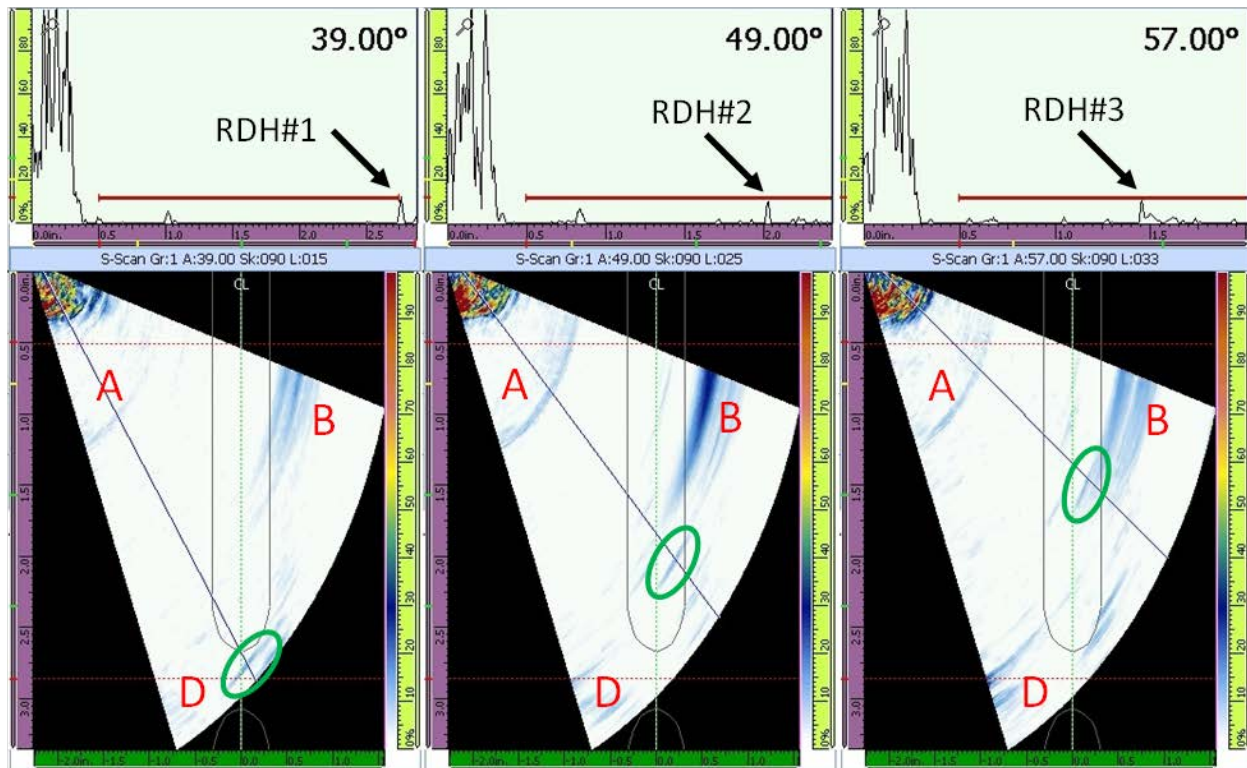


Figure 7.2.5.3-5. Sectorial Exam View of Three Radially Drilled Holes in Weld Root and A-scan of Each Hole at Angle of Peak Response

Although the half-V sectorial exam was effective at detecting most of the included holes within the test block, it also detected several extraneous signals within the part that cannot be associated with the part geometry or with the included flaws. Figure 7.2.5.3-6 shows two S-scans with example extraneous signals. In the left view, a low-amplitude indication (labeled G) is detected close to the weld root. This S-scan also shows a clear presentation of the echoes originating from the various layered plates (labeled C). In the right view, two relatively high amplitude indications (labeled H and I) are detected close to the weld cap. Both of these S-scans were captured in supposedly defect-free regions of the block. Throughout both test blocks, several of these indications have been identified. An attempt to correlate the unidentified indications in one block with those in the other block showed that the unidentified indications were not present at the same positions in both blocks. The presence of these unidentified indications in both blocks and the fact that these indications appear in different locations in each block imply that they are not artifacts of the exam settings and that they are not secondary indications of the included flaws within the first test block. Evaluation with other NDE methods and/or destructive analysis will be required to determine whether these indications correlate to real flaws. Until further work is conducted to determine the source of these unknown indications, it will be difficult to develop this exam approach into an inspection procedure.



Title:

Evaluation of Agency Non-code LPVs

Page #:
159 of 193

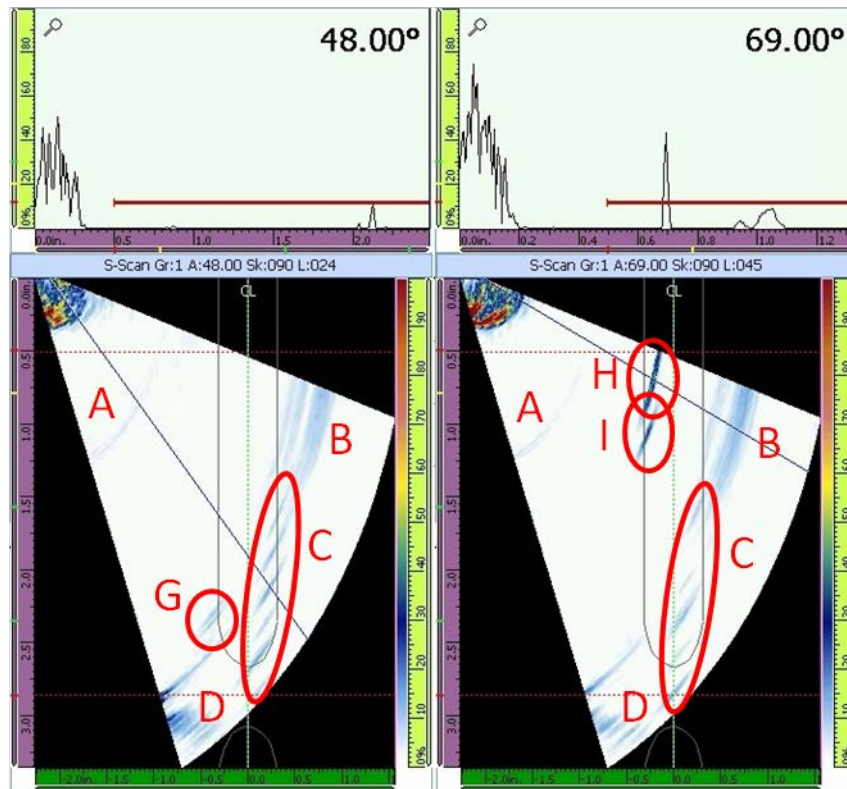


Figure 7.2.5.3-6. Two S-scans Showing Unidentified Indications Not Associated with Known Flaws or Part Geometry

7.2.5.4 Full-V Inspection

Attempts were made to develop a full-V sectorial exam that would provide inspection coverage over the upper portion of the weld that cannot be inspected using the half-V exam. The full-V inspection approach relies upon reflecting the ultrasonic beam off the inner surface of the vessel so that the beam can insonify the part material that is located above the area that can be directly interrogated by the transmitted wave. To focus the beam at the correct location within the part, the phased array instrument attempts to calculate a focal point at some virtual depth that is greater than the thickness of the part. An illustration of this approach showing the full-V beam path to SDH#2 is shown in Figure 7.2.5.4-1.

	<p align="center">NASA Engineering and Safety Center Technical Assessment Report</p>	<p align="center">Document #: NESCP-RP- 13-00852</p>	<p align="center">Version: 1.0</p>
<p align="center">Title: Evaluation of Agency Non-code LPVs</p>			<p align="center">Page #: 160 of 193</p>

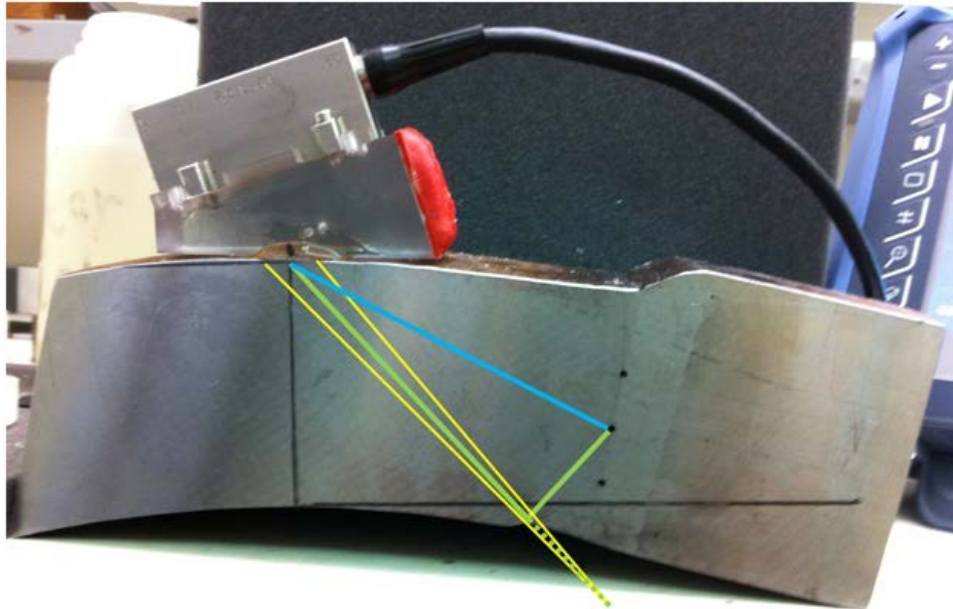


Figure 7.2.5.4-1. Illustration of Full-V Beam Path to SDH#2

The full-V beam path from the probe to SDH#2 is shown in green. An idealization of the beam focus is shown as yellow rays. A unique characteristic of this exam is that each indication can be potentially observed twice. It appears at lower apparent depth but at greater inspection angle along the half-V path (shown in blue) and then at greater apparent depth but lower inspection angle in the full-V path. The obvious disadvantage to this exam approach is that the probe must be further offset from the weld, meaning the metal path to the inspected region must be greater. The increased metal path results in greater attenuation, lower position accuracy, and greater difficulty in correctly focusing the transmitted beam at the intended location.

Unfortunately, while the full-V exam was demonstrated to work in principle, it was shown to be highly inconsistent and difficult to repeat. In addition to the added challenges related to the increased metal path, the irregular curvature of the cap inner surface tended to scatter the reflected beam, resulting in unreliable focusing. As a result, inspection using a full-V sectorial exam is not recommended. It is possible that the performance of the full-V exam can be improved by converting the exam from a sectorial exam to a linear electronic exam. A linear exam could be made to produce a wider focal spot that would be less sensitive to scattering after reflection from the inner surface. At present, this exam has not been attempted.

7.2.5.5 Conclusion

Based on the investigative work conducted to date, it appears that all but the uppermost 0.6 inches (as measured from the shell head side) of the shell-to-head weld can be inspected with phased array half-V sectorial exams. The remaining portion of this weld configuration (extreme taper) cannot be insonified with a half-V sectorial sweep, so flaws close to the weld cap must be detected with another inspection approach. Attempts were made to insonify the uppermost

	NASA Engineering and Safety Center Technical Assessment Report	Document #: NESCP-RP- 13-00852	Version: 1.0
Title: Evaluation of Agency Non-code LPVs		Page #: 161 of 193	

region of the weld using a full-V sectorial sweep exam, but this approach has not proven successful. In future work, SwRI[®] plans to attempt full-V linear electronic exams to inspect this region of the weld. It is believed that the larger focal spot produced by linear electronic exams will be less susceptible to the issues encountered in full-V sectorial exams.

All of the FBHs located within the region of the weld that can be interrogated with the half-V sectorial exam have been demonstrated to be reliably and repeatedly detected, although not without some difficulty. Due to the signal loss within the part, the background noise is often comparable to the signal response of the included flaws. Additional investigation into appropriate instrumentation, including the probe, the wedge, and the driving electronics, may be needed to improve flaw signal-to-noise ratio. Furthermore, several extraneous indications have been detected throughout both test blocks. Because these indications are present regardless of the presence of the flaws and because the locations of these indications do not coincide between the two blocks, it is believed that these indications are not related to either the weld geometry or the flaws included in the first test block. Until the causes of these extraneous indications are better understood (perhaps through destructive testing of a test weld sample), it will be difficult to use PAUT as an inspection procedure for LPVs.

In the remaining period of performance, SwRI[®] will add several EDM notches to the second test block. The successful phased array examination approach developed previously will be tested on these notches to verify the method's capability to detect crack-like flaws within the weld. SwRI[®] will also continue to pursue methods to detect flaws in the uppermost portion of the weld.

7.2.6 AE Laboratory Test Specimen Design

Based on the results from the ARC validation activities, where smaller than expected AE signals were detected from known crack growth, it was decided by the assessment team that laboratory scale testing of AE from crack growth in LPV materials was preferred as the next step, prior to further full-scale validation efforts. Such testing could be performed at lower expense and under more controlled conditions, with better documentation of actual crack growth to correlate with observed AE signals. Further, tests could easily be performed on different material components of these vessels (i.e., head parent material, shell parent material, and weld and HAZ materials) to assess whether these different material components more preferentially generated AE. Results from such tests might define the applicability of AE across the different vessel regions and target regions where it might be more successfully validated and applied.

As such, a low-level Task 2 activity was defined to develop designs for laboratory test coupons. The design effort was based on a plan to utilize materials from the MSFC sacrificed vessel V0032, which has been used for ongoing materials characterization activities. Considerations for the design of the AE laboratory specimens included maximizing the specimen lateral dimensions to minimize the influence of AE signal reflections from the lateral boundaries against a number of constraints that limited the specimen size. These constraints included the curvature of the vessel, thickness of the layers, load capabilities of test load frames to be used, and fracture mechanics considerations for predicting and measuring crack growth. The resulting planned specimen size was defined to be a dog bone specimen 18 inches in length by 3.5 inches wide in

	NASA Engineering and Safety Center Technical Assessment Report	Document #:	Version:
		NESCP-RP-13-00852	1.0
Title:			Page #:
Evaluation of Agency Non-code LPVs			162 of 193

the gage section. This sample is shown in Figure 7.2.6-1. Curvature was retained in the specimen to be as representative as possible of the LPV, which requires custom backing plates. A large center crack 2a of 0.75 inches is designed to produce failure in the gage section. Even with this compromise in specimen dimensions, reflections of AE signals generated by crack growth will quickly reflect and superimpose on the original AE signal. Hamstad [ref. 89] modeled this effect, showing the resultant increase in measured signal amplitude for a particular finite-dimensioned laboratory specimen. This is a low-constraint sample, which will need to be taken into account when applying these data to the structure, but the purpose of this test is to assess AE detection capability and not to directly determine fracture properties. It is planned to run a simple finite element analysis model of this test first to estimate the stress state at tearing and evaluate the feasibility of the sample for the test. The sample will be loaded monotonically at room temperature until crack tearing is observed. While performing the test at cold temperatures with expected cleavage failure would be more distinct and more easily measured by AE, the purpose of this test is to be representative of a proof test on an actual vessel.

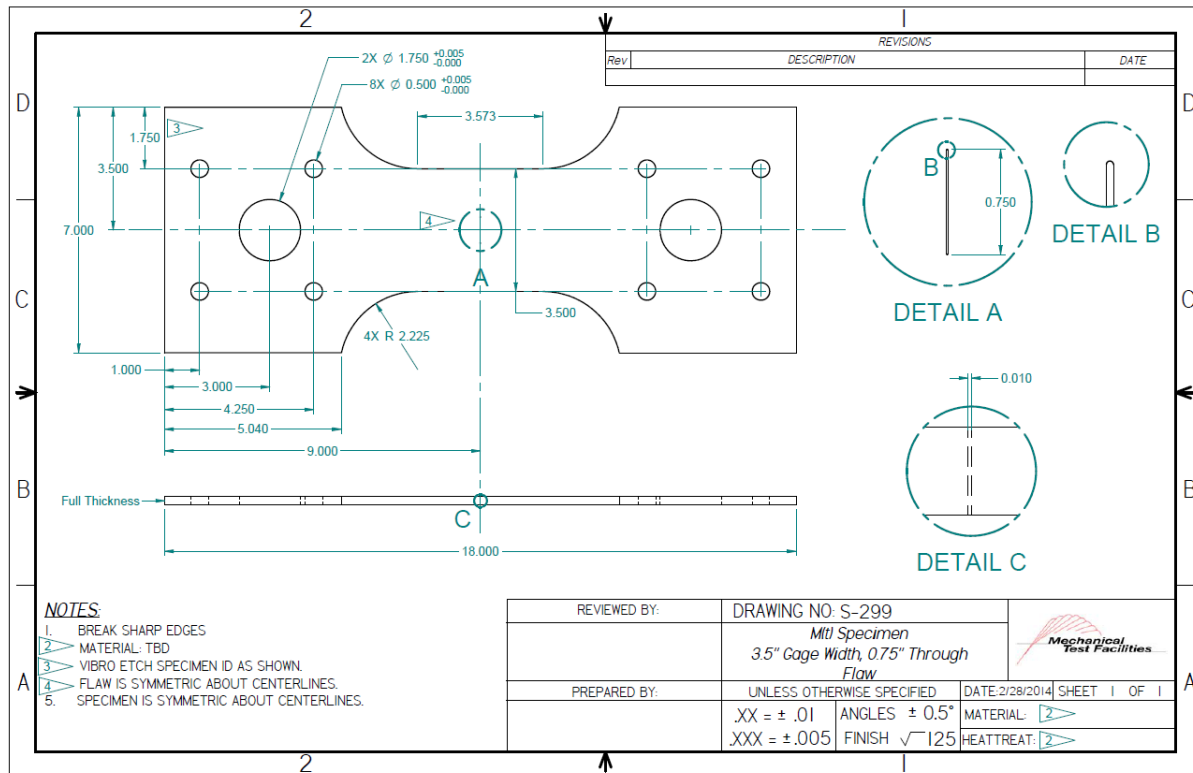


Figure 7.2.6-1. AE Laboratory Specimen to be Tested from V0032 1146a Material

To understand the amplitude enhancement factor that might also occur for the specimens designed for this testing, an additional laboratory investigation of signals from simulated AE signals (generated by pencil-lead breaks) was performed. Specimens of the same crack-growth specimen design were compared with increasingly large plate specimens, and the relative amplitudes of simulated AE signals were compared. Efforts will be made to simulate the same

	NASA Engineering and Safety Center Technical Assessment Report	Document #: NESCP-RP- 13-00852	Version: 1.0
Title: Evaluation of Agency Non-code LPVs		Page #: 163 of 193	

AE signal mode of propagation as might be expected for cracks to better replicate the observed effect.

The additional laboratory investigation involved testing on three steel plates, ¼-inch-thick, with different dimensions: 3 by 6 inches, 4 by 8 inches, and 6 by 12 inches. In addition, a ¼-inch-thick aluminum plate, 36 by 72 inches, was used as a reference for a plate because reflections would be more spread out due to the larger lateral dimensions. Pencil-lead breaks were performed on the surface of each plate, using a Hsu-Nielsen source (0.3-mm leads). Pencil-lead breaks have been demonstrated to provide a good simulation of the time and frequency response of cracks in metals. However, they provide a much more energetic source and, thus, result in much larger detected amplitude signals than are typical for small increments of fatigue crack propagation. However, as this study was only to detect the relative amplitude differences for different geometries and not the absolute amplitude for a real crack source, the use of pencil-lead breaks as a simulated source was deemed appropriate.

For the steel plates, a wide-band AE sensor (DWC model B225.5 (bandwidth 40–330 KHz)) was placed at each plate’s center, and the lead breaks were located midway on the long edge at the edge. For the aluminum plate, the transducer was placed 6 inches from the long edge and 18 inches from the short side. The pencil-lead breaks were performed 6 inches from the sensor at the long edge of the plate. The signals were recorded with a 16-channel DWC model FM1 signal conditioner and a dedicated signal acquisition system/computer, also from DWC. The signals were amplified with 42 dB of gain. The data were band pass filtered from 20 to 750 KHz. The system was set to digitize at 2 MSamples/sec and recorded 16,438 data points (8.219 ms), with 1,024 points before the trigger. Triggering was accomplished by utilizing a second transducer (B1025) located at the pencil-lead break site with a simple threshold trigger. The signal energy (SE) of each recorded waveform was then computed with the following formula:

$$SE = \sum_i^N V_i^2 \Delta t$$

where V_i is the voltage at time i and Δt is the time between measurement samples. Since pencil-lead breaks are manually done, the lead break signals can vary slightly from test to test, so the triggering sensor signal was used to select equivalent signals.

For the four different plates, Figure 7.2.6-2 shows the signal energies (gain corrected) that were measured.



Title:

Evaluation of Agency Non-code LPVs

Page #:
164 of 193

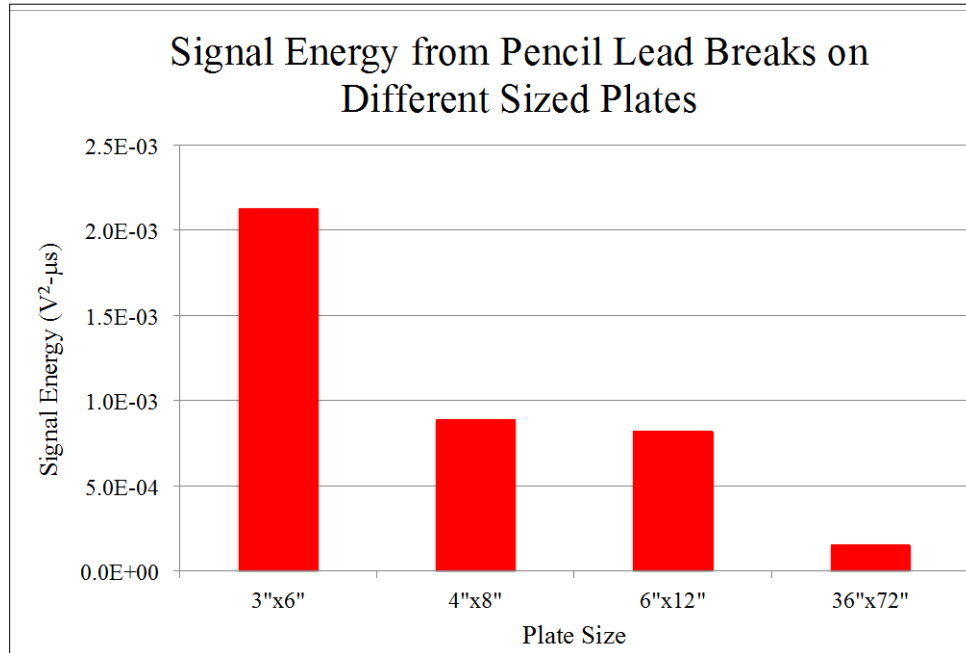


Figure 7.2.6-2. Bar Graph Comparing Measured Signal Energies from Different-sized 1/4-inch-thick Plates

Logically, the smaller plate should suffer more reflections per unit time, which in this example generated the greatest signal energy, followed by the 4- by 8-inch, then the 6- by 12-inch, and then the 36- by 72-inch plate. The smallest plate recorded more than an order of magnitude greater signal energy that the largest plate. Figure 7.2.6-3 shows the initial waveform for the large plate. In the figure, the trigger signal is at about 510 µs. The first arrival signal at the sensors is a symmetric plate wave that arrives at about 535 µs and has an initial amplitude of about 30 to 40 mV. A second plate wave, a flexural wave, follows at about 550 µs. Its amplitude is about 10 times greater. The echoes from the nearest plate edge do not show up until after 800 µs. For contrast, Figure 7.2.6-4 shows the waveform from a similar pencil-lead break on the smallest plate. In that figure, the trigger again occurs at about 510 µs. Because of the small plate size, the first arrivals of the symmetric and flexural plate modes arrive almost simultaneously just after 510 µs. In this specific case, the waveform seems to indicate a phase reversal from the largest plate as the echoes rapidly interfere. In Figures 7.2.6-5 and 7.2.6-6, one can see this progression of echo interference moving to earlier and earlier times as the echoes are arriving earlier and earlier. The results of the echoes are constructive interferences that will increase and make the waveform appear more energetic.



Title:

Evaluation of Agency Non-code LPVs

Page #:
165 of 193

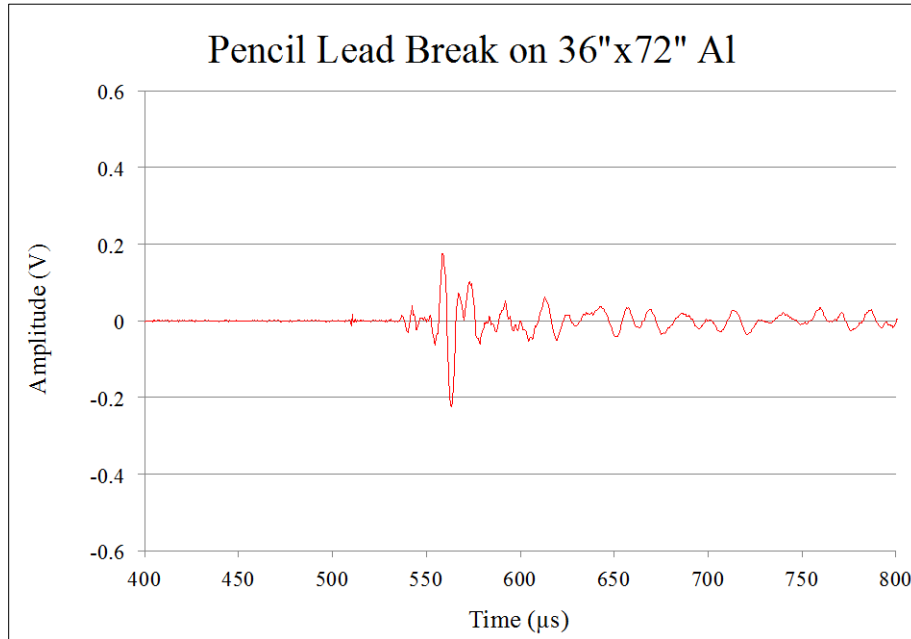


Figure 7.2.6-3. Early Waveform from Pencil-Lead Break on 36- by 72-inch Aluminum Plate

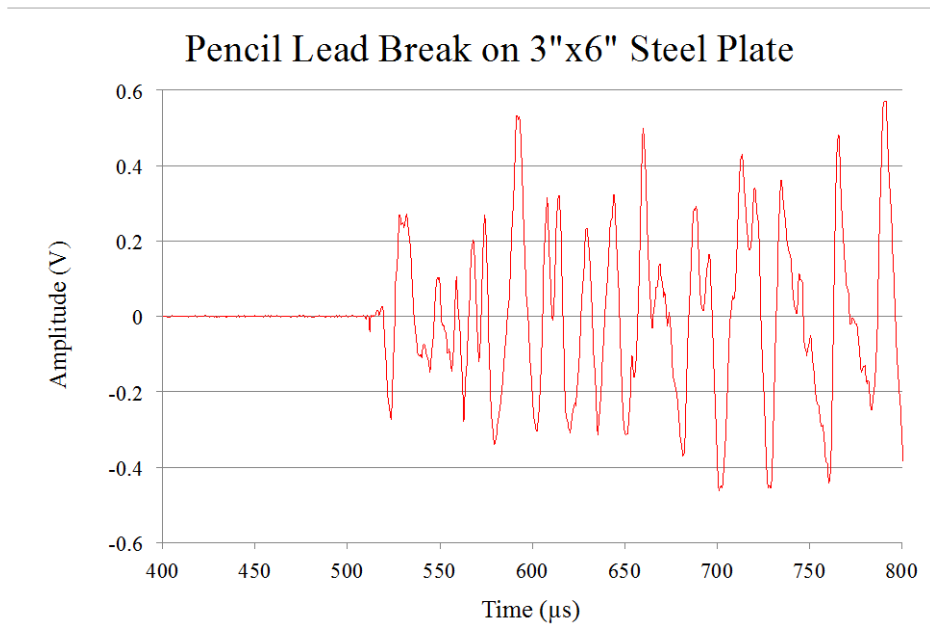


Figure 7.2.6-4. Early Waveform from Pencil-Lead Break on 3- by 6-inch Steel Plate



Title:

Evaluation of Agency Non-code LPVs

Page #:
166 of 193

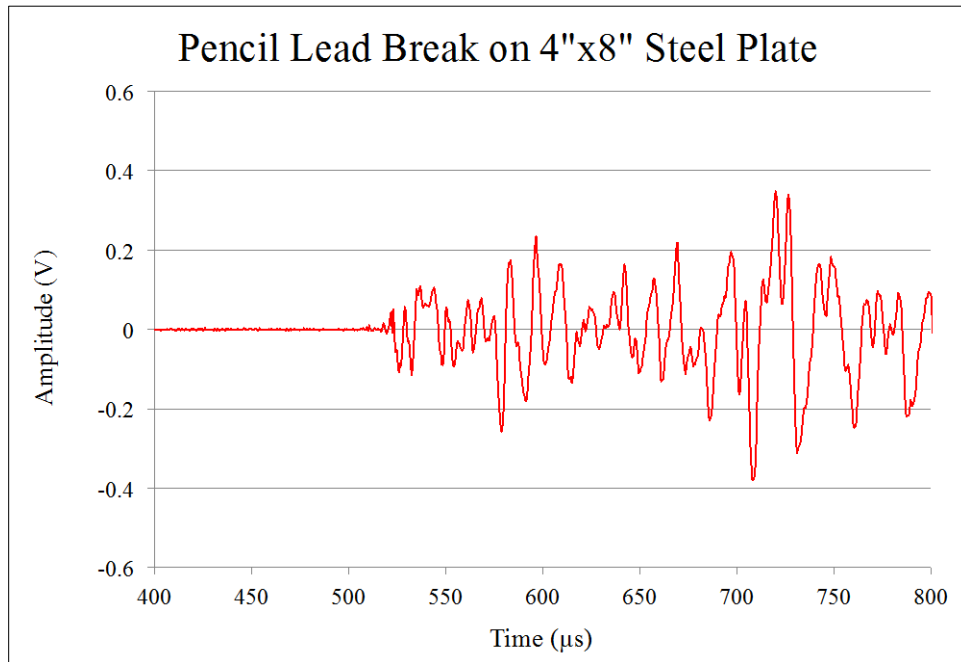


Figure 7.2.6-5. Early Waveform from Pencil-Lead Break on 4- by 8-inch Steel Plate

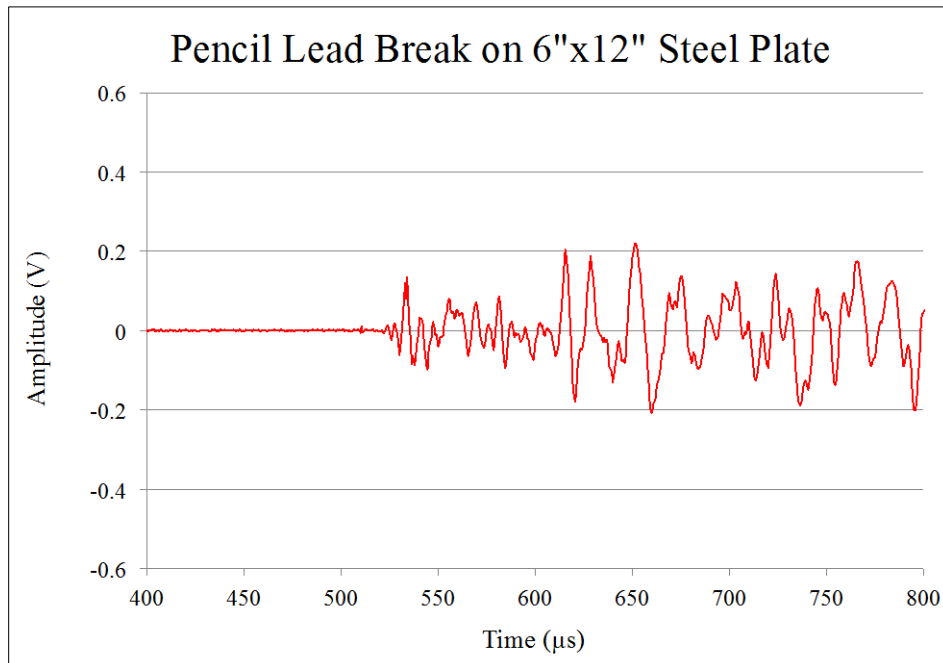


Figure 7.2.6-6. Early Waveform from Pencil-Lead Break on 6- by 12-inch Steel Plate

By comparing the full 8 ms of data from the smallest and the largest samples, one can understand the extent of the impact of this phenomenon on the signal energy measurement. Figure 7.2.6-7

	NASA Engineering and Safety Center Technical Assessment Report	Document #: NESCP-RP-13-00852	Version: 1.0
Title: Evaluation of Agency Non-code LPVs			Page #: 167 of 193

shows the full waveform for the largest plate tested. After about 900 μs , a small echo is evident, and then the signal settles down to a relatively constant level of noise. In contrast, Figure 7.2.6-8 shows the signal immediately interfering and growing in magnitude. It is not until after 4 ms that the amplitude of that signal declines to less than the largest plate's signal.

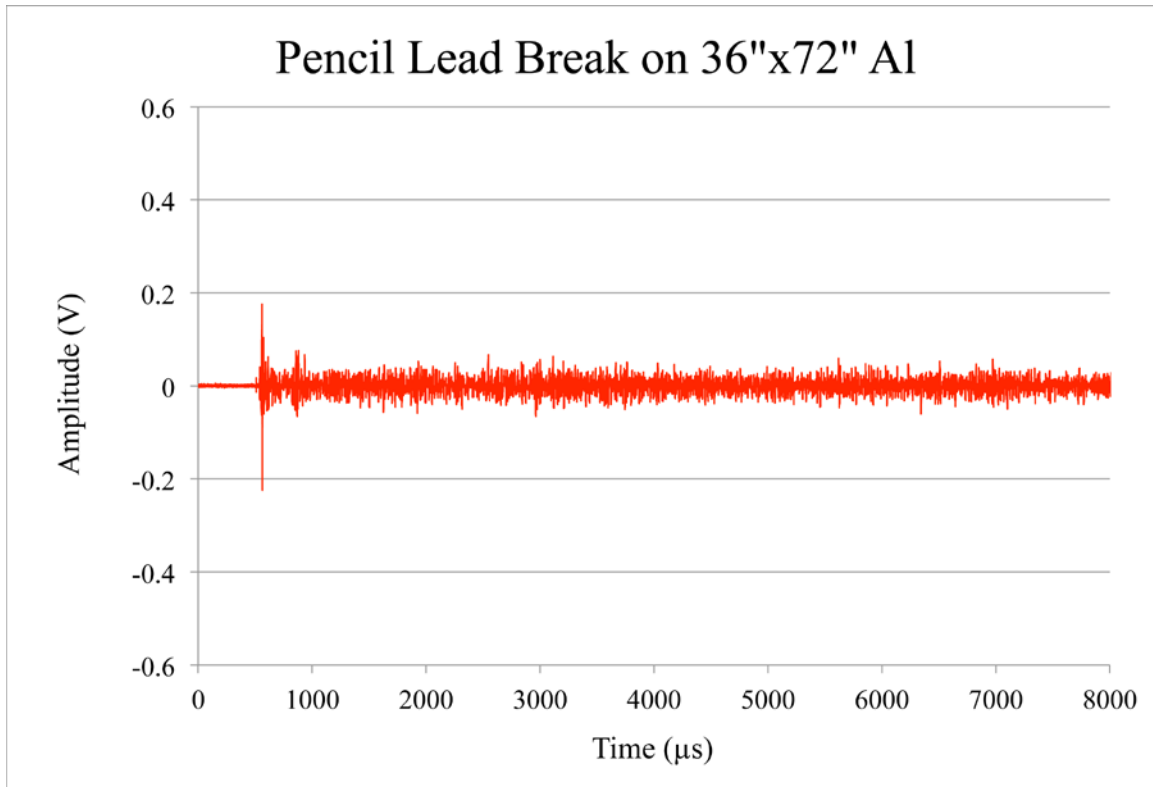


Figure 7.2.6-7. Full Waveform from Pencil-Lead Break on 36- by 72-inch Aluminum Plate



Title:

Evaluation of Agency Non-code LPVs

Page #:
168 of 193

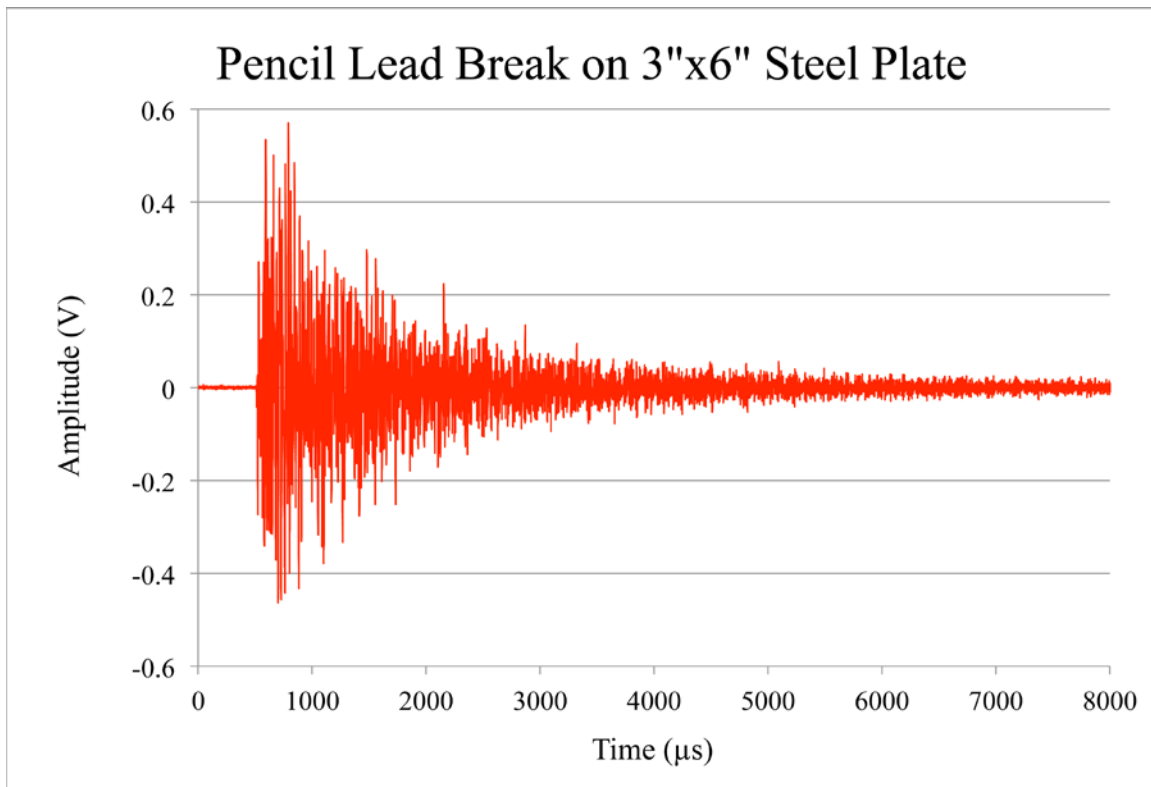


Figure 7.2.6-8. Full Waveform from Pencil-Lead Break on 3- by 6-inch Steel Plate

Based on this testing, we can expect that the crack-growth signals measured in a modest-sized load frame sample will be 5 to 10 times greater than the signals that might be detected near a crack site on a larger-sized LPV.

The crack-growth plan for the specimens is to insert a starter notch and then grow the starter notch in fatigue to produce a sharp crack that well represents an actual crack. The load will monotonically increase until crack growth occurs while monitoring with AE. The driving force for crack growth is the stress-intensity factor which is a function of the load, crack length, and specimen geometry. Accordingly, an overload cycle representative of the overload pressure applied during AE monitoring of an LPV in the field is not directly relevant, since the 0.75-inch crack will not produce an equivalent K at a given load as a 0.75-inch crack would in a given layer (such as the outer shell) of an LPV. This difference is an issue since the two processes can be easily reconciled by fracture mechanics keeping in mind that the goal of this laboratory-scale AE effort is to determine the efficacy of AE for measuring structurally significant crack growth in LPV materials. Both resonant and broadband sensors that are employed by the different AE approaches commonly used for LPV testing (i.e., MONPAC™ and MAE) will be used in this testing to provide additional data relative to comparison of the two techniques. Crack growth will be verified with standard materials testing NDE (potential difference) and post-test measurements after the sample is broken open. Again, tests are planned on the different material components of these vessels including head and shell parent materials, as well as weld and HAZ

	NASA Engineering and Safety Center Technical Assessment Report	Document #: NESCP-RP- 13-00852	Version: 1.0
Title: Evaluation of Agency Non-code LPVs		Page #: 169 of 193	

materials. The expected results are an indication of the signal amplitude as a function of the amount of crack growth under the given stress intensity conditions. Results from the signal amplification study will be used to remove the effect of lateral boundaries on the measured signal amplitudes. These results will provide a basis for evaluating the potential for AE for detecting crack growth in the various materials and regions of LPVs and a basis for decisions on further validation efforts on larger subscale and, eventually, full-scale vessels.

To date, the specimen designs have been completed and are undergoing evaluation by the MSFC materials community and are awaiting specimen fabrication. A block of the V0032 vessel has been designated for this purpose. AE instrumentation and personnel at MSFC and LaRC have been identified to support this testing effort.

7.3 Assessment Team Comments on Proof Testing of LPVs

Proof testing of pressure vessels (i.e., pressurizing a vessel to a level higher than the intended operating pressure) is a long-standing acceptance test procedure following vessel fabrication. Proof testing subsequent to fabrication is expected to ensure the quality and safety of the vessel for its design use and carries additional benefits, such as reducing weld or shell-section residual stresses through cyclic shakedown. The objectives of the proof test procedure commonly fall into two categories: (1) to provide a general screen on the quality of materials and workmanship present in the vessel (most common) and (2) to provide a quantifiable engineering rationale for safe operation of the vessel over a number of pressure cycles based on the stress in the vessel at proof pressure, serving as a sieve to identify flaws greater than a critical size, whereby fracture mechanics principles may be used to evaluate a minimum remaining cyclic life beginning at that proof-critical flaw size (uncommon). The first approach is often referred to as a “workmanship” proof test, and the second, as a “fracture mechanics” based proof test. Both share the goal of providing rationale for the safety of the vessel; the difference is in the quantifiable nature of the latter, which leads to a much clearer understanding of the vessel and its associated structural risks.

All known proof testing performed to date on LPVs has been of the workmanship variety. The acceptance proof test (or “hydrotest”) to $1.5 \times$ MAWP performed at vessel fabrication or following certain vessel repair activity provides an unquantified confidence in the integrity of the vessel. This concept fits with the general ASME code approach of establishing rigorous design, fabrication, and inspection quality requirements, which result in a code-approved vessel in an assumed “undamaged” state. This approach has served the industry well for decades. For older vessels, those with known defects that violate the assumed “undamaged” state, or in the subject case, vessels of non-code construction, rationale for the FFS of the vessel is required. In simple cases, this may involve repair of the vessel to an equivalent undamaged state or, in the case of non-code vessels, may require an alternative engineering rationale. The proof test, either workmanship or fracture-mechanics-based, often plays a key role in this alternative logic. For cases such as the LPVs, the geometric limitations of layered construction reduce the effectiveness of quantifiable NDE throughout the vessel, making the standard NDE-based analytical methods of FFS less practical. The lack of comprehensive quantifiable data from the

	NASA Engineering and Safety Center Technical Assessment Report	Document #: NESCP-RP-13-00852	Version: 1.0
Title: Evaluation of Agency Non-code LPVs		Page #: 170 of 193	

LPV NDE process emphasizes the benefits of quantifiable results from a proof test by enabling a FFS rationale that moves beyond mere risk assessment toward a more anchored and quantified engineering rationale. While the layered construction should not hinder the physics behind the proof logic, as with NDE the layered construction makes quantification of the proof test efficacy considerably more complicated.

Figure 7.3-1 illustrates the basic idea of a fracture-mechanics-based proof test to provide a quantifiable expectation of reliable cyclic life. The curve in the axes reflects the general relationship between critical crack size and pressure in the vessel, showing increasing critical crack size as pressure decreases. The position and shape of the critical crack size curve is a function of the crack geometry (e.g., through crack, surface crack, or embedded crack) and the material toughness, which will vary by material (head, shell, nozzle, or weld) and temperature. The most important aspect to quantifying the cyclic life assured by proof test is the ability to assess accurately the critical flaw size in the vessel at the proof pressure condition and at the maximum operating pressure condition. The ratio of these stress states ($\sigma_{proof}/\sigma_{oper}$) defines the proof factor. For most common pressure vessels, this ratio of stress states is equivalent to the ratio of internal pressures at these conditions because pressure is the primary source of stress. The higher pressure at the proof test condition makes the critical crack size at proof smaller than the critical crack size in operation ($a_{crit,pr} < a_{crit,op}$); therefore, following a successful proof test, there is a range of crack growth of length $\Delta a = a_{crit,op} - a_{crit,pr}$ reserved for cyclic growth in operation. The number of operational pressure cycles available within Δa may be determined through fracture mechanics methods for fatigue crack growth, such as predicted by crack growth

relations like such that $\frac{da}{dN} = C(\Delta K)^n$ such that $N = \int_{a_{pr}}^{a_{op}} \frac{1}{C(\Delta K)^n} da$, where N is the number of

cycles and ΔK is the cyclic range of the crack's stress intensity factor. While simple in concept, an accurate assessment of the Δa (or cycle life N) assured by the proof test is complicated. As illustrated in Figure 7.3-1, the value of the proof factor will be the most direct influence, but the shape and consistency of the critical crack size curve is also extremely crucial.

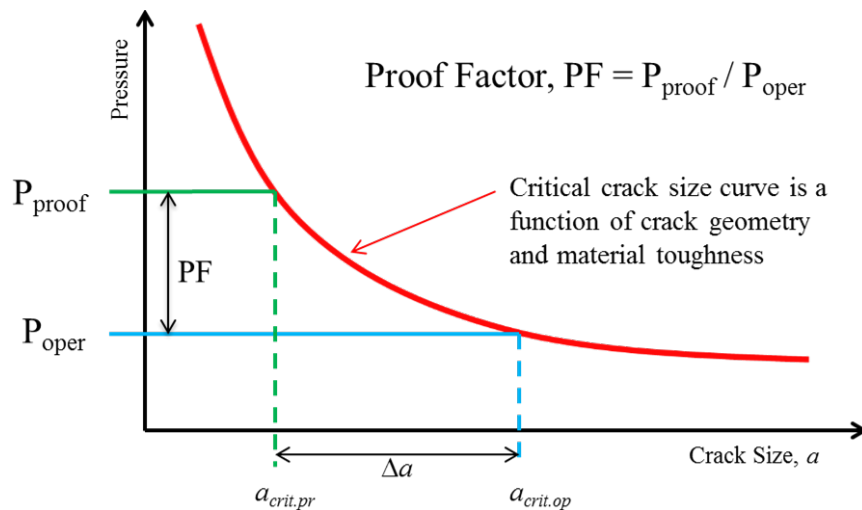


Figure 7.3-1. Proof Test Concept

Considering the concept illustration of Figure 7.3-1, an accurate definition of the critical crack size curve is fundamental to the proof test logic. In this figure, a single critical crack size curve is shown for simplicity. In reality, the two critical events in the proof logic (i.e., proof test and reaching the operational critical crack size) are well separated in time, perhaps by years. The key aspects that define the curve (i.e., crack geometry and material performance) may not be the same over time. For example, as a crack grows over the operational service life, the shape of the flaw may evolve from an embedded crack to through-wall crack, or the temperature of the vessel in operation may differ from that during proof test. Considering this, it is more appropriate to consider a version of the conceptual figure that has a critical crack size curve for both the proof condition and the operational condition, as illustrated in Figure 7.3-2. In this context, the life assured through the proof test, Δa , can appropriately consider the limitations imposed by the proof and operational conditions of the vessel. The life assured through proof is maximized by maximizing Δa . This implies screening for the smallest possible $a_{crit.pr}$ and allowing the largest operational crack size $a_{crit.op}$. However, from a safety perspective, the proof test must be assessed based on the minimum Δa that may exist between proof and operational failure. This requires considering the largest crack that may escape proof test and the smallest that may cause failure, which minimizes Δa . To do this, the toughness of the material during proof must be considered at its upper bound, and worst-case performance must be assumed regarding toughness and material variability during operation. For materials with consistent ductile fracture properties (always upper shelf), the upper bound toughness assumed in proof can often reasonably be assumed to be present in operation as well. This reduces some of the pessimism in the assessment. However, for these LPV ferritic steels, which cleave through a stochastic sampling of crack front cleavage initiators such as carbide particles, the assumption of consistent upper bound toughness values being present for the operational condition are not justified because the crack will have advanced through the material during operational cycles and will not be sampling the same crack front material later in the operational life. At this point for the crack, it is a new draw from the random deck.

	NASA Engineering and Safety Center Technical Assessment Report	Document #:	Version:
		NESCP-RP-13-00852	1.0
Title:			Page #:
Evaluation of Agency Non-code LPVs			172 of 193

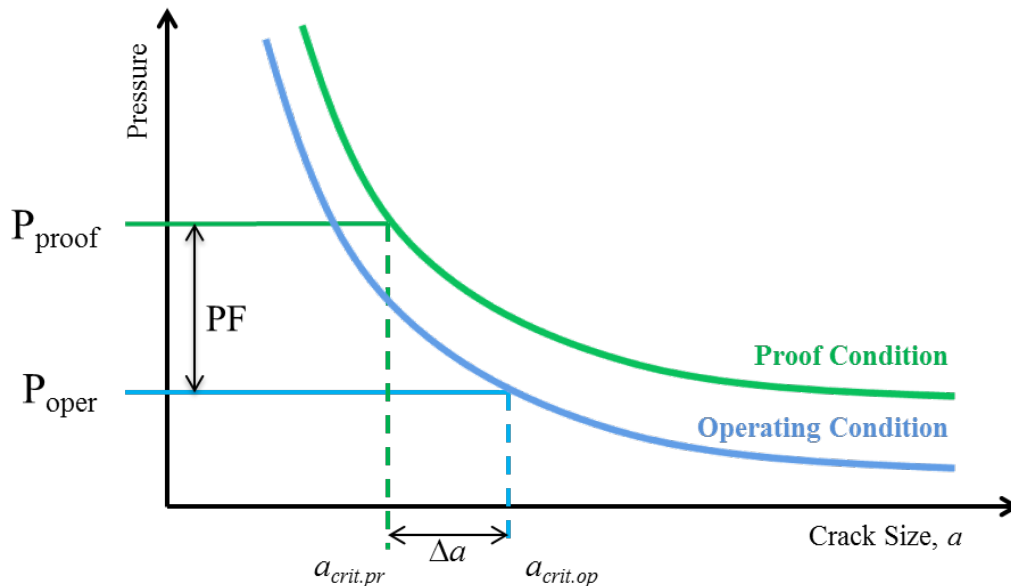


Figure 7.3-2. Proof Test Concept with Proof and Operational Critical Crack Size Curves

For more detail on proof test considerations, see the thorough review of the fundamentals of proof testing provided in reference 90.

7.3.1 Methods of Proof Test Assessment

The efficacy of a proof test may be quantified analytically, experimentally, or through a combination of these. Proper analytical assessments of proof test efficacy are difficult. The use of linear elastic fracture mechanics (LEFM) to determine $a_{crit,pr}$ and $a_{crit,op}$ with the desired accuracy is generally not feasible and could likely lead to nonconservative results. LEFM is generally more robust in evaluating cyclic life in fatigue than in accurately predicting true fracture failure, particularly for ductile materials like the LPV steels. An analytical assessment of the bounding crack sizes for proof and operation may be performed more robustly with a J -integral based failure assessment diagram, such as described in API-579 [ref. 32]. In this case, the main variables affecting the outcome of the Δa assessment will be the material toughness values chosen to represent the two conditions and the choice of assumed crack geometries. For the case of the LPV problem, the latter represents the larger challenge. The material toughness and its expected variability can be assessed and reasonably understood through evaluations, such as those described elsewhere in this report (e.g., Section 7.2.1). Choosing representative and appropriate hypothetical crack geometries to assess the proof test is complicated somewhat by the layered construction relative to traditional solid-wall vessels. There are more potential scenarios to consider, and the load cases are more complicated to assess. The prediction of crack-shape evolution during the operational life is also more complicated. This does not imply that the problem is intractable, but the time required to assess an LPV for proof will be longer than for a typical solid-wall vessel. Fortunately, for structural assessment considerations, an analysis that is reasonably suited to provide a conservative estimate of proof stress conditions at a location in an LVP can generally also be used for the assessment of the operational stress state

	NASA Engineering and Safety Center Technical Assessment Report	Document #: NESCP-RP- 13-00852	Version: 1.0
Title: Evaluation of Agency Non-code LPVs		Page #: 173 of 193	

given that most aspects of the problem governing stress states remain consistent between the two conditions. The only changes from the proof assessment to the operational assessment are typically the applied pressure, the evolved crack shape, and the material properties.

Though more costly, the experimental approach to assessing proof test efficacy is, in principal, more robust, although its practicality for application to NASA's LPV fleet has not been assessed. The issues of elastic-plastic fracture mechanics, material property changes, crack-shape evolution, and fatigue-crack-growth predictions can be rolled into a single test result that requires less specific knowledge about the contributions and interactions of all these complicated behaviors. The experimental methodology commonly used for such an assessment is referred to as an "imminent failure simulated service test." In this method, a crack is fatigued into a representative test specimen. The specimen may simply be a section of the LVP base material or the specimen may be a more complicated, configurational analog of the LPV structure, including layers or welds. The specimen and crack are sized such that the crack will be near failure at a stress level representative of the LPV proof stress. Under environmental conditions representative of the proof test, the specimen is loaded in a test frame to a point of "imminent failure" (i.e., a point where it is anticipated that any additional load would cause failure). The proof load is then removed and the specimen cycled under environmental conditions representative of the operational stress level (i.e., peak load is reduced by the proof factor ratio) and the specimen cycled to failure. This experiment provides a direct measure of the cyclic capability of a crack that barely survives the proof test. Much of the complicated physics that confound the analytical assessment is handled cleanly in the experiment, such as plasticity, crack extension by tearing during proof, fatigue crack-shape evolution, and final failure. A larger number of tests would be needed for cleavage-prone materials such as appear to exist in NASA's LPV fleet than for other more consistently ductile fracture materials due to the stochastic nature of the cleavage mechanism. The variability this may impose on the experimental assessment of proof test efficacy is not clear at this time. The issues of geometric differences between vessels, material property and toughness variations, different manufacturers and manufacturing processes, etc., of NASA's LPV fleet are factors that would further complicate development of an experimental approach. Reference 91 provides a wealth of information regarding proof test assessment.

There are numerous other influences that require investigation related to the proof test assessment in LPV systems. Some effects may be negligible, some helpful, others detrimental. Each should be studied to ensure it does not present an unreasonable limitation or reduction in confidence in the proof test assessment and its influence on perceived vessel reliability. The following are a few items for future consideration:

- Choice of proof factor:** To be effective as a screen for additional safe operating cyclic life, the proof factor must be sufficient to overcome the variability present in the system. As previously described, the material behavior with respect to cleavage failure has a considerable stochastic nature. The need to be conservative in material properties for both $a_{crit,pr}$ (upper bound) and $a_{crit,op}$ (lower bound) can greatly reduce the actual "effective" proof factor. This material variability alone may drive the need for

	NASA Engineering and Safety Center Technical Assessment Report	Document #: NESCP-RP- 13-00852	Version: 1.0
Title: Evaluation of Agency Non-code LPVs		Page #: 174 of 193	

substantial proof factors. The proof factor level should be an integral part of the vessel proof assessment, taking into account system variability and the desired proof-assured life.

- **Proof test temperature:** The need to utilize upper bound toughness properties for the proof evaluation of $a_{crit,pr}$ makes it particularly appealing to mitigate that effect by minimizing the material toughness during proof. This is accomplished by lowering the proof test temperature to the lowest practical degree. It is preferable that the proof test temperature at least bound the allowable minimum operational temperature. Methods to effectively implement such a test in field conditions may require special development.
- **Residual stress state:** Residual stress in and around welds may have a significant effect on the driving force for cracks and failure due to cleavage. Changes in residual stress due to cyclic shakedown of the materials may also influence the material response. An understanding of how these stresses likely evolved from the original vendor proof test to those currently present or following additional proof cycles may be important.
- **Crack-shape evolution:** As previously discussed, the larger the difference between $a_{crit,pr}$ and $a_{crit,op}$, the longer the proof-assured life will be; however, large Δa also means an increased likelihood that the fundamental crack shape will change between the time of proof testing and operational failure. The layered structure offers additional complications. Experiments or simulations may be used to determine likely crack-shape evolution paths. Fracture mechanics tools, most notably LEM boundary element methods, have matured sufficiently to provide good first-order estimates of this crack-shape evolution behavior. An understanding of these trends in LPVs will be important to an accurate general assessment of LPV proof efficacy.
- **Tearing, sharpening, retardation, (i.e., nonlinear effects):** Tearing and sharpening of defects may be aspects of vessel behavior that limit the effectiveness, or reduce the reliability, of the proof test. Stable crack tearing is most likely to occur during or at the peak of the proof loading cycle. Unless reasonably represented in the analytical or experimental assessment of the proof loading cycle, the tearing adds to the length of $a_{crit,pr}$, reducing the available Δa for operation. If tearing occurs and is undetected or unanticipated, the proof test may not be effective. Unanticipated crack tearing may be mitigated by understanding toughness R -curve behavior, representing the tearing in the simulated service tests, listening for it during proof with acoustic emission, or conducting more robust screening via multi-cycle proof testing. Sharpening of defects in proof is also a concern. In this case, initial defects that are not fully crack-like, such as a welding lack of fusion or chain of porosity, is torn to a crack-like condition and then sharpened during the unloading cycle of the proof test. The most effective screen for this consideration is the multi-cycle proof test. A third likely influence of proof test assessment is retardation of fatigue-crack-growth. Unlike tearing and sharpening, retardation effects may tend toward enhancing the realized proof life by increasing the number of cycles required to grow the crack by Δa . This effect is a strong function of the

	NASA Engineering and Safety Center Technical Assessment Report	Document #: NESCP-RP- 13-00852	Version: 1.0
Title: Evaluation of Agency Non-code LPVs		Page #: 175 of 193	

applied proof factor and occurs due to well-characterized crack closure effects following an overload cycle, where the crack opening is suppressed in subsequent loading cycles by the residual compression caused plastic wake following the overload. Each of these phenomena can complicate the proof test assessment by adding what are essentially nonlinear effects to the crack behavior.

- Multi-cycle proof testing:** The multi-cycle proof test concept involves cycling the vessel to the proof condition a number of times (five is common) to improve the reliability of the proof screen. This does not provide a smaller value of $a_{crit,pr}$ and, thus, does not alter the assured Δa , but rather improves the likelihood that any defects close to the $a_{crit,pr}$ size or evolving to that size through tearing or sharpening mechanisms will be screened. Probabilistically, the effectiveness of the proof test in assuring vessel reliability is improved. The additional cycles at proof stress levels are a cost in accumulated damage, but are not likely significant in the overall cyclic life of such vessels. Details can be found in reference 92.
- Other effects, for example, costs and facility threats:** A reliance on proof testing of the LPV fleet to provide service life reliability may overcome many of the inspection and analytical challenges inherent to these vessels, but such testing comes with significant costs and presents potential hazards. The direct costs of implementing a proof test on any given vessel may be significant, especially if there are infrastructure developments needed to provide a cold, hydrostatic condition for proof testing, or vessel cleaning costs post-proof are substantial. Additionally, there will often be costs associated with either moving a vessel to a safe location or providing some other form of protection from collateral damage should a vessel fail in proof. The potential energy release from large vessels can be significant, even in hydrostatic testing, and hazard assessment and mitigation must be taken seriously. Though expensive, these costs are a small fraction of typical replacement costs. Though the loss of a vessel by failure in proof can be considered a substantial cost, a preferred point of view is that the proof test was successful at removing a dangerous vessel from the fleet under controlled circumstances. While undesirable, vessel failure in proof is vastly preferable to failure in service, provided the potential hazards due to such failure have been adequately mitigated.

7.3.2 Proof Test Conclusions

Systematic use of proof testing for FFS assurance in the LPV fleet will require the issues discussed in this section be investigated such that the benefits and risks of proof testing these vessels are better understood. When proof testing is performed, it must be assumed that, although highly unlikely, sudden catastrophic failure could occur, and hazard mitigations must be implemented to protect personnel and, if appropriate, facilities, from such failures.

7.4 Assessment Team Comments on LPV Replacement Strategy

In light of the elevated and indeterminate risks associated with the continued use of aging, non-code LPVs, the assessment team had considerable discussions as to whether to include any

	NASA Engineering and Safety Center Technical Assessment Report	Document #: NESCP-RP-13-00852	Version: 1.0
Title: Evaluation of Agency Non-code LPVs		Page #: 176 of 193	

recommendations regarding replacement of these vessels. In the end, such a recommendation was not included for the following reasons:

- The defined scope of the assessment was to identify work that was required to continue to use these vessels safely. Thus, recommending replacement, although it would eliminate the additional risk associated with these LPVs, is inconsistent with the assessment scope. It is noted that even the likely replacement (i.e., single-walled ASME vessels) are not risk free but have a lower risk that is acceptable based on ASME BPVC and OSHA regulations.
- Although this report must not be taken out of context to indicate that these vessels are entirely safe to operate or will continue to be so for any future period, there were no findings that warranted a recommendation to begin immediate planning for replacement of these vessels.
- The report instead identifies that there is a lack of information with which to adequately assess the immediate risks associated with these vessels or to determine the remaining safe life of any particular vessel in its specific service. Characterization of those risks will be critical information needed to guide replacement decisions. Thus, the recommended longer-term activities are necessary not only to develop a process to ensure continued safe operations but also to provide essential information to support eventual, orderly replacement decisions.
- Further, as replacement of these vessels is an expensive option (i.e., an estimated average cost of around \$2 M per vessel), such decisions regarding replacement should be driven by a risk analysis that incorporates an understanding of costs and benefits associated with available options. Obviously, replacing these vessels with single-walled ASME code vessels eliminates the additional risks associated with non-code LPVs, but at a substantial cost. Analysis of costs and benefits in terms of risk reduction for other options needs to be considered as part of the replacement decisions. The risks of thick-walled single-layer ASME code vessels are generally better understood and more manageable through a variety of validated analysis and NDE methods, but these risks are not zero. Estimates of costs will need to include costs for the recommended efforts that are identified in this report to support continued use, as well as costs that might occur from additional inspections, operational constraints, etc., that will likely originate as a consequence of the results of this work. Thus, again, it is highlighted that the activities recommended in this final report are critical not only for assurance of continued safe operations but also for input into decisions on eventual replacement of these vessels.
- Lastly, as the costs of wholesale replacement of all NASA LPVs is not affordable to the Agency under current budget constraints, such decisions will need to be made on a case-by-case basis, driven by the individual circumstances for specific vessels.

However, all assessment team members were in agreement with the obvious fact that replacement of these vessels eliminates the risks associated with their continued use, albeit

	NASA Engineering and Safety Center Technical Assessment Report	Document #: NESCP-RP- 13-00852	Version: 1.0
Title: Evaluation of Agency Non-code LPVs		Page #: 177 of 193	

substituting for that risk the better understood risks of thick-walled single-layer vessels. Thus, where there are opportunities and funding available to allow replacement of LPVs, this action could be advisable, although an assessment of the particular circumstances would still be required. Further, while a general recommendation for replacement is not being made, identification of certain defects may require removal from service of individual vessels.

8.0 Findings, Observations, and NESC Recommendations

8.1 Findings

General

- F-1.** Non-code LPVs are in use at nine NASA Centers and facilities, with 376 vessels reported, 302 of which are in active service.
- F-2.** Operation of NASA non-code LPVs presents an elevated level of risk compared with conventional code vessels.
- Non-code materials, process controls, and inspection methods used during original vessel fabrication.
 - Uncertain minimum safe-operating temperatures, with indications of likely operation within the transition region to brittle fracture behavior.
 - Inability to currently perform adequate inspections or assessments to ascertain remaining safe life, with no specific LPV guidance provided in the principal post-construction pressure-vessel codes NB-23 and ASME FFS-1/API-579.
 - Potential aging effects that could include fatigue, corrosion, and embrittlement.
 - Noncatastrophic cracks documented in industry and NASA vessels, including those found recently in LaRC high-pressure methane and KSC nitrogen LPVs.
 - Internal corrosion of NASA LPVs not known to be an issue due to operation with noncorrosive gases at ambient temperatures.
 - Some NASA LPVs subject to external corrosion due to proximity to ocean.
 - No known data on embrittlement of NASA LPV materials, although some vessels used for gaseous hydrogen service.
 - At least nine catastrophic LPV failures in industry.
 - Occurred under different usage conditions than NASA LPVs (elevated temperatures with corrosive products).
 - Two occurred after evidence of inner shell failure was observed through product loss at vent holes.
- F-3.** The level of increased risk associated with non-code LPVs and the overall reliability of these vessels cannot be quantitatively estimated.

	NASA Engineering and Safety Center Technical Assessment Report	Document #: NESCP-RP- 13-00852	Version: 1.0
Title: Evaluation of Agency Non-code LPVs		Page #: 178 of 193	

- Lack of historical data associated with design, fabrication, operation, inspection, maintenance, and repair.
 - Available data in disparate formats and locations and difficult to retrieve.
 - Original materials property data in some cases acquired with methods not consistent with current code; cannot be correlated with current methods.
 - Recently acquired materials property data from NASA sacrificed vessels are limited, do not provide sufficient sampling to adequately represent potential fleet variability (material lot to lot and within lot), and in some cases show lower than expected property values or possible undocumented material substitutions.
 - Currently available structural analysis approaches for LPVs are idealized and simplistic and do not accurately reflect some of the key details of construction.
 - Uncertainty in the identification of probable failure modes and associated critical initial and final flaw sizes currently precludes the identification of NDE detection requirements.
 - Currently no validated NDE methods available to inspect certain critical regions of LPVs (e.g., full penetration circumferential welds, shell longitudinal welds, and interior shell layers).
- F-4.** The Agency lacks a consensus approach to addressing the risks associated with these vessels.
- Center PSMs have not reached consensus on certification, recertification, inspection, maintenance, or usage of LPVs.
 - Frequency and methods of reporting LPV risks to Center management, and their awareness of the risks presented by continued use of these vessels, varies from Center to Center.
 - Previous and ongoing efforts at specific Centers to develop data and methods to mitigate risks associated with LPVs have not always been effectively communicated across the Agency.
 - No consistent methodology identified in industry survey.
- F-5.** Near-term actions (identified in R-1 through R-7) are available to reduce the risk of or consequences from catastrophic failure of LPVs. However, for many of these actions, the associated degree of risk reduction cannot be quantified.
- F-6.** Longer-term efforts will be required to characterize and mitigate risks for LPVs. Emphasis should be placed on vessel features and operating conditions that pose the highest risks, accompanied by a focus on the most promising technologies to mitigate these risks.

	NASA Engineering and Safety Center Technical Assessment Report	Document #: NESCP-RP- 13-00852	Version: 1.0
Title: Evaluation of Agency Non-code LPVs		Page #: 179 of 193	

- Load sharing, interlayer friction, and other interactions from the layered construction complicate the application of the traditional fracture mechanics approach for LPVs in their entirety.
- Proof test methodologies may be able to address risk in regions where NDE is inadequate, provided that bounding material properties are available and appropriate analysis methods are developed and validated.
- Operation of NASA LPVs at ambient temperatures in cold weather is a significant concern.
 - MDMT stamped on the nameplate or shown on the design drawings for non-code LPVs was determined via methods seen as inadequate today and does not account for brittle fracture potential at temperatures below the NDT.
 - During recent record cold temperatures (i.e., January through March 2014), an attempt was made to gather pressure and temperature data for a number of NASA LPVs at some Centers.
- Identified high-risk regions of NASA LPVs include circumferential full penetration welds, shell sections near full penetration welds and along longitudinal welds, and welds for drain nozzles through shell sections.
- NDE methodologies that have the potential to detect relevant defects have not been satisfactorily validated.

Specific Discipline Findings

Materials

- F-7.** Strength evaluations of LPV steels and associated welds reflect properties mostly consistent with material records from the time of fabrication. In some cases, strength values have been nearer to assumed design values than typically would be expected. One vessel material tested (i.e., inner layer of MSFC vessel V0032) was of significantly lower strength than the certification records indicate. Uncertainty in the pedigree and consistency of materials in the LPV fleet is recognized as a risk associated with these vessels.
- F-8.** Inconsistencies are present in the historical material specifications from the various LPV manufacturers, including the requirements for chemistry and strength.
- F-9.** Material anisotropy is relatively mild for strength properties but significant with respect to fracture toughness across the head and shell materials evaluated. Anisotropy is not always readily apparent in metallographic evaluations; therefore, toughness or Charpy testing is best used to identify the material orientation of minimum toughness. Materials may not be oriented favorably in vessels with respect to material anisotropy in fracture toughness, so bounding values are necessary.

	NASA Engineering and Safety Center Technical Assessment Report	Document #:	Version:
		NESCP-RP-13-00852	1.0
Title:			Page #:
Evaluation of Agency Non-code LPVs			180 of 193

- F-10.** Initial single-lot measurements of toughness in the transition regime have been made for two-shell-layer materials (i.e., alloys 1143 and 1146) from sacrificed vessels. The toughness measurements were developed in terms of the T_0 parameter per ASTM E1921-13, providing the fracture toughness versus temperature relationship in the transition toughness regime. Once fully developed, the T_0 values for the steels will provide rationale for the allowable service temperatures for the LPV fleet.
- F-11.** The LPV steels tested are less tough than the more modern pressure vessel steels used in the development of the Master Curve method prescribed by ASTM E1921-13. The LPV material toughness presents difficulties in meeting the current requirements and assumptions of the test standard; however, the temperature-dependent material toughness generated by the method is expected to be directly applicable to FFS assessments.
- F-12.** Radiographic comparison of selected sections of longitudinal layer welds for two sacrificial vessels revealed markedly different internal weld qualities between the two vessels, an indicator of potential quality variations that exist within the LPV fleet.

Structural Analysis

- F-13.** The diversity of pressure vessels across the Agency will require unique assessments based on individual vessels or vessel types.
- F-14.** Preliminary models have been developed to estimate residual stresses in LPV full penetration circumferential welds, which were not stress relieved in the fabrication process. The initial results show high residual stresses, which could negatively affect safe life calculations.

Nondestructive Evaluation

- F-15.** Preliminary testing of PAUT methods has demonstrated some potential for volumetric inspection of full-penetration circumferential welds.
- F-16.** Photogrammetric techniques were used to provide LPV full-field surface deformation measurements, which could be useful for validating analysis models. The capability of photogrammetry to detect subsurface flaws will be a function of the magnitude of the change in surface deformation produced by those flaws. It will also require an understanding of the surface deformation produced by other LPV features (e.g., layer gaps, welds, support structure, etc.).
- F-17.** AE has potential for detecting crack growth in internal layered shell sections and welds if cracks can be shown to produce detectable AE in the presence of high background noise associated with layer rubbing.
- F-18.** The capabilities for RT as applied to crack detection in LPVs have not been established.
- The presence of multiple shell layers adds non-relevant indications (i.e., layer wash) to radiographic images that make detection of flaws more difficult.

	NASA Engineering and Safety Center Technical Assessment Report	Document #: NESCP-RP- 13-00852	Version: 1.0
Title: Evaluation of Agency Non-code LPVs		Page #: 181 of 193	

- The flaw detection capability for RT is a function of the overall thickness being inspected, while the critical flaw size for a layer will be based on the layer thickness.

F-19. Low-frequency electromagnetic inspection methods have been developed to detect wall thinning in thick carbon steel pipes. These methods may also have applicability to the detection of flaws in LPVs.

8.2 Observations

O-1. The Center PSMs have demonstrated understanding of the technical issues and concerns associated with non-code LPVs and a willingness to engage across Centers to develop improved approaches to mitigating risks associated with the continued use of these vessels.

O-2. A significant amount of pertinent, valuable testing and development that directly relates to the understanding of and continued safe use of LPVs at NASA is being performed by NASA Centers outside this NESC assessment.

8.3 NESC Recommendations

Near-term Recommendations

In drafting recommendations to the Agency and Centers that operate and maintain LPVs, an attempt was made to provide some near-term recommendations that could, if enacted, reduce the risk of or consequences from catastrophic LPV failure resulting from their continued use. It was recognized that due to the lack of adequate materials property data, inspection methodologies, and analyses methods, the risks associated with the continued use of these vessels and the degree to which these recommendations would reduce that risk cannot be accurately estimated. It was also recognized that these recommendations cannot be uniformly adapted or applied across the Agency because of the unique applications/requirements and local site conditions for specific vessels. These recommendations are as follows:

- R-1.** Agency ensure continued-use rationale is documented for all in service LPVs. *(F-2, F-3)*
- R-2.** Centers inspect LPV vent holes to ensure that they are not corroded, blocked, or plugged, and periodically monitor vent holes for product loss that may indicate inner shell failure. *(F-2, F-5)*
- R-3.** Centers consider imposing service restrictions (e.g., reduced operating pressures or operation at temperatures where material toughness is in the upper shelf region) to reduce the risk of catastrophic failure. *(F-2, F-5, F-6)*
- When data necessary to establish appropriate MDMT are not available, set minimum allowable usage temperature at conservative levels above historical cold usage temperatures where such data are available.

	NASA Engineering and Safety Center Technical Assessment Report	Document #: NESCP-RP-13-00852	Version: 1.0
Title: Evaluation of Agency Non-code LPVs		Page #: 182 of 193	

- R-4.** Centers consider the implementation of physical barriers (e.g., berms) or operational controls (e.g., minimized personnel access) where practical to mitigate the consequences of vessel failure. *(F-2, F-5)*
- R-5.** Agency develop and implement a consistent program of minimum maintenance and vessel inspection requirements. *(F-2, F-4, F-5)*
- R-6.** Centers remove from service any LPV with crack-like indications in critical areas until acceptance rationale (e.g., repair, proof testing, periodic inspection, physical barriers, operational constraints, and/or analysis) and safety/risk assessment are approved by Center management. *(F-2, F-3)*
- R-7.** Agency formulate and support an Agency-wide team to continue efforts to assess and reduce risks associated with LPVs, with the goal of developing a standard Agency process for their continued usage.
 - Team regularly report to Agency and Center management baseline LPV risks and results to reduce risk. *(F-2, F-4, F-5)*
- R-8.** Agency develop a centralized database that documents, to the extent practical, LPV design, fabrication, materials, operation, inspection, maintenance, and repair data. *(F-3, F-5)*

Longer-Term Recommendations

The following are discipline-specific recommendations to develop improved understanding of the risks associated with the continued use of LPVs and to lead to the development of Agency processes to mitigate these risks.

- R-9.** Agency expand efforts to gather LPV weld and parent materials property data.
 - Perform statistical analysis to determine number of LPVs and associated materials testing specimens needed to provide adequate bounding materials property data. *(F-2, F-3, F-6)*
 - Provide for a complete characterization of fracture toughness as a function of temperature for each of the steels used in LPV construction, including welds. The expected variability in fracture toughness across the LPV fleet should be sufficiently characterized to enable developing meaningful MDMT values. Studied influences should include variables such as the steel producer, vessel vendor, manufacturing time period, steel product size, and other known manufacturing process dependencies. *(F-2, F-3, F-6, F-10)*
 - Perform failure analysis to include metallurgical examination and materials property characterization for specimens collected from cracked LPVs. *(F-2, F-3, F-6)*

	NASA Engineering and Safety Center Technical Assessment Report	Document #: NESCP-RP- 13-00852	Version: 1.0
Title: Evaluation of Agency Non-code LPVs		Page #: 183 of 193	

- Collect available and future material property data into a central and complete database sufficient to support all forms of LPV FFS evaluations, proof testing methodology and efficacy evaluations, and critical crack size determinations for NDE detection criteria. Establish and maintain this database in an openly accessible location, such as maptis.nasa.gov. (*F-2, F-3, F-6*)

R-10. Agency expand efforts to develop and validate analysis methods to address identified highest risk conditions and regions of LPVs.

- Assess sensitivity of results to uncertainties in input variables (e.g., material property values, structural configurations, and weld residual stress states). (*F-3*)
- Complete development of analytical models that incorporate key structural details of LPVs. Validate models where possible against deformation measurements from pressurized LPVs. (*F-3*)
- Complete analytical predictions of residual stresses in LPV circumferential full-penetration welds and obtain a sample of WRS measurements to validate predictions. (*F-14*)
- Establish an analytical framework to evaluate proof test logic. (*F-6*)
- In cases where proof testing cannot be applied, establish an analytical framework to evaluate the LBB capability of the system. (*F-3*)
- To aid in NDE development and validation, establish an analytical framework to evaluate critical initial flaw sizes. (*F-3*)
- Predict surface deformations associated with critical flaw sizes to assess the capability of photogrammetry methods for flaw detection in shell sections. (*F-16*)
- Evaluate friction effects between intermediate layers of shell sections. (*F-3*)

R-11. Agency develop and validate the following NDE techniques to address the highest risk conditions and regions of LPVs.

- PAUT for inspection of LPV full-penetration circumferential welds. (*F-15*)
- Photogrammetric techniques for validating analysis methods and assess capability for detecting flaws in shell sections. (*F-16*)
- AE techniques for application to LPVs. (*F-17*)
- RT methods for detecting cracks in shell sections and welds. (*F-18*)
- Low-frequency electromagnetic methods for the detection of flaws in shell sections of LPVs. (*F-19*)

	NASA Engineering and Safety Center Technical Assessment Report	Document #:	Version:
		NESCP-RP-13-00852	1.0
Title:		Page #:	
Evaluation of Agency Non-code LPVs		184 of 193	

9.0 Alternate Viewpoint

There were no alternate viewpoints identified during the course of this assessment by the NESC team or the NESC Review Board quorum.

10.0 Other Deliverables

No unique hardware, software, or data packages, outside those contained in this report, were disseminated to other parties outside this assessment.

11.0 Lessons Learned

No applicable lessons learned were identified for entry into the NASA Lessons Learned Information System as a result of this assessment.

12.0 Recommendations for NASA Standards and Specifications

No recommendations for NASA standards and specifications were identified as a result of this assessment.

13.0 Definition of Terms

Corrective Actions	Changes to design processes, work instructions, workmanship practices, training, inspections, tests, procedures, specifications, drawings, tools, equipment, facilities, resources, or material that result in preventing, minimizing, or limiting the potential for recurrence of a problem.
Finding	A relevant factual conclusion and/or issue that is within the assessment scope and that the team has rigorously based on data from their independent analyses, tests, inspections, and/or reviews of technical documentation.
Lessons Learned	Knowledge, understanding, or conclusive insight gained by experience that may benefit other current or future NASA programs and projects. The experience may be positive, as in a successful test or mission, or negative, as in a mishap or failure.
Observation	A noteworthy fact, issue, and/or risk, which may not be directly within the assessment scope, but could generate a separate issue or concern if not addressed. Alternatively, an observation can be a positive acknowledgement of a Center/Program/Project/Organization's operational structure, tools, and/or support provided.
Problem	The subject of the independent technical assessment.
Proximate Cause	The event(s) that occurred, including any condition(s) that existed immediately before the undesired outcome, directly resulted in its

	NASA Engineering and Safety Center Technical Assessment Report	Document #:	Version:
		NESCP-RP- 13-00852	1.0
Title:		Page #:	
Evaluation of Agency Non-code LPVs		185 of 193	

occurrence and, if eliminated or modified, would have prevented the undesired outcome.

Recommendation A proposed measurable stakeholder action directly supported by specific Finding(s) and/or Observation(s) that will correct or mitigate an identified issue or risk.

Root Cause One of multiple factors (events, conditions, or organizational factors) that contributed to or created the proximate cause and subsequent undesired outcome and, if eliminated or modified, would have prevented the undesired outcome. Typically, multiple root causes contribute to an undesired outcome.

Supporting Narrative A paragraph, or section, in an NESCS final report that provides the detailed explanation of a succinctly worded finding or observation. For example, the logical deduction that led to a finding or observation; descriptions of assumptions, exceptions, clarifications, and boundary conditions. Avoid squeezing all of this information into a finding or observation

14.0 Acronym List

AE	Acoustic Emission
AFRC	Armstrong Flight Research Center (formerly Dryden Flight Research Center)
AMA	Analytical Mechanics Associates, Inc.
ARC	Ames Research Center
ASME	American Society of Mechanical Engineers
ASTM	American Society for Testing and Materials
B&W	Babcock and Wilcox
BPVC	Boiler and Pressure Vessel Code
C	Circumferential (structural orientation)
C(T)	Compact Tension
CB&I	Chicago Bridge & Iron Company
dB	Decibel
DOD	Department of Defense
DOT	Department of Transportation
DP	Dye Penetrant
DWC	Digital Wave Corporation
EDM	Electronic Discharge Machine
FBH	Flat-bottom Hole
FEAM	Finite Element Alternating Method
FFS	Fitness for Service
FS	Factor of Safety
FSH	Full Screen Height
FY	Fiscal Year



NASA Engineering and Safety Center Technical Assessment Report

Document #:
**NESCP-RP-
13-00852**

Version:
1.0

Title:

Evaluation of Agency Non-code LPVs

Page #:
186 of 193

GRC	Glenn Research Center
GSE	Ground Support Equipment
GUI	Graphical User Interface
HAZ	Heat-Affected Zone
HDT	Hit Definition Time
HLT	Hit Lockout Time
Hz	Hertz
ICP	Inductively Coupled Plasma
ID	Inner Diameter
JPL	Jet Propulsion Laboratory
JSC	Johnson Space Center
KAPL	Knolls Atomic Power Laboratory
KSC	Kennedy Space Center
L	Longitudinal (material or structural orientation)
LAPVAT	Layered Pressure Vessel Analysis Tool
LaRC	Langley Research Center
LBB	Leak before Burst
LEFM	Linear Elastic Fracture Mechanics
LPV	Layered Pressure Vessel
M	Meridional, spherical head (structural orientation)
MAE	Modal AE (Acoustic Emission)
MAF	Michoud Assembly Facility
MAWP	Maximum Allowable Working Pressure
MDMT	Minimum Design Metal Temperature
MSFC	Marshall Space Flight Center
MT	Magnetic Particle Testing
MTSO	Management and Technical Support Office
NBIC	National Board Inspection Code
NDE	Nondestructive Evaluation
NDT	Nil Ductility Temperature
NESC	NASA Engineering and Safety Center
NG	Northrop Grumman Corporation
NRC	U.S. Nuclear Regulatory Commission
OD	Outer Diameter
OSHA	Occupational Safety and Health Administration
OSMA	Office of Safety and Mission Assurance
PAUT	Phased Array Ultrasonic Technique
PDT	Peak Definition Time
PSM	Pressure Systems Manager
PT	Penetrant Testing
PWHT	Post-Weld Heat Treated
R	Radial (structural orientation)

	NASA Engineering and Safety Center Technical Assessment Report	Document #:	Version:
		NESCP-RP- 13-00852	1.0
Title:		Page #:	
Evaluation of Agency Non-code LPVs		187 of 193	

RDH	Radially Drilled Hole
RFI	Request for Information
RT	Radiographic Testing
S	Short-transverse (material orientation)
SCC	Stress Corrosion Cracking
SDH	Side-drilled Hole
SE	Signal Energy
SE(B)	Single-edge Notch Bend
SLOFEC™	Saturated Low Frequency Eddy Current
SOW	Statement of Work
SSC	Stennis Space Center
SwRI	Southwest Research Institute
T	Transverse (material orientation)
TIM	Technical Interchange Meeting
U.S.	United States
UT	Ultrasonic Testing
VFT	Virtual Fabrication Technology
VT	Visual Testing
WFF	Wallops Flight Facility
WRS	Weld Residual Stress
WSTF	White Sands Test Facility
XRF	X-ray Fluorescence

15.0 References

1. “ASME Boiler and Pressure Vessel Code, Section VIII – Pressure Vessels,” Division 1, current edition.
2. “Occupational Safety and Health Standards,” 29 CFR 1910, OSHA, U.S. Department of Labor.
3. Basic Program Elements for Federal Employee Occupational Safety and Health Programs and Related Matters: Subpart 1 for Recordkeeping and Reporting Requirements,” 29 CFR 1960, OSHA, U.S. Department of Labor, November 26, 2004.
4. “ASME Boiler and Pressure Vessel Code, Section VIII – Pressure Vessels,” Division 1, 1968 edition.
5. U.S. Patent 1,925,118, “Pressure Vessel and Method of Fabricating It,” Stresau, Richard, Assigned to A. O. Smith Corporation, September 5, 1933.
6. U.S. Patent 2,332,463, “Multilayer Pressure Vessel,” Nilson, E. H., Assigned to A. O. Smith Corporation, October 19, 1943.
7. Gilbertson, M. and Benac, D. J., “Multi-layered Secondary Urea Reactor Failure,” AICHE Ammonia Safety Symposium, Chicago, IL, Paper 1C, September 9–13, 2012.

	NASA Engineering and Safety Center Technical Assessment Report	Document #: NESCP-RP- 13-00852	Version: 1.0
Title: Evaluation of Agency Non-code LPVs		Page #: 188 of 193	

8. “Nondestructive Evaluation Requirements for Fracture Critical Metallic Components,” NASA-STD-5009, April 7, 2008, para. 4.2.4.4.3.
9. ASME BPVC Code, Summer 1979 Addenda to the 1977 Section VIII.
10. “Requirements for Pressure Vessels Fabricated by Layered Construction,” Part UWL, ASME BPVC Code, Winter Edition of 1978 (Section VIII, Divisions 1 and 2).
11. ASME Code for Unfired Pressure Vessels (1956).
12. ASME Code Interpretations Case 1205-3.
13. A. O. Smith Corporation’s specification MLS-30A.
14. A. O. Smith Corporation’s specification dated August 27, 1957.
15. “ASME Boiler and Pressure Vessel Code, Section VIII – Pressure Vessels,” Division 1, 1989 edition.
16. Gross, J. H., “The Effect of Strength and Thickness on Notch Ductility,” presented at Symposium on Testing by Impact at ASTM Annual Meeting, Atlantic City, NJ, June 25, 1969.
17. “ASME Boiler and Pressure Vessel Code, Section II – Materials,” current edition.
18. Cloud, R. L. and Spiering, G. A., “Failure of a High Pressure Vessel in Ammonia Service,” Joint Conference of The Pressure Vessels and Piping, Materials, Nuclear Engineering, and Solar Divisions, June 21-25, 1981, Denver, CO, ASME 81-PVP-8, pp. 1–15.
19. Jojima, T., “Urea Reactor Failure,” *Ammonia Plant Safety*, Vol. 21, 1979, pp. 111–118.
20. Occupational Safety and Health Review Commission Docket 93-0628, 2004, last accessed on April 28, 2014, URL: http://www.oshrc.gov/decisions/html_2004/93-0628.html.
21. Li *et al.*, “Analysis on Layer Cracking of Urea Reactors,” Paper No. PVP2010-25855, ASME 2010 Pressure Vessels and Piping Division/K-PVP Conference, Bellevue, WA, July 18–22, 2010. ISBN: 978-0-7918-4924-8, pp. 265–274.
22. Song, M., Wang, W., Zhao, Y., and Cui, Y., “Urea Reactor Integrity Evaluation Based on Failure Analysis,” *Transactions of the ASME*, Vol. 129, November, 2007, pp. 744–753.
23. Gilbertson, M. and Benac, D. J., “Multi-layered Secondary Urea Reactor Failure,” AICHE Ammonia Safety Symposium, Paper 1C, Chicago, IL, September 9–13, 2012.
24. “NASA Requirements for Ground-Based Pressure Vessels and Pressurized Systems (PVS),” NASA-STD-8719.17.
25. Fowler, T. J., Blessing, J. A., Conlisk, P. J., and Swanson, T. L., “The MONPAC System,” *Journal of Acoustic Emission*, Vol. 8, No. 3, pp. 1–8.

	NASA Engineering and Safety Center Technical Assessment Report	Document #: NESCP-RP- 13-00852	Version: 1.0
Title: Evaluation of Agency Non-code LPVs		Page #: 189 of 193	

26. Ziola, S. M., "Cyclic Crack Growth Testing of an A. O. Smith Multilayer Pressure Vessel with Modal Acoustic Emission Monitoring and Data Assessment," NASA/CR 2014-218156, January 2014.
27. Ziola, S. M., "AE Qualification Test of HPADS Storage Vessel #16 at N250A," Ames Research Center, Moffett Field, CA, Digital Wave Corp., October 10, 2001.
28. Ziola, S. M., "AE Qualification Test of HPADS Storage Vessels 21–36 at N250A," Ames Research Center, Moffett Field, CA, Digital Wave Corp., October 29, 2002.
29. Ziola, S. M., "AE Qualification Test of HPADS Storage Vessels 1–16 at N250A," Ames Research Center, Moffett Field, CA, Digital Wave Corp., August 12, 2009.
30. "SLOFEC™ Fast Corrosion Screening Technique," Innospection, Ltd., 2004, last accessed on April 28, 2014, URL: <http://www.innospection.com/pdfs/SLOFEC%20Technique.pdf>.
31. "Standard Test Method for Determination of Reference Temperature, T_0 , for Ferritic Steels in the Transition Range," ASTM E 1921-13, ASTM International, West Conshohocken, PA.
32. "Recommended Practice for Fitness-For-Service," ASME-FFS-1 (API-579), American Petroleum Institute, Washington, D. C., 2008.
33. "Standard Test Method for Determination of Reference Temperature, T_0 , for Ferritic Steels in the Transition Range," ASTM E 1921-13, ASTM International, West Conshohocken, PA.
34. Graff, K., *Elastic Wave Motion in Solids*, Ohio State University Press, Columbus, 1976.
35. Pao, Y. H., "Theory of Acoustic Emission, Elastic Waves and Nondestructive Testing of Materials," ASME Pub. AMD-Vol. 29, ASME, New York, 1978, pp. 107–128.
36. Gorman, M. R., "Plate Wave Acoustic Emission," *Journal of the Acoustic Society of America*, July 1991, pp. 358–364.
37. "Use of Modal Acoustic Emission and Ultrasonic Examination (AE/UE) in lieu of Hydrostatic Pressure Test and Internal Visual Examination," DOT SP-15322, Digital Wave Corp., April 26, 2012.
38. Blackburn, P. R. and Rana, M. D., "Acoustic Emission Testing and Structural Evaluation of Seamless, Steel Tubes in Compressed Gas Service," *ASME Journal of Pressure Vessel Technology*, 1985.
39. Hudak, Connolly, Hanley, and Lukezich, "A Damage Tolerance Approach for Recertification of Submarine High-Pressure Flasks," SwRI Project No. 06-4557, Southwest Research Institute, March 31, 1995.
40. "Standard Practice for Acoustic Emission Monitoring of Structures during Controlled Stimulation," ASTM E-569, ASTM International, West Conshohocken, PA.
41. "Standard Test Method for Examination of Seamless, Gas Filled Pressure Vessels using Acoustic Emission," ASTM E-1419–02b, ASTM International, West Conshohocken, PA.

	NASA Engineering and Safety Center Technical Assessment Report	Document #: NESCP-RP- 13-00852	Version: 1.0
Title: Evaluation of Agency Non-code LPVs		Page #: 190 of 193	

42. “Standard Practice for Continuous Monitoring of Acoustic Emission from Metal Pressure Boundaries,” ASTM E-1139, ASTM International, West Conshohocken, PA.
43. “Standard Terminology for Nondestructive Examinations,” ASTM E-1316, ASTM International, West Conshohocken, PA.
44. Cardinal, J. W. and Popelar, C. F., “Multilayer Pressure Vessel Materials Testing and Analysis (Phase 2),” NASA/CR 2014-218158, January 2014.
45. Cardinal, J. W., Popelar, C. F., and Page, R. A., “Multilayer Pressure Vessel Materials Testing and Analysis (Phase 1),” NASA/CR 2014-218157, January 2014.
46. Mike Hudson *et al.*, “An Investigation of Fracture Toughness,” NASA TM X-3316, December 1975.
47. ANSI/NB-23 “National Board Inspection Code,” National Board of Boiler and Pressure Vessel Inspectors, 2013 Edition, 2013.
48. “Specification for High Strength Low-Alloy Steel Plates (1143),” Standard 626-1143, Distribution 7, Chicago Bridge and Iron Company, released November 1, 1963.
49. A. O. Smith, “Specification for High Strength Low-Alloy Steel Plates (1146),” Standard 626-1146, published November 8, 1963, Rev. March 1968.
50. A. O. Smith, “Specification for 1146-a, High Tensile Strength – Low Alloy Steel Flange Quality Plates,” Gauges 0.180 in. to 0.580 in., dated April 20, 1956.
51. ASME SA225 Gr. B, 1956 ASME Code Section II.
52. “Materials Standards, Material Specification for MLF-5002 Modified* High Tensile Strength, Low Alloy Steel Forgings for Fusion Welded Pressure Vessels,” Chicago Bridge and Iron Company, March 14, 1963.
53. “Specification for High Strength Low-Alloy Steel Plates (1146),” Standard 626-1146, Distribution 7, Chicago Bridge & Iron Company, released November 8, 1963.
54. Kenyon, N. and Epstein, A. L., “Technical Note: Sulfur and Phosphorus in Low Alloy Steel Welds Containing Up to 6% Nickel,” *Welding Journal*, Vol. 37, No. 11, November 1958, Research Supplement, pp. 481s–492s.
55. Sharp, D., *General Physics Corporation Contact Report*, Submitted to B. Howel and B. Hower of Nooter Corp., St. Louis, MO, November 28, 1989.
56. Private e-mail communication between Maan Jawad (consultant) and Matthew A. Adler, Ph.D. (MSFC, Jacobs ESSSA) on January 15, 2014.
57. “Standard Test Method for Determination of Reference Temperature, T_0 , for Ferritic Steels in the Transition Range,” ASTM E 1921-13, ASTM International, West Conshohocken, PA.
58. Broek, D., *The Practical Use of Fracture Mechanics*, Kluwer Academic Publishers, 1989, pp. 10–12.

	NASA Engineering and Safety Center Technical Assessment Report	Document #: NESCP-RP- 13-00852	Version: 1.0
Title: Evaluation of Agency Non-code LPVs		Page #: 191 of 193	

59. McCabe, D. E., Merkle, J. G., and Wallin, K., “An Introduction to the Development and Use of the Master Curve Method,” ASTM International, West Conshohocken, PA, 2005, p. 6.
60. Wallin, K., *Fracture Toughness of Engineering Materials*, EMAS Publishing, 2011, pp. 115–190.
61. Joyce, J. A. and Tregoning, R. L., “Investigation of Specimen Geometry Effects and Material Inhomogeneity Effects in A533B Steel, European Transactions,” European Conference on Fracture 14, Crakow, Poland, 2002.
62. Fletcher, F. B., “Properties and Selection: Irons, Steels, and High-Performance Alloys, Carbon and Low-Alloy Steel Plate,” ASM Handbook Volume 1, pp. 227–239.
63. <http://www.georgesbasement.com/Microstructures/LowAlloySteels/Lesson-1/Specimen01.htm>.
64. “Standard Test Method for Instrumented Impact Testing of Metallic Materials,” ASTM E 2298-13, ASTM International, West Conshohocken, PA.
65. “Standard Test Method for Measurement of Fracture Toughness,” ASTM E 1820-11, ASTM International, West Conshohocken, PA.
66. Private phone communication between Jim Joyce (Consultant) and Matthew A. Adler, Ph.D. (MSFC, Jacobs ESSSA) on April 9, 2014.
67. Palmer, C., “NASA MSFC Radiography Test Report,” EM20 NDE Work Order No. 2014-0011, January 13, 2014.
68. Palmer, C., “NASA MSFC Radiography Test Report,” EM20 NDE Work Order No. 2014-0276, April 9, 2014.
69. Palmer, C., “NASA MSFC Radiography Test Report,” EM20 NDE Work Order No. 2014-0162, March 6, 2014.
70. *Vessel V125 Data Package Index*, Chicago Bridge and Iron Company, 1963.
71. “VFTTM Manual,” Engineering Mechanics Corporation of Columbus, Emc2, June 2013.
72. Cheston, D., Piascik, R., Larsen, C., Knight, N., Brust, F. W., Womack, J., Phillips, D. R., Raju, I. S., Russel, S., Hudak, S., Reuter, W., Dawicke, D., and Hayes, M., “Independent Evaluation of the Critical Initial Flaw Sixe for Ares I-X (AIX) Upper Stage Simulator (USS) Common Segment to Flange-to-Skin Welds,” NESC Technical Report Document RP-08-09, February 26, 2008.
73. Raju, I. S., Brust, F. W., Phillips, D. R., and Cheston, R., “Ares I-C Upper Stage Simulator Residual Stress Analysis,” NASA/TM-2008-215339 (NESC-RP-08-09/06-081-E), August 2008.
74. Brust, F. W., Dawicke, D., Raju, I. S., and Cheston, D., “Residual Stresses and Critical Initial Flaw Size Analyses of Welds”, Proceedings of the 50th AIAA/ASME/ASCE Structures, Structural Dynamics, and Materials Conference, Palm Springs, CA, May 2009.

	NASA Engineering and Safety Center Technical Assessment Report	Document #: NESCP-RP- 13-00852	Version: 1.0
Title: Evaluation of Agency Non-code LPVs		Page #: 192 of 193	

75. Brust, F. W., Raju, I., Cheston, D., Dawicke, D., and Phillips, D., “Weld Residual Stress and Distortion Analysis of the ARES I-X Upper Stage Simulator,” Proceedings of the ASME Pressure Vessels & Piping PVP 2008 Conference, PVP 2008-61247, Chicago, IL, July 27–31, 2008.
76. Broussard, J., and Crooker, P., “NRC/EPRI Residual Stress Validation Program Phase 1: Experimental Specimen Modeling and Measurement,” Proceedings of ASME Pressure Vessel and Piping Conference, Paper No. PVP2011-57677, Baltimore MD, July 2011.
77. Schmidt, T., *et al.*, “Performance Verification of 3D Image Correlation Using Digital High-Speed Cameras,” Proceedings of 2005 SEM Annual Conference and Exposition, Portland, OR, June 7–9, 2005.
78. Melis, M., *et al.*, “Impact Testing on Reinforced Carbon-Carbon Flat Panels with BX-265 and PDL 1034 External Tank Foam for the Space Shuttle Return to Flight Program,” NASA TM 2009-213642/REV1, 2009.
79. Ambur, D. R., *et al.*, “Progressive Failure Studies of Stiffened Panels Subject to Shear Loading,” *Composite Structures*, Vol. 65, 2004, pp. 129–142.
80. Littell, J. D., *et al.*, “Measurement of Epoxy Resin Tension, Compression and Shear Stress Strain Curves over a Wide Range of Strain Rates Using Small Test Specimens,” *J. Aerosp. Eng.*, Vol. 21, 2008, pp. 162–173.
81. Amsterdam, E., *et al.*, “Failure Mechanisms of Closed Cell Aluminum Foam under Monotonic and Cyclic Loading,” *Acta Materialia*, Vol. 54, 2006, pp. 4465–4472.
82. Lesser, W. P., *et al.*, “Fatigue Crack Closure Analysis Using Digital Image Correlation,” NASA TM 2010-216695, 2010.
83. Chevalier, L., *et al.*, “Digital Image Correlation used to Analyze Multiaxial Behavior of Rubber-like Materials,” *European Journal of Mechanics A/Solids*, Vol. 20, 2001, pp. 167–187.
84. Revilock, D. M., *et al.*, “Three-Dimensional Digital Image Correlation of a Composite Overwrap Pressure Vessel during Hydrostatic Pressure Tests,” NASA TM 2007-214938, 2007.
85. Thornburgh, R. P. and Hilburger, M. W., “Longitudinal Weld Land Buckling in Compression Loaded Orthogrid Cylinders,” NASA TM 2010-216876, 2010.
86. Tyson, J., *et al.*, “Biomechanics Deformation and Strain Measurements with 3D Image Correlation Photogrammetry,” *Experimental Techniques*, Vol. 26, No. 5, 2002, pp. 39–42.
87. Zhang, D., *et al.*, “Evaluating the Material Behavior of Arterial Tissue using Digital Image Correlation,” *Experimental Mechanics*, Vol. 42, No. 2, 2002, pp. 409–416.
88. “Standard Practice for Acoustic Emission Monitoring of Structures during Controlled Stimulation,” ASTM E569/E569M-13, ASTM International, West Conshohocken, PA.

	NASA Engineering and Safety Center Technical Assessment Report	Document #:	Version:
		NESCP-RP- 13-00852	1.0
Title:		Page #:	
Evaluation of Agency Non-code LPVs		193 of 193	

89. Hamstad, M. A., O’Gallagher, A., and Gary, J., “Effects of Lateral Plate Dimensions on Acoustic Emission Signals from Dipole Sources,” *J. of Acoustic Emission*, Vol. 19, 2001, pp. 258–274.
90. Chell, G. G., McClung, R. C., Russell, D. A., Chang, K. J., and Donnelly, B., “Significant Issues in Proof Testing: A Critical Appraisal,” NASA/CR-4628, 1994.
91. Chell, G. G., McClung, R. C., Kuhlman, C. J., Russell, D. A., Garr, K., and Donnelly, B., “Guidelines for Proof Test Analysis,” NASA/CR-1999-209427, 1999.
92. McClung R. C., Chell, G. G., Millwater, H. R., Russell, D. A., and Orient, G. E., “A Comparison of Single-Cycle to Multi-Cycle Proof Testing Strategies,” NASA/CR-1999-209426, 1999.

16.0 Appendices (separate Volume 2)

- Appendix A. Example LPV Procurement Specification
- Appendix B. Center RFI Summaries
- Appendix C. MSFC Sacrificed Vessel General Information
- Appendix D. Current Considerations for the MSFC Non-Code Pressure Vessel Material Properties Assessment Presentation, February 28, 2014
- Appendix E. LPV TIM – September 18, 2013: Current Considerations for the MSFC Non-Code Layered Pressure Vessel Material Testing Tasks Presentation, February 28, 2014
- Appendix F. MSFC LPV Analysis Activities/LAPVAT Presentation, March 17, 2014
- Appendix G. ARC MAE Validation Effort Summary
- Appendix H. SwRI[®] Testing Summary

REPORT DOCUMENTATION PAGE

*Form Approved
OMB No. 0704-0188*

The public reporting burden for this collection of information is estimated to average 1 hour per response, including the time for reviewing instructions, searching existing data sources, gathering and maintaining the data needed, and completing and reviewing the collection of information. Send comments regarding this burden estimate or any other aspect of this collection of information, including suggestions for reducing this burden, to Department of Defense, Washington Headquarters Services, Directorate for Information Operations and Reports (0704-0188), 1215 Jefferson Davis Highway, Suite 1204, Arlington, VA 22202-4302. Respondents should be aware that notwithstanding any other provision of law, no person shall be subject to any penalty for failing to comply with a collection of information if it does not display a currently valid OMB control number.
PLEASE DO NOT RETURN YOUR FORM TO THE ABOVE ADDRESS.

1. REPORT DATE (DD-MM-YYYY) 01-07-2014		2. REPORT TYPE Technical Memorandum		3. DATES COVERED (From - To) April 2013 - June 2014	
4. TITLE AND SUBTITLE Evaluation of Agency Non-code Layered Pressure Vessels (LPVs)				5a. CONTRACT NUMBER	
				5b. GRANT NUMBER	
				5c. PROGRAM ELEMENT NUMBER	
6. AUTHOR(S) Prosser, William H.				5d. PROJECT NUMBER	
				5e. TASK NUMBER	
				5f. WORK UNIT NUMBER 869021.03.07.01.08	
7. PERFORMING ORGANIZATION NAME(S) AND ADDRESS(ES) NASA Langley Research Center Hampton, VA 23681-2199				8. PERFORMING ORGANIZATION REPORT NUMBER L-20446 NESC-RP-13-00852	
9. SPONSORING/MONITORING AGENCY NAME(S) AND ADDRESS(ES) National Aeronautics and Space Administration Washington, DC 20546-0001				10. SPONSOR/MONITOR'S ACRONYM(S) NASA	
				11. SPONSOR/MONITOR'S REPORT NUMBER(S) NASA/TM-2014-218505/Volume I	
12. DISTRIBUTION/AVAILABILITY STATEMENT Unclassified - Unlimited Subject Category 39 Structural Mechanics Availability: NASA CASI (443) 757-5802					
13. SUPPLEMENTARY NOTES					
14. ABSTRACT In coordination with the Office of Safety and Mission Assurance and the respective Center Pressure System Managers (PSMs), the NASA Engineering and Safety Center (NESC) was requested to formulate a consensus draft proposal for the development of additional testing and analysis methods to establish the technical validity, and any limitation thereof, for the continued safe operation of facility non-code layered pressure vessels. The PSMs from each NASA Center were asked to participate as part of the assessment team by providing, collecting, and reviewing data regarding current operations of these vessels. This report contains the outcome of the assessment and the findings, observations, and NESC recommendations to the Agency and individual NASA Centers.					
15. SUBJECT TERMS Layered pressure vessel; NASA Engineering and safety Center; Nondestructive Evaluation; Boiler and Pressure Vessel Code; Phased array ultrasonic technique					
16. SECURITY CLASSIFICATION OF:			17. LIMITATION OF ABSTRACT	18. NUMBER OF PAGES	19a. NAME OF RESPONSIBLE PERSON
a. REPORT	b. ABSTRACT	c. THIS PAGE			STI Help Desk (email: help@sti.nasa.gov)
U	U	U	UU	198	19b. TELEPHONE NUMBER (Include area code) (443) 757-5802